



INVESTIGATING SATELLITE DEVELOPING TECHNOLOGY IN DIFFERENT FIELDS OF SURVEYING

By

Eng. KHALED MAHMOUD ABDEL AZIZ MAHMOUD

Administrator of Surveying Department
Shoubra Faculty of Engineering - Benha University

A Thesis Submitted to the Department of Surveying Engineering,
Shoubra Faculty of Engineering, Benha University

For The Degree of Master of Science in
Surveying Engineering

SUPERVISED BY

Prof. Dr. ALI AHMED ELSAGHEER

Prof. of Surveying and Geodesy
Shoubra Faculty of Engineering

Assoc. Prof. Dr. MAHER MOHAMED AMIN

Assoc. Prof. of Surveying and Geodesy
Shoubra Faculty of Engineering

Dr. Eng. FARAG BASTAWY FARAG

Lecturer of Surveying
Shoubra Faculty of Engineering

2009

ABSTRACT

Artificial satellites play an important role in different fields of surveying. These satellites are used to determine the position of any place in our planet, to supply the image of any area on the earth by different spatial resolutions and to determine the gravity field every where on our planet. These satellite systems are modernized continuously and due to this modernization their accuracy in many surveying applications are improved.

This thesis investigates all satellite systems used in different fields of surveying through three categories; positioning, remote sensing and gravity field. Positioning satellites are used starting from 1957 and since then many systems have been built and modernized. In this research, these systems in the past, currently and in the future are investigated and their contributions to improve their accuracy in different applications are discussed.

Remote sensing satellites are started by launching Landsat-1 satellite in 1972. This is the first satellite from the family of Landsat satellites and then after many of the remote sensing satellites are launched. The different remote sensing satellite systems with different resolutions and accuracies cover different applications and requirements. The remote sensing satellite systems in the past, currently and in the future are illustrated.

The first, gravity field satellite was champ which is launched in 2000, after that many satellites are contributing to compute the gravity field of our planet. These satellite missions are investigated from their beginning till now. A practical part in this thesis is applying supervised

classification techniques for producing recent soil map for northern Sinai Peninsula from Landsat TM-5 medium resolution image.

The obtained results indicate that the best classification performance for images using the supervised technique is obtained with the Maximum Likelihood classifier. Proposals based on using the satellites utilized in the three investigated categories are introduced to contribute in the development of Egypt.

ACKNOWLEDGEMENTS

I would like to express my special gratitude and thanks to my advisers, **Prof. Dr. Ali Ahmed Elsagheer, Assoc. Prof. Dr. Maher Mohamed Amin and Dr. Eng. Farag Bastawy Farag**, for their strong support and inspiration through my research. Their creative ideas and enthusiasm helped me to overcome stumbling blocks and develop a strong approach to conducting research.

I also thank **Prof. Dr. Mahmoud Elnokrashy Osman** and **Prof. Dr. Abdallah Ahmed Saad** for their interest in reviewing the thesis and their constructive comment.

I would like to thank everybody who supported me in one way or the other in making this work come true.

Table of Contents

1. INTRODUCTION

Introduction.	1
1.1 Positioning Satellite Missions.	1
1.1.1 GPS Modernization.	2
1.1.2 GLONASS.	3
1.1.3 GALILEO.	4
1.1.4 Compass Navigation Satellite System (CNSS) or (BeiDou-2).	5
1.1.5 Augmentation Systems.	5
1.1.6 Regional Navigation Satellite Systems (RNSS).	6
1.2 Remote Sensing Satellite Missions.	6
1.2.1 Some of the Remote Sensing Satellites.	8
1.3 Gravity Field Satellite Missions.	9
1.3.1 Gravity Field Determination from Satellite Data.	10
1.3.1.1 Satellite Tracking.	11
1.3.1.1.1 Satellite Laser Ranging (SLR).	11
1.3.1.1.2 High-Low Satellite-to-Satellite Tracking (hl-SST).	11
1.3.1.1.3 Low-Low Satellite-to-Satellite Tracking (ll-SST).	11
1.3.1.2 Satellite Gradiometry.	12
1.3.1.3 Satellite Altimetry.	12
1.4 Objectives of the Present Thesis.	12
1.5 Scope of the Present Thesis.	13

2. POSITIONING SATELLITES

Introduction.	16
2.1 Global Navigation Satellite Systems (GNSS).	19
2.1.1 Navigation System with Time And Ranging (NAVSTAR).	19
2.1.1.1 The GPS System Design.	19
2.1.1.2 How GPS works.	26
2.1.1.3 Denial of Accuracy and Access.	28
2.1.1.4 Techniques for Deployment.	30

2.1.1.5 GPS Modernization.	39
2.1.1.6 Goals of modernization.	41
2.1.1.7 GPS Signal.	45
2.1.1.8 GPS Receivers.	45
2.1.1.9 Coordinate System.	46
2.1.1.10 GPS Constellation Status at (1.11.2008).	47
2.1.2 Global Navigation Satellites System (GLONASS).	48
2.1.2.1 The GLONASS System Design.	48
2.1.2.2 GLONASS Signals.	53
2.1.2.3 Coordinate System.	56
2.1.2.4 GLONASS Receivers.	57
2.1.2.5 GLONASS Modernization Program.	57
2.1.2.6 GLONASS Constellation Status at (21.09.2007).	62
2.1.3 GALILEO.	64
2.1.3.1 The GALILEO System Design.	64
2.1.3.2 Status of Galileo Programme.	71
2.1.3.3 GALILEO Signal.	73
2.1.4 Compass Navigation Satellites System (CNSS) or Beidou-2.	74
2.2 Space Based Augmentation Systems (SBAS).	75
2.2.1 Regional Space Based Augmentation Systems (RSBAS).	76
2.2.2 Global Space Based Augmentation Systems (GSBAS).	87
2.3 Ground-Based Augmentation Systems (GBAS).	91
2.3.1. Local Area Differential GPS.	91
2.3.2. Wide Area Differential GPS.	92
2.3.3. Local-Area Augmentation System (LAAS).	92
2.4 Regional Navigation Satellite Systems (RNSS).	94
2.4.1 Compass Satellite Navigation Experimental System (BeiDou-1).	94
2.4.1.1 The BeiDou-1 System Design.	95
2.4.1.2 Method of Operation.	96

2.4.2 Quasi Zenith Satellite System (QZSS).	99
2.4.2.1 The QZSS System Design.	100
2.4.2.2 QZSS Planned Signals.	101
2.4.2.3 Coordinate system.	103
2.4.2.4 QZSS coverage range.	103
, , Indian Regional Navigation Satellite System (IRNSS)	105
2.4.3.1 The IRNS System Design.	106
2.5 Types of GPS Receivers.	107
2.5.1 Modernization of Receivers.	108
 3. REMOTE SENSING SATELLITES	
 Introduction.	112
3.1 Electromagnetic spectrum used for remote sensing.	112
3.2 Remote Sensing Technology (RST).	113
3.2.1 Passive Remote Sensing Technologies.	114
3.2.1.1 Panchromatic Remote Sensing.	115
3.2.1.2 Multispectral Remote Sensing.	115
3.2.1.3 Hyperspectral Remote Sensing.	116
3.2.1.4 Thermal Remote Sensing.	116
3.2.1.5 Passive Microwave Remote Sensing.	117
3.2.1.6 Aerial Photography.	117
3.2.2 Active Remote Sensing Technologies.	118
3.2.2.1 Synthetic Aperture Radar (SAR) and IfSAR.	120
3.2.2.2 Light Detection and Ranging (LIDAR).	120
3.3 Satellite Orbits.	122
3.3.1 Geostationary orbits.	122
3.3.2 Polar orbiting satellites.	124
3.3.2.1 Sun-synchronous orbits.	124
3.4 Image Resolution.	126
3.4.1 Spatial Resolution.	126

3.4.2 Spectral Resolution.	127
3.4.3 Temporal Resolution.	127
3.4.4 Radiometric Resolution.	128
3.5 Scanner Sensor Systems	129
3.5.1 Across-track(Whiskbroom) scanners.	130
3.5.2 Along-track (pushbroom) scanners.	131
3.6 Digital image and processing.	132
3.6.1 Characteristics of digital image.	132
3.6.2 Image processing and analysis.	133
3.6.2.1 Preprocessing: error correction.	133
3.6.2.1.1 Radiometric corrections.	133
3.6.2.1.2 Geometric correction.	135
3.6.2.2 Image enhancement.	138
3.6.2.3 Image Transformations.	139
3.6.2.4 Texture analysis.	139
3.6.2.5 Data integration.	139
3.6.2.6 Information extraction.	140
3.6.2.6.1 Visual Interpretation	140
3.6.2.6.2 Automatic Classification	140
3.6.2.6.2.1 Unsupervised Classification	140
3.6.2.6.2.2 Supervised Classification	144
3.6.2.6.2.3 Accuracy Assessment	154
3.6.3 Image processing softwares.	156
3.7 Satellite platforms.	156
3.7.1 Optical land imaging satellites.	156
3.7.2 Radar land imaging satellites.	160
3.7.3 Most common optical land imaging satellites in Egypt	161
3.8 Applications of Remote Sensing	165

4. GRAVITY FIELD SATELLITES

Introduction	167
4.1 Basic gravity field quantities.	168
4.2 Gravity field determination from satellite data.	170
4.2.1 Satellite tracking.	172
4.2.1.1 Satellite laser ranging (SLR).	172
4.2.1.2 High-Low Satellite-to-Satellite Tracking (hl-SST).	173
4.2.1.2.1 CHAMP.	173
4.2.1.2.1.1 Spacecraft Components.	176
4.2.1.2.1.2 Global gravity field models from the CHAMP.	178
4.2.1.3 Low-Low Satellite-to-Satellite Tracking (ll-SST).	184
4.2.1.3.1 GRACE.	185
4.2.1.3.1.1 Spacecraft Components.	185
4.2.1.3.1.2 The Workings of GRACE.	189
4.2.1.3.1.3 Global gravity field Models from GRACE.	191
4.2.1.3.1.4 Combined Global gravity field models from CHAMP and GRACE	196
4.2.1.3.1.5 Combined Global gravity field models from GRACE, LAGEOS and Surface Gravity Data.	200
4.2.2 Satellite Gradiometry.	203
4.2.2.1 GOCE.	203
4.2.2.1.1 Mission Orbit.	205
4.2.2.1.2 Mission Profile.	205
4.2.2.1.3 GOCE Spacecraft Elements.	206
4.2.2.1.4 GOCE Measurement System.	208
4.2.2.1.5 Mission Objective.	209
4.2.3 Satellite Altimetry.	212
4.2.3.1 Measurement Method.	213

5. APPLICATIONS FOR THESE SATELLITES IN EGYPT

5.1 positioning satellites applications in Egypt	216
5.1.1 High Accuracy Reference Network (HARN)	216
5.1.2 The National Agriculture Cadastral Network (NACN)	219
5.1.3 Radio Beacon Network	220
5.1.4 Finnmap Project	222
5.1.5 Civil Aviation Project	225
5.2 Remote sensing satellites applications in Egypt	227
5.2.1 Estimation of water loss from Toshka Lakes using remote sensing and GIS	227
5.2.2 Middle Egypt Survey Project 2004	232
5.2.3 Remote Sensing and GIS for Integrated Coastal Zone Management A case Study: The Coral Reefs in the Northwestern Red Sea (HURGHADA, EGYPT)	235

6. PRACTICAL APPLICATION

6.1 Study Area, and Data Sources.	239
6.2 Methodology.	241
6.2.1 Scanning the Available Existing Hard Copy of the Geological Map.	242
6.2.2 Georeferencing the Scanned Map.	242
6.2.3 Image to map georeferencing.	242
6.2.4 Supervised classification.	245
6.2.4.1 Minimum distance classifier.	246
6.2.4.2 Mahalanobis Distance classifier.	247
6.2.4.3 Maximum Likelihood/Bayesian classifier.	248
6.2.5 Accuracy assessment.	249
6.2.5.1 The Error Matrix.	250
6.2.5.2 Kappa Statistics	253
6.3 Results and Analysis	253

7. SUMMARY, CONCLUSIONS AND RECOMMENDATIONS

7.1 Summary	259
7.2 Conclusions	261
7.3 Recommendations	264

List of Figures

Figure	Page
(2-1) TRANSIT configuration.	16
(2-2) Schematic View of the Orbit Paths of the GPS.	20
(2-3) Location of the control segment of the GPS satellite navigation system.	24
(2-4) Position is calculated from distance measurement.	26
(2-5) Effect of the Selective Availability on any position.	29
(2-6) Bad GDOP and Good GDOP.	31
(2-7) GPS Modernization Path.	41
(2-8) Ground Control Segment Expansion.	44
(2-9) WGS-84 Reference Ellipsoids.	47
(2-10) GLONASS Satellite Constellation.	49
(2-11) GLONASS ground control network.	53
(2-12) GLONASS Antipodal Satellites.	54
(2-13) Prediction of the satellite amount in the constellation based on the launch program and statistics.	58
(2-14) Ground Control Segment.	
(2-15) Illustrate GLONASS Accuracy Improvement Plan (AIP)	
(2-16) Difference of GLONASS orbits (range) wrt. ITRF before and after 20 December 2007.	61
(2-17) GLONASS Status at (21.09.2007).	62
(2-18) Numbers of visible GLONASS satellites for earth points	63
(2-19) GALILEO Satellite Constellation.	65
(2-20) GALILEO Architecture.	66
(2-21) Unlike SARSAT-COSPAS, GALILEO's Search And Rescue service also provides a reply to the distress signal	69
(2-22) IOV System Configuration.	72
(2-23) Space Based Augmentation System (SBAS).	76
(2-24) WASS Coverage.	78
(2-25) Wide-Area Augmentation System (WAAS).	79
(2-26) EGNOS GEO Satellites Triple Coverage over Europe and Africa.	82
(2-27) EGNOS offers improved GNSS performance with respect to GPS.	82

(2-28) MSAS Configuration.	84
(2-29) GAGAN Coverage.	85
(2-30) OmniSTAR Worldwide Satellite Coverage and Reference Stations.	88
(2-31) Local-Area Augmentation System (LAAS).	94
(2-32) BeiDou-1 User Terminal: The BeiDou-1 system uses a large-size transmitter/receiver user terminal due to its dual-way transmission operation method.	97
(2-33) BeiDou-1 method of operation.	98
(2-34) The difference of elevation angle between QZS and GSO.	99
(2-35) QZSS Orbit and Ground Track Diagram for the Three-Satellite Constellation.	100
(2-36) Transmission signal spectrum.	102
(2-37) Percentage of time during which at least one QZS in the 3-satellite QZSS can be seen at an elevation angle of 10° or more	104
(2-38) Percentage of time during which at least one QZS in the 3-satellite QZSS constellation can be seen at an elevation angle of 60° or more.	104
(2-39) Regional Coverage for Indian Regional Navigation Satellite System.	105
(3-1) Electromagnetic Spectrum.	113
(3-2) Passive sensors.	114
(3-3) Active sensors.	119
(3-4) Illustration of How the LIDAR Sensing Instrument Captures Elevation Points.	121
(3-5) Geo-stationary Orbit.	123
(3-6) Sun-synchronous orbit.	125
(3-7) Illustrate the different image resolution.	127
(3-8) The different Radiometric Resolution.	129
(3-9) Whiskbroom principle of image acquisition.	130
(3-10) Pushbroom principle of image acquisition.	131
(3-11) Characteristics Digital image.	132
(3-12a) Striping.	134
(3-12b) Dropped lines.	134

(3-13) Principle of geometric correction.	136
(3-14) Nearest neighbour method.	137
(3-15) Bilinear Interpolation method.	137
(3-16) cubic convolution method.	138
(3-17) Measures that define a cluster include the size of a cluster and the distance between clusters.	141
(3-18) ISODATA Clustering Procedure.	144
(3-19) Summarizes the three basic steps involved in a typical supervised classification procedure.	145
(3-20) Parallelepiped classification using plus or minus two standard deviations as limits.	147
(3-21) Minimum spectral distance.	149
(3-22) Maximum likelihood decision rule.	153
(4-1) The geoid height N, the elevation H above the geoid and the ellipsoidal height h.	168
(4-2) The LAGEOS-I satellite.	172
(4-3) The CHAMP Satellites.	175
(4-4) GPS-CHAMP high-low satellite-to-satellite and ground based laser tracking.	176
(4-5) EIGEN-1S Geoid.	179
(4-6) EIGEN-2 Gravity Anomalies.	180
(4-7) EIGEN-2 Geoid.	180
(4-8) EIGEN-3p Gravity Anomalies.	181
(4-9) EIGEN-3p Geoid.	182
(4-10) EIGEN-CHAMP03S Gravity Anomalies.	183
(4-11) EIGEN-CHAMP03S Geoid.	183
(4-12) The components of GRACE.	187
(4-13) The GRACE satellites.	188
(4-14) Shape of the GRACE satellites above different regions.	190
(4-15a) Gravity anomaly map derived from tracking data of 30 Earth orbiting satellites over more than 20 years (GRIM5-S1 model).	192
(4-15b) Gravity anomaly map derived from 16 months of CHAMP data only (EIGEN-CHAMP02S model).	192
(4-15c) Gravity anomaly map derived from 39 days of GRACE data only (EIGEN-GRACE01S model).	192
(4-16) EIGEN-GRACE02S geoid heights.	193
(4-17) EIGEN-GRACE02S anomalies.	193

(4-18) Gravity anomalies (mgal) derived from the EIGEN-CHAMP03S (left) and EIGEN-GRACE02S (right) Models.	194
(4-19) Gravity anomalies (in mgal) over Europe derived from the GRACE/LAGEOS satellite only model EIGEN-GL04S1 (left) and from the combined model EIGEN-GL04C (right).	195
(4-20) EIGEN-CG01C Free Air Gravity Anomalies.	198
(4-21) EIGEN-CG01C Geoid.	198
(4-22) Artist's Impression of the GOCE Satellite	205
(4-23) Schematic illustration of the combined satellite gravity gradiometer (SGG) and satellite-to-satellite (high-low) tracking mission concept.	207
(4-24) Schematic diagram showing geoid accuracy.	211
(4-25) Schematic diagram of satellite radar altimeter system.	214
(5-1) GPS Tracking Network of the International GPS Service for Geodynamics Global Stations.	218
(5-2) Recent Precise GPS Geodetic Control Networks in Egypt	219
(5-3) Radio Beacon Reference Stations in Egypt.	222
(5-4) General Layout of (Finnmap) GPS Satellite Network.	223
(5-5) Basic Civil Aviation Authority Network, CAA-Net1.	226
(5-6) Basic Civil Aviation Authority Network, CAA-Net1 Connected to IGS and HARN Reference Stations.	226
(5-7) Location map of Toshka Lakes.	228
(5-8) Toshka lakes surface area change from 2002 (left) to 2006 (right).	229
(5-9) digitized contours of topographic maps for the study area	230
(5-10) DEM of the Toshka area prior to the formation of lakes.	230
(5-11) Toshka lakes surface area change from 2002 to 2006.	231
(5-12) Toshka lakes water volumes change from 2002 to 2006.	232
(5-13) Landsat Satellite Image Used During the Middle Egypt Survey (Delta and Luxor).	233
(5-14) Close-up photo of the survey region. The red represents agricultural areas and the grey, towns.	234
(5-15) Satellite image of the survey area. The red areas represent archaeological places of interest and the circles mark the locations of the sites surveyed in the 2004 season.	235

(5-16) Overview of the Study Area on a Landsat 7 ETM.	236
(5-17) Schematic Overview of the Integration of Remote Sensing-Derived Products Together with Additional Information into a Monitoring System linked with a Coral Reef-GIS.	237
(5-18) Overall Risk Assessment Map of the Hurghada Study Area.	238
(6-1) Geological Map of Sinai, Arab Republic of Egypt (Sheet No.5).	240
(6-2) Landsat TM-5 Satellite Data for Northern Sinai Peninsula, Egypt.	241
(6-3) Distribution of the Map Reference Points over the TM-5 Image.	244
(6-4) Maximum likelihood Classified Landsat-5 image with 16 Class.	255
(6-5) Maximum likelihood Classified Landsat-5 image with 32 Class.	256
(6-6) minimum distance Classified Landsat-5 image with 16 Class.	256
(6-7) minimum distance Classified Landsat-5 image with 32 Class.	257
(6-8) mahalanobis distance Classified Landsat-5 image with 16 Class.	257
(6-9) mahalanobis distance Classified Landsat-5 image with 32 Class.	258

List of Tables

Table	Page
(1-1) History of Remote Sensing.	8
(2-1) Illustrate important elements of transit.	17
(2-2) Estimates of Standard Position System (SPS) User Equivalent Range Error (UERE).	31
(2-3) Carrier Phase Tracking Techniques.	39
(2-4) With Modernization the availability of GPS frequencies.	43
(2-5) Galileo Services, benefits and Availability.	70
(2-6) Illustrates the Horizontal and Vertical Accuracy for Galileo Service.	70
(2-7) Transmitted bandwidth and center frequency.	73
(2-8) Mapping of Galileo Navigation Signals onto Galileo Navigation Services.	74
(2-9): OmniSTAR Geostationary L-band Satellites	87
(2-10) QZSS orbital parameters.	100
(2-11) Illustrates Most Important Properties of the Four GNSS Systems.	111
(3-1) Spatial resolution class.	126
(3-2) very high resolution satellites (0.41to1m).	157
(3-3) high resolution satellites (1.8 to 2.5m).	157
(3-4) high medium resolution satellites (4 to 8m).	158
(3-5) medium resolution satellites (10 to 20m).	158
(3-6) low medium resolution satellites (30 to 56 m).	159
(3-7) Radar satellites.	160
(3-8) QuickBird satellite.	161
(3-9) IKONOS satellite.	162
(3-10) LANDSAT 7 satellite.	163
(3-11) SPOT-5 satellite.	164
(4-1) The requirements for several geoscientific branches expressed in terms of geoid height and gravity anomaly accuracies.	171
(4-2) Root mean square (RMS) about mean of GPS / leveling minus gravity field model derived geoid heights [m].	184

(4-3) Root mean square (RMS) about mean of GPS / leveling minus gravity field model derived geoid heights [m].	196
(4-4) Root mean square (RMS) about mean of GPS / leveling minus gravity field model derived geoid heights [m].	200
(4-5) Root mean square (RMS) about mean of GPS / leveling minus gravity field model derived geoid heights [m].	202
(4-6) Summary of science applications areas using GOCE data.	212
(4-7) Illustrate history of satellites altimetry.	215
(5-1) Egypt Marine DGPS Station Data.	221
(5-2) 1 st order observation Sessions.	224
(5-3) 2 nd Order Observation Sessions.	224
(5-4) GPS Observation Date and Session Duration at Every Investigated Station.	227
(6-1) Registration Map Reference Points (MRPs).	242
(6-2) Error in Coordinates of Control Points.	245
(6-3) Error Matrix for the Maximum Likelihood Map Produced From Landsat-5 Image Used 16 Classes.	252
(6-4) Illustrates the Producer's Accuracy and User Accuracy For the Maximum Likelihood Classification Map Used 16 Classes.	253
(6-5) Accuracy of Maximum Likelihood Classification at the various numbers of classes.	254
(6-6) Accuracy of Mahalanobis distance Classification at the various number of classes.	254
(6-7) Accuracy of minimum distance Classification at the various number of classes.	255

ABBREVIATIONS

AS	Anti-Spoofing
BIH	Bureau International de l'Heure
ESA	European Space Agency
EU	European Union
FDMA	Frequency division multiple access
FOC	Full Operational Capability
GEO	Geostationary Orbit
GNSS	Global Navigator Satellite System
ICAO	International Civil Aviation Organization (ICAO).
ITRF	International Terrestrial Reference Frame
PPS	Precise Positioning Service
PRN	Pseudo Random Noise
RF	Radio frequency
SA	Selective Availability
SDCM	System of Differential Corrections and Monitoring
SPS	Standard Positioning Service
UTC	Coordinated Universal Time
DOD	Department of Defense
OTF	On The Fly
CGWIC	China Great Wall Industries Corporation

Chapter 1

Introduction

Introduction

The idea of this work resulted due to modernization of the satellite technology in different fields of surveying. This thesis presents the history, stages for modernization, and applications of these satellites in three branches; Positioning, Remote sensing and Gravity field and the integration between these systems to obtain the optimum benefit. The following paragraph will illustrate the early use of the satellites in surveying fields.

1.1 Positioning Satellite Missions

Navigation has been an area of marked interest for human beings. People have been looking for and discovering easy and dependable ways to navigate from one place to another quickly. In the earlier days, position of stars was used for navigation. Then the magnetic compass and sextant came into picture; compass could not tell the exact position of the traveler but used to provide information on which direction he is moving and early sextant used to give only latitude of the position. Thereafter the concept of chronometer made it possible to measure the longitude of a particular point. So sextant along-with chronometer could give the longitude as well as latitude of a particular point [*Prinja,R.,2003*].

Radio-based navigation systems were developed in the early twentieth century, and were used extensively for military purposes in World War II. The drawback in such systems was the tradeoff between the area that can be covered and accuracy as high frequency radio-waves are accurate but can cover only a small area. Satellite navigation systems were built to overcome the drawback of radio-based navigation systems. The idea of satellite based navigation using radio waves started when Sputnik was launched into space by Russia [*Prinja,R.,2003*].

Since the first artificial satellite, the famous Sputnik was launched in 1957[*Soanes,C.,2004*], other orbital navigation systems are launched. These current systems are modernized and new systems planning to contribute the improvement in surveying applications.

1.1.1 GPS Modernization

Motivated by the United States Department of Defense (DoD), the current GPS has experienced three decades' development. Although the original motivation was only for military purposes, GPS has been widely used in civilian applications during the past few decades. However, the integrity, availability, and accuracy still need further improvement for various applications. For the surveying industry, applications can be classified according to the achievable accuracy. Therefore, a GPS modernization program was initiated in the late 1990's, in an attempt to upgrade GPS performance for both civilian and military applications. The GPS modernization program started with the cancellation of SA in 2000. It is followed by the addition of a new second civil code on L2 (L2C), then a third civil frequency L5. Further modernization consists of the assessment and design of a new generation of satellites to meet military and civil requirements through 2030.

[www.aars-acrs.org/acrs/proceeding/ACRS2007/Papers/TS40.5.pdf].

GPS Constellation Status as of 11 January 2008 is 30 Healthy Satellites (Baseline Constellation: 24)

- 13 Block IIA satellites operational
- 12 Block IIR satellites operational
- 5 Block IIR-M satellites operational
- Most Recent Launch

- IIR-18(M) – 5th modernized SV, Launched Wednesday, 20 December 2007 and Set healthy on 2 Jan 08
- IIR-19(M) – March 2008
- IIR-20(M) – June 2008, L5 demo payload
- IIR-21(M) – September 2008
- IIF-1 launch in 2009 [*Crews,M.,2008*].

1.1.2 GLONASS

GLONASS was originally deployed as the Soviet Union's answer to GPS. The design of GLONASS is very similar to GPS except that each satellite broadcasts its own particular frequency with the same codes (this is known as a FDMA, or Frequency Division Multiple Access, scheme), while GPS satellites broadcast the same frequencies and a receiver differentiates between satellites by recognizing the unique code broadcast by a given satellite (this is known as a CDMA, or Code Division Multiple Access, scheme). Current activity centers on launching GLONASS-M satellites with an improved 7-year design lifetime, which will broadcast in the L1 and L2 bands (though not on the same frequencies as GPS). It is planned to launch GLONASS-K satellites with improved performance, which will also transmit a third civil signal known as L3 (not the same frequency as GPS's L5). The stated intention is to achieve a full 24 satellite constellation transmitting the two civil L1 and L2 signals by 2010. The full constellation is planned to be broadcasting three sets of civil signals by 2012

[www.aars-acrs.org/acrs/proceeding/ACRS2007/Papers/TS40.5.pdf].

In the 21th of September 2007, the GLONASS constellation consists of eleven satellites, seven new GLONASS-M and four old GLONASS. Healthy 9 satellites, one satellite in commissioning and one satellite in maintenance [*Revnivkykh,S.,2007*].

1.1.3 GALILEO

The European Union wants to become independent of GPS which is under control of the Department of Defense of the United States. Additionally the EU wants to profit from the growing market "Satellite based positioning and navigation [*Eissfeller et. al.,2007*]. Technical progress on the European Galileo navigation system, comprising of 30 future navigation satellites (27 active satellites in a 3- plane 27/3/1 Walker configuration plus 3 spare satellites, one per plane) in MEO orbits [*Pullen,s.,2008*].

On December 28, 2005, the first experimental satellite GIOVE-A was launched into orbit from the Russian Cosmodrome at Baikonur in Kasachstan. On January 12, 2006, GIOVE-A transmitted its first signal. The signals were registered and analyzed at the observation station for Atmospheric and Radio wave Research in Chilbolton in Britain as well as the ESA ground station at Redu in Belgium

[[http://telecom.tlab.ch/~zogg/Dateien/GPS_Compendium\(GPS-X-02007\).pdf](http://telecom.tlab.ch/~zogg/Dateien/GPS_Compendium(GPS-X-02007).pdf)]. A second GIOVE satellite is planned to be launched in April 2008 [http://en.wikipedia.org/wiki/Galileo_positioning_system].

With GIOVE-A and B the EU will secure the frequency bands for GALILEO operation and determine the orbitals for the test phase satellites. These pioneer satellites will also serve in the testing of important technology, such as atomic clocks, in the hard conditions of space. GIOVE-A has two Rubidium atomic clocks and GIOVE-B will have two passive Hydrogen-Maser atomic clocks onboard.

[[http://telecom.tlab.ch/~zogg/Dateien/GPS_Compendium\(GPS-X-02007\).pdf](http://telecom.tlab.ch/~zogg/Dateien/GPS_Compendium(GPS-X-02007).pdf)]. The next technical step for Galileo beyond completion of GIOVE activities is known as "In Orbit Validation" or (IOV). As part of IOV, the first four operational Galileo satellites to be launched will be used with the initial set of ground monitor stations (Galileo Sensor Stations, or

GSS's) and uplink antennas to test all facets of the performance of the eventual end-state Galileo system.

The first launch of IOV satellites planned in 2009, the “operational phase” of Galileo's life cycle will not begin before 2012 and it seems very optimistic to expect the 30-satellite constellation to be completed before 2015 even if no significant program setbacks are encountered

[Pullen,s.,2008].

1.1.4 Compass Navigation Satellite System (CNSS) or (BeiDou-2)

China is planning to build a navigation satellite constellation known as Compass Navigation Satellite System (CNSS), or (BeiDou-2) in its Chinese name. The system will be based on its current Compass Satellite Navigation Experimental System (BeiDou-1), which provides navigation and positioning services to users in China and its neighbouring countries since 2008. The system will be gradually expanded into a navigation satellite constellation comprising 5 Geostationary Earth Orbit (GEO) satellites and 30 medium Earth orbit satellites, which can provide navigation and positioning services to global users.

China successfully launched a medium Earth orbit BeiDou navigation satellite codenamed Compass-M1 on 14 April 2007. The satellite will operate at an altitude of 21,500 km orbit.

[www.sinodefence.com/strategic/spacecraft/beidou2.asp].

1.1.5 Augmentation Systems

In addition to these global systems, regional geostationary systems and global systems are used to complement the GPS or GLONASS constellations. These additional systems are known as Regional Space Based Augmentation Systems (RSBAS). The current active RSBAS are EGNOS in Europe, WAAS in the USA and MSAS in Japan (system under validation,

IOC in 2007). Several other SBAS systems are now in study or development phase for the coverage of other regions (GAGAN in India, CWAAS in Canada and SNAS in China [*Francois,R.,2007*], Nigeria is also planning NIGCOMSAT [*Dempster,A.,2007*], Russia is also planning SDCM this is Wide-area (Russia) [www.unoosa.org/pdf/icg/2007/algeria/01.pdf] and other systems already active are known as Global Space Based Augmentation Systems (GSBAS) for example OmniSTAR, StarFire and VueStar [*Kemppi,p.,2007*], and Ground based augmentation systems(GBAS).

1.1.6 Regional Navigation Satellite Systems (RNSS)

China launched Beidou-1, which was the first Regional Navigation Satellite System (RNSS), Japan tried to solve the urban canyon problem by planning their own regional augmentation to GPS: the Quasi-Zenith Satellite System (QZSS) and India proposed the Indian RNSS (IRNSS) [*Dempster,A.,2007*].

1.2 Remote Sensing Satellite Missions

Remote sensing (RS), also called earth observation, refers to obtaining information about objects or areas at the Earth's surface without being in direct contact with the object or area. Humans accomplish this task with aid of eyes or by the sense of smell or hearing; so, remote sensing is day-today business for people. Reading the newspaper, watching cars driving in front of you are all remote sensing activities. Most sensing devices record information about an object by measuring an object's transmission of electromagnetic energy from reflecting and radiating surfaces.

Remote sensing techniques allow taking images of the earth surface in various wavelength region of the electromagnetic spectrum (EMS). One of the major characteristics of a remotely sensed image is the wavelength region it represents in the EMS. Some of the images represent reflected solar

radiation in the visible and the near infrared regions of the electromagnetic spectrum, others are the measurements of the energy emitted by the earth surface itself i.e. in the thermal infrared wavelength region. The energy measured in the microwave region is the measure of relative return from the earth's surface, where the energy is transmitted from the vehicle itself. This is known as active remote sensing, since the energy source is provided by the remote sensing platform. Whereas the systems where the remote sensing measurements depend upon the external energy source, such as sun are referred to as passive remote sensing systems [*Aggarwal,S.,1998*]. Table (1-1) Illustrates history of remote sensing before launching the first land observation satellite (Landsat-1) in 1972.

Table (1-1): History of Remote Sensing

[www.isprs.org/caravan/documents/Lao_Basic_RS.pdf]

1826	The invention of photography
1850's	Photography from balloons
1873	Theory of electromagnetic energy by James Clerk Maxwell
1909	Photography from airplanes
1910's	World War I: aerial reconnaissance
1920's	Development and applications of aerial photography and photogrammetry
1930's	Development of radar in Germany, USA, and UK
1940's	World War II: application of Infrared and microwave regions
1950's	Military Research and Development
1960's	The satellite era: Space race between USA and USSR
1960	The first meteorological satellite (TIROS-1)
1960's	First use of term “ remote sensing ”
1972	Launch of the first earth resource satellite (Landsat-1)

1.2.1 Some of the Remote Sensing Satellites

RADARSAT, the Canadian satellite uses SAR, an active microwave sensor, allowing 24- hour data collection, independent of weather conditions and illumination.

The LANDSAT program is the longest running exercise in the collection of multispectral digital data of the Earth's surface from space. Since LANDSAT-1 was launched on July 23, 1972, data is being collected in a continuous stream, through one after another launch of LANDSAT (LANDSAT 7 is the latest in orbit). SPOT 1, the first French satellite, was launched in 1986. SPOT 2, 3 and 4 followed in 1990, 1993 and 1998 respectively. SPOT 5 has been launched in Oct, 2001 to ensure continuity of

service. On September 24, 1999 United States launched IKONOS satellite, has the world's most powerful digital camera system making it the only commercial imaging system for the space borne remote sensing in this time. It is designed and built so powerful that it can see objects less than one square meter on the ground and well enough to outline narrow alleys and streets. The satellite will simultaneously collect panchromatic imagery with one-meter resolution, and multispectral data with four-meter resolution, across and 11-km swath of the Earth's surface. The highly detailed topographical images of remote cities and unique geoinformation at a very high resolution make IKONOS an important part of disaster mitigation planning and decision-making. Digital Globe launched a low altitude (450km) satellite, QuickBird, on October 18, 2001 opening a new commercial channel with highest publicly available resolution. The satellite has 61cm panchromatic and 2.44 m multispectral sensors [Simonovic,S.,2002].

Since the launch of the first earth resource satellite (Landsat-1) in 1972 the modernization of the remote sensing satellites technology are continuous. Today many generations of remote sensing satellites are launched from many countries; each generation improved the data collection from earth land cover.

1.3 Gravity Field Satellite Missions

One of the major tasks of geodesy is the determination of the geoid, which is defined as an equipotential surface of the Earth gravity field, which coincides on average with mean sea level. The geoid surface is more irregular than the ellipsoid of revolution often used to approximate the shape of the physical Earth, but considerably smoother than the Earth's physical surface. Nowadays, with technology advancing so quickly, GPS positioning can offer

a very accurate determination of ellipsoid height h relative to the adopted reference ellipsoid. Precise knowledge of the geoid undulation relative to the ellipsoid N , can lead to the estimation of orthometric height H by using the equation $h = H + N$ which connects those three values. Thus, one of the primal goals of geodesy is to develop a precise geoid model, which can then be used for computing the orthometric heights. The determination and availability of a high-resolution and more accurate geoid model, is a necessity in several geosciences e.g. detecting the variations of the ocean currents, study of the interior properties of the Earth in geophysics, seismology and plate tectonics since it serves as the reference surface for other measurements and phenomena. Geoid is also important information for other disciplines related to Geomatics engineering like navigation, mapping, surveying and construction [*Daras,I.,2008*].

1.3.1 Gravity Field Determination from Satellite Data

The big advantage of satellite gravity data is that we can obtain a global coverage of the Earth. By tracking the orbit of a satellite, one can strengthen the estimation of the low-degree part of the gravitational field and fill in the gaps in some remote areas. Altimetry is an accurate technique to obtain an estimate of the geoid in the oceanic regions. A constellation of multiple satellites, with an inter-satellite tracking, is able to obtain the temporal changes in the gravity field and gradiometry is used to estimate the high-degree spherical harmonics of the Earth's gravitational field. In this thesis, the different measurement techniques used in satellite gravity modeling will be discussed [*Loon,J.,2008*].

1.3.1.1 Satellite Tracking

The orbit of a satellite is highly influenced by the gravity field of the Earth. Inversely, a time series of the position of a satellite can give extra information on this gravity field.

1.3.1.1.1 Satellite Laser Ranging (SLR)

Satellite laser ranging is the most accurate technique (within the centimeter level) to determine the position of a satellite. It measures the round trip time of pulses of light to satellites equipped with retro-reflectors. With a network of ground stations measuring the distances to the satellite, one can determine the position of the satellite's centre of mass very precisely [*Loon,J.,2008*].

1.3.1.1.2 High-Low Satellite-to-Satellite Tracking (hl-SST)

An alternative method to measure the position of a satellite is to use high-low satellite-to-satellite tracking (hl-SST) by means of GPS measurements e.g., CHAMP satellite [*Reigber et. al., 1999*]. On July 15, 2007, CHAMP has finished its 7th year in orbit. All satellite subsystems, science instruments and ground segment components are performing excellent and are still providing an almost continuous flow of highly valuable gravity, magnetic field and atmosphere sounding observations, two years beyond CHAMP's predicted life time. It is expected that CHAMP will continue to provide highly valuable data for another 2 years from low altitude [www-app2.gfz-potsdam.de/pb1/op/champ/more/newsletter_CHAMP_016.html].

1.3.1.1.3 Low-Low Satellite-to-Satellite Tracking (ll-SST)

A constellation of multiple satellites measuring their mutual distances (ll-SST), combined with an absolute positioning technique (hl-SST / SLR) can improve the estimation of the Earth's gravity field, especially its temporal variations, considerably [*Jekeli,1999*]. The GRACE mission, launched in

2002, is such a mission, measuring the distance between two low-altitude (≈ 500 km) satellites in identical near-polar orbits [*Tapley et al., 2004a, 2004b*].

1.3.1.2 Satellite Gradiometry

Gradiometry measures the difference in acceleration of test masses over small distances with two accelerometers for each direction. In this way, components of the gravity tensor can be measured, which will mainly provide information on the high-degree spherical harmonics of the Earth's gravity field [*Rummel and Colombo, 1985*].

The GOCE satellite will be the first satellite carrying a gradiometer on board. Successfully launched on 2009, with an expected lifetime of two years [*Fehringer, M., et. al., 2007*].

1.3.1.3 Satellite Altimetry

Satellite altimetry is a method to estimate the sea surface height, by measuring the distance between the satellite and the sea surface using an on board altimeter [*Lemoine et. al., 1998*]. Examples of altimetry satellites are the GEOS-3 (1975-1978), SEASAT (1978), GEOSAT (1985-1990), ERS-1 (1991-2000), ERS-2 (1995-), TOPEX/Poseidon (1992- 2005), Jason-1 (2001-) and Envisat (2002-) satellites. Just recently (June 2008), the Jason-2 satellite is put into orbit [*Loon, J., 2008*].

1.4 Objectives of the Present Thesis

Based on the above discussions, it can be stated that, the main point of our interest, will be studying the past, current and future of the satellite missions used in different fields of surveying and how could they contribute in the different applications in Egypt. To verify that, the following will be done:

- a. Studying stages of the improved technologies for the positioning satellites, remote sensing satellites and gravity field satellites and studying the effect of improving their accuracies on the different fields of surveying.
- b. The integration among those satellite missions for the optimum use.
- c. The practical part in this thesis is using supervised classification techniques for producing recent soil map for northern Sinai Peninsula from Landsat TM-5 medium resolution image.
- d. Investigating the effect of using these satellite missions or some of them in different applications in Egypt, and introducing recommendations based on that.

1.5 Scope of the Present Thesis

The remainder of the material of this thesis will be presented in the next six chapters, whose contents may be summarized as follows:

Chapter (2) concerned with the Global Navigation Satellite Systems (GNSS) as NAVSTAR, GLONASS, GALILEO and BeiDou-2. They will be illustrated through their history, components, theory of operation, and stages of modernization. Space Based Augmentation Systems (SBAS) as WAAS, EGNOS, MSAS, CWAAS, SNAS, GAGAN, SDCM and NIGCOMSAT-1 will be explained through their components, theory of operation and available accuracy. Global Space Based Augmentation Systems (GSBAS) as OmniSTAR, StarFire and VueStar will be investigated through their components and their theory of operation. Ground-Based Augmentation Systems (GBAS) as Local Area Differential GPS, Wide Area Differential GPS and LAAS will be explained through their components and the theory of operation and available accuracy. Regional Navigation Satellite Systems

(RNSS) as BeiDou-1, QZSS and IRNSS will be also shown via their components and the theory of operation and available accuracy. Finally, the used receivers and their modernization will be illustrated.

Chapter (3) consists of a detailed description of Remote Sensing Technology; Passive Remote Sensing Technologies and Active Remote Sensing Technologies, Satellite Orbits, Image Resolution, Scanner Sensor Systems, Digital image and their processing, Satellite platforms from two categories, Optical land imaging satellites and Radar land imaging satellites and applications of Remote Sensing. In this chapter the most common optical land imaging satellites in Egypt will be presented.

Chapter (4) consists of a detailed description of basic gravity field quantities, Gravity field determination from satellite data, Satellite tracking, High-Low Satellite-to-Satellite Tracking (hl-SST) as CHAMP, Low-Low Satellite-to-Satellite Tracking (ll-SST) as GRACE, Satellite Gradiometry as GOCE and Satellite Altimetry. In this chapter, the components and the theory of operation, applications of the above systems will be explained in details. Global gravity field models from the CHAMP, global gravity field models from GRACE, combined global gravity field models from CHAMP and GRACE, combined global gravity field models from GRACE, LAGEOS and Surface Gravity Data, are illustrated.

Chapter (5) presents the proposals which could be achieved by those satellite missions separately or integrated in different fields of applications in Egypt.

Chapter (6) contains the practical part of this research which is using supervised classification techniques for producing recent soil map for northern Sinai Peninsula from Landsat TM-5 medium resolution image. Then the obtained results will be analyzed and checked out against a reference geological map of northern Sinai Peninsula.

Chapter (7) summarizes the basic work performed in this research. Then, the important conclusions as deduced from the obtained results will be given. Also, some recommendations based upon the extracted conclusions for both the preformed work herein and for future researches connected with the subject matter, will be stipulated.

Chapter 2

Positioning Satellites

Introduction

The use of satellites for surveying purposes first became a practical reality with the development of the Transit system by the United States Navy [www.gs.rmit.edu.au/commimg/Surveying%20using%20the%20GNSS.pdf]. It is launched in 1958. It became operational in 1964 and was made available to civilian users in 1967 [Kulkarni, M., 2000]. The Transit system used Doppler measurements from six satellites arranged in six polar orbits to determine position and trajectory. The orbits of the six satellites form a circular birdcage effect with an orbital altitude approximately 1100 km above the surface of the Earth Figure (2-1).

The system was used for geodetic surveying applications in the 1970's and 1980's. However, due to the limited number of satellites, positioning was performed by observing for long periods. The low altitude of the satellites also meant that satellites were not visible at all times and gaps of 90 minutes between satellite passes Table (2-1). Typically, several satellite passes were required to position marks accurately on the ground.

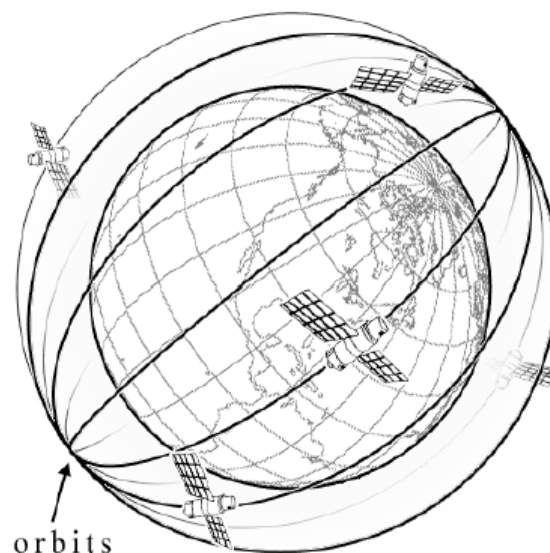


Figure (2-1): Transit Configuration.

The primary limitations of the Transit system that have been rectified in the development of GPS include the ability to now observe 24 hours per day and to coordinate features to a higher accuracy. The former has been achieved by increasing the number of satellites, the latter by placing the GPS satellites in significantly higher orbits than the Transit satellites [www.gs.rmit.edu.au/comming/Surveying%20using%20the%20GNSS.Pdf].

Table (2-1): Illustrate Important Elements of Transit
[www.gmat.unsw.edu.au/snap/work/2005/cr36-05proj.pdf]

	TRANSIT
No. of Satellites	6
Altitude	1,100 km
Accuracy	$20 \text{ cm} < x < 25 \text{ m}$
Satellites necessary to get a position	1
Time between Position Determination	$\geq 1 \text{ hour}$
Time taken to complete one orbital cycle	1hour 47 mins
Transmission Freq	F1 = 150 MHz F2 = 400 MHz
Navigation data	2D : X, Y

In the near future, there could be as many as four global navigation satellite systems (GNSS) and three regional navigation satellite systems (RNSS) [Dempster,A.,2007].

Global Navigation Satellite Systems (GNSS) is the generic name given to navigation systems which use satellite positioning. There are currently two active global navigation satellite systems: the American Global

Positioning System (GPS) and the Russian GLONASS system [*Francois, R., 2007*]. Third global positioning system, Galileo, is under development by the European Union through the European Space Agency. It is expected to be fully operable from 2012 with up to 30 satellites orbiting the earth broadcasting on 4 frequencies. A fourth global positioning system, the COMPASS Navigation Satellite System, is under development in China. GNSS is used to determine precise latitude, longitude and altitude by tracking signals from satellites [*NovAtel, 2006*].

In addition to these global systems, regional geostationary systems and global systems are used to complement the GPS or GLONASS constellations. These additional systems are known as Regional Space Based Augmentation Systems (RSBAS). The current active RSBAS are EGNOS in Europe, WAAS in the USA and MSAS in Japan (system under validation, IOC in 2007). Several other RSBAS systems are now in study or development phase for the coverage of other regions (GAGAN in India, CWAAS in Canada and SNAS in China [*Francois, R., 2007*], Nigeria is also planning NIGCOMSAT [*Dempster, A., 2007*].

Russia is also planning SDCM, this is a Wide-area system (Russia) [www.unoosa.org/pdf/icg/2007/algeria/01.pdf]. There are other systems already active known as Global Space Based Augmentation Systems (GSBAS), for example OmniSTAR, StarFire and VueStar [*Kemppi, p., 2007*], and Ground based augmentation systems (GBAS).

China launched Beidou-1, which was the first Regional Navigation Satellite System (RNSS), Japan tried to solve the urban canyon problem by planning their own regional augmentation to GPS: the Quasi-Zenith Satellite System (QZSS) and India proposed the Indian RNSS (IRNSS) [*Dempster, A., 2007*].

2.1 Global Navigation Satellite Systems (GNSS)

2.1.1 Navigation System with Time And Ranging (NAVSTAR)

The first Navstar satellite was launched in 1978 with the system being declared operational in 1989 although the full satellite constellation was not completed until 1994. The system requires twenty-four satellites (twenty-one operating and three spare) *[Soanes,C.,2004]*.

The NAVSTAR milestones can be stated as follows:

- 1973 – Program began
- 1978 – Developmental satellites began launch
- 1989 – Operational satellites began launch
- 1993 – Initial Operational Capability
- 1994 – ICAO Council accepted the GPS SPS to support the need of international civil aviation
- 1995 – Full Operational Capability
- 2000/05/01 – SA turned off *[Chou,H., 2006]*.

2.1.1.1 The GPS System Design

GPS system design consists of three main parts:

A. Space Segment

B. Control Segment

C. User Segment

The following is explanation of each segment:

The Space Segment (SS) is composed of the orbiting GPS satellites or Space Vehicles (SV) in GPS parlance. The GPS design calls for 24 SVs to be distributed equally among six circular orbital planes Figure (2-2). The orbital planes are centered on the Earth, not rotating with respect to the

distant stars. The X planes have approximately 55° inclination (tilt relative to Earth's equator) and are separated by 60° right ascension of the ascending node (angle along the equator from a reference point to the orbit's intersection). Orbiting at an altitude of approximately 20,200 kilometers orbital radius of 26,600 km, each SV makes two complete orbits each sidereal day, so it passes over the same location on Earth once each day. The orbits are arranged so that at least six satellites are always within line of sight from almost any where on Earth [<http://geodesy.eng.ohio-state.edu/course/gs609/>].

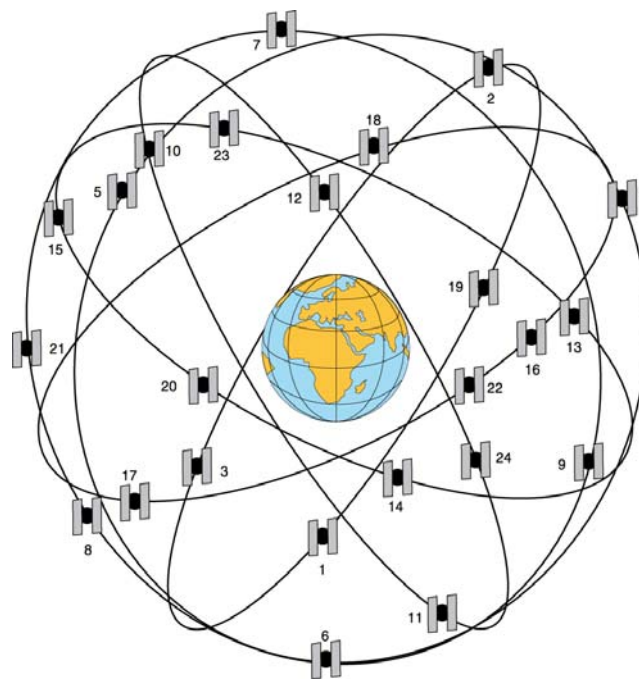


Figure (2-2): Schematic View of the Orbit Paths of the GPS.

Types of GPS satellites, past, current and proposed are as follow:

Block I

- Vehicle numbers (SVN) 1 through 11
- Launched between 1978 and 1985
- Concept validation satellites
- Developed by Rockwell International

- Circular orbits
- Inclination 63 deg
- One Cesium and two Rubidium clocks
- Design life of 5 years (not operational)

Block II

- Vehicle numbers (SVN) 13 through 21
- Launched between 1989 and 1990
- Developed by Rockwell International
- Nearly circular orbits
- Inclination 55 deg
- Two Cesium and two Rubidium clocks
- Design life of 7.3 years
- AS/SA capabilities (not operational)

Block IIA

- Vehicle numbers (SVN) 22 through 40
 - Launched since 1990 (total of 19)
 - Developed by Rockwell International
 - Nearly circular orbits
 - Inclination 55 deg
 - Two Cesium and two Rubidium clocks
 - Design life of 7.3 years
 - AS/SA capabilities
[<http://geodesy.eng.ohio state.edu/course/gs609/>]
 - Status of Block IIA in 11 January 2008 is 13 healthy satellites
[Crews,M.,2008].
-

Block IIR

- Vehicle numbers (SVN) 41 through 62
- Total of 13(1 unsuccessful) as of January 2005
- Operational replenishment satellites
- Developed by Lockheed Martin
- Nearly circular orbits
- Inclination 55 deg
- One Cesium and two Rubidium clocks
- Design life of 7.8 years
- AS/SA capabilities
[<http://geodesy.eng.ohio state.edu/course/gs609/>]
- Status of Block IIR in 11 January 2008 is 12 healthy satellites
[Crews,M.,2008].

The satellites of Block IIA and IIR send the standard GPS signal. i.e the Coarse/Acquisition (C/A) code on the L1 band (1575.42 MHz) and the P(Y) code (only for DOD-authorized user) on the L1 and L2 (1227.60 MHz) band. The modernization of the GPS system began in 2005 with Block IIR-M *[Eissfeller et. al.,2007].*

Block IIR-M

- First IIR-M launched in 25 September 2005
- 8 Satellites
- SPS signals: L1C/A, L2C
- PPS signals: L1-L2P(Y), L1-L2M
- Status of Block IIR-M in 11 January 2008 is 5 healthy satellites

Block IIF

- Scheduled for launch in 2009

- 12 Satellites
- 2 Rubidium and 1 Cesium clock
- 12 year design life
- SPS signals: L1C/A, L2C, 3rd civil signal (L5)
- PPS signals: L1-L2P(Y), L1-L2M [*Crews, M., 2008*].

Block III

- Scheduled for launch in 2014
- New code on the L1 frequency (the so-called L1C),
- Increased accuracy
- Signal integrity
- Search and Rescue [*Crews, M., 2008*].

A. Control Segment

The Control Segment of GPS consists of:

Master Control Station: The master control station, located at Falcon Air Force Base in Colorado Springs, Colorado, is responsible for overall management of the remote monitoring and transmission sites. GPS ephemeris being a tabulation of computed positions, velocities and derived right ascension and declination of GPS satellites at specific times, replace "position" with "ephemeris" because the Master Control Station computes not only position but also velocity, right ascension and declination parameters for eventual upload to GPS satellites Figure (2-3).

Monitor Stations: Six monitor stations are located at Falcon Air Force Base in Colorado, Cape Canaveral, Florida, Hawaii, Ascension Island in the Atlantic Ocean, Diego Garcia Atoll in the Indian Ocean, and Kwajalein Island in the South Pacific Ocean. Each of the monitor stations

checks the exact altitude, position, speed, and overall health of the orbiting satellites. The control segment uses measurements collected by the monitor stations to predict the behavior of each satellite's orbit and clock. The prediction data is up-linked, or transmitted, to the satellites for transmission back to the users. The control segment also ensures that the GPS satellite orbits and clocks remain within acceptable limits. A station can track up to 11 satellites at a time. This "check-up" is performed twice a day, by each station, as the satellites complete their journeys around the earth. Noted variations, such as those caused by the gravity of the moon, sun and the pressure of solar radiation, are passed along to the master control station.

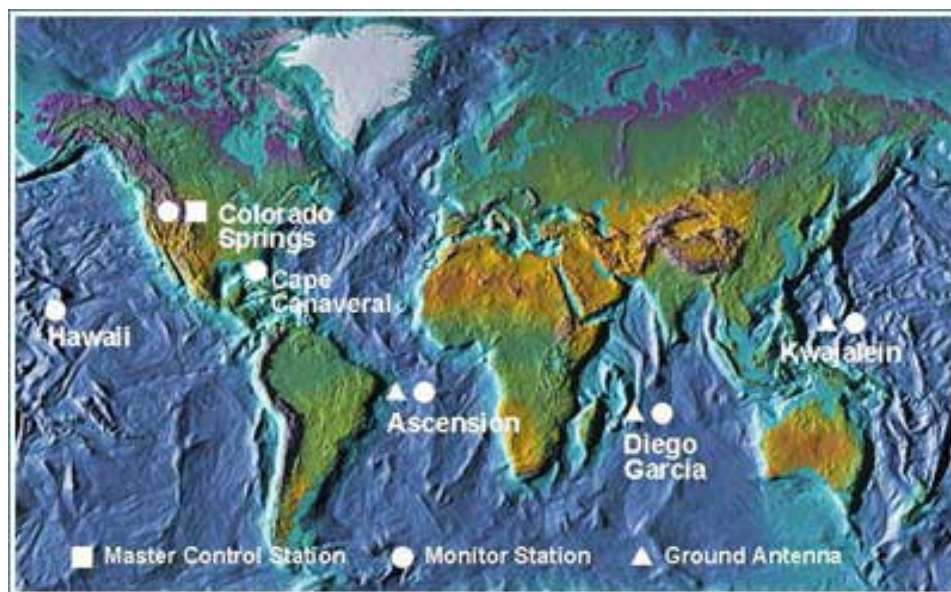


Figure (2-3): Location of the control segment of the GPS satellite navigation system.

Ground Antennas: Ground antennas monitor and track the satellites from horizon to horizon. They also transmit correction information to individual satellites.

[www.faa.gov/about/office_org/headquarters_offices/ato/service_units/t echops/navservices/gnss/gps/controlsegments].

B. User Segment

The User Segment refers to who use the signals generated by the GPS satellites some of which are described below:

- 1. Military:** GPS allows accurate targeting of various military weapons including cruise missiles, tanks, vehicles, submarines, ships, precision-guided munitions and etc, as well as improved command and control of forces through improved locational awareness.
- 2. Navigation:** GPS is used by people around the world as a navigation aid in cars, airplanes, and ships. Personal Navigation Devices (PND) such as hand-held GPS is used by mountain climbers and hikers.
- 3. Location-based services:** GPS functionality can be used by emergency services and location-based services to locate mobile phones. Assisted GPS is a GPS technology often used by the mobile phone because it reduces the power requirements of the mobile phone and increases the accuracy of the location obtained.
- 4. Road and Highways:** GPS can be used to route the traffic effectively to avoid congestion on the busy highways in conjunction with GIS.
- 5. Aviation:** Aviators use Global Positioning System (GPS) to increase the safety and efficiency of flight
- 6. Marine:** GPS provides the fastest and most accurate method for mariners to navigate, measure speed, and determine location. This enables increased levels of safety and efficiency for mariners worldwide
- 7. Environment:** GPS when coupled with GIS can provide better data which can be very helpful in predicting and reacting to the environment conditions.

8. **Surveying:** More costly and precise receivers are used by land surveyors to locate boundaries, structures, and survey markers, and for road construction
9. **Agriculture:** GPS Machine Guidance is used for tractors and other large agricultural machines.
10. **Public Safety and Disaster Relief:** Time plays an important part in the rescue operations to be effective after the disaster. Knowing the precise location of landmarks, streets, buildings, and disaster relief sites reduces that time and saves lives. GPS has made accurate data available easily [*Prinja,R.,1997*].

2.1.1.2 How GPS Works

A. Trilateration: The basis of GPS is ‘triangulation’ or ‘trilateration’ using satellites. It is a method of determining the relative positions of objects using the geometry of triangles. By accurately measuring our distance from three satellites we can "triangulate" our position anywhere on earth. This can be illustrated in Figure (2-4)

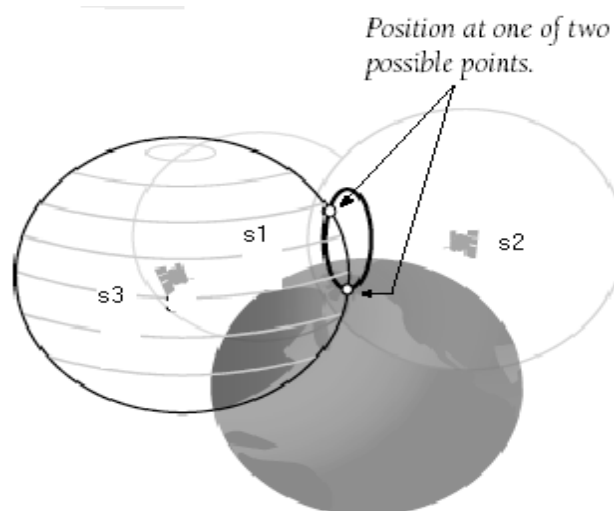


Figure (2-4): Position is calculated from distance measurement.

S1, S2 and S3 are three satellites and User represents a GPS user on earth's surface. In a diagram shown above, the intersection of 3 circles

is a collection of points but when this diagram is extrapolated to 3-dimensional surface; it can be found that 3 spheres intersect at 2-points. By measuring distance from another satellite (S4), the accurate position of the user on earth can be found as geometrically distances from 4 spheres will intersect at only one point.

B. Measuring Distance: Distance to a satellite is determined by measuring how long a radio signal takes to reach the receiver from that satellite. Multiply that travel time by the speed of light gives the distance.

a. Each satellite in the message it sends, includes the time (T1) at which it sends message based on the atomic clock inside the satellite. When the signal hits the receiver, that time T2 is noted. T2-T1 gives the total time (T) taken by the signal in space.

b. Speed of light is taken to be 2.997925×10^8 m/sec

c. Distance = Speed X T (in meters)

C. Getting Perfect Timing: Accurate timing is the key to measuring distance to satellites. Satellites are accurate because they have atomic clocks on board. Since atomic clocks are very costly, receivers generally have quartz clock but it looks at signals coming from four satellites and gauges its own accuracy. The receiver calculates the necessary adjustment in its clock that will cause the four spheres (as described in # A) to intersect at one point. Based on this, it resets its clock to be in sync with the satellite's atomic clock. The receiver does this constantly whenever it's on, which means it is nearly as accurate as the expensive atomic clocks in the satellites.

D. Satellite Positions: To use the satellites as references for range measurements, their exact positions are required to be known. GPS

satellites are so high up that their orbits follow the same designated path almost all the times. Minor variations in their orbits are measured by the Department of Defense and the error information is sent to the satellites, to be transmitted along with the timing signals.

E. Error Corrections: Finally the delay of the signals has to be corrected. The delay in the signal in turn affects the distance calculation and hence the calculation of the triplet (longitude, latitude, altitude) [*Prinja,R.,2003*].

2.1.1.3 Denial of Accuracy and Access

There are two primary methods for denying unauthorized users full use of the Global Positioning System. The first is Selective Availability (SA) and the second is Anti-Spoofing (A-S).

A. Selective Availability (SA)

Selective Availability, the intentional degradation of positioning accuracy, was discontinued by presidential directive on 1 May 2000 and there is no intent to ever use SA again. The SA feature allows the intentional introduction of errors into the satellite's navigation data to prevent unauthorized users from receiving full system accuracy. The errors can come from altering the satellite's atomic clocks (dithering) or altering the orbital data in the satellite's navigation messages (epsilon) or a combination of the two. The epsilon error in satellite position roughly translates to a like position error in the receiver. Encrypted correction parameters are included in the navigation signals that allow PPS receivers with the correct crypto keys to remove the SA errors from the navigation data. SA was originally activated on 4 July 1991. For almost ten years national policy set the level of SA to limit SPS accuracy to the 100 meter

(95 percent) specification. Now that SA is set to zero (it's always turned on), the SPS accuracy is 10-20 meters (95 percent) Figure (2-5).
[\[www.aa.washington.edu/courses/aa420/references/GPS_intro_2.pdf\]](http://www.aa.washington.edu/courses/aa420/references/GPS_intro_2.pdf)

Termination of Selective Availability

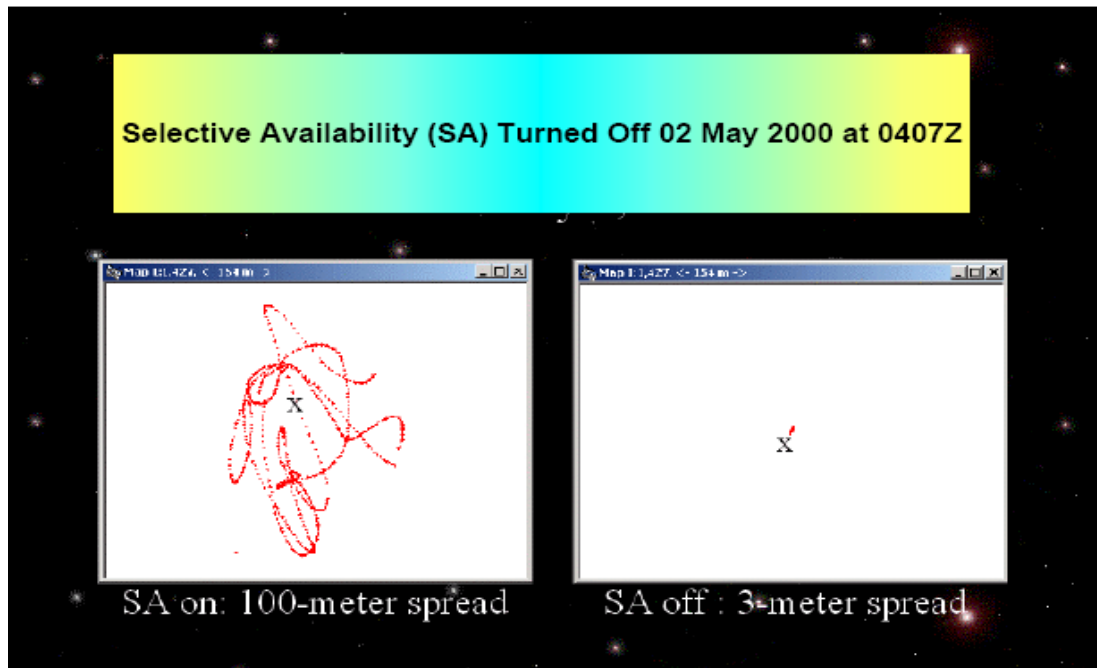


Figure (2-5): Effect of the Selective Availability on any position.

[After, Alan Zor. ,2002].

B. Anti-Spoofing (AS)

A-S is meant to negate hostile imitation of the GPS signals (i.e., fake satellite transmissions) by encrypting the P-code into the Y-code. Otherwise, the false transmissions could lead to false position solutions. The encrypted code is usually referred to as the P(Y) code. The A-S feature was activated when the system became operational. To decrypt the P(Y) code back into usable P-code, a GPS receiver must have special decryption device. The first generation device was called the Auxiliary Output Chip (AOC). An improved device called the PPS Security Module came next. A receiver that has the ability to decrypt the SA

correction parameters or the P(Y) code or both is considered to be a PPS receiver. SPS receivers, by definition, have neither SA nor A-S decryption capability.

[www.aa.washington.edu/courses/aa420/references/GPS_intro_2.pdf]

2.1.1.4 Techniques for Deployment

Deployment and collection techniques may be separated into two general categories: absolute positioning and relative (including differential) positioning. Within each of these categories there are code-based solutions and carrier phase-based solutions.

Background on GPS Positioning Accuracies

The accuracies which can be achieved by any of the following techniques are based on two values: Dilution of Precision (DOP) and User Equivalent Range Error (UERE). DOP is essentially a measure of the strength of the trilateration figure used to estimate the receiver position and receiver clock bias. It generally varies smoothly as the satellites move through space but exhibits extreme changes as satellites rise above and drop below the horizon Figure (2-6). DOP can be reported in several forms, the most common of which is Position Dilution of Precision, or PDOP. PDOP is a measure of the precision of the estimated three-dimensional coordinates of the receiver and is the most frequently used. However, most systems are capable of reporting Horizontal DOP (HDOP) and Vertical DOP (VDOP) as well. Other measures of precision include Time DOP (TDOP), which predicts the precision of the receiver clock offset estimate and Geometric DOP (GDOP) which takes into account both position and time. These various DOP measures are often used in mission planning because they can be computed for any given

past or future location and time based only on the approximate satellite ephemeris [Tullis, J et al., 2005].

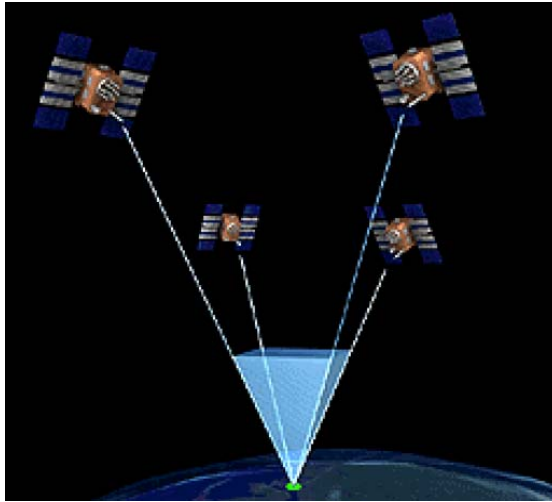
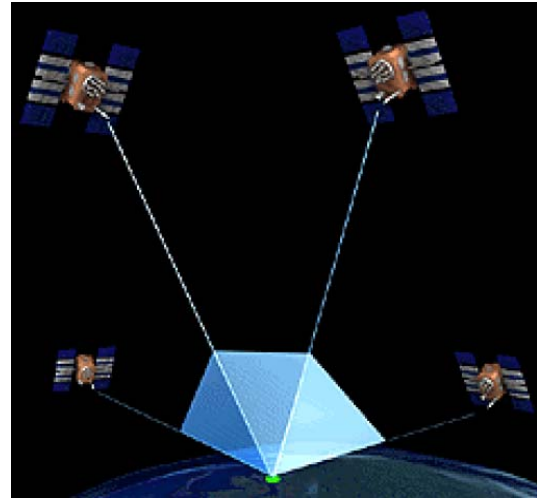


Figure (2-6): Bad GDOP



Good GDOP

UERE is the estimated precision of a single pseudorange measurement from a receiver to a satellite it also varies with time as the atmosphere and noise characteristics of the signal and receiver change. The contribution of various error sources such as tropospheric and ionospheric delays, clock errors, receiver noise, ephemeris errors, and multipath all contribute to the UERE Table (2-2) [Tullis, J et. al., 2005].

Table (2-2): Estimates of Standard Position System (SPS) User Equivalent Range Error (UERE) [After, Tullis, J et. al., 2005].

Error Source	User Range Error Contribution (meters)
Tropospheric delay	0.25
C/A Code phase bias	0.27
Orbit	1.20
Receiver noise	0.80
Satellite clock bias	1.43
Ionospheric delay	5.00
UERE (95%)	8.95

The relationship between a position solution, range error, and dilution of precision (DOP) can be approximated as:

$$\mathbf{S}_{\text{position}} = \mathbf{S}_{\text{range}} \times \mathbf{DOP} \quad (2-1)$$

Where $\mathbf{S}_{\text{position}}$ is the precision at the 95% confidence level of the position, $\mathbf{S}_{\text{range}}$ is the range error or 95% UERE, and \mathbf{DOP} is dilution of precision. If, for example, the UERE is estimated to be 5 meters, and the observed Horizontal Dilution of Position (HDOP - Northing and Easting only) is 2.0, then the horizontal positional precision is estimated to be 10 meters. Most processing software utilizes this or similar formulas to predict absolute positional accuracies [Tullis, J et. al., 2005].

A. Absolute Positioning

Absolute positioning refers to the use of a single receiver using code or carrier phase measurements to determine a position estimate. The position estimate may be the result of a single observation, as is the case of a moving vehicle or of multiple observations in which a receiver is set up over a stationary position. The following sub-section illustrates the absolute positioning based on code or carrier phase measurements.

1. Code-Based Absolute Positioning

Code-based absolute positioning is the technique envisioned by the designers of GPS in which a single low-cost receiver is used to determine a three-dimensional coordinate somewhere on the surface of the earth. It is the simplest, least expensive, and least accurate of all GPS techniques. Two services are provided by the system for absolute positioning, the Standard Positioning Service (SPS) and the Precise Positioning Service (PPS). The C/A code is the only observable of the Standard Positioning Service – the only code-based absolute positioning service currently available to civilians. Prior to May 2, 2000, the UERE associated with the

SPS was approximately 25 meters due the effects of Selective Availability (SA). Without SA, the UERE associated with SPS is around 5 meters so that, depending on the satellite configuration (measured by the DOP values), SPS now provides instantaneous horizontal accuracies (with 95% confidence) in the 10 to 20 meter range. Vertical accuracies are generally 1.7 to 2.1 times worse than horizontal accuracies. The Precise Positioning Service (PPS) is available to users with access to the P(Y) code. The UERE associated with the PPS is in range of 1-2 meters and can thus provide real-time horizontal accuracies in the 2-5 meter range depending on the DOP at observation time. PPS is also much more resistant to jamming and spoofing. In the case of both SPS and PPS, multiple estimates of the same position may be recorded and averaged (or more likely incorporated into the least-squares adjustment) for slightly improved precision.

2. Carrier-Based Absolute Positioning

Absolute positioning using L1 and L2 carrier phase measurements requires very long observation times (as long as several hours) to obtain a precise position estimate. This is due to the number of observations and changing satellite geometry required to determine the integer ambiguity. This technique is often used for geodetic measurements in which receivers can be positioned and observe for hours and even days, undisturbed. Various filtering techniques applied to the resulting time series (in x, y, and z) can detect velocities in the mm/year range (as in geologic movements) [Tullis, J et. al., 2005].

B. Relative Positioning

Relative positioning refers to a number of techniques which use two or more receivers simultaneously observing the same satellites (a minimum

of four) to improve the accuracy of a computed position. Code-based solutions of this type are commonly known as Differential GPS, or DGPS. Carrier phase-based solutions of this type determine the relative position – or base line vector – between two receivers. The following sub-section illustrate the relative positioning based on code or carrier phase measurements [*Tullis, J et. al., 2005*].

1. Code-Based Relative Positioning

The degraded accuracy caused by Selective Availability (SA) contributed to the development of relative positioning techniques which use two or more receivers to negate the effects of SA. Because many of the error sources that contribute to UERE are similar over tens of kilometers (especially ionospheric delays), it is possible to use measurements from two receivers to achieve better accuracies. One receiver (the base station) is placed on a known position and set to observe pseudoranges of all satellites in view. Another receiver (the rover) travels to points of interest and also observes pseudoranges from at least four of the same satellites. While the base station observes the satellite constellation the receiver position estimate is compared to the known point at individual epochs. The vector between the known and estimated position at each point in time may be used in one of two ways to improve the position of the rover as long as the base and rover observe at least four common satellites at the given epoch. The most straight-forward method is to apply the vector directly to the rover's position. The more common (and more accurate) method is for the base station to use the known coordinates to compute pseudorange corrections to each satellite at each epoch. The corrections presumably account for the various contributions to UERE and are applied to the pseudorange observations of the rover. These code based techniques can increase post-processed accuracy to anywhere from 0.5 to

5.0 meters for SPS users depending on the geometry of the network and the distance between the rover and base. Typically rover-base separations of up to 100 km can yield the accuracies cited above. Some software is capable of integrating more than one base station in the solution. This not only tends to increase accuracy, but perhaps more importantly, provides redundant data that can eliminate poor observations at the rover and or base station.

In fact, this type of code base solution resembles the survey-like deployments and processing described in the next section. If both the rover and base record and store pseudoranges (almost no navigation receivers are capable of this), no communication between these receivers is required since the differential corrections may be applied as a post-processing step.

Many base stations across the world upload their observation data to an internet server and make it available for a fee or for free to users in the area. Many of these base stations are from the networks of Continuously Operating Receiver Sites (CORS) managed by the National Geodetic Survey. If a real-time radio link is available then the corrections may be applied immediately in the field. This can be important for certain problems in which one must navigate to a known set of coordinates or precisely navigate in real-time such as in a narrow waterway. In 1985 the Radio Technical Commission for Maritime Services proposed a standard for the transmission of correction data via radio links. The RTCM format is now provided as an option by virtually all manufacturers of real-time DGPS solutions. Real-time solutions are generally less accurate than post-processed solutions because of the latency of the radio link. It can take as long as two seconds for the receiver to receive and process the signal from the base and in that time the conditions affecting UERE can

change. In fact, most real-time, code-based systems don't modify pseudoranges but simply apply a vector offset to the receiver position as described above. A more recent development in DGPS is the deployment of Wide-Area Differential GPS networks. Rather than using a single base station to compute pseudorange corrections, WADGPS systems employ a network of base stations scattered across a much larger area of operation. Observations from these base stations are used to compute a regional set of corrections which are either stored for post-processing or, more typically, broadcast to users with receivers equipped to read the correction signal [Tullis, J et. al., 2005].

2. Carrier-Based Relative Positioning

To achieve the high level of accuracy required for most surveying applications it is necessary to use the carrier phase observable. Relative positioning using the carrier phase observable can provide positional information to centimetre - millimetre level accuracy if the appropriate survey techniques are used. These techniques include the following: [www.gs.rmit.edu.au/commimg/Surveying%20using%20the%20GNSS.pdf].

a. Static

This method requires relatively long observation times (at least one hour and often as many as 8 – 10 hours). Observation time requirements depend on available satellite geometry, baseline length, and accuracy. This method can achieve sub-centimeter baseline accuracies. Both single and dual frequency carrier phase receivers can be used.

b. Rapid Static

This method is slightly less accurate for determining baselines (centimeter level) but does not require long observation times. In fact, 5-20 minute occupation times are possible over short baselines and the rover can lose lock on one or all satellites in transit between occupation sites. Typically, only dual frequency receivers can be used for this method because of their ability to combine L1 and L2 carriers into a signal for which the integer ambiguities are easier to resolve.

c. Kinematic

This technique allows for positioning a moving rover (briefly stopping at an occupation site or even in continuous motion) within the centimeter-level relative to the base. However, this technique requires an initialization (resolution of all integer ambiguities) of the rover by various methods such as setting the rover and base on a known baseline, “On-the-Fly” ambiguity resolution, antenna swap, and others.

d. Pseudo-Kinematic

This method does not require an initialization period but does require that occupation sites be visited twice. Five to ten minute visits separated by at least one hour allowing sufficient satellite geometry change are relied upon to resolve the integer ambiguities. Maintaining lock on all satellites throughout the survey is not required. Centimeter accuracies are possible with this technique.

e. Real-Time Kinematic (RTK)

Equipment requirements for this method are more extensive; in addition to base and rover receivers a high frequency radio transmitter is

necessary. However, it delivers very high performance with baseline accuracies at the centimeter level in real time. A brief initialization period is required to establish the integer ambiguity to each satellite (5-10 minutes) and the rover must retain lock on all satellites while moving from site to site. If lock is lost, the rover must be reinitialized (usually only 2-5 minutes depending on the distance to the base and the number of integers lost). RTK solutions typically allow baselines of up to 10 km Table (2-3) (although baseline accuracy deteriorates with baseline length) and are usually limited by the power of the data link radio [*Hofmann-Wellenhof, et. al., 2001 and Leick, 2005*].

Table (2-3): Carrier Phase Tracking Techniques

*[www.usace.army.mil/publications/eng-manuals/em1110-1-1003/c
5.pdf]*

Concept	Minimum Requirements	Applications	Accuracy
Static (Post-processed)	L1 or L1/L2 GPS receiver 30 min to 1 hour minimum observation time	Control surveys (high-accuracy) Slow point positioning	Sub-centimeter
Rapid Static (Post-processed)	L1/L2 GPS receiver 5-20 min observation time Single occupation only No continuous satellite lock required	Control surveys (medium to high accuracy)	Sub-centimeter
Stop-and-Go Kinematic (Post-processed)	L1 GPS receiver Initialization required 1-2 minute baseline occupation Continuous satellite lock required	Control surveys (Medium accuracy) Fast point positioning	Centimeter +
Pseudo Kinematic (Post-processed)	L1 GPS receiver 5-10 minutes static observations Double occupations required between 1 and 4 hours No initialization required Loss of satellite lock permitted	Control surveys (Medium accuracy)	Few centimeters
Real-Time Kinematic (Real-time)	L1/L2 GPS Receiver Data-Link required Baselines should be < 10 km OTF initialization or conventional initialization Maintain satellite lock	Real-time hydro tides and heave corrections Location surveys Photo control (ABGPS) Real-time topo Construction stake out (Medium to high accuracy)	Centimeter +

2.1.1.5 GPS Modernization

The US has embarked on a program of GPS Modernization to provide better accuracy and more powerful and secure signals from future GPS satellites. While there are a range of planned improvements, noteworthy are the extra signals to be broadcast by the modernized GPS satellites:

- An improved code (instead of the current L1 C/A-code) on the L2 frequency of GPS (the so-called L2C) is being implemented to enable civilian receivers to better account for ionospheric error, as well as to be more immune to RF interference and multipath. The first Block IIR-M satellite to broadcast L2C was launched 26 September 2005,

the second was launched on 25 September 2006, and the third on 17 November 2006 [*Rizos,C.,2007*]. Status of Block IIR-M in 11 January 2008 is 5 Healthy Satellites [*Crews,M.,2008*]. The launch schedule to replace existing satellites is difficult to predict but full operational capability for L2C will not be declared until all 24 satellites in the constellation are broadcasting the new signal, and that is not expected to occur until 2013 or beyond.

- The radio spectrum for the L2 signal is not fully ‘protected’ through the International Telecommunications Union (ITU), as it does not lie in the ITU’s Aeronautical Radio Navigation Services band (the L1 frequency does). This means that L2C cannot be relied upon for so-called safety of life applications such as navigation to aid civil aviation. Therefore a third civil frequency at 1176.45MHz (the so-called L5) is planned for launch on the Block IIF satellites [*Rizos,C.,2007*]. The first Block IIF satellite launch is scheduled for 2009[*Crews,M.,2008*], Figure (2-7), with Full Operational Capability (FOC) of L1-L2-L5 GPS satellites i.e 24 satellites, unlikely until 2015 at the earliest.
- GPS-III will incorporate the extra L2 and L5 signals of the Block IIR-M and Block IIF satellites, as well as a new code on the L1 frequency (the so-called L1C), which will be compatible with GALILEO’s L1 signal. However, to preserve ‘backward compatibility’ with legacy user equipment, all current and planned GPS Block II signals will also be broadcast. The 30 GPS-III satellites are planned for launch from about 2013 until 2017.

The implications for GPS user equipment is that low-cost receivers may not just be L1-only, as is currently the case, but they may be L2-only or L5-only, or even dual-frequency. (e.g. L1-L5). However, top-of-the-line

user equipment for centimeter-level accuracy will take advantage of Triple-Carrier Ambiguity Resolution (TCAR) based on L1-L2-L5 pseudorange and carrier phase observations [Rizos, C., 2007].

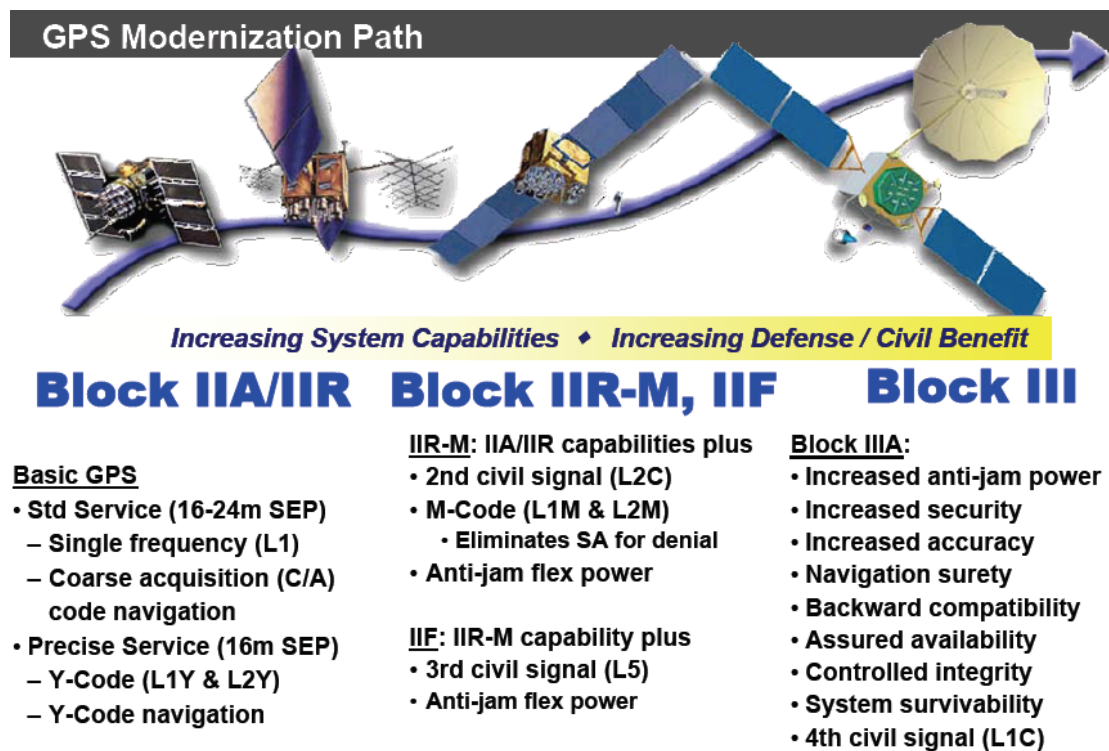


Figure (2-7): GPS Modernization Path [After, Pat Norris, 2006].

2.1.1.6 Goals of Modernization

A. Civil Goals (SPS)

o C/A Code Transmitted on L2 1227.6 MHz

Currently, Block II/IIA and Block IIR NAVSTAR GPS satellites transmit the civilian C/A code on the L1 frequency, and the military P(Y) code on both the L1 and L2 frequencies. The new Block IIR-M satellites will transmit the same signals as the previous two blocks, but will also have a new signal, called L2C, on the L2 frequency. L2 has a carrier frequency of 1227.60 MHz. L2C has two codes, the moderate length code (CM) and the long code (CL). The CM code carries data while the CL is the pilot

signal. The CM code is 10,230 chips long and repeats every 20 milliseconds. The CL code is 767,250 chips long and repeats every 1.5 second. The L2C and L1C/A codes ensure that there are always two accessible civilian codes *[NovAtel,2006]*.

◦ **C/A Code Transmitted on New L5 Carrier (1176.45 MHz)**

Civilian use signal, broadcast on the L5 frequency (1176.45 MHz) and planned to be available with first GPS IIF launch (2009) *[Crews,M.,2008]*.

The following can be gained:

- Improves signal structure for enhanced performance
- Higher power than L1/L2 signal (~3db, or twice as powerful)
- Longer spreading codes (10x C/A)
- Aeronautical Radionavigation Services band

◦ **New Civilian L1 (L1C)**

Civilian use signal, broadcast on the L1 frequency (1575.42 MHz), which currently contains the C/A signal used by all current GPS users. The L1C will be available with first Block III launch, currently scheduled for 2013.

[http://en.wikipedia.org/wiki/GPS_modernization]

B. Military Goals (PPS)

◦ **New M-Code on L1 and L2**

Major component of the modernization process, a new military signal called M-code was designed to further improve the anti-jamming and secure access of the military GPS signals. The M-code is transmitted in the same L1 and L2 frequencies already in use by the previous military code, the P(Y) code.

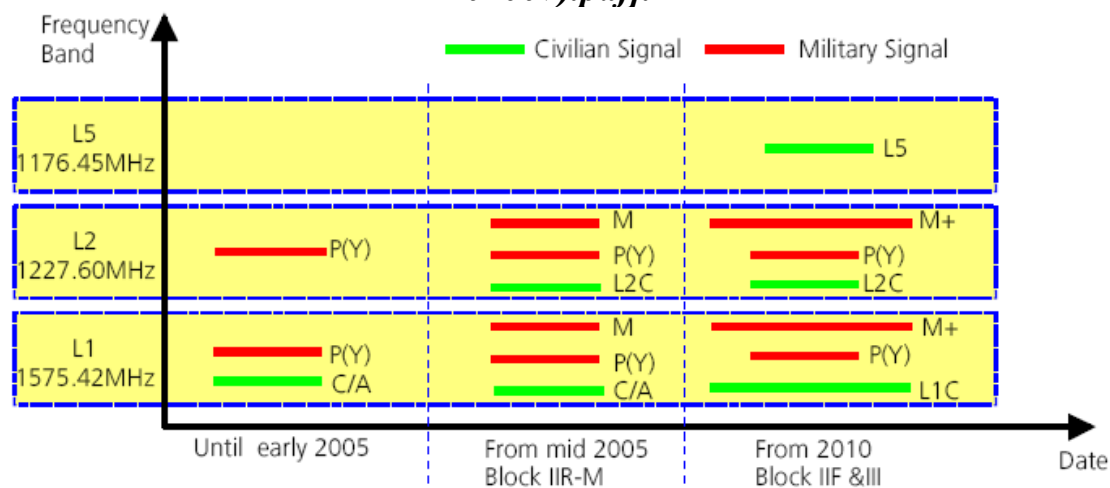
The new signal is shaped to place most of its energy at the edges (away from the existing P(Y) and C/A carriers). Unlike the P(Y) code, the M-code is designed to be autonomous; meaning that a user can calculate the position using only the M-code signal. Users of the P(Y) code must typically first lock onto the C/A code and then transfer to lock onto the P(y)-code. In a major departure from previous GPS designs, the M-code is intended to be broadcast from a high-gain directional antenna, in addition to a full-Earth antenna. This directional antenna's signal, called a spot beam, is intended to be aimed at a specific region (several hundred kilometers in diameter) and increase the local signal strength by 20 db, or approximately 100 times stronger.

A side effect of having two antennas is that the GPS satellite will appear to be two GPS satellites occupying the same position to those inside the spot beam. While the full-Earth M-code signal is available on the Block IIR-M satellites, the spot beam antennas will not be deployed until the Block III satellites are deployed, tentatively in 2013 Table (2-4).

[http://en.wikipedia.org/wiki/GPS_modernization].

Table (2-4): With Modernization the availability of GPS frequencies will be increased

[[http://telecom.tlab.ch/~zogg/Dateien/GPS_Compendium\(GPS-X-02007\).pdf](http://telecom.tlab.ch/~zogg/Dateien/GPS_Compendium(GPS-X-02007).pdf)].



C. Ground Control Modernization

The main features of the ground control after modernization are:

- New Master Control Station with:
 - Improved operator interfaces
 - IIR-M capabilities
 - Integrated Mission Operations Support Center
- Legacy Accuracy Improvement Initiative
 - Information from additional reference stations:
 - Doubles amount of data being used for signal integrity and constellation performance monitoring Figure (2-8)
 - Doubles amount of data used for satellite time and position estimation, resulting in more accurate satellite orbital position and clock data available to user [Miller, J. J.,2006].

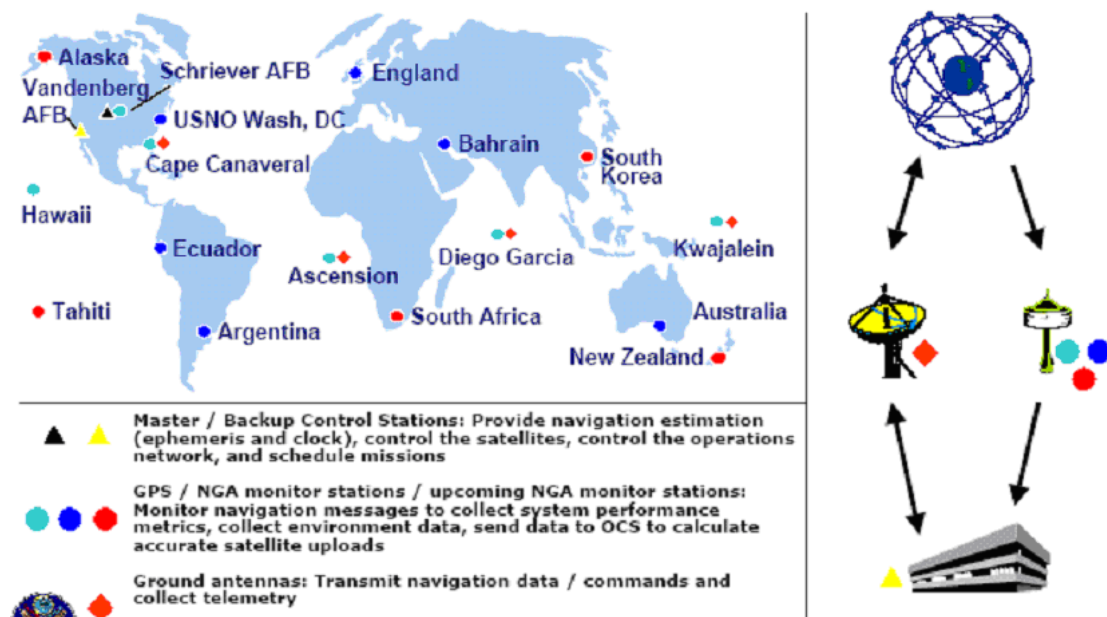


Figure (2-8): Ground Control Segment Expansion.

[<http://pnt.gov/public/2006/2006-06-zambia/ken2.ppt>]

2.1.1.7 GPS Signals

Each GPS satellite carries a cesium and/or rubidium atomic clock to provide timing information for the signals transmitted by the satellites. Internal clock correction is provided for each satellite clock. Each GPS satellite transmits two spread spectrum, L-band carrier signals—an L1 signal with carrier frequency $f_1 = 1575.42$ MHz and an L2 signal with carrier frequency $f_2 = 1227.6$ MHz. These two frequencies are integral multiples $f_1 = 154f_0$ and $f_2 = 120f_0$ of a base frequency $f_0 = 10.23$ MHz. The L1 signal from each satellite uses binary phase-shift keying (BPSK), modulated by two pseudorandom noise (PRN) codes in phase quadrature, designated as the C/A-code and P-code. The L2 signal from each satellite is BPSK modulated by only the P-code [*Mohinder, S., 2001*].

- **Navigation Message**

A 50 Hz navigation message is superimposed on both the P(Y) code and the C/A-code. The navigation message includes data unique to the transmitting satellite and data common to all satellites. The data contain the time of transmission of the message, a Hand Over Word (HOW) for the transition from C/A-code to P(Y)-code tracking, clock correction, ephemeris, and health data for the transmitting satellite, almanac and health data for all satellites, coefficients for the ionospheric delay model, and coefficients to calculate UTC [*Lindstrom, G., Gasparini, G., 2003*].

2.1.1.8 GPS Receivers

Overall, there are three different types of GPS terminals, categorised according to the code they can acquire:

- C/A (SPS) receiver: which are available to the wider public for civilian applications

- C/A (PPS) receiver: used exclusively by military personnel
- Direct P(Y) military receivers: these last generation military receiver does not have to go through the C/A signal to track the P(Y) signal. Once all military personnel have access to direct P(Y) receivers, military commanders can switch off the C/A signal on the battlefield without fear of a negative repercussion for friendly military forces [*Lindistrom, G., Gasparini, G., 2003*].

2.1.1.9 Coordinate System

The details displayed and calculations made by a GNSS receiver primarily involve WGS-84 (World Geodetic System 1984) reference system. The WGS-84 coordinate system is geocentrically positioned with respect to the center of the earth. Such a system is called ECEF (Earth Centered, Earth Fixed).

The positive X- axis of the ellipsoid Figure (2-9) lies on the equatorial plane and extends from the centre of mass through the point at which the equator and the Greenwich meridian intersect (the zero meridian).

The Y- axis also lies on the equatorial plane and is offset 90° to the east of the X- axis.

The Z- axis lies perpendicular to the X and Y- axis and extends through the geographical North Pole.

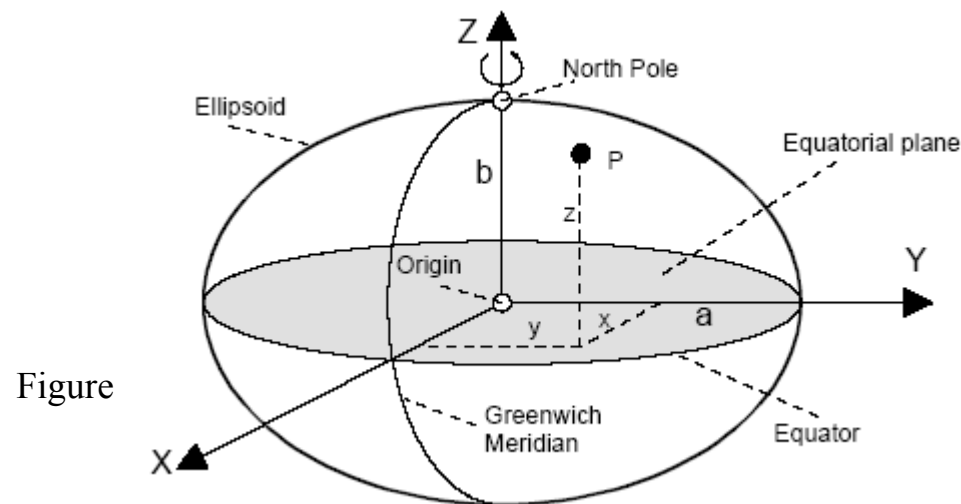


Figure (2-9) WGS-84 Reference Ellipsoid

Parameter of WGS-84 Reference Ellipsoids

Semi major axis a (m)	Semi minor axis b (m)	Flattening (1:)
6,378,137.00	6,356,752.31	298,257223563

[[http://telecom.tlab.ch/~zogg/Dateien/GPS_Compendium \(GPS-X-02007\).pdf](http://telecom.tlab.ch/~zogg/Dateien/GPS_Compendium%20(GPS-X-02007).pdf)]

2.1.1.10 GPS Constellation Status at (11.01.2008)

GPS Constellation Status as of 11 January 2008 is 30 Healthy Satellites (Baseline Constellation: 24)

- 13 Block IIA satellites operational
- 12 Block IIR satellites operational
- 5 Block IIR-M satellites operational
- Most Recent Launch

–IIR-18(M) – 5th modernized SV, Launched Wednesday, 20 December 2007 and set healthy on 2 Jan 08[Crews,M.,2008].

2.1.2 Global Navigation Satellite System (GLONASS)

The other GNSS Russian system is called GLONASS, a system similar in operation to GPS. GLONASS was started in 1982 and declared operational in 1996, and initially for the civilian user. GLONASS was more precise than that of GPS as it was not degraded in any way. GLONASS uses L1 at 1602MHz, However, unlike GPS, each satellite broadcasts the same PRN, but on a unique frequency. This is the carrier offset by satellite modifier multiplied by 0.5265MHz. The GLONASS system requires twenty four satellites to function accurately. However, due to funding problems, following the break up of the Soviet Union, the system was at one time reduced to about seven satellites. New funding appears to have been allocated and the launch program has been restarted [Soanes,C., 2004].

The GLONASS milestones, can be stated as follows:

- 1970 – Program began
- 1982 – Developmental satellites began launch
- 1990 – Operational satellites began launch
- 1994 – Initial Operational Capability
- 1996 – ICAO Council accepted the GLONASS to support the needs of international civil aviation
- 2010 – Full Operational Capability [Chou,H., 2006].

2.1.2.1 The GLONASS System Design

GLONASS system design consists of three segments explained in the next titles;

A. Space Segment

A complete GLONASS constellation consists of 24 satellites, including three spares, traveling in three orbital planes at height of 19,100 kilometers. The satellites orbit the earth with a period of 11 hours and fifteen minutes at an inclination of 64,8 degrees with respect to the equator Figure (2-10). Through this relatively high inclination, a fully operational GLONASS would provide a better coverage of the poles than GPS. In the earlier years the lifespan of each satellite is relatively short at about three years, requiring a large number of replacement satellites. The current and next generation satellites, including the GLONASS-M, GLONASS-K, and GLONASS-KM are expected to increase both lifespan and transmission power [www.iss-eu.org/occasion/occ44.pdf].

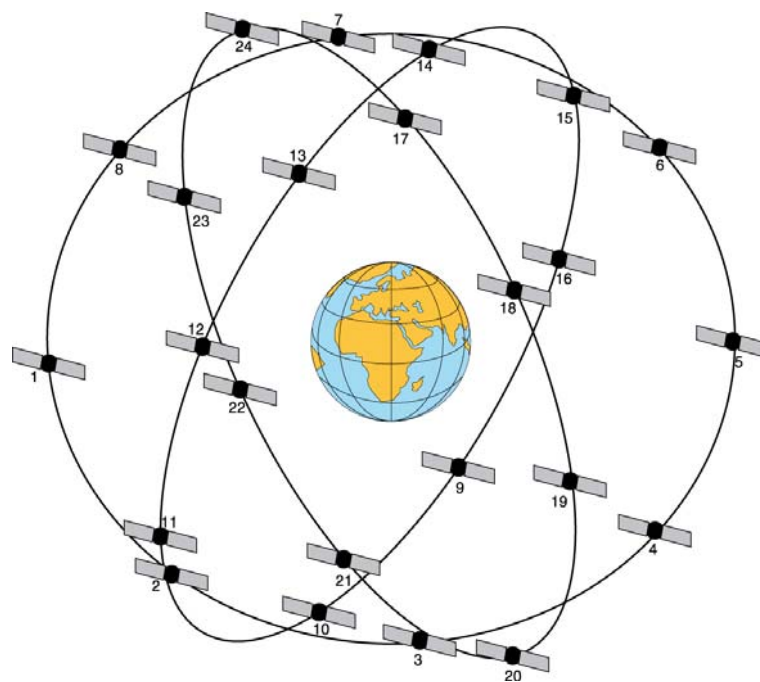


Figure (2-10): GLONASS Satellite Constellation

The GLONASS constellation, past, current and proposed are as follow:

There have been different versions of the GLONASS satellites launched so far and there have also been plans for updated versions in the future.

The following sub-section illustrates the first launches of GLONASS satellites, GLONASS-M, GLONASS-K and GLONASS-KM.

- **Block I:** One year expected lifetime. Ten satellites launched of 1982 to 1985,
- **Block IIa:** One year expected lifetime, new time and frequency standards and increased frequency stability by an order of a magnitude. Six satellites launched of 1985 to 1986,
- **Block IIb:** expected lifetime of two years, twelve satellites launched of 1987 to 1988,
- **Block IIc:** expected lifetime of three years. Since April 1991– enhanced radiation-hardening design, which suggests lifetimes up to approximately five years. Fifty one satellites launched of 1989 [*Borjesson, J. ,2000*].
- **GLONASS-M:** The new civil signal at L2 frequency band is already broadcasted by the GLONASS-M satellites. It is expected to provide higher positioning accuracy [*Kemppi,p.,2007*]. These satellites possess a substantially increased lifetime of seven years. Laser corner-cube reflectors are installed as aid for precise orbit determination and geodetic research. GLONASS satellites are equipped with Cesium clocks onboard to provide time and frequency standards [*Eissfeller et. al., 2007*]. This satellites launched since 2003 [*Rizos, C.,2007*].
- **GLONASS-K:** A third civil signal will be broadcasted by the GLONASS-K these satellites scheduled for launch in 2009. L3 signal will provide higher reliability and accuracy and is especially intended for safety-of-life applications as it will provide GNSS integrity

information to guarantee the reliability of the navigation service [Kempfi,p.,2007]. Ten years expected life time [Rizos,C.,2007].

- **GLONASS-KM:** Proposed to be available by 2025.

The following summarizes GLONASS space segment:

- The orbit period of each satellite is approximately 8/17 of a sidereal day such that, after eight sidereal days, the GLONASS satellites have completed exactly 17 orbital revolutions. A sidereal day is the rotation period of the Earth relative to the equinox and is equal to one calendar day (the mean solar day) minus approximately four minutes.
- Because each orbital plane contains eight equally spaced satellites, one of the satellites will be at the same spot in the sky at the same sidereal time each day.
- The satellites are placed into nominally circular orbits with target inclinations of 64.8 degrees and an orbital height of about 19,100 km, which is about 1,100 km lower than GPS satellites.
- The GLONASS satellite signal identifies the satellite and provides:
 - The positioning, velocity and acceleration vectors at a reference epoch for computing satellite locations
 - Synchronization bits
 - Data age
 - Satellite health
 - Offset of GLONASS time from UTC (SU) (formerly Soviet Union and now Russia)
- Almanacs of all other GLONASS satellites [NovAtel ,2006].

B. Control Segment

Spread throughout the former Soviet Union are a small number of GLONASS monitoring ground stations, the Command Tracking Stations (CTS) located in St. Petersburg, Ternopol, Eniseisk and Komsomolsk-na-Amure , see Figure (2-11). They are in contact with the System Control Center (SCC) in the Moscow area. This whole structure, CTS and SCC combined, together with Quantum Optical Tracking Stations (QOTS) – laser ranging stations, is referred to as the Ground-based Control Complex or GCC. Every CTS station tracks the GLONASS satellites in view and calculates satellite ranges and receives the satellite messages. These data give, together with radar ranging, an accuracy of some two to three meters in satellite orbit parameters. They are fed on to the SCC where clock corrections, satellite status messages and navigation messages are calculated and sent back to the CTS for upload to the satellites. Periodically the radar ranges measured by the CTS stations are calibrated by measurements using the satellite laser ranging equipment at the QOTS sites [*Borjesson,J., 2000*].

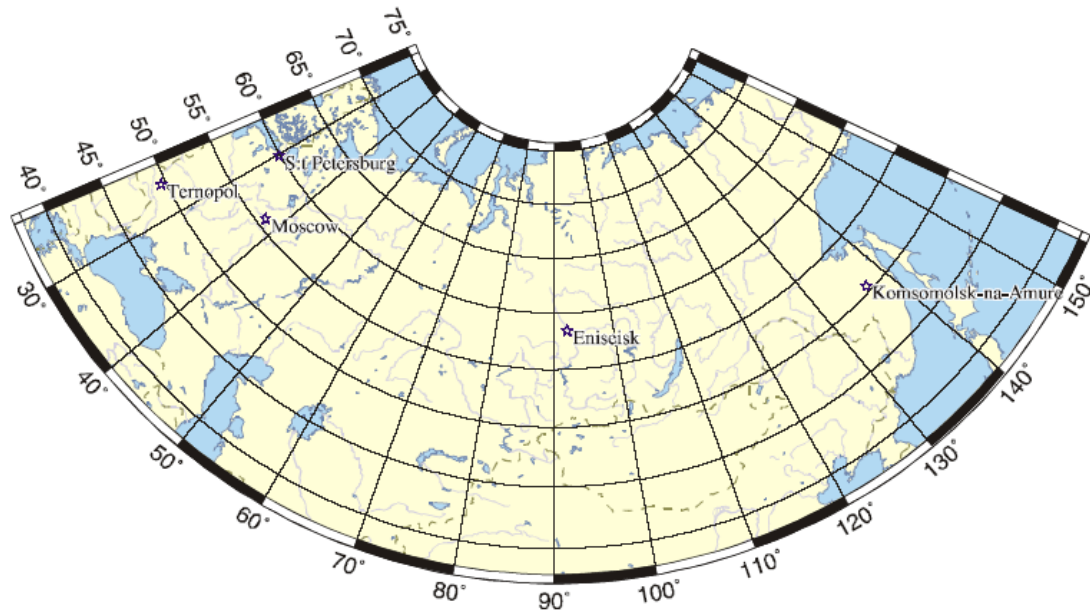


Figure (2-11) GLONASS Ground Control Network

[After, Borjesson, J., 2000].

C. User Segment

The user segment consists of equipment that tracks and receives the satellite signals. This equipment must be capable of simultaneously processing the signals from a minimum of four satellites to obtain accurate position, velocity and timing measurements. Like GPS, GLONASS is a dual military/civilian-use system. The system's potential civil applications are many and mirror those of GPS *[NovAtel, 2006]*.

2.1.2.2 GLONASS Signals

GLONASS, being a Frequency Division Multiple Access (FDMA) system, transmits on several different carrier frequencies. Each satellite transmits on two sub-bands, called L1 and L2, in the L-band region. The navigation signals are modulated onto the carrier using Bipolar Phase-Shift Keying (BPSK). The civil so called Standard Positioning Service (SPS) has a chip rate of 511 kbps and the other one is the secret military code known as Precise Positioning Service (PPS) with a ten time higher

chip rate of 5.11 Mbps, The nominal carrier frequencies for the L1 and L2 bands can be calculated from

$$f_{k1} = f_{o1} + k\Delta f_1 \quad (2-2)$$

$$f_{k2} = f_{o2} + k\Delta f_2 \quad (2-3)$$

Where K is a frequency number as used by GLONASS. The respective channel number for each satellite is transmitted within the almanac.

For L1 the values are $f_{o1} = 1602$ MHz and $\Delta f_1 = 562.5$ kHz while the L2 values are $f_{o2} = 1246$ MHz and $\Delta f_2 = 437.5$ kHz respectively. These carrier frequencies are derived aboard each satellite using the onboard frequency standards, usually of the cesium type [Borjesson, J., 2000].

GLONASS accomplishes system operation (24 satellites and only 12 channels) by having antipodal satellites transmit on the same frequency. Antipodal satellites are in the same orbit plane separated by 180 degrees in argument of latitude. This is possible because the paired satellites will never appear at the same time in view of an operational receiver that is on the Earth's surface see Figure (2-12) [NovAtel, 2006].

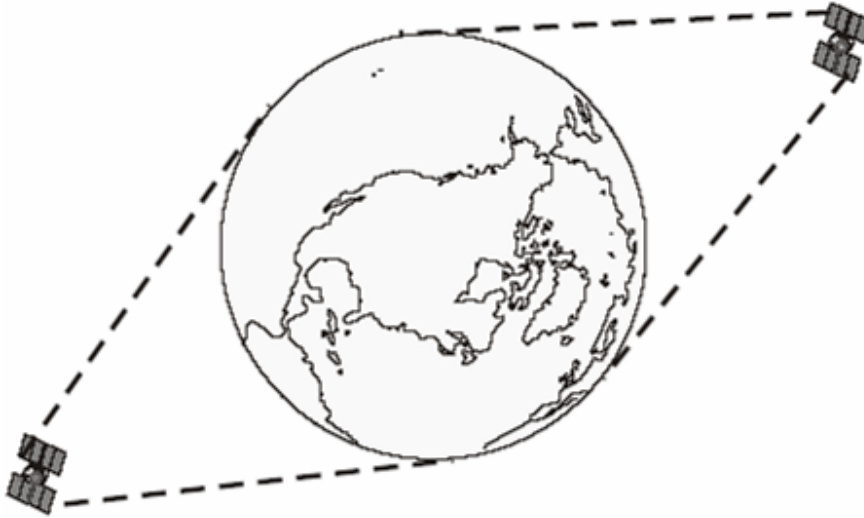


Figure (2-12): GLONASS Antipodal Satellites
[After, NovAtel, 2006].

A. Navigation Message

All GLONASS satellites transmit navigation messages with low bit rates as part of their normal signaling. This message provides users with the required information for positioning, timing and planning of measurement campaigns. The navigation message is structured as a superframe consisting of five subframes with 15 strings each. Each subframe of data consists of 15 strings and lasts for 30 s. Thus, the entire superframe takes 2.5 minutes to transmit before it is repeated again. The 15 strings in the subframes are divided into two parts; the first 5 strings, identical for all subframes, contain detailed ephemeris and clock information for the transmitting satellite. The latter 10 strings contains almanac information for the whole constellation where information for each satellite takes two strings leaving room for five satellites within each subframe and 25 satellites in the superframe [*Borjesson,J., 2000*].

- **Ephemeris Representation**

The most detailed part of the navigation message is the first five strings. These strings contain not only the information needed for calculating the transmitting satellite's position and velocity but also parameters for estimating the satellite's clock difference from the GLONASS system time together with one of the most important parameters, namely the health bit. The health bit signals if the satellite is "healthy" or not, i.e. if it is performing according to specifications. Note that this health bit is not generated in the satellite itself but is set by the ground control network. This means that if the satellite experience some kind of difficulty when not in sight of command tracking stations in Russia then the health bit will not be set to "unhealthy" until the satellite is in view from Russia and the malfunction is detected.

Hence it is useful to have knowledge about how old the data is. This is also provided with a parameter in the ephemeris message, namely the “age-of-data of ephemeris” [*Borjesson,J., 2000*].

- **Almanac Structure**

The almanac is the second part of the navigation message and it contains non-immediate data for the whole system, divided into three parts;

- Status almanac; giving the operating status of all satellites in the system.
- Phase almanac; giving coarse corrections of all onboard time scales compared to GLONASS system time.
- Orbital almanac; giving orbital parameters of all satellites.

Apart from this the almanac information also contains a term for the difference between UTC (Russia) and GLONASS system time [*Borjesson,J., 2000*].

2.1.2.3 Coordinate System

The GLONASS broadcast ephemeris describes a position of transmitting antenna phase, center of given satellite in the PZ-90 Earth-Centered Earth-Fixed reference frame defined as follows:

The Origin is located at the center of the Earth's body;

The Z-axis is directed to the Conventional Terrestrial Pole as recommended by the International Earth Rotation Service (IERS);

The X-axis is directed to the point of intersection of the Earth's equatorial plane and the zero meridian established by BIH;

The Y-axis completes the coordinate system to the right-handed one.

Geodetic coordinates of a point in the PZ-90 coordinate system refers to the ellipsoid which semi-major axis is 6378136 m and flattening is $1/298.257\ 839\ 303$ [www.glonass-ianc.rsa.ru/i/glonass/ICD02_e.pdf].

2.1.2.4 GLONASS Receivers

While GLONASS receivers were traditionally only available to military users, commercial receivers are available on the market today. Recent developments include a combined GLONASS/GPS multi-code and multi-channel receiver that can track both GPS and GLONASS signals. However, given an incomplete constellation, separate GLONASS receivers are not widely used due to low levels of accuracy, integrity and system availability [*Lindstrom, G and Gasparini, G., 2003*].

2.1.2.5 GLONASS Modernization Program

Since the collapse of the Soviet Union, the Russian Federation has struggled to find sufficient funds to maintain GLONASS and there were 10 satellites functioning (as opposed to the 24 necessary for FOC).

However, the Russian Federation has commenced a program to revitalize GLONASS [*Rizos, C., 2007*].

1. Continuous Global Navigation by 2010

- 24 satellites in constellation Figure (2-13)

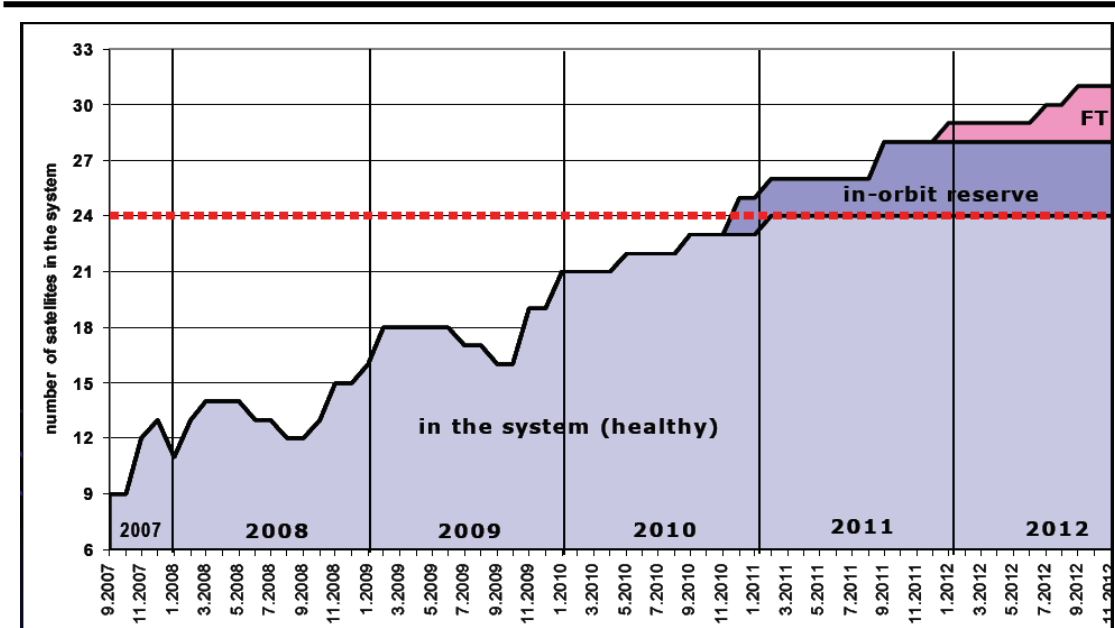


Figure (2-13): Prediction of The Satellite Amount in the Constellation Based on the Launch Program and Statistics [After, *Revnivkh,S.,2007*].

2. Ground Control Segment Modernization

- Monitoring station network extension (Russia) Figure(2-14)
- System time scale improvement
- Monitoring network outside Russia [*Revnivkh,S.,2007*].

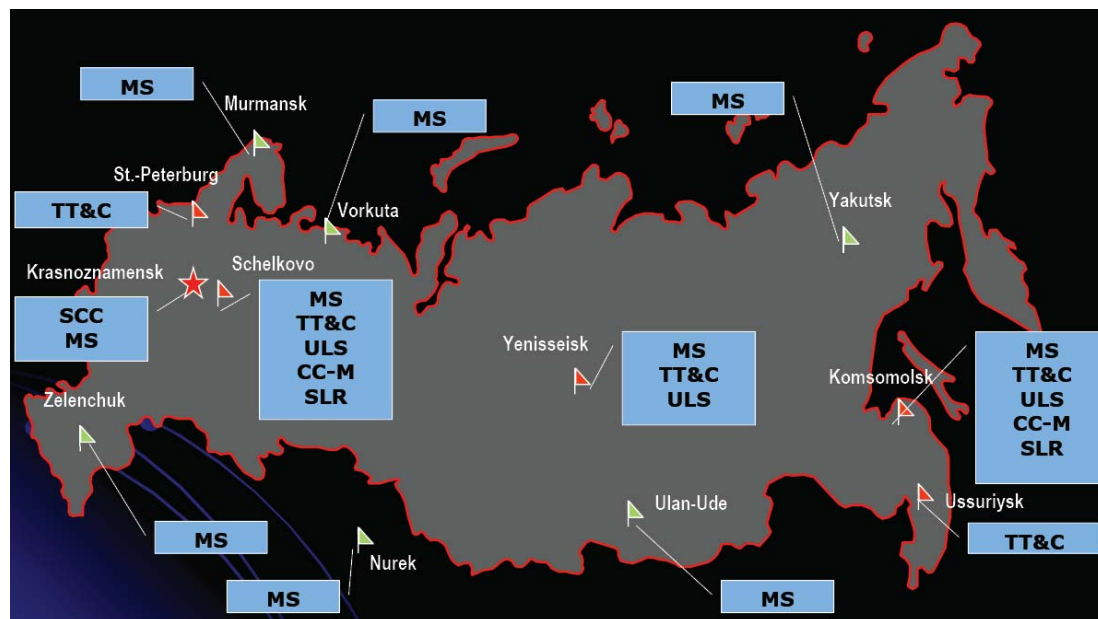


Figure (2-14): Ground Control Segment [After, Revnivykh, S., 2007].

3. GLONASS Accuracy Improvement Plan (AIP)

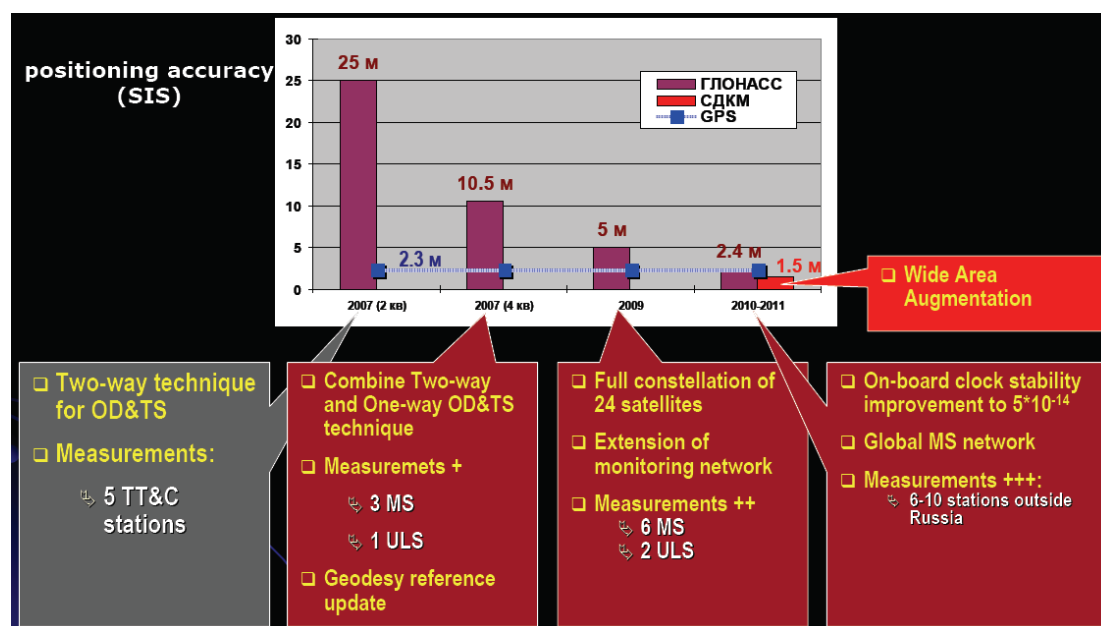


Figure (2-15): Illustrate GLONASS Accuracy Improvement Plan (AIP)

[After, Revnivykh, S., 2007].

4. Signal Modernization

- Second civil signal at L2 (since GLONASS-M in 2003)

Current activity centers on launching GLONASS-M satellites with an improved 7-year design lifetime, which broadcast the second civil signal at L2 frequency band (though not on the same frequencies as GPS). [*Rizos, C., 2007*].

- Third civil signal at L3 (since GLONASS-K in 2009-2010)

GLONASS-K satellites with improved performance, and which will also transmit a third civil signal known as L3 in the Aeronautical Radio Navigation Services band near (but not identical) to GPS's L5 frequency. A full constellation broadcasting three sets of civil signals is unlikely before the middle of the next decade.

Recently there has been discussion of at least the L1 frequency on the new GLONASS-K satellites being of a CDMA design, in order to make these signals compatible with GPS and GALILEO. Greater efforts are likely to be made in the future to increase the degree of interoperability of GPS and GLONASS (and GALILEO), by having frequency overlaps at the L1 and L5 bands, at the very least [*Rizos, C., 2007*].

5. Interoperability with GPS and Future GALILEO Geodesy System

- Geodesy System

Improved geodesy reference

A. Governmental Decision of 20 June 2007:

- PZ-90.02 implementation in GLONASS

- Further permanent improvement toward ITRF Figure (2-16)

B. New geodesy reference in GLONASS

- To be introduced at 20 September 2007

C. PZ-90.02 coordination to ITRF:

- No rotation, Delta X:-36 cm , Delta Y:+8 cm, Delta Z:+18 cm

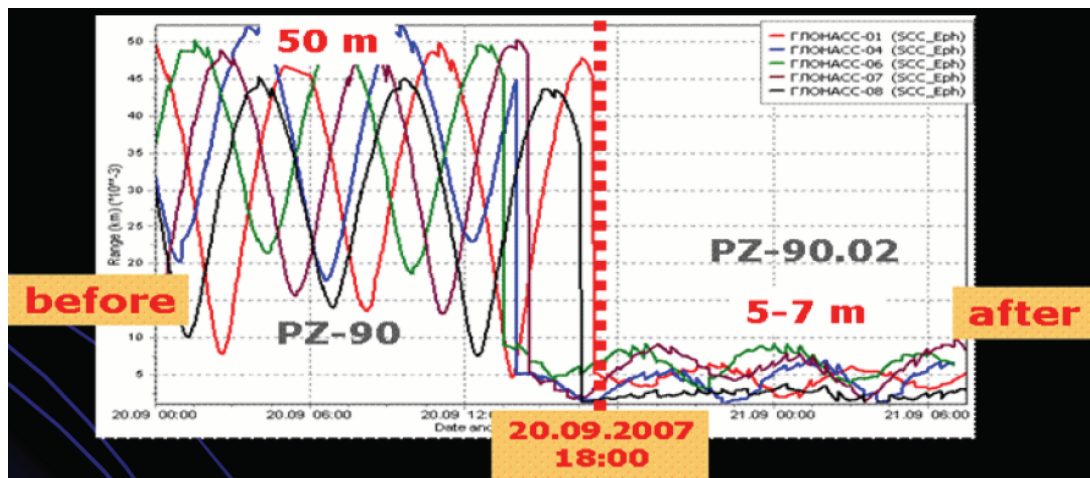


Figure (2-16): Difference of GLONASS Orbits (range) wrt. ITRF Before and After 20 December 2007/[After,Revnivkykh,S.,2007].

- Time system

Improved time reference

- GloST wrt. UTC (SU) <120 ns with accuracy 12 ns

6. Further modernization of GLONASS Based on New GLONASS-KM Satellite [Revnivkykh,S.,2007].

2.1.2.6 GLONASS Constellation Status at (21.09.2007)

In the 21th of September 2007, the GLONASS constellation consists of eleven satellites. GLONASS-M is seven satellites and four old GLONASS satellites. Healthy 9 satellites, one satellite in commissioning and one satellite in maintenance Figure (2-17) *[Revnivykh,S.,2007]*. And Figure (2-18) illustrate numbers of visible GLONASS satellites in 12 July 2007 for earth points *[Parkinson,B.,2007]*.

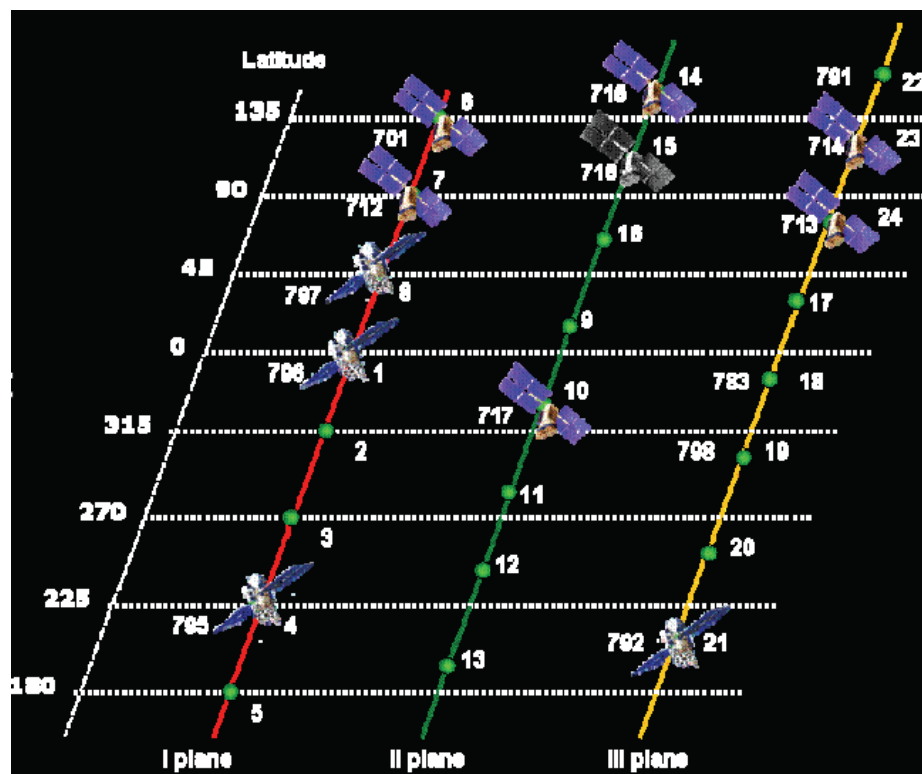


Figure (2-17) GLONASS Status at (21.09.2007)*[After, Revnivkykh, S., 2007]*

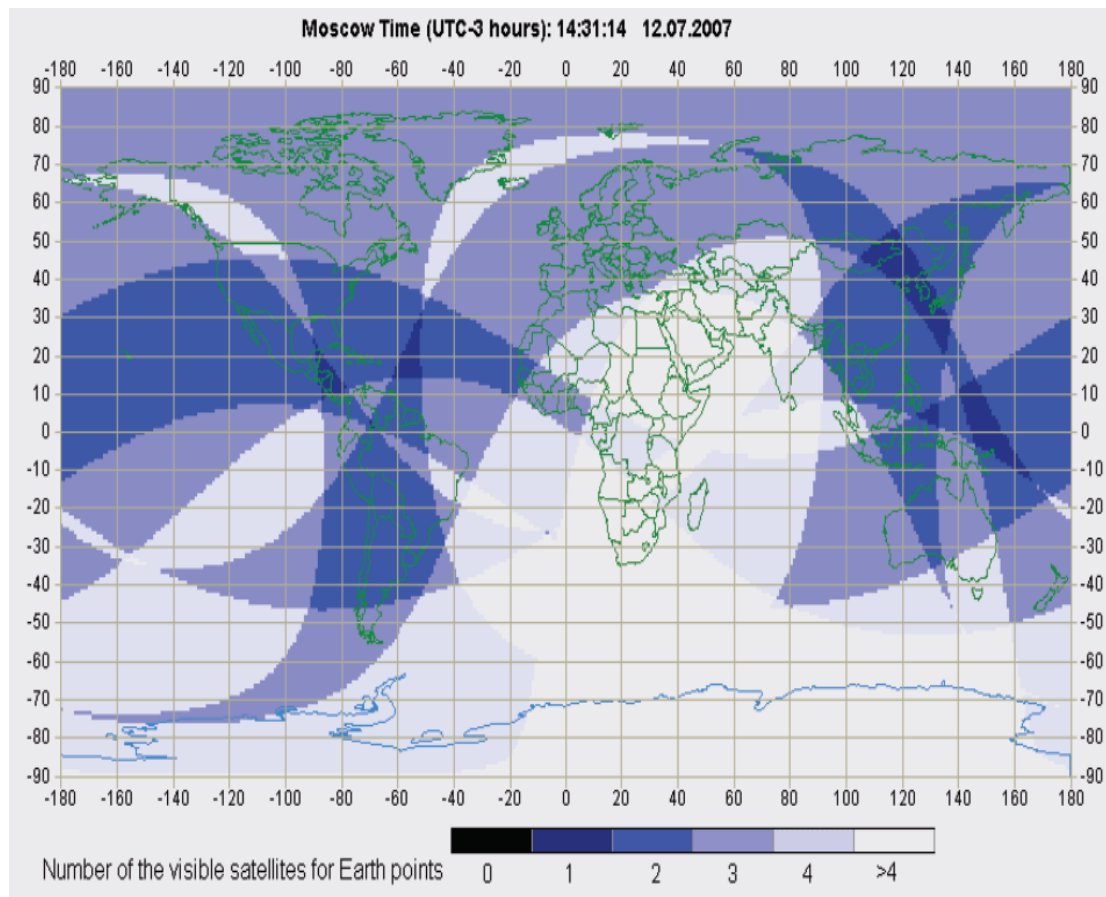


Figure (2-18): Numbers of Visible GLONASS Satellites for Earth Points
[After, Parkinson, B., 2007].

2.1.3 GALILEO

The European Union wants to become independent of GPS which is under control of the Department of Defense of the United States. Additionally the EU wants to profit from the growing market "Satellite based positioning and navigation " which today is dominated by US products and infrastructure. The final decision for funding and developing Galileo, however, was not taken until 26.03.2002 by the European Council of the Ministers of Transport. The reason for this delay was along discussion about the funding concept and therefore the decision who should lead the Galileo project. The result was a 20,9% funding of Germany, 17,0% of France, 16,0% of Great Britain and 15,2% of Italy, with one Control Centre and the headquarters of Galileo Industries in Germany and one Control Center in Italy. A major topic in the built-up of Galileo, which still was not clarified up to July 2007 is the so-called "public-private partnership" (PPP): A private company or a consortium of companies establish the Ground Segment, take responsibility for the launch of the 30 Galileo satellites and will then operate the final system [*Eissfeller et. al.,2007*].

2.1.3.1 The GALILEO System Design

GALILEO system design consists of three segments explained in the next titles;

A. Space Segment

- 30 satellites in three Medium Earth Orbit MEO planes at 23616 km altitude
- Walker 27/3/1 plus 3 in-orbit spares (1/plane) Figure (2-19)

- 1 satellites per orbital plane is a spare
- Inclination of orbital planes 56 degrees
- One revolution 14 hours 4 min
- Ground track repeat 10 days *[Berkes, U.,2002]*.

Once this is achieved, the Galileo navigation signals will provide a good coverage even at latitudes up to 75 degrees north, which corresponds to the North Cape, and beyond. The large number of satellites together with the optimization of the constellation, and the availability of the three active spare satellites, will ensure that the loss of one satellite has no discernible effect on the user *[NovAtel,2006]*.

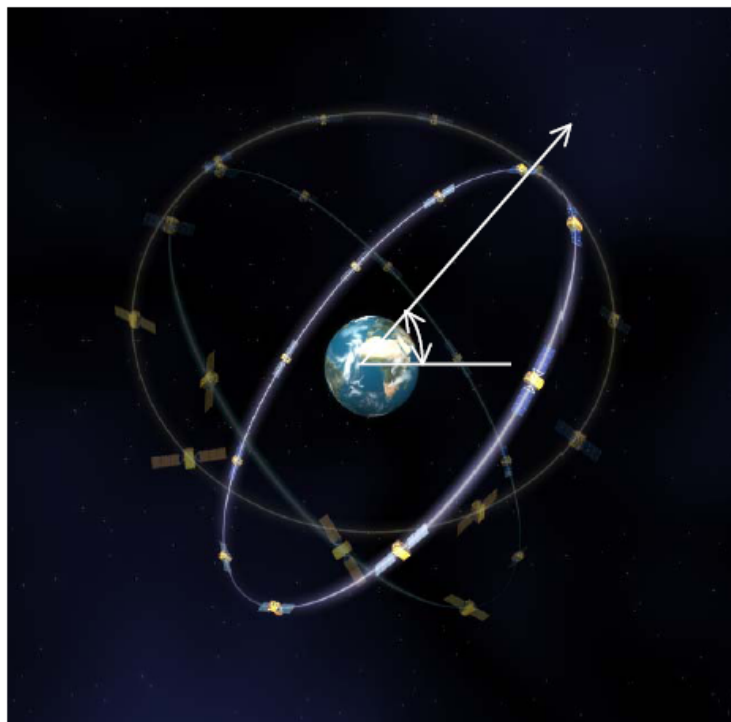


Figure (2-19): GALILEO Satellite Constellation.

B. Ground Segment

Two Galileo Control Centers (GCC) will be implemented on European ground to provide for the control of the satellites and to perform the navigation mission management. The data provided by a global network of 30-40 Galileo Sensor Stations (GSS) will be sent to the Galileo Control Centers through a redundant communications network. The GCC's will use the data of the Sensor Stations to compute the integrity information and to synchronize the time signal of all satellites and of the ground station clocks. The exchange of the data between the Control Centers and the satellites will be performed through so-called up-link stations. Five S-band up-link stations and 10 C-band up-link stations will be installed around the globe for this purpose Figure (2-20) [Dumesnil, N.,2007].

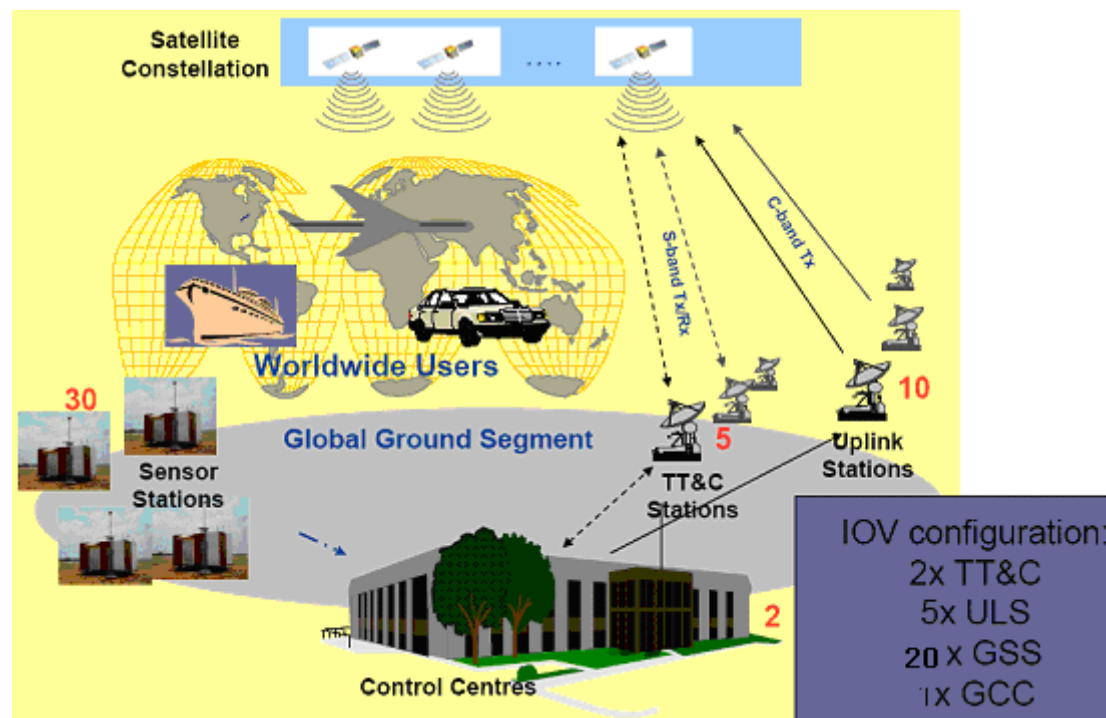


Figure (2-20): GALILEO Architecture [After, Peckham, R., 2006]

C. User Segment

The five categories of GALILEO service are as follows:

1. Open Service (OS)

The open service (OS) is an open, free basic service, which will provide position and timing performances competitive with other GNSS systems. It will be interoperable with GPS for the consumer mass market - personal communication and navigation, cars / motorcycles, trucks and buses, light commercial vehicles, personal outdoor recreation, games. All the targeted segments will require their low costs, low power consumption, small size, user friendly, and best performance for best price [*Dumesnil, N., 2007*].

2. Commercial Service (CS)

The CS service is intended for applications requiring performance higher than that offered by the OS. Users of this service pay a fee for the added value. CS is implemented by adding two additional signals to the OS signal suite, Table (2-5). The additional signals are protected by commercial encryption and access protection keys are used in the receiver to decrypt the signals. Typical value-added services include service guarantees, precise timing, ionospheric delay models, local differential correction signals for very high-accuracy positioning applications, and other specialized requirements [*Andrews, A. P., 2007*].

3. Safety of Life Service (SOL)

The Safety of Life Service allows similar accuracy as the Open Service but with increased guarantees of the service, including improved integrity monitoring to warn users of any problems [*Rizos, C., 2007*].

4. Public Regulated Service (PRS)

The Public Regulated Service (PRS) is to be available to EU public authorities providing civil protection and security (e.g. police, quasi-military), with encrypted access for users requiring a high level of performance and protection against interference or jamming

[Rizos,C.,2007].

5. Search And Rescue (SAR)

This is not a navigation service *[Francois, R.,2007]*, the SAR service will be used by humanitarian search and rescue services. Emergency transmitters and satellites enable the location of individual persons, crafts and vehicles in aviation, land and maritime emergencies. At the end of the 1970s the USA, Canada, the USSR and France developed a satellite system for the location of activated distress beacons. The system is referred to as SARSAT (Search And Rescue Satellite-Aided Tracking). The Russian name for the system is "COSPAS". The COSPAS-SARSAT system employs six LEO (Low Earth Orbit) and five GEO (geostationary) satellites. The GALILEO-SAR service is planned to expand and improve the existing COSPAS-SARSAT system in the following ways:

- Almost instantaneous reception of emergency calls from any location on earth (currently there are delays of an average of one hour).
- Exact determination of position of the distress beacons (to within meters instead of the current accuracy of 5 km).
- Improved effectiveness of the Space Segment through the availability of more satellites to overcome localized hindrances

during suboptimal condition (30 GALILEO satellites in medium orbitals will supplement the existing LEO and GEO satellites of the COSPAS-SARSAT system).

GALILEO will introduce a new SAR function; the distress signal reply (from the SAR operator to the emergency transmitter radio) will begin Figure (2-21). This should simplify rescue measures and reduce the number of false alarms.

The GALILEO SAR service will be defined in cooperation with COSPAS-SARSAT, with the characteristics and functions of the service being governed by the IMO (International Maritime Organization) and ICAO (International Civil Aviation Organization) [[http://telecom.tlab.ch/~zogg/Dateien/GPS_Compendium\(GPS-X-02007\).pdf](http://telecom.tlab.ch/~zogg/Dateien/GPS_Compendium(GPS-X-02007).pdf)].

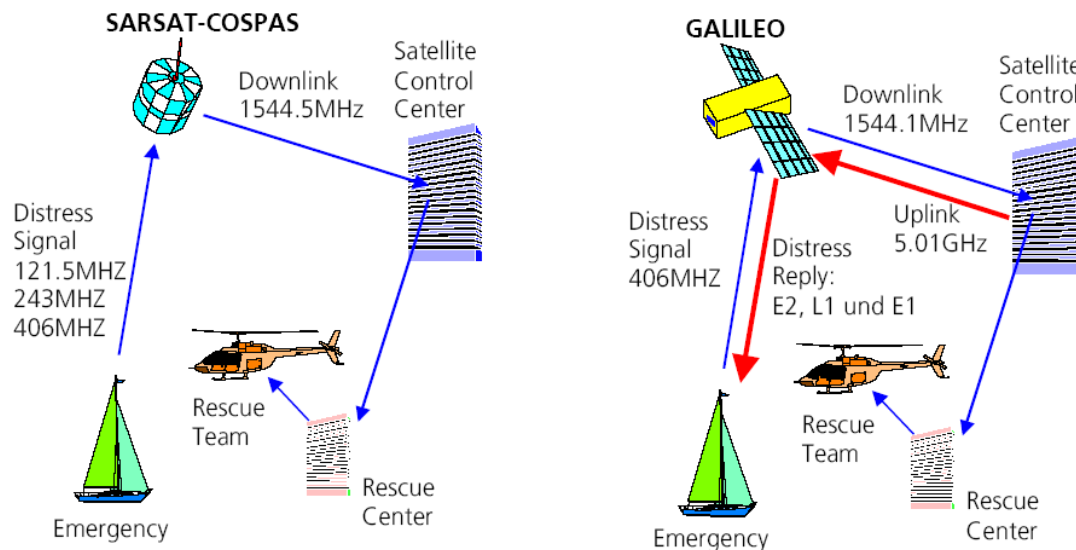


Figure (2-21): Unlike Sarsat-Cospas, GALILEO's Search and Rescue Service Also Provides A reply To the Distress Signal [[http://telecom.tlab.ch/~zogg/Dateien/GPS_Compendium\(GPS-X-02007\).pdf](http://telecom.tlab.ch/~zogg/Dateien/GPS_Compendium(GPS-X-02007).pdf)].

Table (2-5): Galileo Services, Benefits and Availability [After, Ludwig,D.,2007]








Service			Receiver	Benefits	Target user groups	Availability
Open Service	OS		Single frequency	<ul style="list-style-type: none"> Additional satellites for better multi-system coverage (e.g., deep urban) Coding and modulation advances for increased sensitivity and multi-path mitigation Pilot signal for fast acquisition 	Low end mass market (e.g., LBS, outdoor)	Open
			Double frequency	<ul style="list-style-type: none"> As above + increased accuracy with 2nd frequency 	High end mass market (e.g., car navigation, maritime)	Open
Commercial Service	CS		Double frequency	<ul style="list-style-type: none"> Increased accuracy using additional frequencies and signals Additional features under investigation (e.g., data rate capacity) 	Professional markets (e.g., surveying, precision agriculture)	Commercial basis
Safety of Life Service	SoL		Single frequency (Level B)	<ul style="list-style-type: none"> As OS + Integrity and authentication of signal Continuity and service guaranty 	Aviation (en route)	Certified receivers
			Double frequency (Level A and C)	<ul style="list-style-type: none"> As above at higher performance levels suitable for stringent dynamic conditions 	<ul style="list-style-type: none"> Aviation (A) Maritime (C) Road, Train (A) 	Certified receivers
Public Regulated Service	PRS		Dual frequency	<ul style="list-style-type: none"> As OS + High Continuity (in times of crisis) Improved Robustness (vs jamming, spoofing) 	<ul style="list-style-type: none"> Law enforcement Strategic infrastructure 	Regulated
Search and rescue	SAR		Single frequency	<ul style="list-style-type: none"> Almost instantaneous reception of emergency calls Exact positioning of emergency beacon 	Emergencies	Certified & registered beacons

Table (2-6): Illustrates the Horizontal and Vertical Accuracy for Galileo Service [After, Enderle,W.,2009]

Galileo Service	Horizontal Accuracy (95%)	Vertical Accuracy (95%)	Availability	Integrity
Open Service	4 m	8 m	> 99.8%	NO
Safety of Life	4 m	8 m	> 99.8%	YES
Commercial Service	Detailed performance requirements under elaboration			
Public Regulated Service	6.5 m	12 m	> 99.8%	YES

2.1.3.2 Status of Galileo Programme

On December 28, 2005, the first experimental satellite GIOVE-A was launched into orbit from the Russian Cosmodrome at Baikonur in Kazakhstan. On January 12, 2006, GIOVE-A transmitted its first signal. The signals were registered and analyzed at the observation station for Atmospheric and Radio wave Research in Chilbolton in Britain as well as the ESA ground station at Redu in Belgium

[[http://telecom.tlab.ch/~zogg/Dateien/GPS_Compendium\(GPS-X-02007\).pdf](http://telecom.tlab.ch/~zogg/Dateien/GPS_Compendium(GPS-X-02007).pdf)]. A second GIOVE satellite launched on 27 April 2008 *[www.esa.int/esaCP/SEM9GD2QGFF_index_0.html]*. With GIOVE-A and B the EU will secure the frequency bands for GALILEO operation and determine the orbitals for the test phase satellites. These pioneer satellites will also serve in the testing of important technology, such as atomic clocks, in the hard conditions of space. GIOVE-A has two Rubidium atomic clocks and GIOVE-B will have two passive Hydrogen-Maser atomic clocks onboard. When the experimental phase with GIOVE-A and GIOVE-B be successful, GALILEO has moved into the In Orbit Validation (IOV) phase, four satellites will be launched into orbit and tested

[[http://telecom.tlab.ch/~zogg/Dateien/GPS_Compendium\(GPS-X-02007\).pdf](http://telecom.tlab.ch/~zogg/Dateien/GPS_Compendium(GPS-X-02007).pdf)].

A. The In-Orbit Validation phase consists in a constellation of four satellites expected to be deployed by 2009 complemented with a global ground segment of reference and up-link stations to communicate with the satellites Figure (2-22):

- 20 sensor stations
- 5 uplink stations
- 2 TT&C stations

- 1 control centre [Dumesnil, N., 2007].

With this "minimum constellation" scientists can test if the satellite can deliver exact position and time data to test locations on the ground [http://telecom.tlab.ch/~zogg/Dateien/GPS_Compendium(GPS-X-02007).pdf].

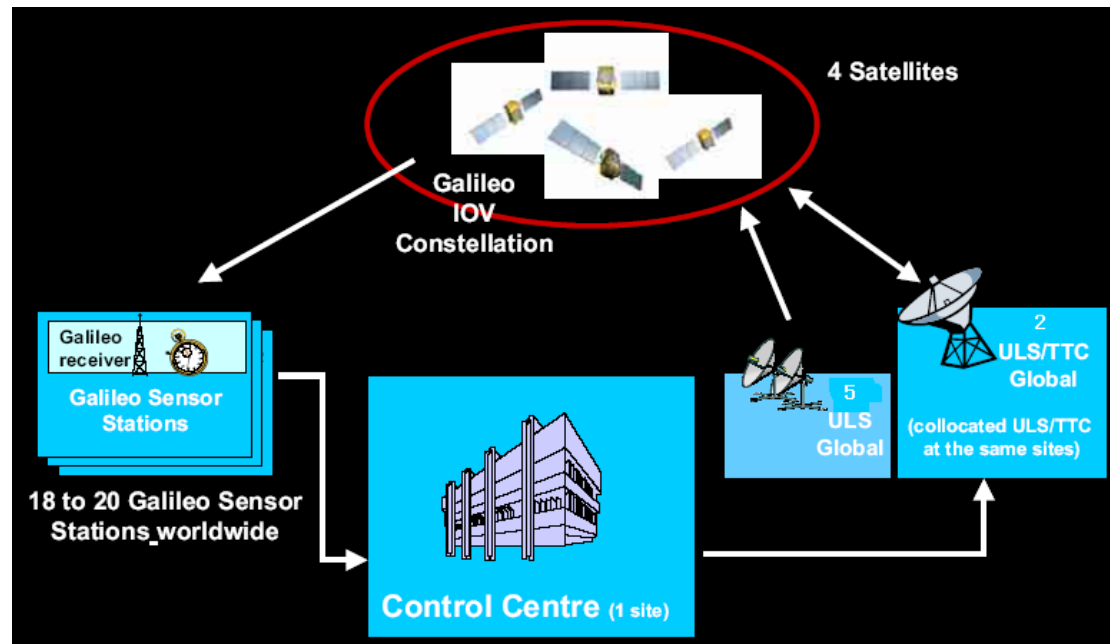


Figure (2-22): IOV System Configuration [After, Steciw, A., 2006]

B. The Full Operational Capability consists of 30 satellites in three MEO planes:

- 56° inclination
- 23616 km altitude
- 10 satellites per plane: 9 satellites per plane active & 1 spare satellite per plane
- 17 orbits in 10 days
- 2 Control Centers (Europe)
- 30-40 reference stations (worldwide)
- 10 mission up-link stations (worldwide)

- 5 TT&C stations (worldwide) [*Ludwig,D.,2007*].

It is unlikely that FOC will be available until 2012-2013, perhaps only a few years before GPS-III's FOC [*Rizos,C.,2007*].

2.1.3.3 GALILEO Signal

A. GALILEO Frequency Plan

The Galileo navigation signals are transmitted in the four frequency bands these four frequency bands are: the E5a band, the E5b band, the E6 band and the E2L1E1 band See Table (2-7).

Table (2-7): Transmitted bandwidth and center frequency
[www2.matimop.org.il/1/foreign/Galileo%20Signal.pdf]

Frequency Band		Carrier Frequency
E5a/L5	Band	1176.450 MHz
E5b	Band	1207.140 MHz
E5 (E5a+E5b) Band		1191.795 MHz
E6	Band	1278.75 MHz
E2-L1-E1	Band	1575.42 MHz

B. GALILEO Navigation Signals Description

Each Galileo Satellite transmits six Navigation Signals, which are named L1F, L1P, E6C, E6P, E5A, and E5B signals See Table (2-8).
[www2.matimop.org.il/1/foreign/Galileo%20Signal.pdf]

Table (2-8): Mapping of Galileo Navigation Signals onto Galileo Navigation Services

[\[www2.matimop.org.il/1/foreign/Galileo%20Signal.pdf\]](http://www2.matimop.org.il/1/foreign/Galileo%20Signal.pdf)

Signal s	Open Service Users	Safety-Of-life Service Users	Commercial Service Users	Public Regulated Service Users
L1F	x(*)	x(*)	x(*)	
L1P				x
E6C			x	
E6P				x
E5a	x	x	x	
E5b	x(*)	x(*)	x	

(*) with no access to encrypted commercial

2.1.4 Compass Navigation Satellite System (CNSS) or (BeiDou-2)

China is planning to build a navigation satellite constellation known as Compass Navigation Satellite System (CNSS), or (BeiDou-2) in its Chinese name. The system will be based on its current Compass Satellite Navigation Experimental System (BeiDou-1), which provides navigation and positioning services to users in China and its neighbouring countries since 2008. The system will be gradually expanded into a navigation satellite constellation comprising 5 Geostationary Earth Orbit (GEO) satellites and 30 medium Earth orbit satellites, which can provide navigation and positioning services to global users.

The CNSS will provide two types of services: a free service for civilian users will have positioning accuracy within 10 meters, velocity accuracy within 0.2 meter per second and timing accuracy within 50 nanoseconds; and a licensed service with higher accuracy for authorized and military users only. The system will initially cover China and its neighbouring

countries only but will eventually extend into a global navigation satellite network.

Unlike the current Beidou-1 Satellite Navigation Experimental System, which requires dual-way transmissions between the user and the central control station via the satellite, the new generation CNSS will allow ground receiver to calculate its position by measuring the distance between itself and three or more satellites, similar to the method of operation of the GPS and GLONASS systems.

- **Compass-M1 (14 April 2007)**

China successfully launched a medium Earth orbit BeiDou navigation satellite codenamed Compass-M1 on 14 April 2007. A CZ-3A space launch vehicle carrying the satellite lifted off from XSLC at 20:11 GMT on 13 April 2007 (04:11 local time on 14 April 2007). The satellite will operate at an altitude of 21,500km orbit.

Launch Records

Satellite	Launch Date	Launch Site	Launch Vehicle	Notes
Compass-M1 (#05)	14 Apr 07	Xichang	CZ-3A	In orbit

[<http://www.sinodefence.com/strategic/spacecraft/beidou2.asp>]

2.2 Space Based Augmentation Systems (SBAS)

As an aid to aviation, primarily to provide integrity, various SBAS systems have been developed to augment GPS, with extension to other GNSS possible. Because these satellites also provide ranging signals, they can also be considered as contributing to the “system of systems” receiver. The satellites are all geostationary and transmit at the L1

frequency (and some at L5). Europe's EGNOS has three satellites, the US WAAS has four, Japan's MSAS has two and India's GAGAN will have three, Figure (2-23). Nigeria is also planning NIGCOMSAT [Dempster,A.,2007], Russia is also planning SDCM this is Wide-area (Russia)[www.unoosa.org/pdf/icg/2007/algeria/01.pdf]. These are known as Regional Space Based Augmentation Systems (RSBAS) and other systems already active are known as Global Space Based Augmentation Systems (GSBAS) for example OmniSTAR, StarFire and VueStar [Kempfi,p.,2007]

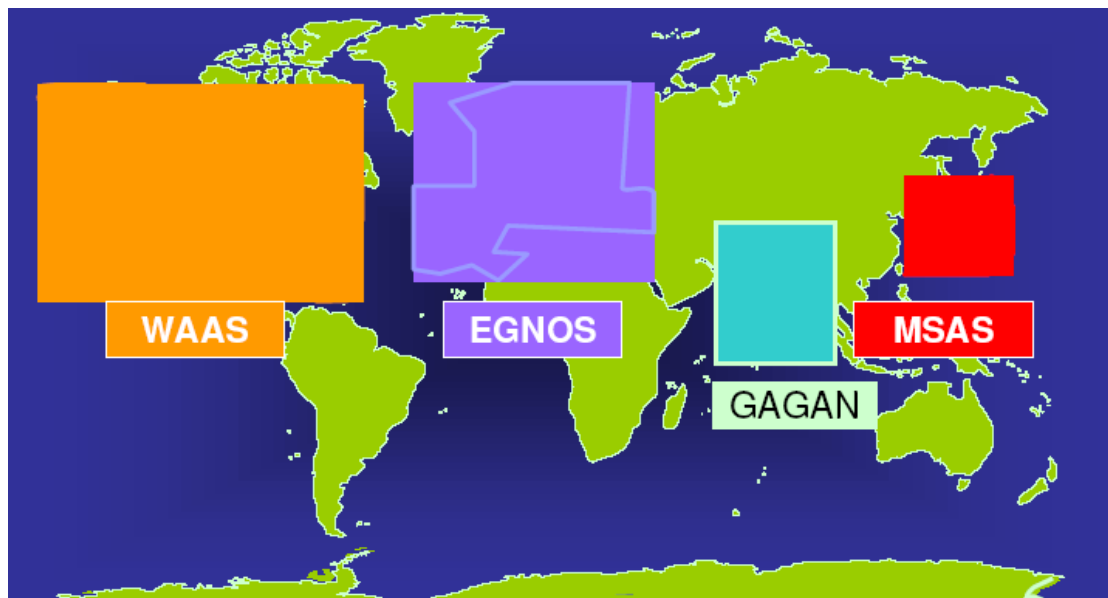


Figure (2-23): Space Based Augmentation Systems (SBAS)

[After, Radhakrishnan, 2007].

2.2.1 Regional Space Based Augmentation Systems (RSBAS)

A. Wide-Area Augmentation System (WAAS)

In 1995 the United States began development of the Wide Area Augmentation System (WAAS) under the auspices of the Federal Aviation Administration (FAA) and the Department of Transportation (DOT), to provide precision approach capability for aircraft. Without

WAAS, ionospheric disturbances, satellite clock drift, and satellite orbit errors cause too much error in the GPS signal for aircraft to perform a precision landing approach. Additionally, signal integrity information as broadcast by the satellites is insufficient for the demanding needs of public safety in aviation. WAAS provides additional integrity messages to aircraft to meet these needs.

WAAS includes a core of approximately 25 Wide-area Ground Reference stations (WRSs) positioned throughout the United States that has precisely surveyed coordinates. These stations compare the GPS signal measurements with the measurements that should be obtained at the known coordinates. The WRS send their findings to a WAAS master station (WMS) using a land-based communications network and the WMS calculates correction algorithms and assesses the integrity of the system. The WMS then sends correction messages via a ground uplink system (GUS) to geostationary (GEO) WAAS satellites covering the United States. The satellites in turn broadcast the corrections on a per-GPS satellite basis at the same L1 1575.42 MHz frequency as GPS. WAAS-enabled GPS receivers receive the corrections and use them to derive corrected GPS signals, which enable highly accurate positioning.

On July 10, 2003, Phase 1 of the WAAS system was activated for general aviation, covering 95% of the conterminous United States and portions of Alaska. In September 2003, improvements enabled WAAS-enabled aircraft to approach runways to within 250 ft altitude before requiring visual control.

In March 2005 two additional WAAS GEO satellites were launched and are now operational. These satellites plus the two existing satellites will improve coverage of North America and all except the northwest part of

Alaska. The four GEO satellites will be positioned at 54°, 107°, and 133° west longitudes, and at 178° east longitude Figure (2-24).

WAAS is currently available over 99% of the time, and its coverage will include the full continental United States and most of Alaska. Although primarily intended for aviation applications, WAAS will be useful for improving the accuracy of any WAAS-enabled GPS receiver. Such receivers are already available in low-cost handheld versions for consumer use. Positioning accuracy using WAAS is currently quoted at less than 2 m of lateral error and less than 3 m of vertical error Figure (2-25), which meets the aviation category. Precision approach requirement of 16 m lateral error and 4 m vertical error [Andrews, A. P et. al 2007].

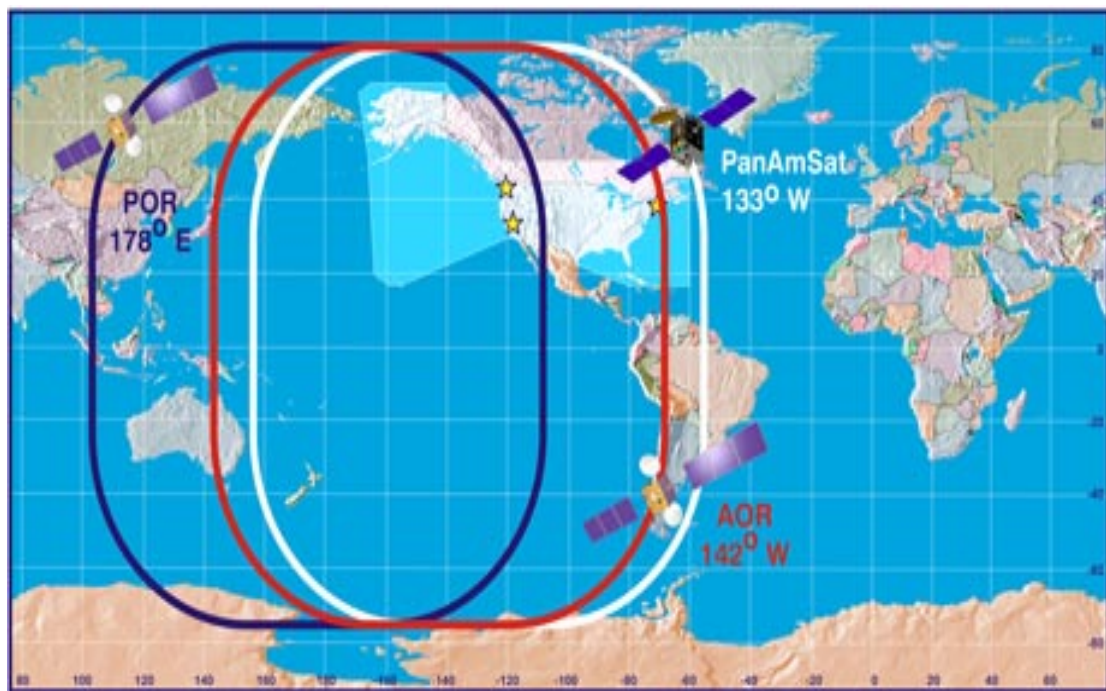


Figure (2-24): WAAS Coverage

[www.faa.gov/about/office_org/headquarters_offices/ato/service_units/techops/navservices/gnss/waas/news/].

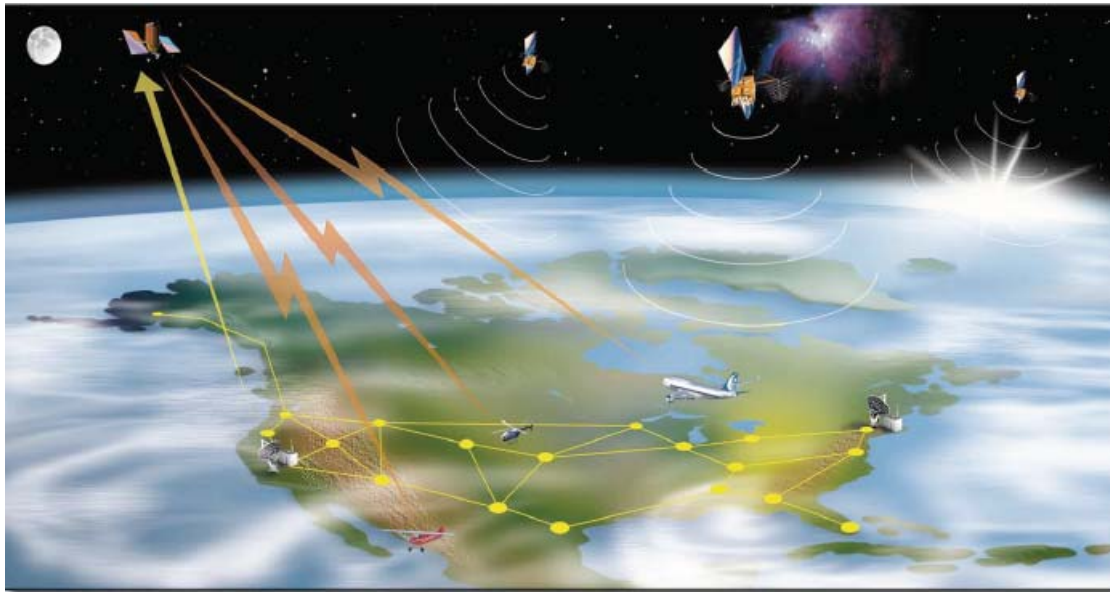


Figure (2-25): Wide-Area Augmentation System (WAAS)

[After, Parkinson, B., 2007].

B. European Geostationary Navigation Overlay System (EGNOS)

The European Geostationary Navigation Overlay System (EGNOS) is Europe's first venture into satellite navigation. It is a joint project of the European Space Agency (ESA), the European Commission (EC), and Euro control, the European organization for the safety of air navigation. Inasmuch as Europe does not yet have its own standalone satellite navigation system, initially EGNOS is intended to augment both the United States GPS and the Russian GLONASS systems, providing differential accuracy and integrity monitoring for safety-critical applications such as aircraft landing approaches and ship navigation through narrow channels.

EGNOS has functional similarity to WAAS, and consists of four segments: space, ground, user, and support facilities segments.

1. Space Segment

The space segment consists of three geostationary (GEO) satellites, the Inmarsat-3 AOR-E, Inmarsat-3 AOR-W, and the ESA Artemis, which transmit wide-area differential corrections and integrity information throughout Europe. Unlike the GPS and GLONASS satellites, these satellites will not have signal generators aboard, but will be transponders relaying uplinked signals generated on the ground, Figure (2-26).

2. Ground Segment

The EGNOS ground segment includes 34 Ranging and Integrity Monitoring Stations (RIMSs), four Mission/Master Control Centers (MCCs), six Navigation Land Earth Stations (NLEs), and an EGNOS Wide-Area Network (EWAN). The RIMS stations monitor the GPS and GLONASS signals. Each station contains a GPS/GLONASS/EGNOS receiver, an atomic clock, and network communications equipment. The RIMS tasks are to perform pseudorange measurements, demodulate navigation data, mitigate multipath and interference, verify signal integrity, and transmit data to the MCC.

The MCC monitor and control the three EGNOS GEO satellites, as well as perform real-time software processing. The MCC tasks include integrity determination, calculation of pseudorange corrections for each satellite, determination of ionospheric delay, and generation of EGNOS satellite ephemeris data. The MCC then sends all the data to the NLEs stations. Every MCC has a backup station that can take over in the event of failure. The NLEs stations receive the data from the MCC centers and generate the signals to be sent to the GEO satellites. These include a GPS-like signal, an integrity channel, and a wide-area differential (WAD) signal. The NLEs send this data on an uplink to the GEO satellites.

3. User Segment

This segment consists of the user receivers. Although EGNOS has been designed primarily for aviation applications, it can also be used with land or marine EGNOS-compatible receivers, including low-cost handheld units.

4. Support Facilities Segment

Support for development, operations, and verifications are provided by this segment. The EGNOS system is currently operational. Positioning accuracy obtainable from use of EGNOS is approximately 5 m Figure (2-27), as compared to 10–20 m with unaided GPS. There is the possibility that this can be improved with further technical development [*Andrews, A. P et. al 2007*].

5. EGNOS coverage

The EGNOS coverage area includes all European states, and could be extended to include other regions, such as South America, Africa, and parts of Asia and Australia, within the coverage of three geostationary satellites being used [*Dumesnil, N., 2007*]

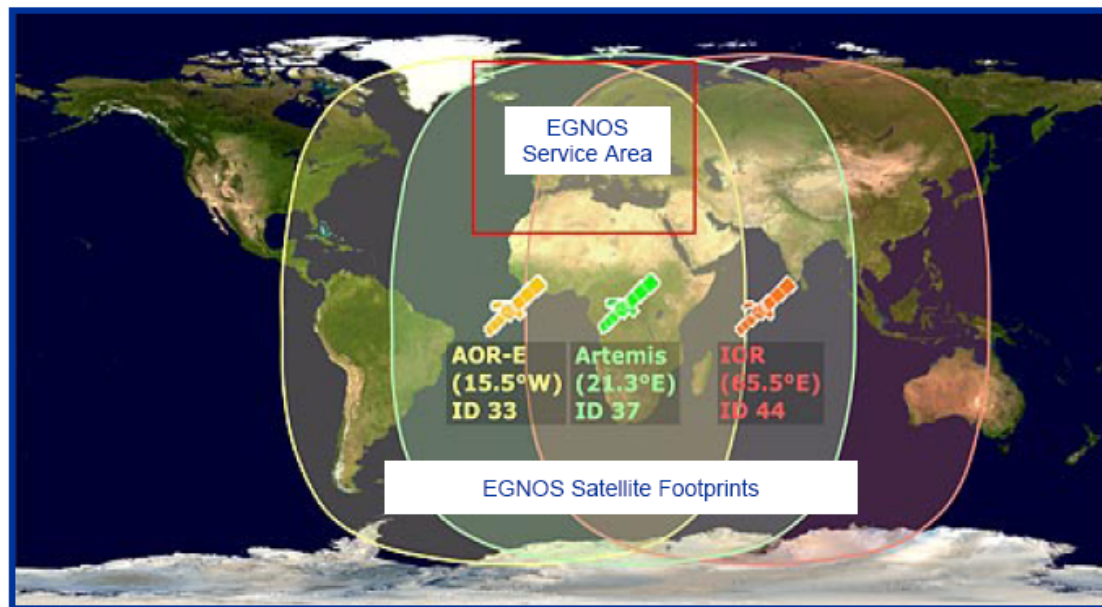


Figure (2-26): EGNOS GEO Satellites Triple Coverage over Europe and Africa [After, Ludwig,D.,2007]

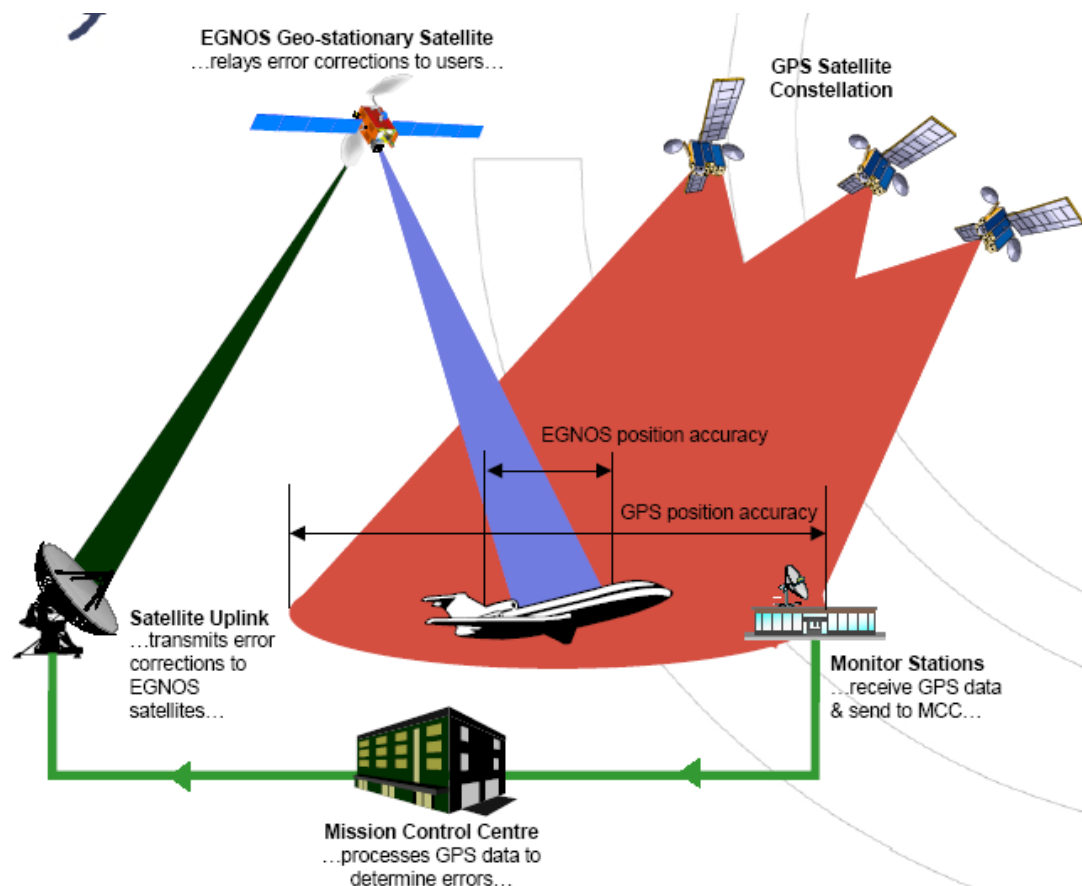


Figure (2-27): EGNOS Offers Improved GNSS Performance with Respect to GPS [After, Dumesnil, N.,2007].

C. Japan's MTSAT Satellite-Based Augmentation System (MSAS)

The Japanese MSAS system, developed by Japan Space Agency and the Japan Civil Aviation Bureau, will improve the accuracy, integrity, continuity, and availability of GPS satellite signals throughout the Japanese Flight Information Region (FIR) by relaying augmentation information to user aircraft via Japan's Multifunctional Transport Satellite (MTSAT) geostationary satellites. The system consists of a network of Ground Monitoring Stations (GMS) in Japan, Monitoring and Ranging Stations (MRSs) outside of Japan, Master Control Stations (MCSs) in Japan with satellite uplinks, and two MTSAT geostationary satellites, Figure (2-28).

MSAS will serve the Asia-Pacific region with capabilities similar to the United States WAAS system. MSAS and WAAS will be interoperable and are compliant with the International Civil Aviation Organization (ICAO) Standards and Recommended Practices (SARP) for SBAS systems [*Andrews ,A. P et. al 2007*].

MSAS Status

- MTSAT-1R was launched in 2005 and Located at 140 E
- MTSAT-2 was launched in February 2006 and Located at 145 E
- MSAS Initial Operational Capability (IOC) from en-route to NPA (Non Precision Approach) with dual MTSAT coverage achieved and commissioned on 27 September 2007 [*Satoshi Kogure,2007*].

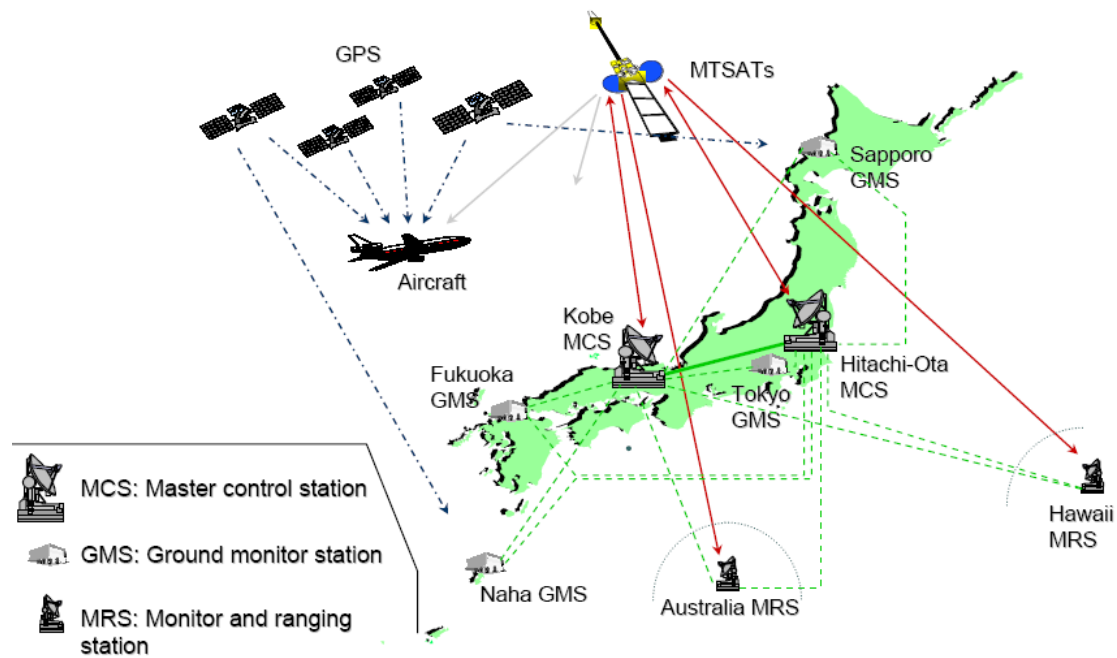


Figure (2-28): MSAS Configuration [After Satoshi KOGURE, 2007]

D. Canadian Wide-Area Augmentation System (CWAAS)

The Canadian CWAAS system is basically a plan to extend the U.S. WAAS coverage into Canada. Although the WAAS GEO satellites can be received in much of Canada, additional ground reference station sites are needed to achieve valid correctional data outside the United States. At least 11 such sites, spread over Canada, have been evaluated. The Canadian reference stations are to be linked to the U.S. WAAS system.

E. China's Satellite Navigation Augmentation System (SNAS)

China is moving forward with its own version of a SBAS. Although information on their system is incomplete, at least 11 reference sites have been installed in and around Beijing in Phase I of the program, and further expansion is anticipated [Andrews, A. P et. al 2007].

F. Indian GPS and GEO Augmented Navigation System (GAGAN)

The Indian Space Research Organization is developing a satellite based augmentation systems for civil aviation with the Aviation Authority of India. The system is named as Geostationary Earth Orbit Augmented Navigation, Figure (2-29). The space segment will consist of India's GSAT-4 satellites. In addition to GPS L1 signal, GAGAN will also broadcast the new safety-of-life signal L5. The ground segment consists of eight Indian reference stations, a master control centre, a land uplink station and associated navigation software and communication links. India and the US have signed a joint statement to facilitate broad and effective use of WAAS and GAGAN as civil space-based regional augmentations to the GPS [Kemppi, P.,2007].

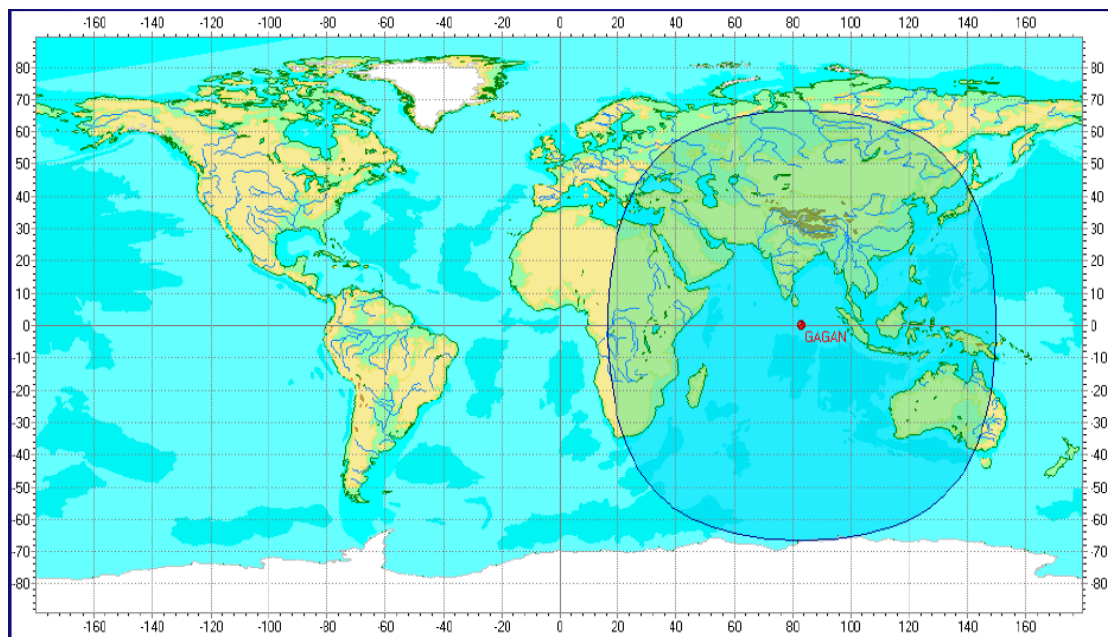


Figure (2-29): GAGAN Coverage [After, Radhakrishnan,2007].

G. System of Differential Correction and Monitoring (SDCM)

The Russian system of differential correction and monitoring (SDCM) is intended for development and real-time transfer of the adjusting information for GLONASS, GPS and GALILEO systems (integrity data,

wide-area and local correction data) to civilian customers. It is expected that SDCM based on GLONASS/GPS signals will provide increased (in comparison with basic level) accuracy of position determination in real time at any point in the Russian Federation.

[www.unoosa.org/pdf/publications/icg_book01E.pdf].

H. Nigerian Communication Satellite (NIGCOMSAT-1)

With its Nigerian Communications Satellite (NIGCOMSAT-1), Nigeria is the first African country planning to enter the field of GNSS *[www.unoosa.org/pdf/publications/icg_book01E.pdf]*. Nigeria reportedly signed in December 2004 a contract with CGWIC for the design, manufacture and launch of the NIGCOMSAT 1. The satellite was successfully launched on 13.05.2007. In April 2008, NIGCOMSAT 1 lost power from the southern solar array. The satellite failed in November 2008 due to a technical error of the satellite northern solar array and was sent to a graveyard orbit as it became apparent, that the satellite could not be recovered.

In March 2009 Nigeria signed a contract for the free delivery and launch of a replacement satellite called NIGCOMSAT 1R. It will be launched in 2011 *[http://space.skyrocket.de/index_frame.htm?http://space.skyrocket.de/doc_sdat/nigcomsat-1.htm]*.

NigComSat-1 Application Areas, Telecommunications, Broadcasting, Internet & Multimedia, Real Time Monitoring Services, and Navigation & Global Positioning Systems. NigComSat-1 is a hybrid geostationary satellite and located on 42°E

[<http://www.space.gov.za/conferences/alc2007/programme/Alale.pdf>].

2.2.2 Global Space Based Augmentation Systems (GSBAS)

A. OmniSTAR

OmniSTAR provides differential corrections for GPS and Glonass via geostationary satellite channels. These differential corrections are based on data from Fugro's worldwide network of reference stations combined with precise orbit and clock information for every satellite in the GNSS satellite constellation. Fugro is group of companies. Fugro collects and interprets data related to the earth's surface and the soils and rocks beneath and provides advice, for purposes related to the oil and gas industry, the mining industry and the construction industry.

OmniSTAR differential corrections are broadcast by a total of nine high power geo-stationary satellites Table (2-9), located at 36,000 km above the equator. In order to receive the OmniSTAR broadcast a combined L1/OmniSTAR or L1/L2/OmniSTAR antenna is required [Visser, H.,2006].

Table (2-9): OmniSTAR Geostationary L-band Satellites [After. Visser, H.,2006].

Satellite name	Area of Coverage	Frequency (kHz)	Data rate	Centre Longitude	East Border	West Border	South Border	North Border
AM-SAT	North and South America	1535.137500	1200 bps	98° West	179° W	17° W	76° S	76° N
AORWH	Atlantic Ocean West	1535.185000	600 bps	54 West	132° W	24° E	76° S	76° N
AOREH	Atlantic Ocean Coast East	1535.125000	600 bps	16° West	94° W	62° E	76° S	76° N
AF-SAT	Africa, Middle East	1535.180000	1200 bps	25° East	56° W	106° E	76° S	76° N
IORH	India, Pakistan Middle East, Russia	1535.157500	600 bps	66° East	14° W	142° E	76° S	76° N
AP-SAT	Asia, India, Australia, New Zealand	1535.137500	1200 bps	109° East	28° E	168° W	76° S	76° N
OC-SAT	Pacific Ocean, Australia, New Zealand	1535.185000	1200 bps	144° East	62° E	136° W	76° S	76° N
MSVW	USA-West	1557.855000	1200 bps	120° West	115° W	80° W	25° N	67° N
MSVC	USA-Central	1557.835000	1200 bps	94° West	25° N	67° N	25° N	67° N
MSVE	USA-East	1557.845000	1200 bps	80° West	100° N	60° N	25° N	67° N

A.1 OmniSTAR Services

A.1.1 OmniSTAR VBS (Virtual Base Station)

The Omnistar VBS service is based on the L1 Code measurements of reference stations Figure (2-30) that are used to calculate optimized GPS range corrections for the location of the user. These distance corrections are passed to the GPS receiver to create an optimized DGPS solution. Accuracy is better than 1 Meter (2DRMS) horizontal at mid-latitudes inside the network. Outside the network the solution is valid up to a range of 1000 km. In the equatorial zone submeter VBS operation may be limited to a few 100 km's when there is Ionospheric activity [Visser, H.,2006].

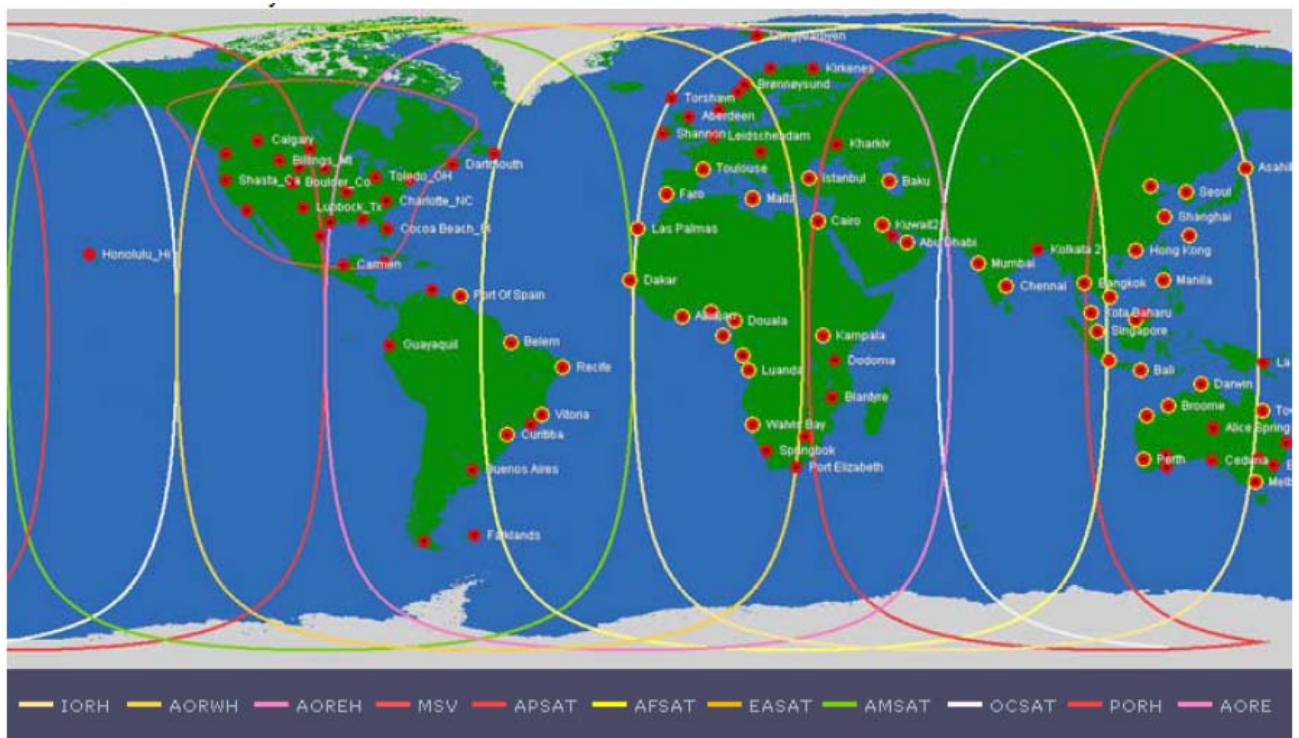


Figure (2-30): OmniSTAR Worldwide Satellite Coverage and Reference Stations [After, Visser, H.,2006].

A.1.2 OmniSTAR HP (High Performance)

OmniSTAR HP is a dual frequency DGPS service based on reference station network technology. The OmniSTAR HP broadcast consists of phase and code measurements from a network of reference stations inside a satellite footprint. Due to the fact that dual frequency reference stations are used, the information is already free of ionosphere signal delay errors. OmniSTAR HP uses measurements from the nearest surrounding reference stations. Up to a distance of 1000 km there are enough common satellites to guarantee good position accuracy. Beyond 1000 km the positional accuracy slowly degrades [*Visser, H.,2006*].

A.1.3 OmniSTAR XP (Extended Performance)

OmniSTAR XP positioning is based on precise orbit and clock information for GPS satellites. Precise satellite orbit information is broadcast every minute and precise clock information every ten seconds. Provided the position of the satellites is known within 20-30 cm and the satellite clock error is known within a nanosecond (which equals 30 cm), it is possible to estimate positions up to the decimeter level without the need for a user to work close to one of our reference stations. This technique is also referred to as “Precise Point Positioning” (PPP).

A.1.4 OmniSTAR G2 (GPS & Glonass)

The OmniSTAR G2 broadcast contains the orbit and clock corrections for the Russian Glonass system as well as for GPS. OmniSTAR G2 uses Glonass Orbit and Clock corrections derived from a separate (OmniSTAR owned) independent network of reference station. At present, the GPS constellation consists of 30 satellites available, whereas Glonass presently (February 2009) consists of 18 satellites and is

expected to expand to 24. Currently at 42, G2 will eventually provide corrections for more than 50 satellites. This high number of satellites allows for improved position availability in semi-urban areas and in locations with blockage due to tree canopy.

A.1.5 Combining Different Services

OmniSTAR can combine HP & XP or HP, XP & G2 into a very robust positioning solution with a high availability [*Visser, H.,2006*].

B. StarFire

NavCom Technology Inc. has developed a global satellite based augmentation system that provides decimeter level positioning accuracy on a worldwide basis. NavCom is the only GPS manufacturer providing both GSBAS signal service and high-precision GPS products of its own design. The StarFire global subscription service provides real-time accuracy, which is normally better than 10 cm. Its globally corrected signal is available virtually anywhere on the Earth's surface on land or at sea, from 76°N to 76°S latitude. The system utilizes a network of more than 60 GPS reference stations around the world and three geostationary satellites to broadcast the real time corrections to the users around the world. Since 2001, NavCom has cooperated with NASA's Jet Propulsion Laboratory to combine JPL's GDGPS together with StarFire. NavCom offers two types of StarFire subscription licenses: Land Only (excludes all oceans/offshore) and All Areas (global coverage) [<http://www.navcomtech.com/StarFire/>].

C. VueStar

VueStar is a complete global satellite based augmentation system that is configured specifically for all aerial survey applications developed by

NavCom Technology Inc. It utilizes the global satellite based StarFire network to provide precise positioning worldwide without the need for RTK base stations or GPS post processing [www.navcomtech.com/Products/GPS/vuestar.cfm]. Photogrammetry, LIDAR, SAR and other Remote Sensing Aerial Survey applications can rely on the real-time, decimeter results provided by VueStar [<http://www.geoinfo.rs/Pdf/NavCom/vuestar.pdf>].

2.3 Ground-Based Augmentation Systems (GBAS)

GBAS is a system that provides augmentation messages through the use of terrestrial radio network. GBAS uses augmentation information provided by a network of ground based reference stations. These reference stations are used to monitor GNSS signals and determine the error components including satellite ephemeris errors and those introduced by ionospheric and tropospheric disturbances. Ground based augmentation systems can be divided into subcategories based on the scale of the reference network and purpose of use [*Kemppi, P.,2007*].

2.3.1 Local Area Differential GPS

Local Area Differential GPS services improve the accuracy of GPS by placing high quality reference receivers into known, surveyed locations. These reference stations estimate the slowly varying error components of each satellite's range measurements, formulate the differential corrections and broadcast them to local users e.g. on commercial AM frequencies. The performance of Local Area DGPS receivers degrades as the distance from the reference receiver's increases. Local Differential GPS is mainly utilized by the maritime vessels and national coast guards [*S. Raman, L. Garin,2005*].

2.3.2 Wide Area Differential GPS

In Wide Area Differential GPS (WADGPS), a broad network of reference stations is used to form a vector correction for each satellite [S. Raman, L. Garin, 2005]. The vector consists of individual corrections for the satellite clock, ephemeris and ionospheric delay model. The vector correction is valid over much broader geographical area than Local DGPS corrections. One of the WADGPS implementations is the patented Global Differential GPS System (GDGPS) provided by NASA Jet Propulsion Laboratory (JPL). It is a complete, highly accurate, and extremely robust real-time GPS augmentation and monitoring system. GDGPS employs a large ground network of real-time reference receivers (over 70 reference stations) to track the GPS civil signals on the L1 and L2 frequencies. The measurements from the reference receivers are streamed via redundant communication paths to GDGPS Operation Centers (GOC) (3 centers as of October 2006) to be processed into the real-time differential corrections. The GDGPS System provides decimeter (10 cm) positioning accuracy and sub-nanosecond time transfer accuracy anywhere in the world. However, in the low latitude, and during ionospheric storms the positioning error may be notably worse [www.gdgps.net/].

2.3.3 Local-Area Augmentation System (LAAS)

LAAS is an augmentation to GPS that services airport areas approximately 20–30 mi in radius, and has been developed under the auspices of the Federal Aviation Administration (FAA). It broadcasts GPS correction data via a very high-frequency (VHF) radio data link from a ground-based transmitter, yielding extremely high accuracy, availability, and integrity deemed necessary for aviation Categories I, II, and III precision landing approaches. LAAS also provides the ability for

flexible, curved aircraft approach trajectories. Its demonstrated accuracy is less than 1 m in both the horizontal and vertical directions.

A typical LAAS system, which is designed to support an aircraft's transition from en route airspace into and throughout terminal area airspace, consists of ground equipment and avionics. The ground equipment consists of four GPS reference receivers, a LAAS ground facility, and a VHF radio data transmitter Figure (2-31). The avionics equipment includes a GPS receiver, a VHF radio data receiver, and computer hardware and software.

The GPS reference receivers and the LAAS ground facility work together to measure errors in GPS position that are common to the reference receiver and aircraft locations. The LAAS ground facility then produces a LAAS correction message based on the difference between the actual and GPS-calculated positions of the reference receivers. The correction message includes integrity parameters and approach-path information. The LAAS correction message is sent to a VHF data broadcast transmitter, which broadcasts a signal containing the correction/integrity data throughout the local LAAS coverage area, where it is received by incoming aircraft.

The LAAS equipment in the aircraft uses the corrections for position, velocity, and time to generate instrument landing system (ILS) lookalike guidance as low as 200 ft above touchdown. It is anticipated that further technical improvements will eventually result in vertical accuracy below 1 m, enabling ILS guidance all the way down to the runway surface, even in zero visibility (Category III landings).

A major advantage of LAAS is that a single installation at a major airport can be used for multiple precision approaches within its local service

area. Furthermore, it is generally agreed that the Category III level of accuracy anticipated for LAAS cannot be supported by WAAS

[Andrews ,A. P et. al 2007].

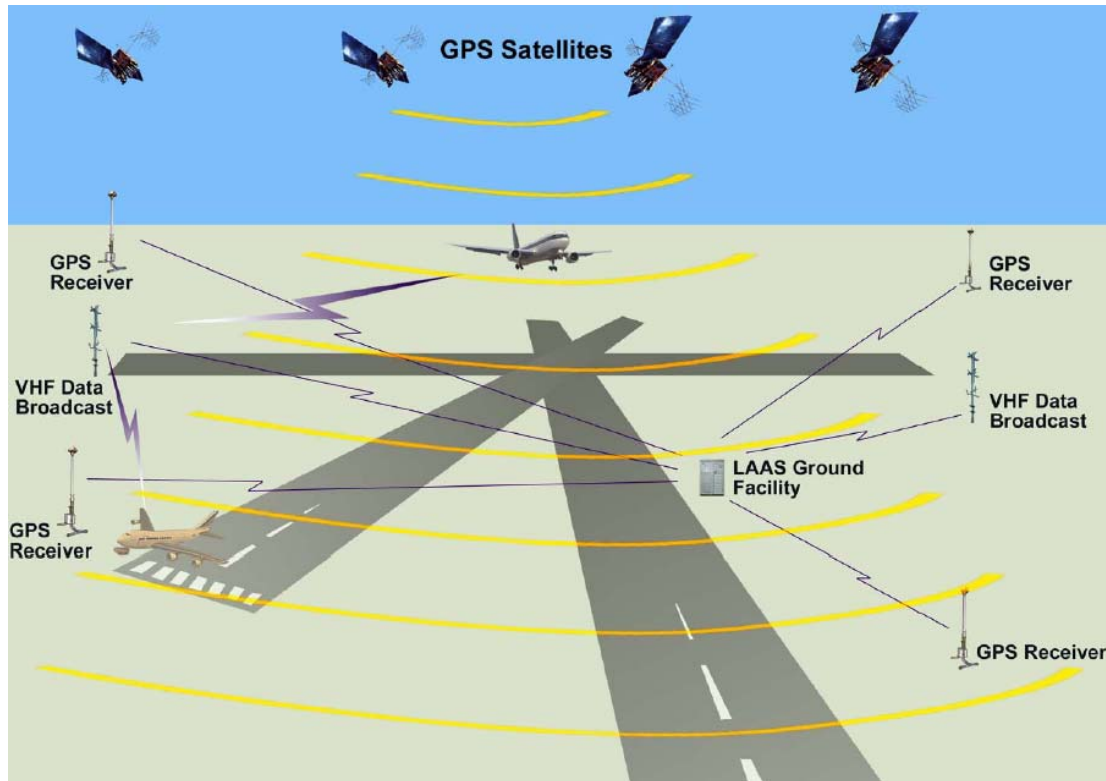


Figure (2-31): Local-Area Augmentation System (LAAS)
[After, Carroll,J.,2004]

2.4 Regional Navigation Satellite Systems (RNSS)

2.4.1 Compass Satellite Navigation Experimental System (BeiDou-1)

The Compass Navigation Satellite Experimental System, or BeiDou-1 in its Chinese name, is the three-satellite constellation developed by China Academy of Space Technology (CAST). It is China's first space-based regional navigation and positioning network. The system provides all-weather, two-dimensional positioning data for both military and civilian users. The network covers most areas of East Asia region and has both navigation and communication functions. The satellite network comprises three BeiDou-1 satellites (two operational and one backup).

The first two satellites of the BeiDou-1 navigation experimental system, the BeiDou-1A and BeiDou-1B, were launched from Xichang Satellite Launch Centre on 31 October 2000 and 21 December 2000 respectively. The system began to provide navigation and positioning services in late 2001. The third satellite (backup) BeiDou-1C was launched on 25 May 2003, bringing the system fully operational. The navigation and positioning services became available to civilian users in April 2004. This has made China the third country in world to have deployed an operational space-based navigation and positioning network.

2.4.1.1 The BeiDou-1 System Design

BeiDou-1 system design consists of three parts:

A. Space Segment

The BeiDou-1 Satellite Navigation Experimental System covers the region between Longitude $70^{\circ}\sim 140^{\circ}$ E and Latitude $5^{\circ}\sim 55^{\circ}$ N. Two satellites are positioned in geosynchronous orbit at 80° E and 140° E. The third (backup) satellite is positioned at 110.5° E.

B. Ground Segment

The ground systems include the central control station, three ground tracking stations for orbit determination (at Jamushi, Kashi and Zhanjiang), ground correction stations, and user terminals (receivers/transmitters).

The satellites transmit at $2491.75\pm 4.08\text{MHz}$ and the ground receiver can transmit back to the satellite on 1615.68MHz . The BeiDou-1 reference-frame is the Beijing 1954 Coordinate System, with time referenced to China UTC as determined in Beijing.

The system provides positioning data of 100m accuracy. By using ground correction stations, the accuracy can be increased to 20m. The system capacity is 540,000 users per hour.

C. User Segment

The navigation and positioning services are available to civilian and military users, Figure (2-32).

2.4.1.2 Method of Operation

Firstly, the central control station sends inquiry signals to the users via two satellites. When the user terminal received the signal from one satellite, it sends responding signal back to both satellites. The central station receives the responding signals sent by the user from two satellites, and calculates the user's 2D position based on the time difference between the two signals. This position is then compared with the digital territorial map stored in the database to get the 3D position data, which is then sent back to the user via satellites using encrypted communications.



Figure (2-32): BeiDou-1 User Terminal: The BeiDou-1 System Uses A large-size Transmitter/Receiver User Terminal Due to its Dual-Way Transmission Operation Method

[www.sinodefence.com/strategic/spacecraft/beidou1.asp]

Because BeiDou-1 system requires dual-way transmissions between the user and central control station via satellites at high-altitude geostationary orbit Figure (2-33), its user segment needs extra space for transmitter and a more-powerful battery. Therefore the BeiDou-1 system's user segments are much bigger, heavier and more expensive compared to GPS user receivers. Additionally, the number of users can be served by the system is limited by the communication capacity of the network.

[www.sinodefence.com/strategic/spacecraft/beidou1.asp]



Figure (2-33): BeiDou-1 method of operation

[www.sinodefence.com/strategic/spacecraft/beidou1.asp]

- **BD-1D (3 February 2007)**

Following the three successful launches of the BeiDou-1 satellites in 2000 and 2003, a fourth GEO satellite was launched by a CZ-3A launch vehicle from Xichang Satellite Launch Centre (XSLC) at 16:28 GMT on 2 February 2007 (00:28 local time on 3 February 2007). The fourth satellite was presumably to complement the three existing regional Beidou-1 geostationary satellites by occupying the open slots at Longitudes 58.75 and 160 degrees east.

Launch Records

Satellite	Launch Date	Launch Site	Launch Vehicle	Notes
BeiDou-1A	31 Oct 00	Xichang	CZ-3A	In orbit
BeiDou-1B	21 Dec 00	Xichang	CZ-3A	In orbit
BeiDou-1C	25 May 03	Xichang	CZ-3A	In orbit
BeiDou-1D	3 Feb 07	Xichang	CZ-3A	In orbit

[www.sinodefence.com/strategic/spacecraft/beidou1.asp]

2.4.2 Quasi Zenith Satellite System (QZSS)

Quasi-Zenith Satellite System (QZSS) is a regional space-based positioning system that uses a constellation of satellites placed in multiple orbital planes. QZSS consists of several QZS (Quasi-Zenith Satellites) the first QZSS satellite will be launched in 2009 and ground segment comprised of master control station, monitoring stations, and satellite tracking & control stations. Its orbit is highly inclined elliptical orbit (HEO). Japan has a lot of mountainous areas and narrow roads surrounded tall buildings as a geographical feature. Japan is also located in middle latitude. In such areas, mobile vehicles and mobile phones can hardly receive signals from satellites; especially Geo-Stationary Orbit satellites. The elevation angle of QZS is much higher than GSO see Figure (2-34).

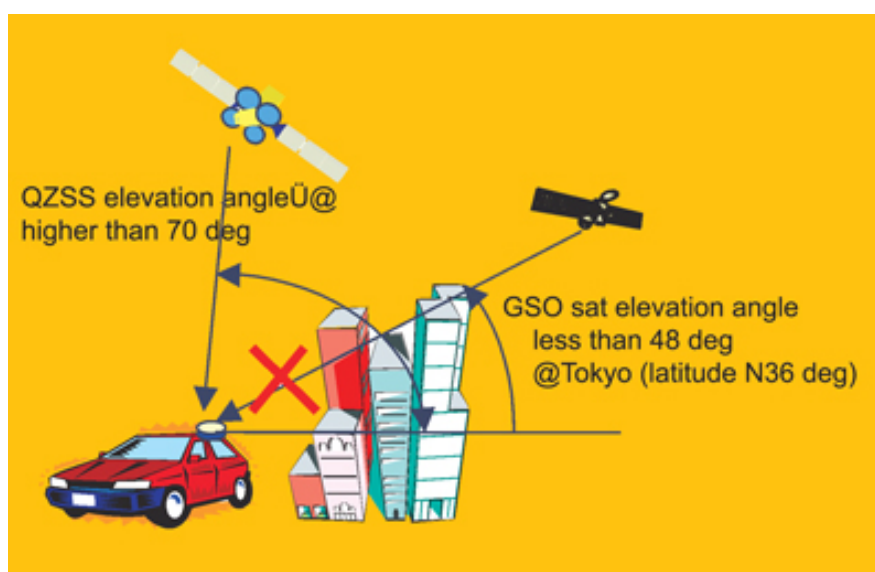


Figure (2-34): The Difference of Elevation Angle between QZS and GSO

[www.location.net.in/magazine/2007/jan-feb/30_3.htm]

If the signals are broadcast from high elevation satellite (QZS), the positioning availability will improve. Eccentricity and inclination are selected so that minimum elevation angle through 24 hours in Japan is

larger than 60 degrees. Table (2-10) shows our baseline of the QZSS orbital parameters *[Kishimoto,M.,2007]*.

Table (2-10): QZSS Orbital Parameters

[www.location.net.in/magazine/2007/jan-feb/30_3.htm]

	Semi-major axis(km)	Eccentricity	Inclination (degree)	RAAN (degree)	Argument of Perigee (degree)	Mean Anomaly(degree)
QZS 1	42164.136	0.099	45	0	270	239.76
QZS 2	42164.136	0.099	45	120	270	119.76
QZS 3	42164.136	0.099	45	240	270	359.76

2.4.2.1 The QZSS System Design

QZSS system design consists of three segments explained in the next titles;

A. Space Segment

The baseline QZSS constellation is comprised of three satellites. All QZS are in orbits that have the same ground track (passing over Southeast Asia, Australia, etc.) as shown in Figure (2-35) *[JAXA, 2007]*.

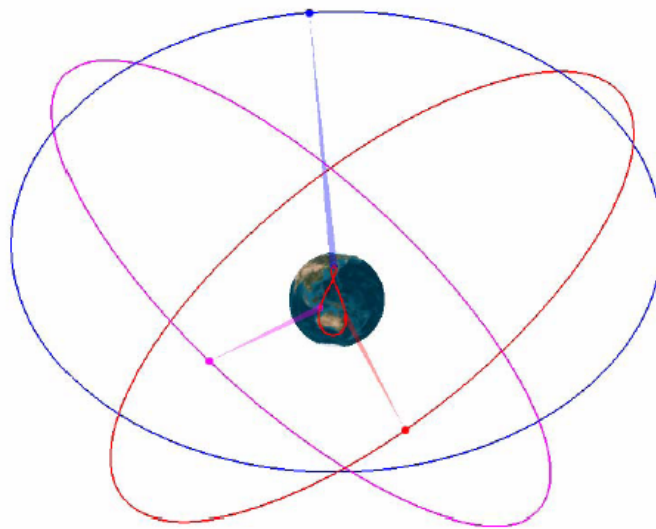


Figure (2-35): QZSS Orbit and Ground Track Diagram for the Three-Satellite Constellation *[After, JAXA, 2007]*.

A. Ground Segment

The QZSS Ground Segment consists of multiple Earth-based stations. These comprise Monitor Stations (MS) that are widely distributed and observe QZS and GPS signals on the ground; a Master Control Station (MCS) that collects the results of monitoring from all of the MS, estimates and predicts QZSS and GPS clock offsets and orbits, generates navigation messages, etc.; and Tracking Control Stations that uplink navigation messages and monitor QZS status.

There are approximately ten MS dispersed throughout the area from which QZS signals can be received. The MCS is located in Japan [*JAXA, 2007*].

B. User Segment

Users can enjoy interference-free communications when they are walking in urban or mountainous areas. In addition, the system, used together with a Global Positioning System (GPS), will provide much more accurate positioning information than before.

2.4.2.2 QZSS Planned Signals

QZSS will transmit navigation signals, which have complete compatibility and interoperability with current and modernized future GPS, on L1 (1575.42MHz), L2 (1227.60MHz) and L5 (1176.45MHz) to whole visible earth surface from the satellite. The signal, called L1-Sub meter class Augmentation with Integrity Function (L1-SAIF), will be planned to provide WDGPS correction message based on SBAS message format adding to above mentioned GPS interoperable signals on L1 band. Moreover, LEX signal on E6 (1278.75MHz) will be transmitted for experimental and augmentation mission. The frequency plan for QZSS is

shown in the Figure (2-36). QZSS will transmit the GPS interoperable signals, that is, L1C, L1-C/A, L2C, and L5 signals. The goal of these signals design is to minimize modifications on user receivers which can receive and calculate user position combining both signals from GPS and QZSS.

There are slight differences on the definition of the message which come from the difference between both systems such as orbit parameters. The complete interoperability and compatibility between QZSS and GPS, including L1-SAIF signal, had been confirmed by the GPS-QZSS Technical Working Group and announced in the joint announcement for the US-Japan Consultations on the Use of the GPS (US-Japan GPS plenary meeting) in January 2006.

The signal characteristics for L1-SAIF and LEX signals are summarized in. L1-SAIF signal is aiming at providing WDGPS correction and integrity message to users in Japan. It uses same methodology as SBAS basically. LEX signal is an experimental signal for technical demonstration [Kishimoto,M.,2007].

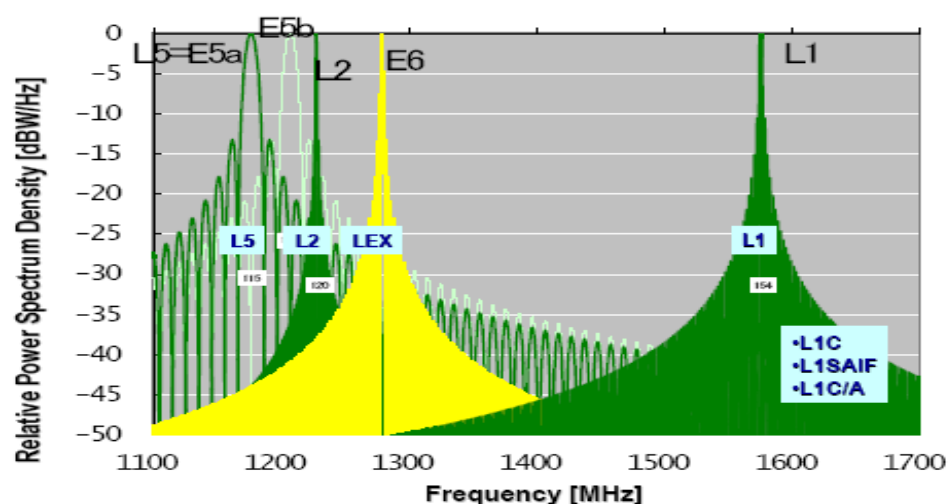


Figure (2-36): Transmission Signal Spectrum [After, JAXA, 2007].

- **Spectrum of Transmission Signals**

The six positioning signals have four center frequencies. With the reference frequency set to $f_0 = 10.23$ MHz, these carrier frequencies will be $154 \times f_0$ (L1), $125 \times f_0$ (LEX), $120 \times f_0$ (L2) and $115 \times f_0$ (L5).

2.4.2.3 Coordinate System

The QZSS coordinate system is known as the Japan satellite navigation Geodetic System (JGS). This coordinate system is operated so as to approach the International Terrestrial Reference System (ITRS) JGS is defined as follows.

- (a) Origin: Ellipsoid GRS80 (earth's center of mass)

The geometrical center of ellipsoid GRS80 (Geodetic Reference System 1980) is established as the Earth's center of mass.

- (b) Z axis: International Earth Rotation Service (IERS) pole direction
- (c) X-axis: Direction of intersection of IERS Reference Meridian (IRM) and plane containing origin and Z-axis
- (d) Y-axis: Direction formed by the right-handed fixed geocentric coordinate system [JAXA,2007]

2.4.2.4 QZSS Coverage Range

Figure (2-37) and Figure (2-38) show the availability of a single QZS in various parts of the world due to the QZSS constellation. For the 3-satellite QZSS constellation, at least one QZS is available 100% of the time not only in Japan but in almost all parts of Southeast Asia and Oceania at an angle of elevation of 10° or more. In Japan, at least one

QZS is available 100% of the time at an elevation angle of 60° or more [JAXA, 2007].

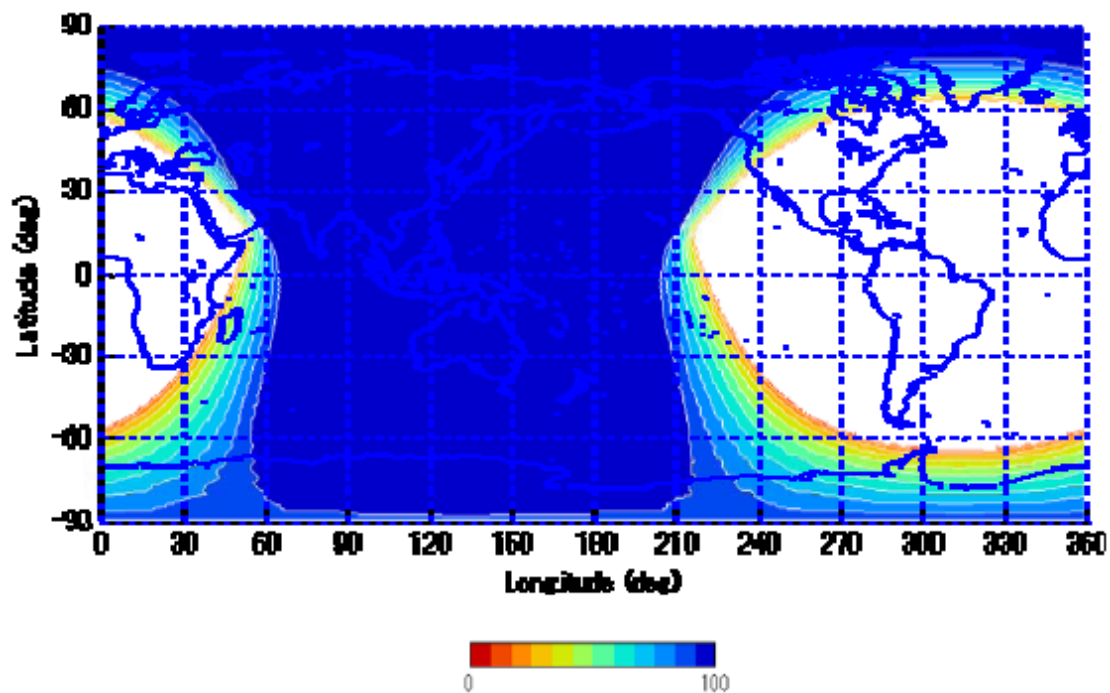


Figure (2-37): Percentage of Time during Which at Least One QZS in The 3-Satellite QZSS can be seen at an Elevation Angle of 10° Or More [After, JAXA, 2007].

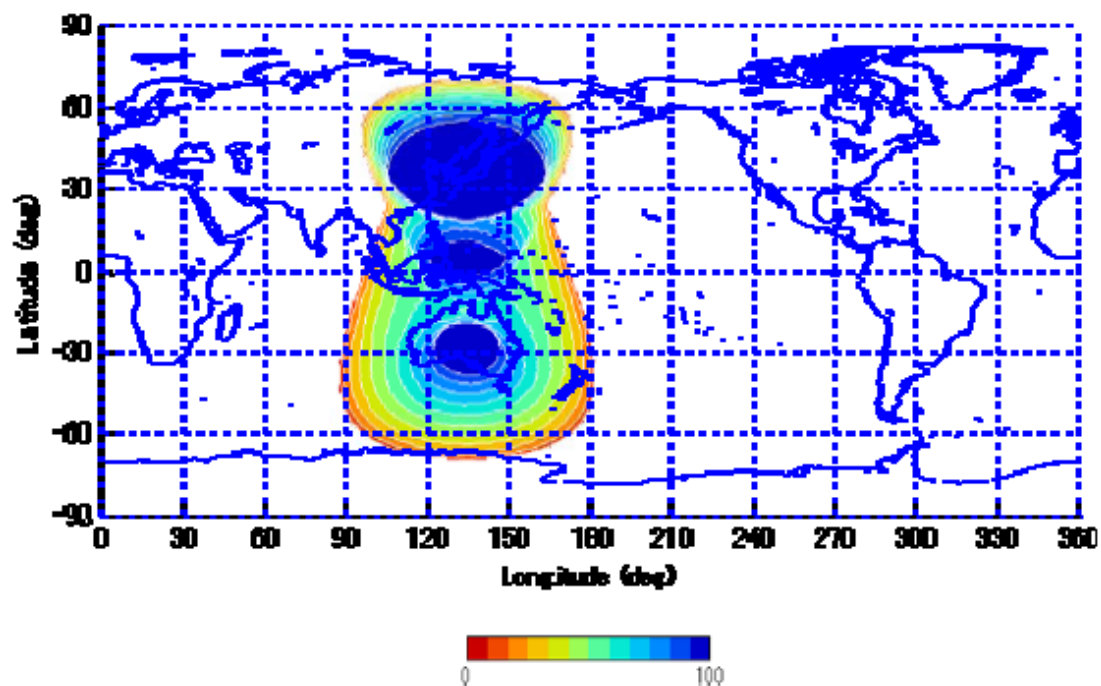


Figure (2-38): Percentage of Time during Which at Least One QZS in The 3-Satellite QZSS Constellation can be seen at an Elevation Angle of 60° or More [After, JAXA, 2007].

2.4.3 Indian Regional Navigation Satellite System (IRNSS)

The Government approved in May 2006, a project to implement an Indian Regional Navigation system (IRNSS) in the next 6-7 years. It will consist of a constellation of seven satellites and a large ground segment. The entire IRNSS system will be under Indian control. The space segment, ground segment and user receivers will be built in India [Nair,M.,2006].

IRNSS is planned to be an independent regional navigation system covering an area of about 1500kms around India, Figure (2-39). It will provide 20 m accuracy over the Indian Ocean Region and <10 m accuracy over India and adjacent countries [Radhakrishnan,2007].



Figure (2-39): Regional Coverage for Indian Regional Navigation Satellite System

[<http://www.fmv.se/upload/Bilder%20och%20dokument/Publikationer/rappporter/Galileo.pdf>].

2.4.3.1 The IRNS System Design

IRNS system design consists of three parts:

A. Space Segment

The proposed system would consist of a constellation of seven satellites, three of the seven satellites in the IRNSS constellation will be placed in Geostationary Earth Orbit (GEO) and four in Geosynchronous Orbits (GSO) inclined at 29° to the equatorial plane. All the seven satellites will have continuous radio visibility with Indian control stations [*Dumesnil, N., 2007*].

B. Ground Segment

The ground segment of the IRNSS constellation will include a Master Control Centre (MCC), IRNSS Ranging and Integrity Monitoring Stations (IRIM) and IRNSS Telemetry Tracking & Command (TT&C) stations. The IRIMs receive the data from all IRNSS satellites through one-way ranging and transmit the data to MCC for processing, MCC will estimate and predict the position (ephemerides) of all IRNSS satellites, calculates integrity, ionospheric corrections, clock corrections and runs the navigation software. The TT&C stations perform the ranging, telemetry and command functions, provide clock corrections to the satellite and upload the ionospheric and tropospheric corrections to the constellation. In order to make the IRNSS truly independent, an Indian standard time infrastructure will be established [*Nair, M., 2006*].

C. User Segment

IRNSS will provide the user, 20 m accuracy over the Indian Ocean Region and <10 m accuracy over India and adjacent countries [*Radhakrishnan, 2007*].

2.5 Types of GPS Receivers

In 1980, only one commercial GPS receiver was available on the market, at a price of several hundred thousand U.S. dollars. This, however, has changed considerably as more than 500 different GPS receivers are available in today's market. The current receiver price varies from about \$100 for the simple handheld units to about \$15,000 for the sophisticated geodetic quality units. The price will continue to decline in the future as the receiver technology becomes more advanced. A GPS receiver requires an antenna attached to it, either internally or externally. The antenna receives the incoming satellite signal and then converts its energy into an electric current, which can be handled by the GPS receiver.

Commercial GPS receivers may be divided into four types, according to their receiving capabilities. These are: single-frequency code receivers, signal-frequency carrier-smoothed code receivers, single-frequency code and carrier receivers, and dual-frequency receivers. Single-frequency receivers access the L1 frequency only, while dual-frequency receivers access both the L1 and the L2 frequencies. GPS receivers can also be categorized according to their number of tracking channels, which varies from 1 to 12 channels. A good GPS receiver would be multichannel, with each channel dedicated to continuously tracking a particular satellite. Presently, most GPS receivers have 9 to 12 independent (or parallel) Channels. Features such as cost, ease of use, power consumption, size and weight, internal and/or external data-storage capabilities, interfacing capabilities, and multipath mitigation (i.e., type of correlator) are to be considered when selecting a GPS receiver[*El-Rabbabny, A.,2002*].

The first receiver type, the single-frequency code receiver, measures the pseudoranges with the C/A – code only. No other measurements are

available. It is the least expensive and the least accurate receiver type, and is mostly used for recreation purposes. The second receiver type, the single-frequency carrier-smoothed code receiver, also measures the pseudoranges with the C/A-code only. However, with this receiver type, the higher-resolution carrier frequency is used internally to improve the resolution of the code pseudorange, which results in high-precision pseudorange measurements. Single-frequency code and carrier receivers output the raw C/A-code pseudoranges, the L1 carrier-phase measurements, and the navigation message. In addition, this receiver type is capable of performing the functions of the other receiver types discussed above. Dual-frequency receivers are the most sophisticated and most expensive receiver type *[El-Rabbabny, A.,2002]*.


2.5.1 Modernization of Receivers


GPS receivers are being manufactured by hundreds of different manufacturers. Some of the well known names are:


Trimble, Leica, Ashtech, Topcon, Sokkia, Magellan. The manufactures are coming out with different models


[\[www.gisdevelopment.net/technology/gps/techgp0012a.htm\]](http://www.gisdevelopment.net/technology/gps/techgp0012a.htm).

Due to the modernization of GPS, increasing the number of satellites of GLONASS and the establishment of the European GALILEO led to the development of the receivers. The next sub-section illustrates the specifications of the receivers.

Brand	Trimble
Model name/Type	R8 GNSS
Introduction date	
Class (GPS, Glonass, Galileo/S, D en T)	GPS & Glonass
Number of Channels	72
Static [mm + ppm]	$\pm 5\text{mm} + 0.5\text{ppm RMS (H)}, \pm 5\text{mm} + 1\text{ ppm RMS (V)}$
RTK [mm + ppm]	$\pm 10\text{mm} + 1\text{ppm RMS (H)}, \pm 20\text{ mm} + 1\text{ppm RMS (V)}$
Single/dual/triple frequency	Triple
Max. no. of satellites tracked parallel (GPS/ Glonass /Galileo/Other)	GPS, Glonass “All in View”
	

Brand	Topcon
Model name/Type	GR-3
Introduction date	July 2006
Class (GPS, Glonass, Galileo/S, D en T)	GPS, Glonass & Galileo/T
Number of Channels	72 Universal Channels
Static [mm + ppm]	$3\text{mm} + 0.5\text{ppm (H)}, 5\text{mm}+0.5\text{ppm (V)}$
RTK [mm + ppm]	$10\text{mm} + 1\text{ppm (H)}, 15\text{mm} + 1\text{ppm (V)}$
Single/dual/triple frequency	Triple
Max. no. of satellites tracked parallel (GPS/ Glonass /Galileo/Other)	36
	

Brand	Leica Geosystems
Model name/Type	Leica GX1230 GG 4) <i>Positioning Satellites</i>
Introduction date	May 2006
Class (GPS, Glonass, Galileo/S, D en T)	GPS & Glonass, Dual-frequency, RTK (prepared for GPS L5 and Galileo E1 and E5)
Number of Channels	72
Static [mm + ppm]	Post-processing (static and rapid static)=5mm+0.5ppm, post-processing kinematic=10+1ppm (horizontal accuracies)
RTK [mm + ppm]	RTK static=5mm+0.5ppm, RTK kinematic=10+1ppm (horizontal accuracies)
Single/dual/triple frequency	Dual
Max. no. of satellites tracked parallel (GPS/ Glonass /Galileo/Other)	28
	

Brand	Sokkia
Model name/Type	GSR2700 ISX
Introduction date	2007
Class (GPS, Glonass, Galileo/S, D en T)	GPS & Glonass
Number of Channels	72 Universal Channels
Static [mm + ppm]	3mm + 0.5ppm (H) 10mm + 1ppm (V)
RTK [mm + ppm]	10mm + 1ppm (H) 20mm + 1ppm (V)
Single/dual/triple frequency	Triple
Max. no. of satellites tracked parallel (GPS/ Glonass /Galileo/Other)	14 L1, 14 L2, 6 L5 GPS, 12 L1, 12 L2 GLONASS, 2 SBAS
	

[www.gim-international.com/files/productsurvey_v_pdfdocument_21.pdf]

Table (2-11) Illustrates Most Important Properties of the Four GNSS Systems

System	GPS	GLONASS	GALILEO	Compass or BeiDou-2
Nominal Constellation	24	24	30	30(MEO)+5(GEO)
Number of operational satellites	30 (January 2008)	9 (September 2007)	None now	1(MEO)+4(GEO) (April 2007)
Mean altitude [km]	20200	19100	23616	21500
Orbital Planes	6	3	3	-
Inclination [degrees]	55	64.8	56	-
Orbital Period	11h 58min	11h 15min	14h 04min	-
Ground Track Repetition [SID]	1	8	10	-
Reference Frame	WGS-84	PZ-90 and now PZ-90.02 (September 2007)	GTRF	-
Time System	GPS-Time	Glomass-Time	GST	-
Signal Characteristic	CDMA	FDMA	CDMA	-
Responsibility	US Department of Defense	Russian Defense Ministry	Civilian Governments of the EU	-
Services	2 (civilian + military)	2 (civilian + military)	5	-
Absolute position accuracy	2.3 m (2007)	10.5 m (2007)	-	-

Chapter 3

Remote Sensing Satellites

Introduction

Remote sensing is a technique to observe the earth surface or the atmosphere from out of space using satellites (space borne) or from the air using aircrafts (airborne). Remote sensing uses a part or several parts of the electromagnetic spectrum. It records the electromagnetic energy reflected or emitted by the earth's surface. The amount of radiation from an object (called radiance) is influenced by both the properties of the object and the radiation hitting the object (irradiance). The human eyes register the solar light reflected by these objects and our brains interpret the colors, the grey tones and intensity variations. In remote sensing various kinds of tools and devices are used to make electromagnetic radiation outside this range from 400 to 700 NM visible to the human eye, especially the near infrared, middle-infrared, thermal-infrared and microwaves [Aggarwal,S.,1998].

3.1 Electromagnetic Spectrum Used for Remote Sensing

The electromagnetic (EM) spectrum is the continuous range of electromagnetic radiation, extending from gamma rays (highest frequency & shortest wavelength) to radio waves (lowest frequency & longest wavelength) and including visible light.

The EM spectrum can be divided into seven different regions, gamma rays, X-rays, ultraviolet, visible light, infrared, microwaves and radio waves, Figure(3-1).

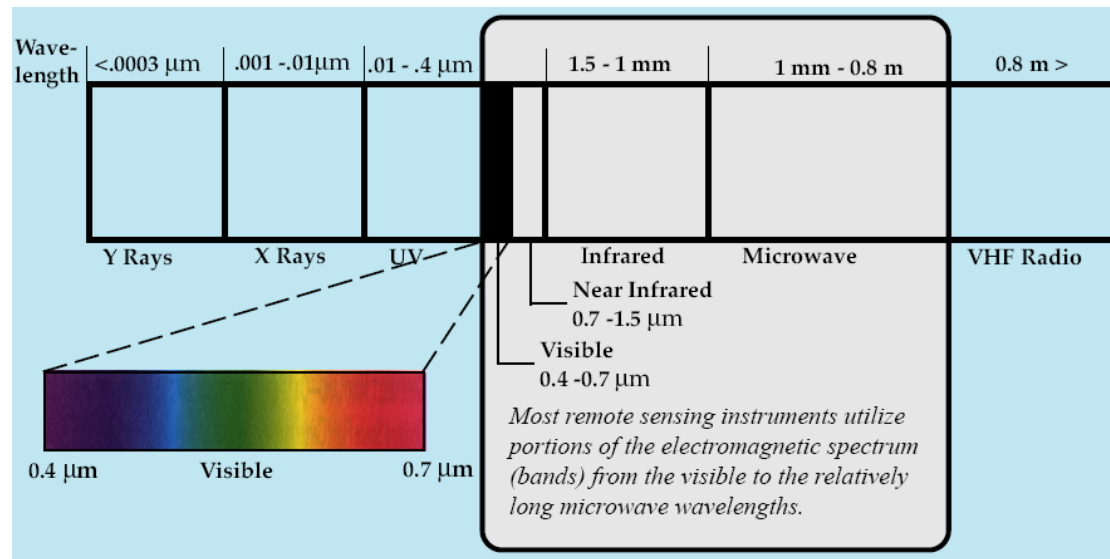


Figure (3-1): Electromagnetic Spectrum

[After, Walton B. Campbell et. al., 1997].

Remote sensing involves the measurement of energy in many parts of the electromagnetic (EM) spectrum. The major regions of interest in satellite sensing are visible light, reflected and emitted infrared, and the microwave regions.

[http://spacegrant.nmsu.edu/statewide/projects/remote_sensing.pdf]

3.2 Remote Sensing Technology (RST)

There are two main types of RST: passive and active. Passive remote sensing scanners detect existing energy, such as reflected sunlight or thermal radiation. Active scanners send out a signal and collect the return, such as radar or sonar.

Electromagnetic energy, which is reflected and/or emitted from objects, can be detected and recorded by a variety of airborne or satellite platforms as remotely sensed data. Scanners are designed to detect the amount of energy within a specified range of wavelengths, referred to as the bandwidth. Within the visible spectrum, the various bandwidths are perceived as individual colors. Some types of scanners/sensors can detect

energy at bandwidths outside the visible spectrum, such as infrared, thermal and microwave wavelengths. Sensors also vary in the number of bandwidths detected. Panchromatic scanners sense one broad bandwidth. Multispectral scanners sense several distinct bandwidths. Hyperspectral scanners detect hundreds of very narrow bandwidths

[www.evergladesplan.org/pm/recover/recover_docs/qasr/qasr_sec_09_2006.pdf].

The following section illustrates in details the Active and Passive Remote Sensing Technology.

3.2.1 Passive Remote Sensing Technologies

Passive sensors record reflected or emitted EM energy. These sensors rely on the external illumination from a light source (such as the sun) Figure (3-2). Some passive sensors can pick up thermal emissions, thus are most effectively used during times of low sun illumination such as sunset or at night [Alspaugh, 2004; Short, 2006].

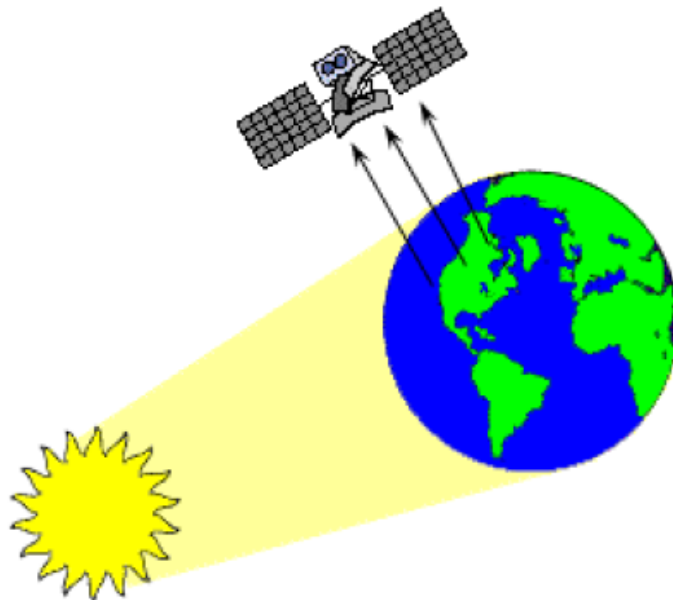


Figure (3-2): Passive sensors

3.2.1.1 Panchromatic Remote Sensing

Panchromatic images are collected by single-band sensors that capture wavelengths in the visible or near infrared (IR) part of the EM spectrum [Lillesand, 2001].

producing a gray scale image similar to a black-and-white photograph [www.evergladesplan.org/pm/recover/recover_docs/qasr/qasr_sec_09_2006.pdf]. The resolution of these black and white images varies, but is often around 5 m. This data can be useful in parts of the world where aerial photography or even maps of adequate scale are not available.

[Short, 2006]

3.2.1.2 Multispectral Remote Sensing

Multispectral sensors commonly collect from four to eight EM bands at intervals through the visible and near IR part of the spectra [Short, 2006]. When evaluating imagery data for its utility, a very important consideration is the resolution or ground sample distance (GSD). The current orbiting sensors can be divided into two major resolution groups: high-resolution systems (0.5-1.8 m) and mid-resolution systems (2.0-39 m). The area that an image can cover is called the swath width; high-resolution swaths are in the 8 to 28 km range and mid-resolution swaths are generally between 70 and 185 km [Stoney, 2006].

Both panchromatic and multispectral images reveal spatial information (shapes) and limited spectral information. Satellite-based panchromatic and multispectral systems are e.g. Landsat, SPOT.

[www.evergladesplan.org/pm/pm_docs/qasr/qasr_ch_09.pdf].

3.2.1.3 Hyperspectral Remote Sensing

Hyperspectral sensors collect EM radiation centered over the visible, extending into the thermal and infrared, and can record this spectrum in over 200 bands. As with other passive sensors, the GSD is related to the height of the platform on which the sensor is housed. Satellite-based hyperspectral sensors produce resolutions from 15 to 90 m, while much higher resolutions can be obtained when sensors are housed on airplanes [Short, 2006]. Thus, hyperspectral remote sensing can distinguish many more spectral features of materials and extract more useful information directly or indirectly for different applications.

[www.evergladesplan.org/pm/recover/recover_docs/qasr/qasr_sec_09_2006.pdf]. Due to the wealth of detailed spectral information that hyperspectral remote sensing can supply, hyperspectral data have been widely used for quantitative analysis in support of variety of applications. A partial list of promising applications supported by hyperspectral remote sensing includes terrestrial ecology, vegetation mapping, oceanography, limnology, geology, volcanology, climatology, agriculture, agronomy, snow and ice hydrology, and environmental management [www.evergladesplan.org/pm/pm_docs/qasr/qasr_ch_09.pdf].

3.2.1.4 Thermal Remote Sensing

In the Thermal InfraRed (TIR) spectral region, most natural surfaces emit electromagnetic radiation that can be used for passive detection purposes. Advances in infrared technologies over the past two decades have been possible by the development of modern electronics and new detector materials. The result is that high-performance TIR imaging systems, utilizing both 3-5 micrometer (μm) and 8-12 μm wavelengths, have become available.

A list of supported applications by thermal remote sensing include geology (e.g. rocks discrimination and mineral deposits mapping), water pollution studies (e.g. thermal plumes and oil spill), earth and water surface temperature mapping, soil moisture determinations, snow and ice hydrology, volcanology, hydrologic modeling (e.g. latent/sensible heat determination), agriculture and vegetation monitoring.

[www.evergladesplan.org/pm/pm_docs/qasr/qasr_ch_09.pdf].

3.2.1.5 Passive Microwave Remote Sensing

Beyond the infrared wavelengths, wave energy in the range ~0.15 cm to ~30 cm forms the basis of remote sensing by microwave radiometry. Passive microwave radiometry applied to investigations of the Earth's surface involves the detection of thermally generated microwave radiation. Although the naturally emitted microwave radiation intensities are much lower than those in the infrared, resulting in poorer brightness temperature resolution, the longer wavelengths allow sensing through cloud cover. Passive microwave sensors also have the advantage of gathering data at night as well as during the day. Currently microwave remote sensing has been utilized mainly in the following areas: water salinity mapping, surface temperature measurement, monitoring of soil moisture content, floodplain delineation, and canal seepage detection

[www.evergladesplan.org/pm/recover/recover_docs/qasr/qasr_sec_09_2006.pdf].

3.2.1.6 Aerial Photography

Aerial photography was traditionally collected by an airborne camera using panchromatic (black and white) or color film. The first aerial photographs were taken in the 1850's from balloons and kites. Modern

advances in aerial photography, typically taken from aircraft, include film that is sensitive beyond the visible spectrum and digital cameras.

Vertical photographs are acquired when the camera is aimed directly at the ground below. Orienting the camera diagonally at a target produces oblique photographs with a much larger field of view and much greater distortion of geometry, resulting in distant objects looking much smaller than nearby objects. Vertical photographs, which typically have less distortion, can be more easily geometrically corrected to produce consistent scale across the entire photograph.

[www.evergladesplan.org/pm/pm_docs/qasr/qasr_ch_09.pdf].

3.2.2 Active Remote Sensing Technologies

Active sensors send an energy signal to the target that is then reflected back to the sensor Figure (3-3). The difference in range and intensity between the source and return signals are measured and recorded by the sensor. Most active systems operate at microwave wavelengths, which can penetrate through clouds. Therefore, active sensors can be utilized at night or during storms, which is an advantage over passive systems

[www.evergladesplan.org/pm/recover/recover_docs/qasr/qasr_sec_09_2006.pdf]. Active sensors, include Radio Detection And Ranging (RADAR), Synthetic Aperture Radar (SAR), Interferometric Synthetic Aperture Radar (IfSAR), Light Detection And Ranging (LIDAR) and Sound Navigation And Ranging (SONAR) *[Wang and Dahman, 2002]*.

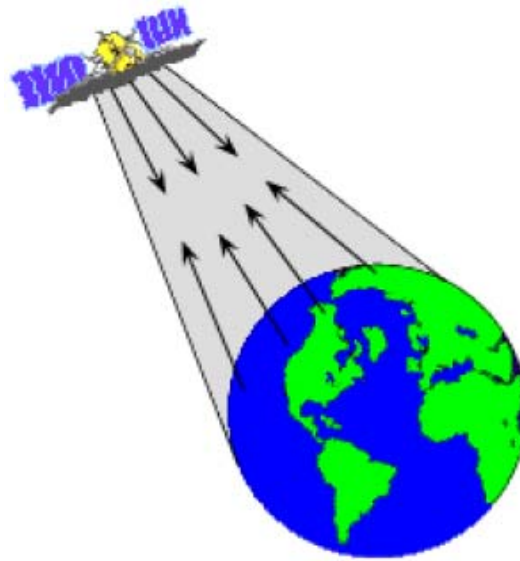


Figure (3-3): Active sensors

These sensors measure the length of time signals take to strike an object and be reflected back. By knowing the location of the sensor, which is provided by yet another technology, distances are transformed into elevations. The result is a digital file containing an array of points that define the surface struck by the signals [*Crane et. al., 2004*].

These files containing horizontal and vertical coordinate values are commonly referred to as digital terrain models (DTM). When evaluating the resulting DTM, two components must be considered: the spacing and the precision at which the data points are collected. To a large extent, both of these components are governed by the capabilities of the sensor; however, the object to sensor distance is also a factor [*Wang and Dahman, 2002*].

Active sensors can be placed on a variety of platforms including satellites, airplanes, unmanned airborne vehicles and surveying tripods.

Radar is an active sensing system, sending microwave energy and capturing the return signal. Typically, radar remote sensing refers to synthetic aperture radar (SAR)

[www.evergladesplan.org/pm/recover/recover_docs/qasr/qasr_sec_09_2006.pdf].

3.2.2.1 Synthetic Aperture Radar (SAR) and IfSAR

Often satellite-based systems, are not limited by light conditions, thus data collection can occur at any time of day or night. The wide wavelengths of SAR and IfSAR can penetrate haze, clouds, water, snow and even sand. The DTMs resulting from these systems make a good supplement to imagery obtained by photogrammetry and are suitable for orthorectifying medium- and high-resolution satellite images. In addition, overlapping SAR images can be viewed in stereo and used to construct three-dimensional models [Wang and Dahman, 2002]. SAR, IfSAR, and Side-Looking Airborne Radar (SLAR) have been successfully used to analyze and monitor geologically active areas such as eolian dune fields, volcanic terrain and tectonically active areas [Ford et. al., 1998].

3.2.2.2 Light Detection and Ranging (LIDAR) system

It is an active system similar to microwave radar, but operating in that part of the spectrum comprising ultraviolet to near infrared regions [www.evergladesplan.org/pm/recover/recover_docs/qasr/qasr_sec_09_2006.pdf]. Light Detection and Ranging (LIDAR) systems emit and receive pulses from an optically-safe laser; the return provides horizontal and vertical coordinates and intensity values, figure(3-4). The intensity values correspond to the reflectance of the material returning the signal and can greatly assist with post processing of the data. There are both aerial- and ground-based LIDAR systems. Aerial LIDAR data is often

used in conjunction with aerial photography to produce digital orthophotographs [Wang and Dahman, 2002] and can be used in the production of high resolution topography (contour intervals of one meter or greater). Ground based LIDAR (GBLIDAR) systems, also known as laser scanning [Louden, 2003] are high-speed, high-accuracy three-dimensional data collectors with the capability to capture hundreds of points per second. Currently, these data points have a positional accuracy of ± 6 mm (or better) when scanning at distances of less than 50 m [Matthews et. al., 2001a]. Ground based laser systems are transportable, robust, field units that provide near real-time access to the data. An advantage of these systems is that measurements can be made directly from the raw three-dimensional digitized or point cloud data while in the field. This data can be utilized in a variety of software packages for the production of three-dimensional surfaces, contours and site visualization [Matthews et. al., 2001a].

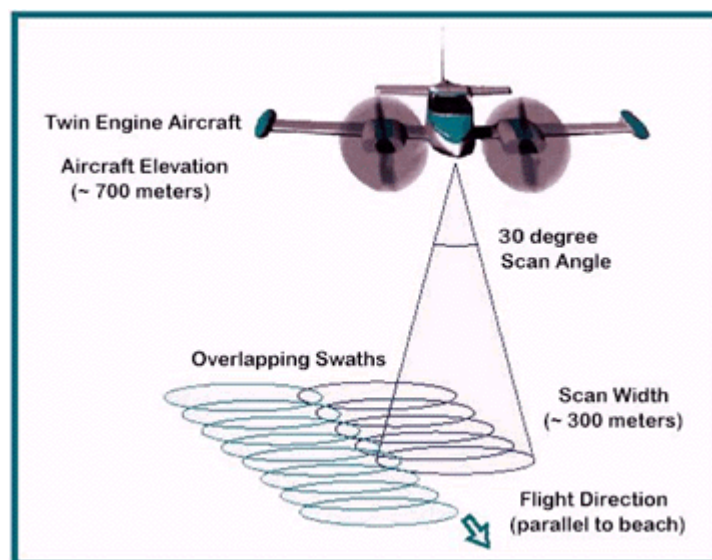


Figure (3-4): Illustration of How the LIDAR Sensing Instrument Captures Elevation Points

[www.csc.noaa.gov/products/sccoasts/html/tutlid.htm]

3.3 Satellite Orbits

Two satellite orbits are important for remote sensing observation of the Earth: the geo-stationary orbit and Sun-synchronous near-polar orbits (simply referred to as polar orbits).

3.3.1 Geostationary Orbits

Characteristics

- The geostationary satellites, at altitudes of about 36,000 km, go around the Earth at speeds which match the rotation of the Earth so they seem stationary relative to the Earth's surface. Geostationary satellites complete an orbit in 24 hours Figure (3-5). This allows the satellites to remain over specific areas and monitor and collect information continuously and constantly.
- The orbit is circular and its inclination is zero degrees, which means that it is above the Earth's equator.
- Weather and communications satellites commonly have these types of orbits. Due to their high altitude (almost three times the diameter of the earth) some geostationary weather satellites can monitor weather and cloud patterns covering an almost entire hemisphere of the Earth.
- Ideal for making repeated observations of a fixed geographical area centered on the equator, polar areas are always covered poorly. Geostationary satellite images of the polar regions are distorted because of the low angle the satellite sees the region.
- Geostationary satellites in orbit include:

- * Meteosat (ESA, covering Europe and Africa)
- * GOES-EAST (NOAA, covering North and South America)
- * GOES-WEST (NOAA, covering Eastern Pacific)
- * GMS (Japan, covering Japan and Australia, Western Pacific)
- * Fengyun-2 (China, covering China and the Indian Ocean)
- * GOMS (Elektro) ((Russia, covering Central Asia and the Indian Ocean)
- * INSAT (India)

[http://geog.tamu.edu/~liu/courses/g489/note7_1.pdf]



Figure (3-5): Geo-stationary Orbit

[http://dprg.geomatics.ucalgary.ca/files/Courses/435/435_CH3_6.pdf]

3.3.2 Polar Orbiting Satellites

Characteristics

- Most of the remote sensing satellite platforms today are in near-polar orbits for meteorological and geophysical applications.
- Polar orbiting satellites closely parallel the earth's meridian lines. They pass over the north and south poles each revolution.
- Polar orbiting satellites can provide global or near global coverage of the atmosphere and Earth surface.
- Polar satellites circle at a much lower altitude (~800km) providing higher quality remote sensing data (more detailed information) than geostationary satellites.
- Most satellites with near polar orbits have altitudes ranging from 600 to 800 km, with orbital periods of 98 to 102 minutes.

3.3.2.1 Sun-synchronous Orbits

- A sun synchronous orbit means that a satellite pass over each area of the Earth's surface at a constant local time of day called local solar time. To achieve this condition, the orbit cannot exactly follow a true north-south track to go over the poles. Actually, the orbit must be slightly tilted towards the northwest with a steep inclination angle of about 98°.
- With the sun synchronous orbit, at any given latitude the position of the sun in the sky as the satellite passes overhead will be the same within the same season. This ensures consistent illumination

conditions when acquiring images in a specific season over successive years.

- Typically, equatorial crossing times of satellites are selected to avoid early morning mists or afternoon cloud in the tropics [<http://geog.tamu.edu/~liu/courses/g661/orbits.pdf>].
- Having a sun-synchronous orbit, however, does not mean that the solar illumination angles are constant throughout the orbit. Most obviously, the sun will generally be lower in the sky as you move northward or southward towards the poles, Figure (3-6).

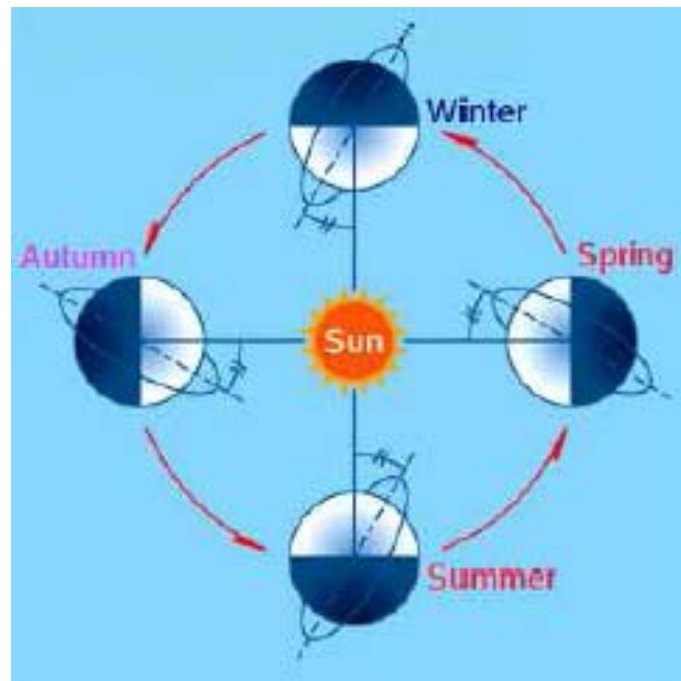


Figure (3-6): Sun-synchronous Orbit [After, Giannoni, F., 2006].

Examples of Polar Orbiting Satellites in Orbits include:

POES, DMSP, Landsat, SPOT, IRS, etc.

[http://geog.tamu.edu/~liu/courses/g489/note7_1.pdf]

3.4 Image Resolution

Resolution (or resolving power) is a measure of the ability of an optical system to distinguish between signals that are spatially near or spectrally similar. In remote sensing, there are four types of resolutions to be considered [*Jensen, 1996*]. This will be explained in the following subsections.

3.4.1 Spatial Resolution

The spatial resolution is the minimum ground area observed by the instrument from a fixed altitude at a fixed moment. It is measured as the size of a pixel on the ground (also called GSD - Ground Sample Distance), when the image is displayed at full resolution [*Giannon, F., 2006*].

The spatial resolution of the satellite imagery is classified in the following Table:

Table (3-1): Spatial resolution class [*After, Giannon, F., 2006*].

spatial resolution [m]	class
< 1	very high
1 - 5	high
5 - 20	mean
20 - 50	low
> 50 m	very low

High-resolution imagery allows details, like houses and cars, to be seen sharply and clearly, Figure (3-7). This type of imagery is often used for community and urban planning and for agricultural purposes. Imagery of lower resolution can be used when studying or planning larger regions on the earth, such as a country and state.

[www.csc.noaa.gov/products/sccoasts/html/tutlid.htm]



80m pixel size

30m pixel size

10m pixel size

Figure (3-7): Illustrates the different image resolutions

3.4.2 Spectral Resolution

The spectral resolution of a remote sensing system can be described as its ability to distinguish different parts of the range of measured wavelengths [Randall B. Smith,2006]. The spectral resolution depends on the kind of sensor, the satellite sensor usually acquires the image in panchromatic, multispectral or hyperspectral mode:

- Panchromatic sensor is sensitive to all wavelengths of visible and near-infrared; the final image is in black and white
- Multispectral sensor can distinguish different spectral bands in the visible and near-infrared; an image is created for each individual wavelength interval
- Hyperspectral sensor is an advanced multispectral sensor; it can detect hundreds of very narrow spectral bands throughout the visible, near-infrared and mid-infrared [Giannon,F.,2006].

3.4.3 Temporal Resolution

In addition to spatial, spectral, and radiometric resolution, the concept of temporal resolution is also important to consider in a remote sensing

system. The revisit period of a satellite sensor is usually several days. Therefore the absolute temporal resolution of a remote sensing system to image the exact same area at the same viewing angle a second time is equal to this period. However, the actual temporal resolution of a sensor depends on a variety of factors, including the satellite/sensor capabilities, the swath overlap, and latitude.

The ability to collect imagery of the same area of the Earth's surface at different periods of time is one of the most important elements for applying remote sensing data. Spectral characteristics of features may change over time and these changes can be detected by collecting and comparing multi-temporal imagery. By imaging on a continuing basis at different times we are able to monitor the changes that take place on the Earth's surface, whether they are naturally occurring (such as changes in natural vegetation cover or flooding) or induced by humans (such as urban development or deforestation).

3.4.4 Radiometric Resolution

Radiometric is the number of data bits used to represent the intensity of the signal arriving at the sensor (a 4 bit representation or 16 levels of the full range from full brightness to full darkness is much less than that in an 8 bit or 256 levels radiometric resolution instrument) the different Radiometric Resolutions are illustrated in Figure (3-8) [*Walton B. Campbell et. al., 1997*].



2-bit image



8-bit image



Figure (3-8): The Different Radiometric Resolutions

3.5 Scanner Sensor Systems

In the following sections, the two scanning features, (whiskbroom and pushbroom principle), will be explained.

3.5.1 Across-track (Whiskbroom) Scanners

Across-track scanners scan the Earth in a series of lines Figure (3-9). The lines are oriented perpendicular to the direction of motion of the sensor platform (i.e. across the swath). Each line is scanned from one side of the sensor to the other, using a rotating mirror. As the platform moves forward over the Earth, successive scans build up a two-dimensional image of the Earth's surface. So, the Earth is scanned point by point and line after line. The incoming reflected or emitted radiation is separated into several spectral components that are detected independently. A bank of internal detectors, each sensitive to a specific range of wavelengths, detects and measures the energy for each spectral band and then, as an electrical signal, they are converted to digital data and recorded for subsequent computer processing [Aggarwal,S.,1997].

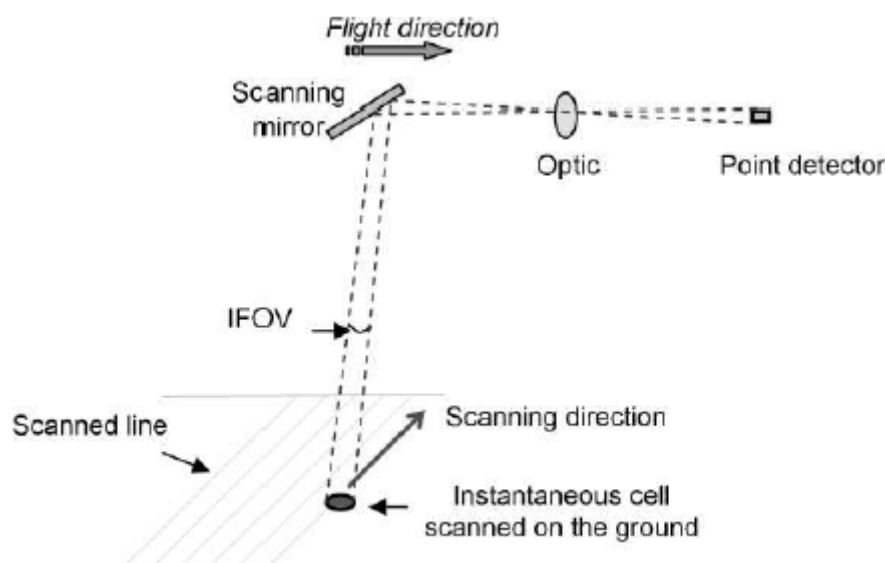


Figure (3-9): Whiskbroom Principle of Image Acquisition

[After, Giannon,F.,2006].

Whiskbroom scanners with their moving mirrors tend to be large and complex to build (e.g. on LANDSAT). The moving mirrors create spatial distortions that must be corrected with preprocessing by the data provider before image data is delivered to the user. An advantage of whiskbroom

scanners is that they have fewer sensor detectors to keep calibrated as compared to other types of sensors [www.amesremote.com/section2.htm]

3.5.2 Along-track (pushbroom) Scanners

Another type of scanner, which does not use rotating mirrors, is the pushbroom scanner also referred to as an along-track scanner (e.g. on SPOT) [www.amesremote.com/section2.htm]. In the pushbroom scanner the acquisition of the image comes with one or more CCD linear arrays, each for each spectral band, placed in the focal plane of optical system. The CCD linear array is perpendicular with respect to the flight direction.

As in whiskbroom sensors, the progressive movement of the platform allows the arrays to acquire a scene Figure (3-10). The length of array projected through the optical system defines the swath width and the dimension of a single CCD element defines the dimension of ground resolution cell [*Giannon,F.,2006*].

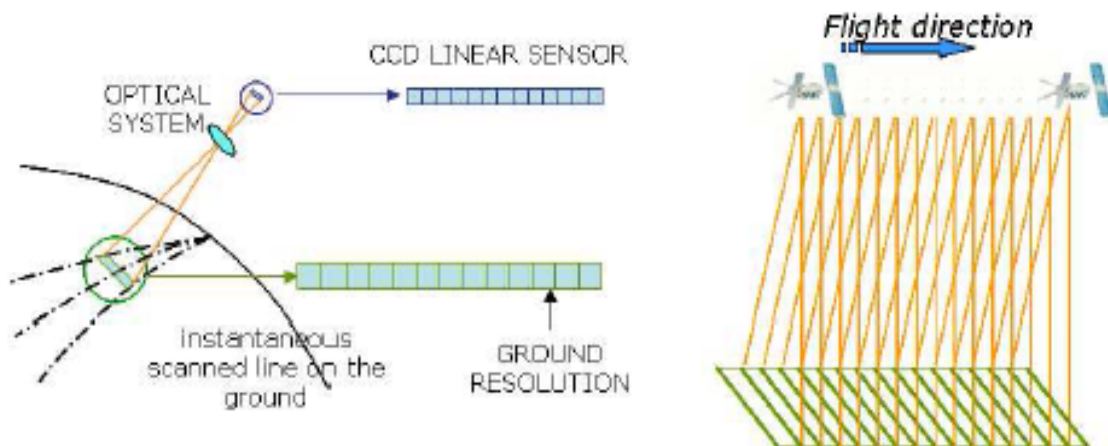


Figure (3-10): Pushbroom Principle of Image Acquisition

[After, *Giannon,F.,2006*].

Pushbroom scanners are lighter, smaller and less complex because of fewer moving parts than whiskbroom scanners. Also they have better radiometric and spatial resolution. A major disadvantage of pushbroom

scanners is the calibration required for a large number of detectors that make up the sensor system [www.amesremote.com/section2.htm].

3.6 Digital Image and Processing

3.6.1 Characteristics of Digital Image

While aerial photography produces analogue images of the terrain, that is, an image represented by continuous variation in tone, images obtained by satellite remote sensing are digital. Digital images are reduced into numbers arranged in two-dimensional matrix (or raster data) of individual picture elements, known as pixels Figure (3-11). When an image is represented as numbers, brightness can be manipulated. Digital images have advantages over analogue film images because computers can store, process, enhance, analyze, and render images visible on a computer screen [*Campbell, J. B., 2002*].

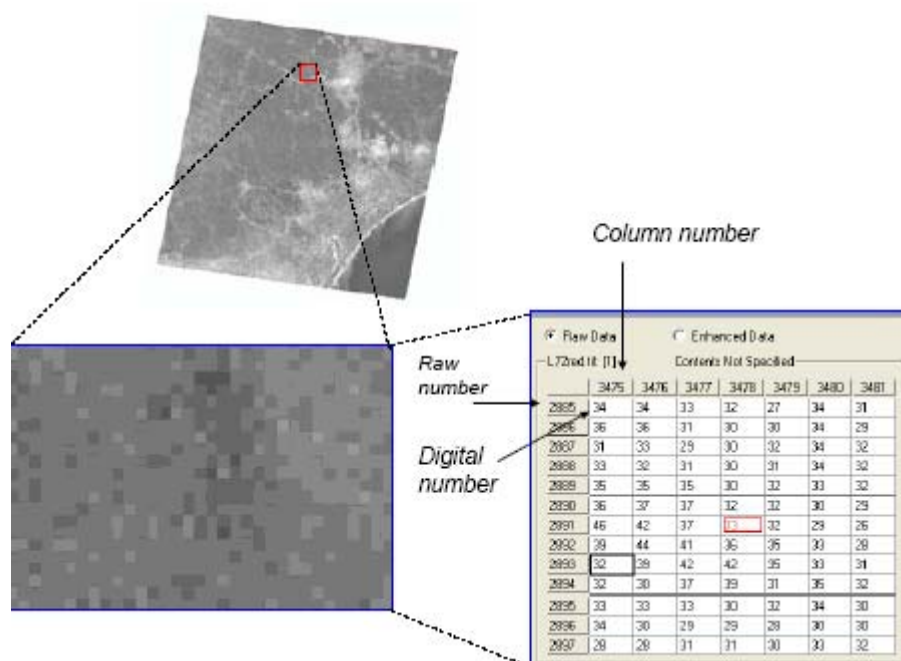


Figure (3-11): Characteristics of Digital Image [*After, Campbell, 2002*].

Each pixel represents an area on the earth's surface and stores two information: (1) the intensity value or pixel value and (2) location address numbers (given by its row and column number) [Franklin, 2001].

3.6.2 Image Processing and Analysis

3.6.2.1 Preprocessing: Error Correction

Preprocessing operations, sometimes referred to as image restoration and rectification, are intended to correct for sensor- and platform-specific radiometric and geometric distortions of data. Preprocessing operations also referred to registration of image [Ouattara, T. et. al., 2004]. Image restoration, which comprehend radiometric and geometric corrections are generally done by the image provider before delivering the data to the costumer [Pereira, C., 2006].

3.6.2.1.1 Radiometric Corrections

A) Variations in Illumination and Viewing geometry Between Images

Variations in illumination and viewing geometry between images (for optical sensors) can be corrected by modeling the geometric relationship and distance between the area of the Earth's surface imaged, the sun, and the sensor [Ouattara, T. et. al., 2004].

B) Atmospheric Correction

The radiance values registered by the sensors do not directly reflect the ground reflectance because of the light scattering of a constantly changing atmosphere, also known as haze. Haze has an additive effect resulting in higher digital number values, decreasing the general contrast of the image [Pereira, C., 2006].

C) Noise

Noise in an image may be due to irregularities or errors that occur in the sensor response and/or data recording and transmission. Common forms of noise include systematic striping or banding and dropped lines Figure (3-12a) and (3-12b).

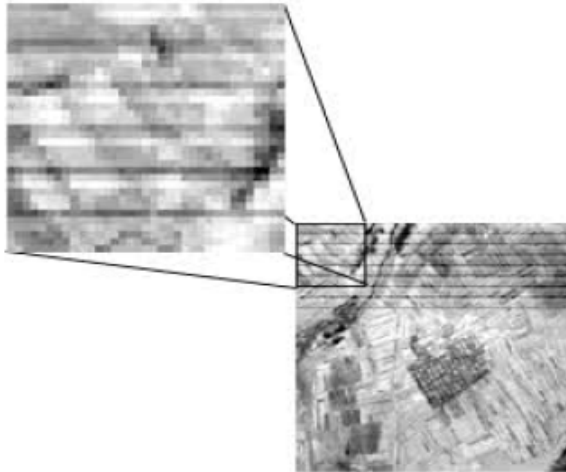


Figure: (3-12a) Striping

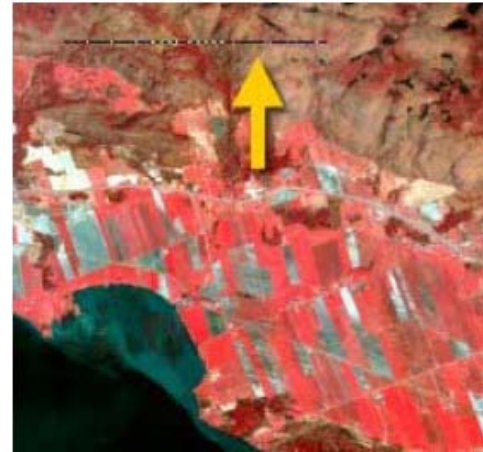


Figure: (3-12b) Dropped lines

[After, Ouattara, T. et. al., 2004].

D) Analog-to-Digital Conversion

For many quantitative applications of remote sensing data, it is necessary to convert the digital numbers to measurements in units which represent the actual reflectance from the surface. This is done based on detailed knowledge of the sensor response and the way in which the analog signal (i.e. the reflected or emitted radiation) is converted to a digital number, called analog-to-digital (A-to-D) conversion. By solving this relationship in the reverse direction, the absolute radiance can be calculated for each pixel, so that comparisons can be accurately made over time and between different sensors *[Ouattara, T. et. al., 2004].*

3.6.2.1.2 Geometric Correction

The distortions may be due to several factors, including: the perspective of the sensor optics; the motion of the scanning system; the motion of the platform; the platform altitude, attitude, and velocity; the terrain relief; and, the curvature and rotation of the Earth. Geometric corrections are intended to compensate for these distortions so that the geometric representation of the imagery will be as close as possible to the real world. Many of these variations are systematic, or predictable in nature and can be accounted for by accurate modeling of the sensor and platform motion and the geometric relationship of the platform with the Earth. Other unsystematic, or random, errors cannot be modeled and corrected in this way. Therefore, geometric registration of the imagery to a known ground coordinate system must be performed.

The geometric registration process involves identifying the image coordinates (i.e. row, column) of several clearly discernible points, called ground control points (or GCPs), in the distorted image (A - A1 to A4), and matching them to their true positions in ground coordinates (e.g. latitude, longitude) Figure (3-13). The true ground coordinates are typically measured from a map (B - B1 to B4), either in paper or digital format. This is image to-map registration. Once several well-distributed GCP pairs have been identified, the coordinate information is processed by the computer to determine the proper transformation equations to apply to the original (row and column) image coordinates to map them into their new ground coordinates. Geometric registration may also be performed by registering one (or more) images to another image, instead of to geographic coordinates. This is called image-to-image registration [Ouattara, T. et. al., 2004].

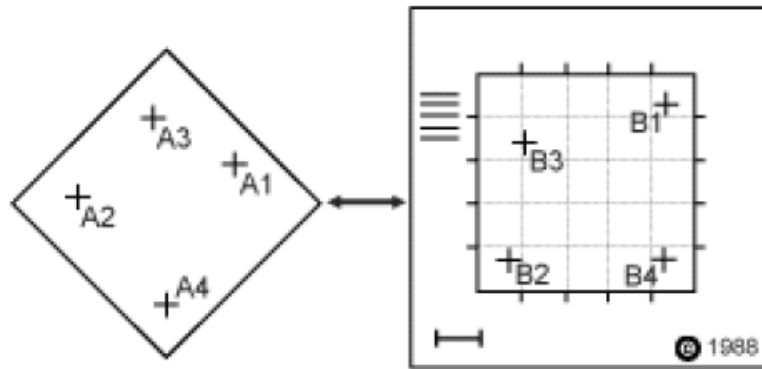


Figure (3-13): Principle of Geometric Correction

[After, Ouattara, T. et. al., 2004].

In order to actually geometrically correct the original distorted image, a procedure called resampling is used to determine the digital values to place in the new pixel locations of the corrected output image. The resampling process calculates the new pixel values from the original digital pixel values in the uncorrected image. There are three common methods for resampling: nearest neighbor, bilinear interpolation, and cubic convolution [Ouattara, T., et. al., 2004].

A) Nearest Neighbour Resampling

In nearest neighbour resampling the DN value of the closest neighbour is chosen as the DN for the new image. In Figure (3-14) the actual location of a pixel is w, however the closest pixel in the original image is d. The DN value is therefore taken from d [Zhou.Q.,1999].

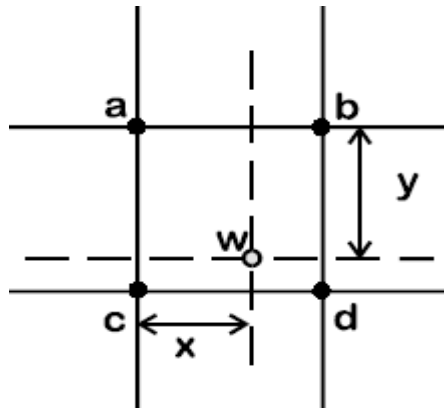


Figure (3-14): Nearest Neighbour Method [After, Zhou.Q., 1999].

B) Bilinear Interpolation

Uses the proximity-weighted for the 4 nearest pixels in the original image around to the output pixel location [Lillesand, 2001].

The new DN is essentially a weighted average of the neighbouring points. Figure (3-15) shows how a DN for point w is determined first by estimating u and v, where u is the weighted average of a and b, and v is the weighted average of c and d. The distance between all points are known. The final value for w is calculated from the weighted average of u and v [Zhou.Q.,1999].

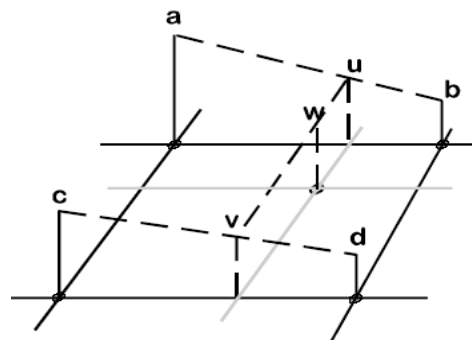


Figure (3-15): Bilinear Interpolation Method [After, Zhou.Q., 1999].

C) Cubic Convolution

The cubic convolution resampling algorithm which weighted averages the 16 closest pixels from the targeted pixel Figure (3-16) [Lillesand, 2001].

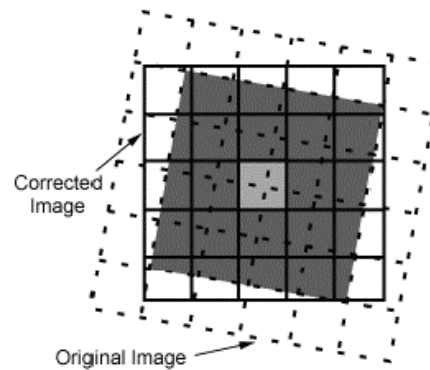


Figure (3-16): Cubic Convolution Method

[After, Ouattara, T., et. al., 2004].

Since the 2D models do not use elevation information, the accuracy of the resulting rectified image will depend on the image viewing/look angle and the terrain relief. On the other hand, 3D models take into account the elevation distortion, a DEM is thus needed to create precise orthorectified images. This rectification should then be called an orthorectification. But if no DEM is available, different altitude levels can be input for different parts of the image (a kind of rough DEM) to minimize this elevation distortion [Touti.T.,2004].

3.6.2.2 Image Enhancement

That is the enhancement of image features through several techniques such as contrast and stretching in order to prepare the data to be easily interpreted [Lillesand, 2001].

3.6.2.3 Image Transformations

Image transformations typically involve the manipulation of multiple bands of data, whether from a single multispectral image or from two or more images of the same area acquired at different times (i.e. multitemporal image data). Image transformations generate "new" images from two or more sources, which highlight particular features or properties of interest, better than the original input images.

3.6.2.4 Texture Analysis

Texture is the spatial variation of tones in an image. Image texture may be qualitatively described as having properties like fineness, coarseness, smoothness, granulation, randomness, lineation, mottled, irregular, hummocky.

3.6.2.5 Data Integration

A) Image Fusion

Image fusion, also called pan-sharpening, is a technique used to integrate the geometric detail of a high-resolution panchromatic (Pan) image and the color information of a low-resolution multispectral (MS) image to produce a high-resolution MS image. This technique is particularly important for large-scale applications [*Zhang,Y.,2004*].

B) Image and Auxiliary Data Integration

Combining data of different types and from different sources is the pinnacle of data integration and analysis. Generally one uses the GIS to combine or integrate the auxiliary and image data.

3.6.2.6 Information Extraction

In remote sensing, there are two great methods of extraction of information (or classification) from an image:

3.6.2.6.1 Visual Interpretation

Recognizing targets is the key to image visual interpretation. Observing the differences between targets and their backgrounds involves comparing different targets based on any, or all, of the visual elements of tone, shape, size, pattern, texture, shadow, and association. One uses the same methods like in photo-interpretation [*Ouattara, T. et. al., 2004*].

3.6.2.6.2 Automatic Classification

Automatic classification uses the spectral information represented by the digital numbers in one or more spectral bands, and attempts to classify each individual pixel based on this spectral information [*Ouattara, T. et. al., 2004*].

There are two main groups of classification, which are known as supervised and unsupervised classification.

3.6.2.6.2.1 Unsupervised Classification

Unsupervised classification, sometimes referred to as clustering, uses the identification of natural groups, or clusters present in the multi-spectral image without prior knowledge of data. This classification technique does not use training data as the basis of classification. The pixels with similar spectral characteristics are grouped into unique clusters according to some statistically determined criteria [*Jensen, 1996*].

Clustering algorithms use predefined parameters to identify cluster locations in data space, and then to determine whether individual pixels

are in those clusters or not. In many algorithms the number of clusters may be defined at the start, while others just use cluster size and separation parameters to control the number of clusters that are found [Zhou,Q., 1999]. In addition to specifying the desired number of classes, the analyst may also specify parameters related to the separation distance among the clusters and the variation within each cluster [Drobnjak,S., 2006]. Figure (3-17) illustrates the type of parameters that can be used to define clusters, and whether pixels belong in that cluster. Clustering algorithms either pass once through the data, grouping pixels during that pass, or they pass through a number of times to adjust and improve the clustering assignments [Zhou, Q., 1999].

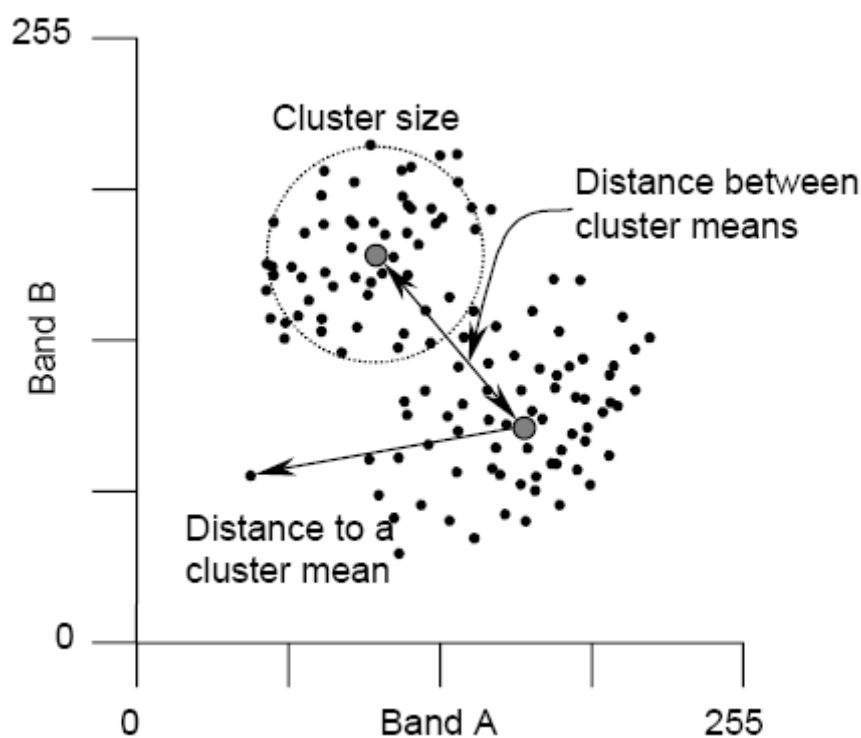


Figure (3-17): Measures that Define A cluster Include the Size of A cluster and the Distance Between Clusters [After, Zhou.Q., 1999].

Unlike the supervised classification, the classes that result from unsupervised classification are spectral classes. Because they are solely

based on the clusters in the image values, the identity of the spectral classes is not initially known. The analyst must compare the classified data with some form of reference data to determine the identity and informational value of the spectral classes [Zhou, Q., 1999].

The analyst may merge or split and recode some clusters in order to assign meaningful information class. Moreover, the analyst may repeat the clustering process with different number of output classes depending on his field experience and ground truth knowledge

[www.gitta.info/PrimSources/en/multimedia/remotesensing.pdf].

The K-means and ISODATA algorithms have been widely used as unsupervised training techniques [Hung, 1992].

A- ISODATA Method

The ISODATA method uses minimum spectral distance to assign a cluster for each candidate pixel. This algorithm is iterative in that it repeatedly performs an entire classification and recalculates statistics. Three parameters must be specified for ISODATA clustering:

- N – The maximum number of clusters to be considered. Since each cluster is the basis for a class, this number becomes the maximum number of classes to be formed;
- T – A convergence threshold, which is the maximum percentage of the pixels whose class values are allowed to be unchanged between iterations; and
- M – The maximum number of iterations to be performed. ISODATA process, Figure (3-18) begins by determining N arbitrary cluster means. The spectral distance between the candidate pixel and each cluster

means is calculated. The pixel is assigned to the cluster whose mean is the closest.

After each iteration, the means for each cluster are recalculated, based on the actual spectral locations of the pixels in the clusters, causing them to shift in feature space.

Then these new means are used for defining clusters in the next iteration. The entire process is repeated-each candidate pixel is compared to the new cluster means, and assigned to the closest cluster mean. The process will terminate until either the convergence threshold T or the maximum number of iterations M is reached.

The ISODATA method has three major advantages. First, Clustering is not geographically biased to the top or bottom pixels of the data file, because it is iterative. Second, this algorithm is highly successful at finding the spectral clusters that inherent in the data. It does not matter where the initial arbitrary cluster means are located, as long as enough iterations are allowed. Third, the resulting thematic raster layer from ISODATA clustering method is similar to using minimum distance classifier. This thematic layer can be used for analyzing and manipulating the signatures before actual classification is performed.

Time consuming is a major disadvantage of this algorithm. Obviously, this is a result of the iterations needed. Another deficit of the ISODATA clustering method is that it does not account for pixel spatial homogeneity [ERDAS Field Guide 1997].

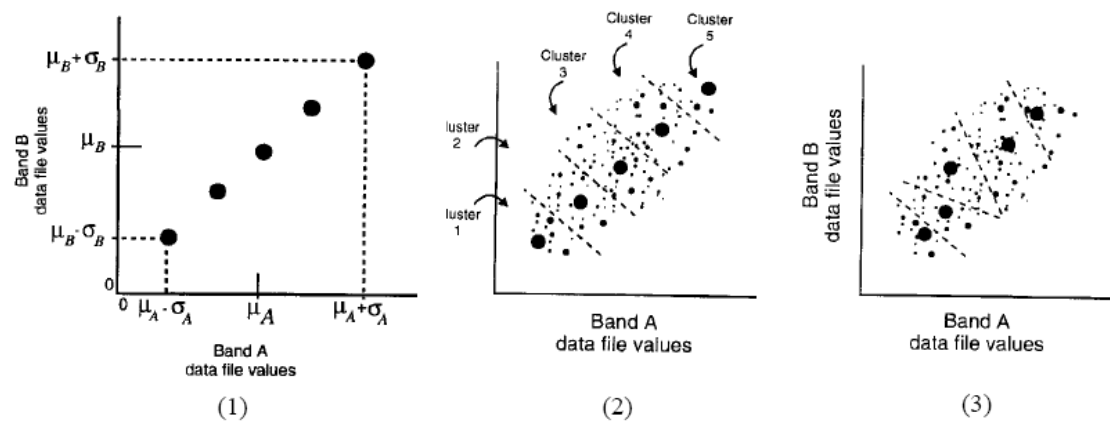


Figure (3-18): ISODATA Clustering Procedure

B- K-Means Method

K-Means unsupervised classification calculates initial class means evenly distributed in the data space, then iteratively clusters the pixels into the nearest class using a minimum-distance technique. Each iteration recalculates class means and reclassifies pixels with respect to the new means. All pixels are classified to the nearest class unless a standard deviation or distance threshold is specified, in which case some pixels may be unclassified if they do not meet the selected criteria. This process continues until the number of pixels in each class changes by less than the selected pixel change threshold or the maximum number of iterations is reached.

[http://faculty.missouristate.edu/x/XinMiao/class/GRY551/Classification_Methods.pdf].

3.6.2.6.2.2 Supervised Classification

The supervised classification relies on the analyst who provides the ‘training’ for computers to recognize different cover types. Usually there are three basic steps involved in a typical supervised classification procedure, namely training, classification and output [Zhou.Q.,1999].

In the training stage (1), the analyst identifies representative training areas and develops a numerical description of the spectral attributes of each land cover type of interest in the scene. Next, in the classification stage (2), each pixel in the image data set is categorized into the land cover class it most closely resembles. If the pixel is insufficiently similar to any training data set, it is usually labeled "unknown". The category label assigned to each pixel in this process is then recorded in the corresponding cell of an interpreted data set. Thus, the multidimensional image matrix is used to develop a corresponding matrix of interpreted land cover category types. After the entire data set has been categorized, the results are presented in the output stage (3) Figure (3-19) [El-Gafy, M., 2005].

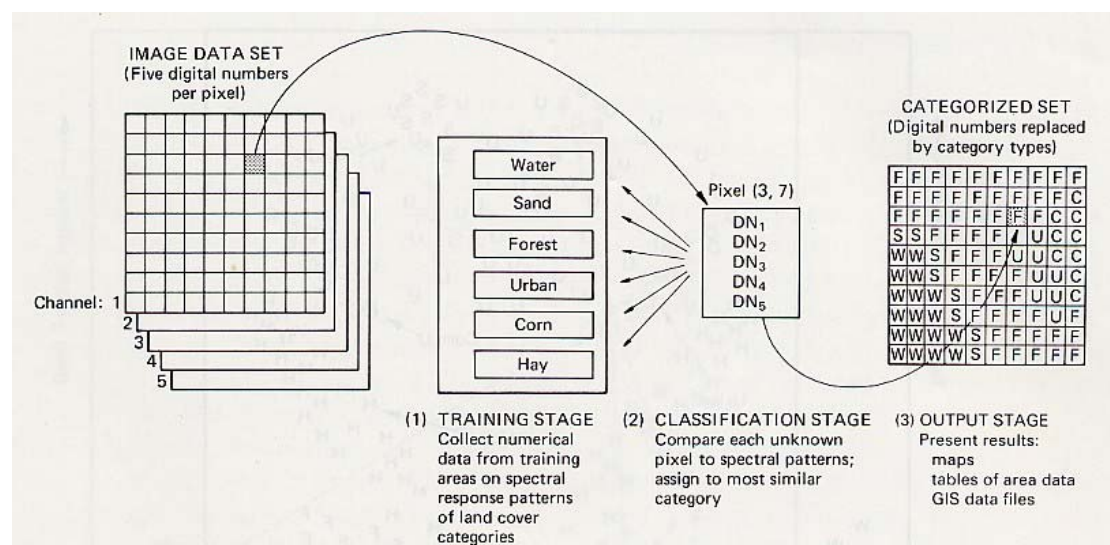


Figure (3-19): Summarizes the Three Basic Steps Involved in A typical Supervised Classification Procedure [After, Kumar, M., 1997].

The most common classification methods used for the classification of remote sensing data are Maximum likelihood, Mahalanobis distance, Minimum distance, and Parallelepiped classifications.

A- Non-Parametric Classification Techniques:

A nonparametric classifier uses a set of nonparametric signatures to assign pixels to a class based on their location, either inside or outside the area in the feature space image. A nonparametric signature is based on an AOI that you define in the feature space image for the image file being classified.

1- Parallelepiped: or the “Box Decision Rule Classifier”

There are upper and lower limits for every signature in every band. Figure (3-20) is a two-dimensional example of a parallelepiped classification. The large rectangles are called parallelepipeds [Erlangung,Z.,1999]. An unknown pixel is classified if it lies inside any of the parallelepipeds, If the pixel does not lie inside any of the regions defined by the parallelepipeds, such pixels are of unknown type [Pal,M.,2002].

The limits for every signature can be either the minimum and maximum data file values of each band in the signature, the mean of each band, plus and minus a number of standard deviations, or any limits that the user specifies, based on the user's knowledge of the data and signatures [Erlangung,Z.,1999].

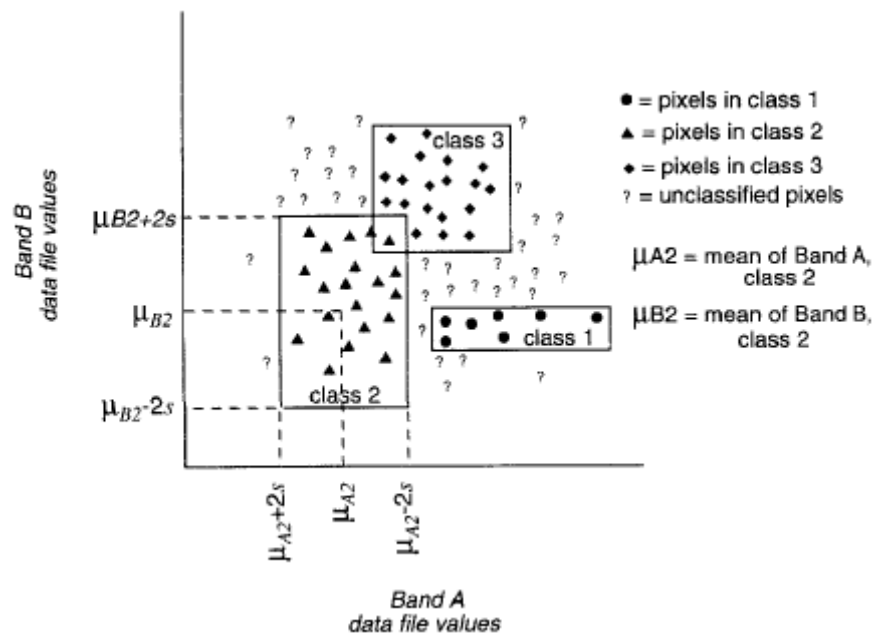


Figure (3-20): Parallelepiped Classification Using Plus or Minus Two Standard Deviations as Limits [After, *ERDAS Field Guide 1997*].

The parallelepiped classifier is a very simple, and fast supervised classifier [Erlangung,Z.,1999]. Because of its simplicity several drawbacks are apparent. Firstly gaps are possible between parallelepipeds. Pixels that fall outside of these regions will not be classified [Richards, 1999]. The second problem occurs when a pixel lies inside two or more overlapping parallelepipeds, which makes the labeling process difficult. Classification of such pixels and allotting these pixels to their correct class is of great importance, as overlapping parallelepipeds are common in remotely sensed data analysis. Several suggestions have been made to overcome this problem. The easiest way for these types of problems is to allocate the pixel to the first or some other arbitrary-selected parallelepiped inside whose boundaries it falls. The problem with this approach is to select the correct parallelepiped and there is no rule that can be used to find out the correct parallelepiped. The second

solution is to employ another, generally more complicated, decision rule, such as to calculate *[Pal,M.,2002]*.

B- Parametric Classification Techniques

Parametric methods of supervised classification take a statistical approach. A parametric signature is based on statistical parameters (e.g., mean and covariance matrix) of the pixels that are in the training sample or cluster. A parametric signature includes the following attributes in addition to the standard attributes for signatures:

- The number of bands in the input image (as processed by the training program)
- The minimum and maximum data file value in each band for each sample or cluster (minimum vector and maximum vector)
- The mean data file value in each band for each sample or cluster (mean vector)
- The covariance matrix for each sample or cluster
- The number of pixels in the sample or cluster

1- Minimum Distance Classifier

The mean spectral value in each band for each information class is determined. These spectral values comprise the mean vector for each class *[Lillesand,2001]*. The minimum distance decision rule calculates the spectral distance between the measurement vector for the pixel to be classified and the mean vector for each signature, Figure (3-21) *[Erlangung,Z.,1999]*. The unclassified pixel is assigned to class

membership based on the closest mean class value, or minimum distance [El-Gafy, M., 2005].

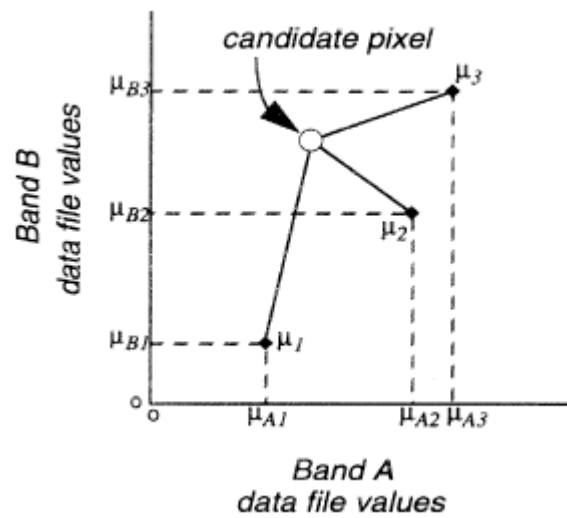


Figure (3-21): Minimum Spectral Distance [After, *ERDAS Field Guide 1997*].

The equation for classifying by spectral distance is based on the equation for Euclidean distance

$$SD_{xyc} = \sqrt{\sum_{i=1}^n (\mu_{ci} - X_{xyi})^2} \quad (3-1)$$

where:

n : number of bands (dimensions)

i : a particular band

c : a particular class

X_{xyi} : data file value of pixel x,y in band i

μ_{ci} : mean of data file values in band i for the sample for class c

SD_{xyc} : spectral distance from pixel x,y to the mean of class c

When spectral distance is computed for all possible values of c (all possible classes), the class of the candidate pixel is assigned to the class for which SD is the lowest [*Swain and Davis, 1978*].

There are no unclassified pixels in the minimum distance classification as every pixel is spectrally close to one sample mean. Minimum distance is a fast decision rule.

A disadvantage of this technique is that pixels which should be unclassified, because they are not spectrally close to the mean of any sample, will become classified. This problem can be alleviated by thresholding out the pixels that are farthest from the means of their classes [*Erlangung, Z., 1999*].

Thresholding is the process of identifying the pixels in a classified image that are the most likely to be classified incorrectly. These pixels are put into another class (usually class 0). These pixels are identified statistically, based upon the distance measures that were used in the classification decision rule [*ERDAS Field Guide, 2005*].

Another limitation of this method is that it does not consider class variability. For example, an urban class may be improperly classified, because an urban area consists of pixels with high variance, which may tend to be far from the mean of the signature. Inversely, a class with less variance, like water, may tend to over classify (that is, classify more pixels than are appropriate to the class), because the pixels that belong to the class are usually spectrally closer to their mean than those of other classes to their means [*Erlangung, Z., 1999*].

2- Mahalanobis Distance Classifier

The Mahalanobis distance algorithm assumes that the histograms of the bands have normal distributions. In addition to the mean value of the signature class the covariance matrix (covariance and variance) is included in the calculation [Andersen, G., 1998].

Mahalanobis distance is similar to minimum distance, except that the covariance matrix is used in the equation. Variance and covariance are figured in so that clusters that are highly varied lead to similarly varied classes, and vice versa. For example, when classifying urban areas—typically a class whose pixels vary widely—correctly classified pixels may be farther from the mean than those of a class for water, which is usually not a highly varied class [Swain and Davis, 1978].

The equation for the Mahalanobis distance classifier is as follows:

$$D = (X - M_c)^T (Cov_c^{-1}) (X - M_c) \quad (3-2)$$

Where:

D : Mahalanobis distance

c : a particular class

X : the measurement vector of the candidate pixel

M_c : the mean vector of the signature of class c

Cov_c : the covariance matrix of the pixels in the signature of class c

Cov_c^{-1} : inverse of Cov_c

T : transposition function

The pixel is assigned to the class, c , for which D is the lowest [ERDAS Field Guide,2005].

Unlike minimum distance or parallelepiped, the Mahalanobis distance classifier takes into account the variability of classes. It may be more useful than minimum distance in cases where statistical criteria must be taken into account, but the weighting factors that are available with the Maximum Likelihood/Bayesian option are not needed.

There are several disadvantages of the Mahalanobis distance classifier. First, it tends to overclassify signatures with relatively large values in the covariance matrix. If there is a large dispersion of the pixels in a cluster or training sample, then the covariance matrix of that signature will contain large values. Second, it is slower to compute than minimum distance and parallelepiped classifier. Third, Mahalanobis distance is parametric, meaning that it relies heavily on a normal distribution of the data in each band. If this is not the case, better results can be achieved with minimum distance or parallelepiped decision rule [Erlangung,Z.,1999].

3- Maximum Likelihood/Bayesian Classifier

This classification method uses the training data as a means of estimating means and variances of the classes, which are then used to estimate probabilities. Maximum likelihood classification considers not only the mean or average values in assigning classification, but also the variability of brightness values in each class [Campbell,J.,2001].

The maximum likelihood algorithm is the most common decision rule for supervised classification. This decision rule is based on the probability that a pixel belongs to a particular class. It assumes that these

probabilities are equal for all classes, and that the input bands have normal distributions, Figure (3-22) [Erlangung,Z.,1999].

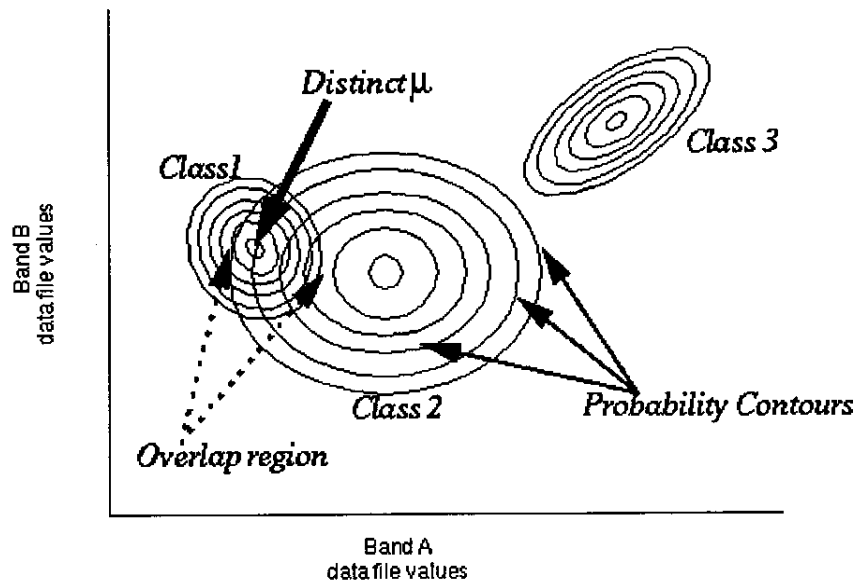


Figure (3-22): Maximum Likelihood Decision Rule

Bayesian Classifier

If you have a priori knowledge that the probabilities are not equal for all classes, you can specify weight factors for particular classes. This variation of the maximum likelihood decision rule is known as the Bayesian decision rule [Hord, 1982]. Unless you have a priori knowledge of the probabilities, it is recommended that they not be specified. In this case, these weights default to 1.0 in the equation.

The equation for the maximum likelihood/Bayesian classifier is as follows:

$$D = \ln(a_c) - [0.5 \ln(|Cov_c|)] - [0.5 (X-M_c)^T (Cov_c^{-1}) (X-M_c)] \quad (3-3)$$

D : weighted distance (likelihood)

c : a particular class

-
- X : the measurement vector of the candidate pixel
- M_c : the mean vector of the sample of class c
- a_c : percent probability that any candidate pixel is a member of class c (defaults to 1.0, or is entered from a priori knowledge)
- Cov_c : the covariance matrix of the pixels in the sample of class c
- $|Cov_c|$: determinant of Covc (matrix algebra)
- Cov_c^{-1} : inverse of Covc (matrix algebra)
- Ln : natural logarithm function
- T : transposition function (matrix algebra)

The pixel is assigned to the class, c, for which D is the lowest.

Disadvantages

- 1- An extensive equation that takes a long time to compute. The computation time increases with the number of input bands.
- 2- Maximum likelihood is parametric, meaning that it relies heavily on a normal distribution of the data in each input band.
- 3- Tends to overclassify signatures with relatively large values in the covariance matrix. If there is a large dispersion of the pixels in a cluster or training sample, then the covariance matrix of that signature contains large values [*ERDAS Field Guide,2005*].

3.6.2.6.2.3 Accuracy Assessment

No classification is complete until its accuracy has been assessed [*Lillisand,2001*]. In this context, the accuracy means the level of agreement between labels assigned by the classifier and the class allocation on the ground collected by the user as test data [*Congalton and*

Green,1998]. The following are two methods commonly used to do the accuracy assessment.

A- Confusion Matrix

The accuracy of classification has traditionally been measured by the overall accuracy by generating a confusion matrix and determining accuracy levels by dividing the total number of correctly classified pixels (sum of major diagonal of confusion matrix, also called actual agreement) by the total number of reference pixels. However as a single measure of accuracy, the overall accuracy gives no insight into how well the classifier is performing for each of the different classes [*Fitzgerald and Lees, 1994*]. In particular, a classifier might perform well for a single class that accounts for a large proportion of the test data and this will create a bias in overall accuracy, despite low class accuracies for other classes. To avoid such a bias when assessing the accuracy of a classifier, it is important to consider the individual class accuracies. Individual class accuracy can be obtained by dividing the total number of correctly classified pixels in that category by the total number of pixels of that category. Individual class accuracy can be determined by using the reference data (called producer's accuracy). The resulting percentage accuracy indicates the probability that a reference pixel will be correctly classified [*Pal,M.,2002*]. The producer's accuracy is a measure of error of omission. However, a misclassification error is not only an omission from the correct class but also a commission into another class. Individual class accuracy obtained from the classified data in that category (user's accuracy) is a measure of error of commission [*Story and Congalton,1986*].

B- Kappa Statistics

Which is an other measure of agreement or accuracy this measure of agreement is based on difference between the actual agreement in error matrix (i.e, the agreement between the remotely sensed classification and the reference data as indicate by the major diagonal) and the chance agreement, which is indicate by the row and column totals [*Geo Yan,2003*]. It provides a better measure of the accuracy of a classifier than the overall accuracy, and it takes into account the whole confusion matrix rather than the diagonal elements alone [*Pal,M.,2002*].

3.6.3 Image Processing Softwares

There are several image processing softwares but the principal are:

- PCI Geomatics: www.pcigeomatics.com
- ERDAS: www.erdas.com/home.asp
- ENVI: www.rsinc.com/envi/index.asp
- IDRISI: www.clarklabs.org [*Ouattara,T., et. al., 2004*].

3.7 Satellite Platforms

Two techniques are used, optical imaging and Radar imaging. Satellite missions of both of them will be illustrated here.

3.7.1 Optical Land Imaging Satellites

This section includes all optical civil land imaging satellites with resolutions equal to or better than 57 meters in orbit or currently planned to be in orbit by 2011. The optical systems can be divided into five resolution groups very high resolution (0.41 to 1m), high resolution (1.8 to 2.5 m), high medium resolution (4 to 8 m), medium resolution (10 to 20 m) and low medium resolution (30 to 56 m).

Table (3-2): Illustrates Very High Resolution Satellites (0.41to1m)

[www.sani-ita.com/pdf/SatelliteGuide.pdf]

SATELLITE	COUNTRY	LAUNCH	PAN RES. M	MS RES. M	SWATH KM
GeoEye-1	US	03/16/07	0.41	1.64	15
WorldView -1	US	07/01/07	0.5	Null	16
WorldView -2	US	07/01/08	0.5	1.8	16
QuickBird-2	US	10/18/01	0.6	2.5	16
EROS B1	Israel	04/25/06	0.7	Null	7
EROS C	Israel	03/21/08	0.7	2.5	16
Pleiades-1	France	07/01/08	0.7	2.8	20
Pleiades-2	France	07/01/09	0.7	2.8	20
IKONOS-2	US	09/24/99	1.0	4	11
OrbView 3	US	06/26/03	1.0	4	8
Resurs DK-1 (01-N5)	Russia	06/15/06	1.0	3	28
KOMPSAT-2	Korea	07/28/06	1.0	4	15
IRS Cartosat 2	India	08/15/06	1.0	Null	10

Table (3-3): Illustrates High Resolution Satellites (1.8 to 2.5m)

[www.sani-ita.com/pdf/SatelliteGuide.pdf]

SATELLITE	COUNTRY	LAUNCH	PAN RES. M	MS RES. M	SWATH KM
EROS A1	Israel	12/05/00	1.8	-	14
FormoSat (RocSat2)	Taiwan	04/20/04	2.0	8	24
THOES	Thailand	06/30/07	2.0	15	22, 90
SPOT-5	France	05/04/02	2.5	10	120
IRS Cartosat 1	India	05/04/05	2.5	Null	30
TopSat (SSTL)	UK	10/27/05	2.5	5	10, 15
ALOS	Japan	01/24/06	2.5	10	35, 70
RazakSat	Malaysia	11/01/06	2.5	5	20
Spain Sat	Spain	07/01/10	2.5	-	

Table (3-4): Illustrates High Medium Resolution Satellites (4 to 8m)

[www.sani-ita.com/pdf/SatelliteGuide.pdf]

SATELLITE	COUNTRY	LAUNCH	PAN RES. M	MS RES. M	SWATH KM
Beijing-1 (SSTL)	China	10/27/05	4.0	32	600
VinSat-1 (SSTL)	Vietnam	11/01/06	4.0	32	600
MTI	US	03/12/00	-	5, 20	12
CBERS-3	China/Brazil	05/01/08	5.0	20	60, 120
CBERS-4	China/Brazil	07/01/10	5.0	20	60, 120
IRS 1C	India	12/28/95	6.0	23	70, 142
IRS 1D	India	09/29/97	6.0	23	70, 142
IRS ResourceSat-1	India	10/17/03	6.0	6, 23, 56	24, 140, 740
IRS ResourceSat-2	India	12/15/06	6.0	6, 23, 56	24, 140, 740
RapidEye- A,B,C,D,E	Germany	06/01/07	-	6.5	78
KOMPSAT-1	Korea	12/20/99	6.6	Null	17
R26m	South Africa	09/01/06	-	7.5	
Proba	ESA	10/22/01	8.0	18, 36	14
MONITOR-E -1	Russia	08/26/05	8.0	20	94, 160

Table (3-5): Illustrates Medium Resolution Satellites (10 to 20m)

[www.sani-ita.com/pdf/SatelliteGuide.pdf]

SATELLITE	COUNTRY	LAUNCH	PAN RES. M	MS RES. M	SWATH KM
SPOT-2	France	01/22/90	10.0	20	120
SPOT-4	France	03/24/98	10.0	20	120
EO-1	US	11/21/00	10.0	30	37
X-Sat	Singapore	04/16/08		10	50
LDCM	US	07/01/11	10.0	30	177
DMC BilSat (SSTL)	Turkey	09/27/03	12.0	26	24, 52
Landsat 7	US	04/15/99	15.0	30	185
TERRA (ASTER)	Japan/US	12/15/99	-	15, 30, 90	60
CBERS-2	China/Brazil	10/21/03	20.0	20	113
CBERS-2B	China/Brazil	06/15/07	20.0	20	113

Table (3-6): Illustrates Low Medium Resolution Satellites (30 to 56 m)

[www.sani-ita.com/pdf/SatelliteGuide.pdf]

SATELLITE	COUNTRY	LAUNCH	PAN RES. M	MS RES. M	SWATH KM
Landsat 5	US	03/01/84	-	30	185
DMC AlSat-1 (SSTL)	Algeria	11/28/02	-	32	600
ThaiPhat (SSTL)	Thailand	12/01/04	-	36	600
DMC NigeriaSat-1 (SSTL)	Nigeria	09/27/03	-	32	600
DMC UK (SSTL)	UK	09/27/03	-	32	600
IRS ResourceSat-1 AWIFS	India	0/17/03	-	56	740
IRS ResourceSat-2 AWIFS	India	12/15/06	-	56	740

3.7.2 Radar Land Imaging Satellites

This section includes radar satellites in orbit or currently planned to be in orbit by 2008.

Table (3-7): Illustrate Radar Satellites

[http://volkskunde.at/alp_2006/report_red_team.pdf]

SATELLITE	COUNTRY	LAUNCH	RES. M	SWATH KM
<i>COSMO-Skymed-1 (military)</i>	Italy	11/1/2006	1.0	10-200
<i>COSMO-Skymed-2 (military)</i>	Italy	5/1/2007	1.0	10-200
<i>COSMO-Skymed-3 (military)</i>	Italy	11/1/2007	1.0	10-200
<i>COSMO-Skymed-4 (military)</i>	Italy	5/1/2008	1.0	10-200
<i>TerraSAR L</i>	Germany	8/15/2008	1.5-30	10-200
<i>TerraSAR X</i>	Germany	10/31/2006	1.5-30	10-200
<i>RadarSat 2</i>	Canada	12/15/2006	3-28-100	20-100-500
<i>RadarSat 1</i>	Canada	11/4/1995	8.5-100	50-500
<i>RISAT</i>	India	1/30/2007	10.0-50.0	10-240
<i>ALOS</i>	Japan	1/24/2006	10-20-100	35-50-70-250
<i>JERS-1</i>	Japan	1992-1998	18	75
<i>ERS-2</i>	ESA	4/21/1995	25	500
<i>ENVISAT</i>	ESA	3/1/2002	30	60-100

3.7.3 Most Common Optical Land Imaging Satellites in Egypt

This section illustrates by details the most common optical land imaging satellites in Egypt.

Table (3-8): QuickBird Satellite

Name:	QuickBird
Launch:	October 18, 2001
Country:	USA
Bands:	1 Panchromatic and 4 Multispectral
Resolutions:	Spatial resolution: For Panchromatic 0.61m at nadir, 0.72m at 25° off-nadir and For Multispectral 2.44 at nadir, 2.88m at 25° off-nadir Spectral resolution: For Panchromatic 450—900 nanometers and For Multispectral Blue: 450—520 nanometers, Green: 520—600 nanometers, Red: 630—690 nanometers, Near-IR: 760—900 nanometers Temporal resolution: 3 - 7 days Radiometric resolution: 11 bits
Stereo Y/N:	Pan(Y) and MS (Y)
Swath Width:	16.5 Km at nadir
Data cost:	Raw: \$14/km ² , Processed: \$24/km ²
Proven uses:	Invasive species mapping, photogrammetric mapping, aerial photo substitute, data fusion with other lower resolution sensors, coastline change, emergency response, coral reef mapping, land cover assessment
Equipment/softw are needed:	Handheld spectrometer desirable, image processing software such as ERDAS Imagine

[www.amsa.gov.au/Marine_Environment_Protection/National_Plan/Environment_and_Scientific_Coordinators_Toolbox/Workshop_Proceedings/2004/Day1/Remote_flyer.pdf].

[www.evergladesplan.org/pm/pm_docs/qasr/qasr_ch_09.pdf].

[www.researchplanning.com/pubs/RemoteSensing.pdf].

[www.realvista.it/products/docs/P_S.pdf].

Table (3-9): IKONOS Satellite

Name:	IKONOS 1, 2
Launch:	launched on September 24, 1999 by the United States (IKONOS 2 failed)
Country:	USA
Bands:	1 Panchromatic and 4 Multispectral
Resolutions:	Spatial resolution: 1 m (panchromatic), 4 m (visible). Spectral resolution: For Panchromatic 450—900 nanometers and For Multispectral Blue: 450—520 nanometers, Green: 520—600 nanometers, Red: 630—690 nanometers, Near-IR: 760—900 nanometers. Temporal resolution: ~ 3 days Radiometric resolution: 11 bits
Sensor:	MMS, PAN
Stereo Y/N:	Pan(Y) and MS (Y)
Swath Width:	11 km x 11 km (Single Scene)
Data cost:	
Proven uses:	Roads, vehicles, buildings, infrastructure (panchromatic) Land use, agricultural uses, vegetation (color imager)
Equipment/software needed:	Image processing software such as ERDAS Imagine

[www.usyd.edu.au/su/agric/acpa/people/james/Thesis/Chapter%203_Taylor2004.pdf].

[www.amsa.gov.au/Marine_Environment_Protection/National_Plan/Environment_and_Scientific_Coordinators_Toolbox/Workshop_Proceedings/2004/Day1/Remote_flyer.pdf].

[http://sedac.ciesin.columbia.edu/remote_sens/RemoteSensing.pdf].

[www.researchplanning.com/pubs/RemoteSensing.pdf].

[www.csc.noaa.gov/crs/rs_apps/sensors/ikonos.htm].

Table (3-10): LANDSAT 7 Satellite

Name:	LANDSAT 7 (1, 2, 3, 6 are inactive)		
Launch:	launched on 15 April 1999		
Country:	USA		
Bands:	1 pan and 7 Multispectral bands		
Resolutions:	Band Number	Spectral resolution	Spectral resolution
	1	0.450-0.515 (B) μm	30 m
	2	0.525-0.605 (G) μm	30 m
	3	0.630-0.690 (R) μm	30 m
	4	0.750-0.900(NIR) μm	30 m
	5	1.550-1.750 (Mid-IR) μm	30 m
	6	10.40-2.50 (Thermal IR) μm	60 m
	7	2.090-2.350 (Mid-IR) μm	30 m
	8	0.52-0.900 (pan) μm	15 m
	Temporal resolution: 16 days Radiometric resolution: 8 bits		
Sensor:	ETM + (Enhanced Thematic Mapper)		
Stereo Y/N:	Pan(N) and MS (N)		
Swath Width:	185 Km		
Data cost:	Raw: \$600/scene		
Proven uses:	Water color, landscape and land use, general vegetation/ecosystem mapping, land change detection, vegetation spatial variation/seasonal dynamics, coastal line change, emergency preparation and damage assessment, regulatory compliance, water permitting		
Equipment/software needed:	Image processing software such as ERDAS Imagine		

[www.evergladesplan.org/pm/pm_docs/qasr/qasr_ch_09.pdf].

[www.amsa.gov.au/Marine_Environment_Protection/National_Plan/Environment_and_Scientific_Coordinators_Toolbox/Workshop_Proceedings/2004/Day1/Remote_flyer.pdf].

[http://sedac.ciesin.columbia.edu/remote_sens/RemoteSensing.pdf].

Table (3-11): SPOT-5 Satellite

Name:	SPOT-5						
Launch:	launched in May 2002,						
Country:	France						
Bands:	(2 HRG): 1 PAN (5m combined to generate 2.5m), 3 MS (10 m), 1 SWIR (20m) (HRS): 1 PAN (10 m) (VEG 2): 3 MS(1000 m), 1 SWIR (1000m)						
Resolutions, Sensor and Swath Width	Sensor	Bands	Spectral	Spatial	Temporal	Swath (km)	
	2 HRG	Pan	0.48 - 0.71 μm	(5 meter), combined to generate a 2.5 meter product	26 day	60	
		green	0.50 - 0.59 μm	10 meter			
		red	0.61 - 0.68 μm	10 meter			
		NIR	0.78 - 0.89 μm	10 meter			
		SWIR	1.58 - 1.75 μm	20 meter			
	HRS	Pan	0.49 - 0.69 μm	(10 meter) (resampled every 5 meter along track)	26 day	120	
	VEG 2	blue	0.45 - 0.52 μm	1 kilometer	1 day	2200	
		red	0.61 - 0.68 μm	1 kilometer			
		NIR	0.78 - 0.89 μm	1 kilometer			
		SWIR	1.58 - 1.75 μm	1 kilometer			
	Radiometric resolution: 8-bits						
	Stereo Y/N:	(Y)					
Data cost:	\$1-3 /km2						
Proven uses:	Topographic Mapping , Cadastral Mapping ,Forecasting Crop Yields, Characterizing Urban Growth, Identification and Monitoring of Disaster-Prone Areas, Emergency Response Planning and Monitoring Land Cover Change						

Equipment/software needed:	<p>Editing and image processing and analysis will require specialized software, including these examples:</p> <ul style="list-style-type: none"> • ESRI products (ArcView, ArcInfo, ArcGIS, etc.) • ERDAS Imagine (OrthoBASE adds more capability when working with SPOT data in Imagine, but is not required) • RSI ENVI • SOCET SET
-----------------------------------	---

[http://calval.cr.usgs.gov/documents/LDGST_overview_LDCM.pdf].

[www.scanex.ru/en/publications/pdf/publication22.pdf].

[www.waterandfood.org/gga/Lecture%20Material/SKSrivastav_Overview.pdf].

[www.csc.noaa.gov/crs/rs_apps/sensors/spot.htm].

3.8 Applications of Remote Sensing

Meteorology - profiling of atmospheric temperature, pressure, water vapor, and wind velocity.

Oceanography - measuring sea surface temperature, mapping ocean currents, and wave energy spectra.

Glaciology - measuring ice cap volumes, ice stream velocity, and sea ice distribution.

Geology - geomorphology, identification of rock type, mapping faults and structure.

Geodesy - measuring the figure of the earth and its gravity field.

Topography and cartography - improving digital elevation models.

Agriculture, forestry, and botany - monitoring the biomass of land vegetation, monitoring the health of crops, mapping soil moisture, forecasting crop yields.

Hydrology - assessing water resources from snow, rainfall and underground aquifers.

Disaster warning and assessment - monitoring of floods and landslides, monitoring volcanic activity, assessing damage zones from natural disasters.

Planning applications - mapping ecological zones, monitoring deforestation, monitoring urban land use.

Oil and mineral exploration - locating natural oil seeps and slicks, mapping geological structures, monitoring oil field subsidence.

Military - developing precise maps for planning, monitoring military infrastructure, monitoring ship and troop movements [*Sandwell,D.,2007*].

Chapter 4

Gravity Field Satellites

Introduction

One of the major tasks of geodesy is the determination of the geoid, which is defined as an equipotential surface of the Earth gravity field, which coincides on average with mean sea level. The geoid surface is more irregular than the ellipsoid of revolution often used to approximate the shape of the physical Earth, but considerably smoother than the Earth's physical surface. Nowadays, GPS positioning can offer accurate ellipsoid height h relative to the ellipsoid. Precise knowledge of the geoid undulation N relative to the ellipsoid can lead to the estimation of orthometric height H by using the equation $h = H + N$ which connects those three values Figure (4-1). Thus, one of the goals of geodesy is to develop a precise geoid model, which can then be used for computing the orthometric heights. The determination and availability of a high-resolution and more accurate geoid model, is a necessity in several geosciences e.g. detecting the variations of the ocean currents, study of the interior properties of the Earth in geophysics, seismology and plate tectonics since it serves as the reference surface for other measurements and phenomena. Geoid is also important information for other disciplines related to Geomatics engineering like navigation, mapping, surveying and construction [*Daras,I.,2008*].

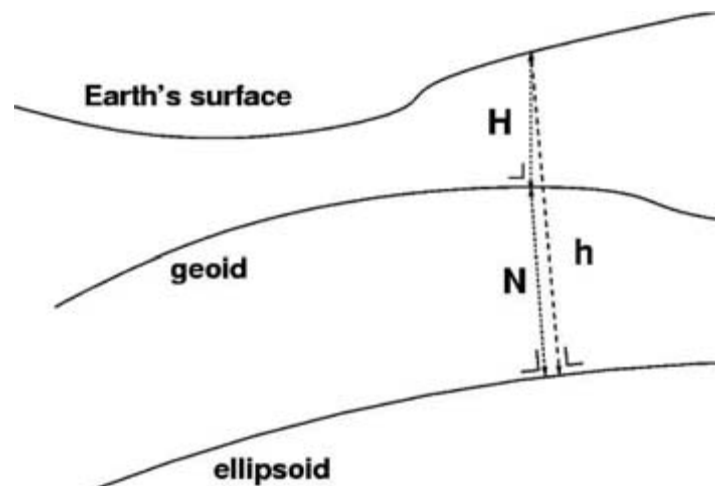


Figure (4-1): The Geoid Height N , the Elevation H Above the Geoid and the Ellipsoidal Height h [Loon,J.,2008].

4.1 Basic Gravity Field Quantities

The gravity potential, W , is the sum of the potential generated by the attraction of masses (V) and the centrifugal potential. Differences between values in two points may be obtained by levelling. A surface where W is equal to a constant is an equipotential surface. Points on one such surface may be determined regionally by tide-gauges, which define regional mean sea level. A height datum is defined by the equipotential surface which best agrees with local mean sea level calculated from tide-gauges for a specific time period. The equipotential surface which approximates the global mean sea level, i.e. a global set of tide-gauges and leveling benchmarks, after subtraction of the dynamic components, is the geoid [Balmino G et. al.,1998].

The mean Earth ellipsoid is an ellipsoid of revolution, rotating with the Earth around its Z -axis, and centered at the Earth's centre of mass. It is determined as the surface which gives best fit in some sense to mean sea-level. The height above this ellipsoid, h , is measured along the normal to the ellipsoid. It is obtained indirectly by satellite positioning from the determined Cartesian coordinates (X,Y,Z). The geoid height, N , is the

height of a point on the geoid above the ellipsoid. It can be observed by determining h by satellite technique at a tide-gauge or at a levelling point. The orthometric height, H , is measured from the geoid along the plumbline (it is often called the height above mean sea-level). It is observed by levelling: the measurements (level differences and gravity) yield the geopotential number which is converted to metric units by dividing by the mean gravity along the plumbline.

Gravity, g , is the magnitude of the gradient of W at the Earth's surface and of V in space. It may be observed by absolute technique (e.g. in a free fall experiment) or relatively (as a difference) by a spring gravimeter. Gravity gradients are derivatives of the gravity vector, i.e. second order derivatives of W . Certain linear combinations may be measured by a torsion-balance at Earth's surface, and by forming differences of accelerometer measurements in space [*Balmino G et. al.,1998*].

A model (normal) gravity potential, U , with the ellipsoid as an equipotential surface, is used to calculate normal gravity, γ . At any point of given latitude and orthometric height, the gravity anomaly Δg is the value derived by subtracting measured and normal gravity ($\Delta g = g - \gamma$). The gravity γ is calculated at a point with the ellipsoidal height put equal to the orthometric height. This is the modern definition of Δg according to Molodensky, which differs from the gravity anomaly at sea level which is still used sometimes. The difference $T = W - U$ is called the anomalous potential. It is small and allows linearization, such as the Bruns equation $N = T/\gamma$, which directly relates potential and geoid height [*Balmino G et. al.,1998*]. The potential V (or T) may be expanded as a series of spherical harmonic functions which are the spherical equivalent of Fourier series in a plane. The coefficients of the series are numbered according to degree and order, l and m respectively ($m \leq l$), which correspond to wave-

numbers in the plane [*Balmino G et. al.,1998*]. In practice the series expansion has to be limited to an upper maximum degree ***lmax***. Today's gravity field models are complete to degree and order 180 or 360, but their accuracy is decreasing for degrees beyond 70 to 80. The following formula shows the connection between the degree ***lmax*** and the spatial resolution ***D***.

$$D[\text{km}] = 20000 / lmax \quad (4-1)$$

For ***lmax*** = 80, we get a spatial resolution of about 250 km. Comparing this resolution with the requirements of different applications (cf. Table 1.1), we see that most of the applications need a resolution up to 100 km, which corresponds with to a degree of ***lmax*** = 200 [*Christoph,2005*].

4.2 Gravity Field Determination from Satellite Data

The big advantage of satellite gravity data is that we can obtain a global coverage of the Earth. By tracking the orbit of a satellite, one can strengthen the estimation of the low-degree part of the gravitational field and fill in the gaps in some remote areas. Altimetry is an accurate technique to obtain an estimate of the geoid in the oceanic regions. A constellation of multiple satellites, with an inter-satellite tracking, is able to obtain the temporal changes in the gravity field and gradiometry is used to estimate the high-degree spherical harmonics of the Earth's gravitational field. In this section, we will shortly discuss the different measurement techniques used in satellite gravity modeling [*Loon,J.,2008*].

Table (4-1): The Requirements for Several Geoscientific Branches
Expressed in Terms of Geoid Height and Gravity Anomaly Accuracies

[After, Rebhan et. al.,2000]

Application	Accuracy		Spatial Resolution (half wavelength - D) [km]
	Geoid [cm]	Gravity [mgal]	
<i>Solid Earth</i>			
Lithosphere and upper-mantle density structure		1-2	100
Continental lithosphere			
sedimentary basins		1-2	50-100
rifts		1-2	20-100
tectonic motions		1-2	100-500
seismic hazards		1	100
Ocean lithosphere and interaction with asthenosphere		0.5-1	100-200
<i>Oceanography</i>			
Short-scale	1-2		100
	0.2		200
Basin-scale	~ 0.1		1000
<i>Ice Sheets</i>			
Rock basement		1-5	50-100
Ice vertical movements	2		100-1000
<i>Geodesy</i>			
Levelling with GPS	1		100-1000
Unification of world-wide height systems	1		100-20000
Inertial Navigation System		~1-5	100-1000
Orbits (1 cm radial orbit error for altimetric satellites)	~1-3		100-1000
<i>Sea-level Change</i>	Many of the above applications, with their specific requirements, are relevant to studies of sea-level change.		

4.2.1 Satellite Tracking

The orbit of a satellite is highly influenced by the gravity field of the Earth. Inversely, a time series of the position of a satellite can give extra information on this gravity field.

4.2.1.1 Satellite Laser Ranging (SLR)

Satellite laser ranging is the most accurate technique (within the centimeter level) to determine the position of a satellite. It measures the round trip time of pulses of light to satellites equipped with retro-reflectors. With a network of ground stations measuring the distances to the satellite, one can determine the position of the satellite's centre of mass very precisely.

Some satellites, e.g., LAGEOS-I (1976-), LAGEOS-II (1992-) and GFZ-1 (1995-1999), have been especially designed for this purpose. The shape of these passive satellites is spherical and they are fully equipped with retro-reflectors. The LAGEOS satellites fly at a high altitude (5, 900 km), increasing their lifetime and improving the lower degrees spherical harmonics. The GFZ-1 satellite flew at a much lower altitude (230 – 398 km), reducing its lifetime considerably [*Loon,J.,2008*].



Figure (4-2): The LAGEOS-I Satellite

4.2.1.2 High-Low Satellite-to-Satellite Tracking (hl-SST)

An alternative method to measure the position of a satellite is to use high-low satellite-to-satellite tracking (hl-SST) by means of GPS measurements. Together with an on board accelerometer to measure the non-conservative forces (mostly atmospheric drag), this hl-SST technique is a highly accurate technique to measure the Earth's gravitational field. A recently launched satellite to have GPS receivers and accelerometer on board is the CHAMP satellite [Reigber et. al., 1999].

4.2.1.2.1 CHAMP

The CHAMP (CHAllenging Minisatellite Payload) mission was proposed by the GeoForschungsZentrum Potsdam in 1994 in cooperation with the German Aerospace Center (Deutsches Zentrum fuer Luft- und Raumfahrt, DLR) and a consortium of industrial companies from the former East and West Germany [Eicker, A., 2008].

The three primary science objectives of the CHAMP mission are to provide

- Highly precise global long-wavelength features of the static Earth gravity field and the temporal variation of this field.
- Unprecedented accuracy global estimates of the main and crustal magnetic field of the Earth and the space/time variability of these field components
- A large number of GPS signal refraction data caused by the atmosphere and ionosphere, which can be converted into temperature, water vapor and electron content [www.lsespace.com/missions/champ.php].

The development and manufacturing phase began in January 1997 resulting in the launch of the CHAMP mission on July 15, 2000, from Plesetsk, Russia. It was launched into a near polar and near circular orbit (inclination of ≈ 87 , eccentricity of ≈ 0.0004) with an original altitude of 454 km Figure (4-3). After seven years in orbit, it has descended to an orbit height of approximately 340 km. The given altitude constitutes a compromise between the research interests of the CHAMP mission comprising gravity, magnetism as well as atmosphere and ionosphere [Eicker,A.,2008].

The latter two would have preferred an even higher orbit, and a rather lower orbit would have been more suitable for gravity field research. The satellite moves with a speed of about 28,000km/h and has a mean period of 1.5 h resulting in approximately 15 revolutions per day.

Concerning the task of gravity field recovery, the satellite itself can be regarded as a sensor. It carries an on-board GPS antenna to enable the determination of the precise orbit by the Global Positioning System. As the satellite's orbit is influenced by gravity field disturbances, the analysis of the orbit data can provide information about the structure of the gravity field. Thus the satellite positions represent the primary observable for the task of gravity field determination. This primary measurement principle is known as satellite-to-satellite tracking in the high-low mode (hl-SST), as the orbit of the low flying CHAMP satellite is determined by the higher-flying GPS satellites [Eicker,A.,2008].



Figure (4-3): The CHAMP Satellites.

The benefit of using hl-SST is that complete orbits will be tracked instead of the limited orbital arcs that can be tracked using ground-based stations Figure (4-4). Another benefit is that the CHAMP satellite will 'see' up to ~12 GPS satellites with a good constellation geometry for complete orbits, while being in a sufficiently low Earth orbit to sense medium frequencies in the Earth's gravity field. The large number of visible GPS satellites with a good geometrical configuration will improve the determination of the CHAMP satellite's orbit from which the gravitational perturbations are inferred [*Featherstone, W., 2003*].

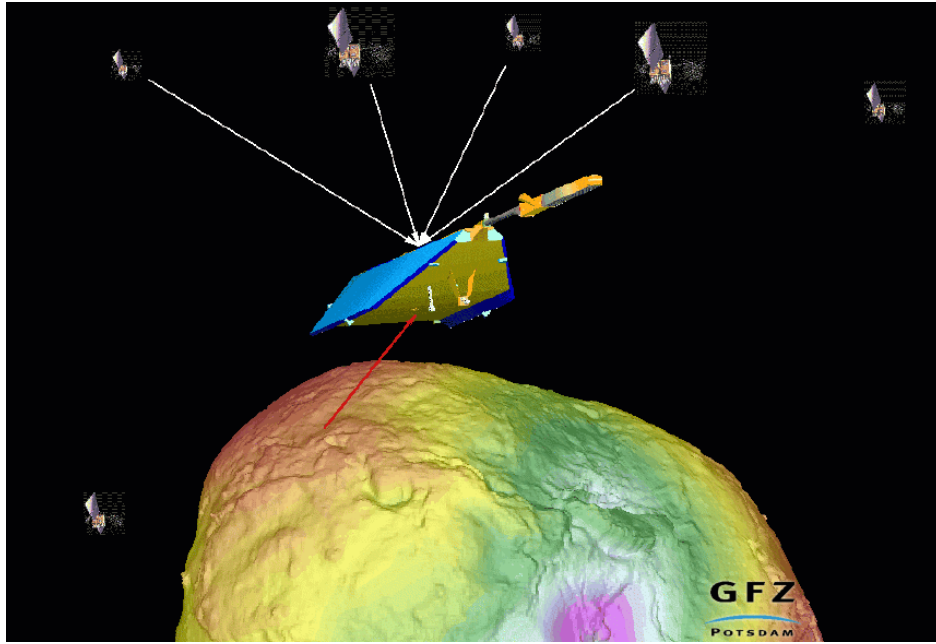


Figure (4-4): GPS-CHAMP High-Low Satellite-to-Satellite and Ground Based Laser Tracking.

Additionally, CHAMP is equipped with an on-board accelerometer to account for non-gravitational forces acting on the satellite such as atmospheric drag, solar radiation, and earth albedo which influence the orbit as well [Eicker, A., 2008]. The Laser Retro-Reflector (LRR) consists of four corner-cube prisms in an array which reflects short laser pulses back to a transmitting ground station. The measurements reflected by the LRR, a technique known as Satellite Laser Ranging (SLR), can be used to validate the GPS-based CHAMP orbit accuracy [Tae-Suk Bae, 2006]. The following section will illustrate CHAMP instrumentation onboard

4.2.1.2.1.1 Spacecraft Components of CHAMP

a- Electrostatic STAR Accelerometer

It serves for measuring the non-gravitational accelerations such as air drag, Earth albedo and solar radiation acting on the CHAMP satellite.

b- GPS Receiver TRSR-2

In combination with the STAR accelerometer it serves as the main tool for high-precision orbit determination of the CHAMP satellite and by this for the Earth's gravity field recovery. The low orbiting CHAMP satellite and each spacecraft of the high orbiting GPS satellite configuration establish a so-called high-low satellite-to-satellite (SST) link. Each of the GPS satellites transmits a PRN modulated L1 and L2 signal which the TRSR-2 receiver acquires for a maximum of 12 satellites at the same time.

c- Laser Retro Reflector

The Laser Retro Reflector is a passive payload instrument consisting of 4 cube corner prisms intended to reflect short laser pulses back to the transmitting ground station. This enables to measure the direct two-way range between a ground station and the satellite with a single shot accuracy of <1 cm without any ambiguities. These data are used for precise orbit determination in connection with GPS for gravity field recovery, calibration of the on-board microwave orbit determination system (GPS) and allows for two-colour ranging experiments to verify existing atmospheric correction models.

d- Fluxgate Magnetometer

The FGM is probing the vector components of the Earth magnetic field. It is therefore regarded as the prime instrument for magnetic field investigations in the CHAMP mission.

e- Overhauser Magnetometer

The purpose of this scalar magnetometer is to provide an absolute in-flight calibration capability for the FGM vector magnetic field measurements.

f- Advanced Stellar Compass

The ASC on the spacecraft body provides attitude data primarily for the three component STAR accelerometer and the Digital Ion Driftmeter. This information is however also required for the proper reduction of GPS data, laser ranging data and attitude control

g- Digital Ion Driftmeter

The purpose of this instrument is to make in-situ measurements of the ion distribution and its moments within the ionosphere [*Reigh.C, et al.,2001*].

4.2.1.2.1.2 Global Gravity Field Models from the CHAMP**1- EIGEN-1S**

EIGEN-1S is first earth gravity field model including CHAMP tracking data. EIGEN-1S model is a combination of

- GRIM5-1S normal equation system
- Lageos-1,-2, Starlette derived constraints on zonals
- additional Lageos-1,-2, Starlette and Stella laser tracking data (year 2000)

- CHAMP GPS satellite-to-satellite tracking data: 88days within the periods 2000, July 30 - Aug. 10, and Sept. 24 - Dec. 31 (accelerometry used for surface force reduction).

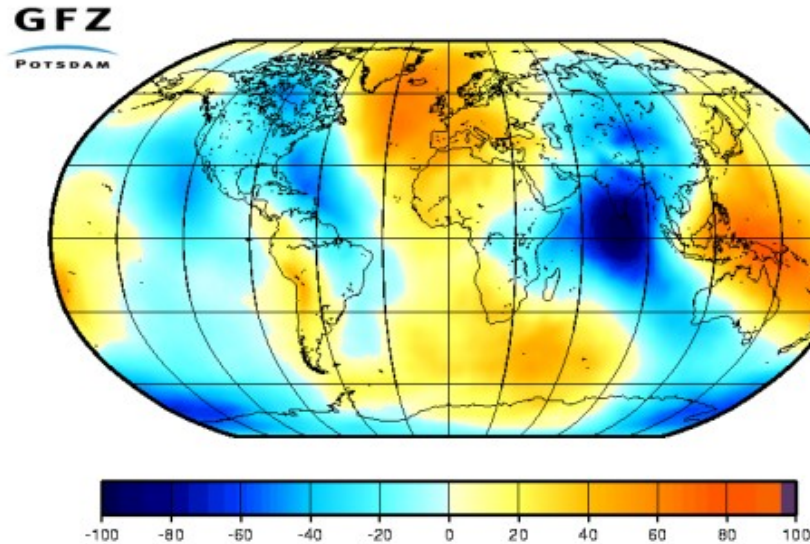


Figure (4-5): EIGEN-1S Geoid ($a=6378136.46$, $1/f=298.25765$) in meter
[\[http://op.fz-potsdam.de/champ/results/index_RESULTS.html\]](http://op.fz-potsdam.de/champ/results/index_RESULTS.html).

GRIM5-S1 is the latest pre-CHAMP satellite-only model (based on tracking data from 24 satellites and multi-year tracking records) [Knig,R et. al.,2004].

Model	Year	Degree	Data
EIGEN-1S	2002	119	GRIM5,S (Champ, Lageos-1,-2, Starlette, Stella)

S=Satellite Tracking Data

[\[http://icgem.gfz-potsdam.de/ICGEM/ICGEM.html\]](http://icgem.gfz-potsdam.de/ICGEM/ICGEM.html)

2- EIGEN-2

EIGEN-2 is CHAMP-only earth gravity field model derived from altogether six months of CHAMP data, EIGEN-2 is a CHAMP-only gravity field model derived from CHAMP GPS satellite-to-satellite and

accelerometer data out of the period 2000, July to December, and 2001, September to December.

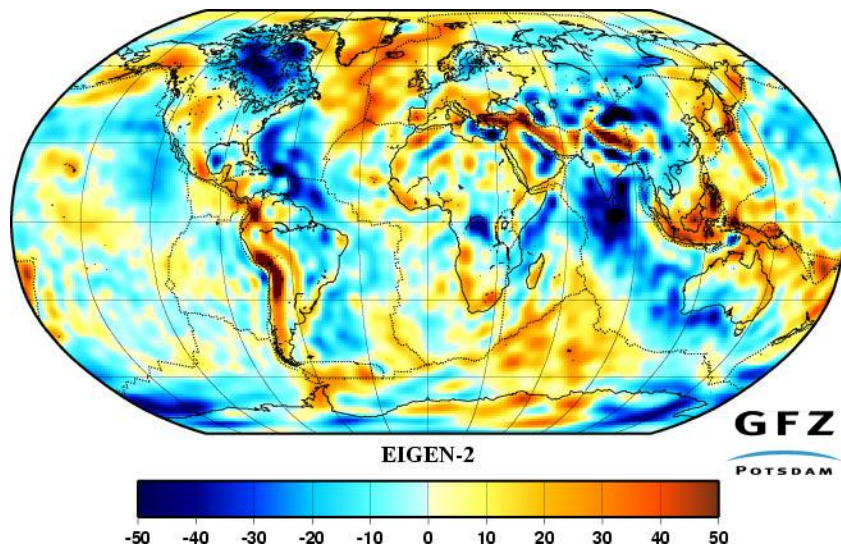


Figure (4-6): EIGEN-2 Gravity Anomalies ($a=6378136.46$, $1/f=298.25765$) in mgal

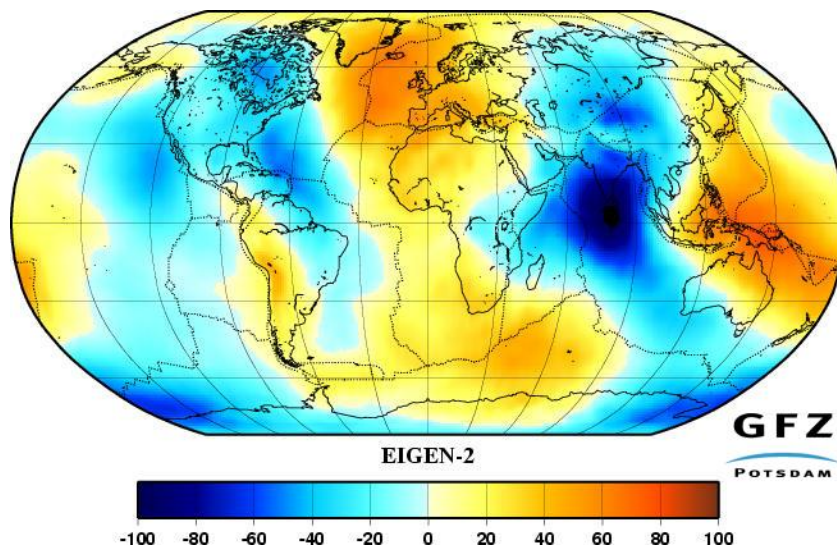


Figure (4-7): EIGEN-2 Geoid ($a=6378136.46$, $1/f=298.25765$) in meter

[http://op.gfz-potsdam.de/champ/results/index_RESULTS.html].

Model	Year	Degree	Data
EIGEN-2	2003	140	S(Champ)

S=Satellite Tracking Data

[\[http://icgem.gfz-potsdam.de/ICGEM/ICGEM.html\]](http://icgem.gfz-potsdam.de/ICGEM/ICGEM.html)

3- EIGEN-3P

EIGEN-3P is CHAMP only earth gravity field model derived from three years of CHAMP data, EIGEN-3p (EIGEN-3 preliminary) is a CHAMP-only gravity field model derived from CHAMP GPS satellite-to-satellite and accelerometer data out of the period July 2000 through June 2003. EIGEN-3p differs from EIGEN-2 not only by the six times larger amount of CHAMP data but also by a different parameterization of the accelerometer calibration parameters (partly, reprocessing ongoing) and a different normal equation regularization (starting at degree 65 instead of 30)

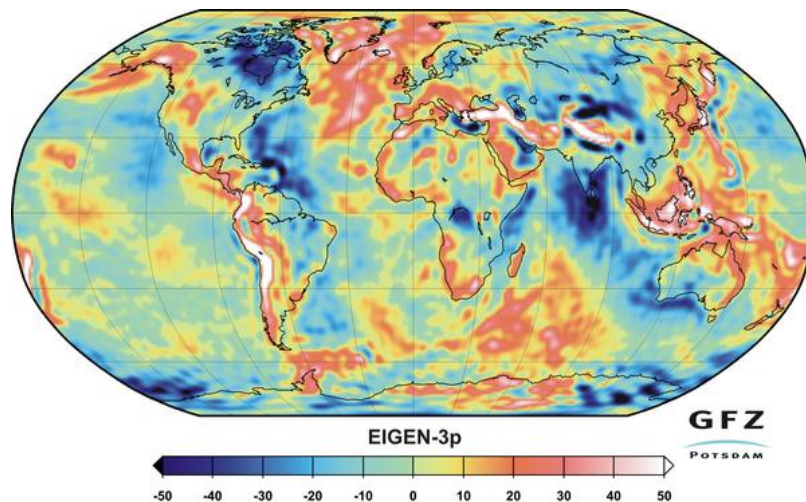


Figure (4-8): EIGEN-3p Gravity Anomalies ($a=6378136.46$,
 $1/f=298.25765$) in mgal

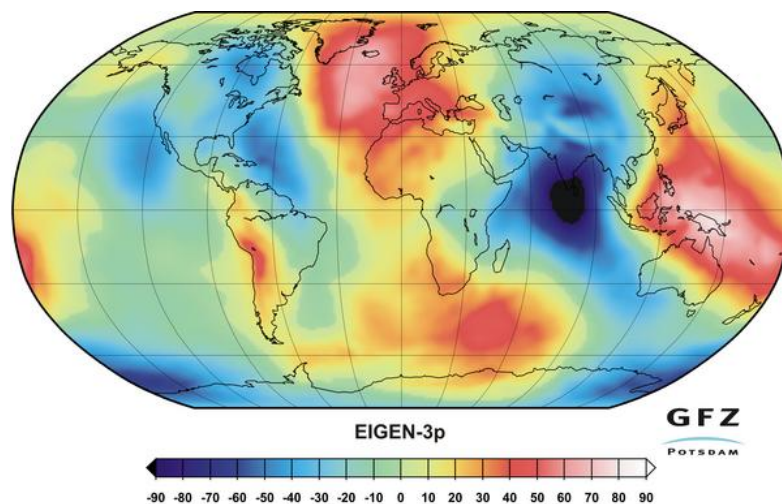


Figure (4-9): EIGEN-3p Geoid ($a=6378136.46$, $1/f=298.25765$) in meter

Model	Year	Degree	Data
EIGEN-3P	2003	140	S(Champ)

[\[http://op.gfz-potsdam.de/champ/results/index_RESULTS.html\]](http://op.gfz-potsdam.de/champ/results/index_RESULTS.html).

4- EIGEN-CHAMP03S

EIGEN-CHAMP03S is CHAMP-only earth gravity field model derived from 33 months of CHAMP data, EIGEN-CHAMP03S is a CHAMP-only gravity field model derived from CHAMP GPS satellite-to-satellite and accelerometer data out of the period October 2000 through June 2003. EIGEN-CHAMP03S is the final version of the preliminary model EIGEN-3p and results from a homogeneous reprocessing of all normal equations including the improved parameterization of the accelerometer calibration parameters. Normal equation regularization starts at degree 60.

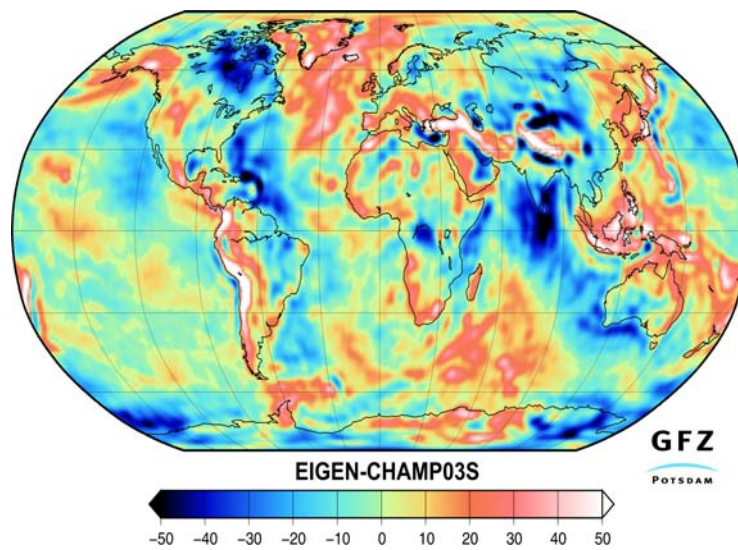


Figure (4-10): EIGEN-CHAMP03S Gravity Anomalies ($a=6378136.46$, $1/f=298.25765$) in mgal

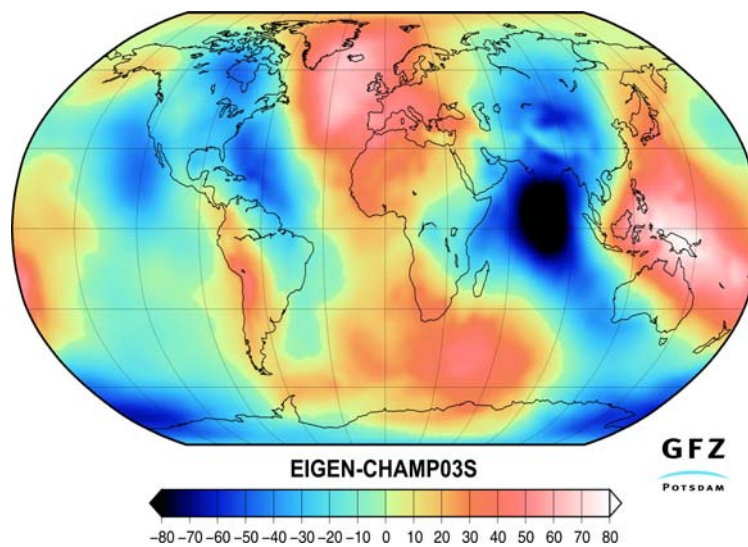


Figure (4-11): EIGEN-CHAMP03S Geoid ($a=6378136.46$, $1/f=298.25765$) in meter

[http://op.gfz-potsdam.de/champ/results/index_RESULTS.html].

Model	Year	Degree	Data
EIGEN-CHAMP03S	2004	140	S(Champ)

Table (4-2) Root Mean Square (RMS) about Mean of GPS / Levelling
Minus Gravity Field Model Derived Geoid Heights [m]

Model	Nmax	USA 6169 points	Canada 1930 points	Europe 1235 points	Australia 201 points
EIGEN1S	119	0.935 m	1.073 m	1.659 m	1.221 m
EIGEN1	119	0.973 m	1.067 m	1.793 m	1.397 m
EIGEN2	140	0.966 m	1.080 m	1.655 m	1.074 m
EIGEN-CHAMP03SP	140	0.823 m	0.861 m	1.440 m	0.853 m
EIGEN-CHAMP03S	140	0.816 m	0.842 m	1.451 m	0.849 m

[<http://icgem.gfz-potsdam.de/ICGEM/ICGEM.html>].

On July 15, 2007, CHAMP has finished its 7th year in orbit. All satellite subsystems, science instruments and ground segment components are performing excellent and are still providing an almost continuous flow of highly valuable gravity, magnetic field and atmosphere sounding observations, two years beyond CHAMP's predicted life time. We can expect that CHAMP will continue to provide highly valuable data for another 2 years from low altitude *[www-app2.gfz-potsdam.de/pb1/op/champ/more/newsletter_CHAMP_016.html].*

4.2.1.3 Low-Low Satellite-to-Satellite Tracking (ll-SST)

A constellation of multiple satellites measuring their mutual distances (ll-SST), combined with an absolute positioning technique (hl-SST / SLR) can improve the estimation of the Earth's gravity field, especially its

temporal variations, considerably [*Jekeli,1999*]. The GRACE mission, launched in 2002, is such a mission, measuring the distance between two low-altitude (≈ 500 km) satellites in identical near-polar orbits [*Tapley et al., 2004a, 2004b*].

4.2.1.3.1 GRACE

The Gravity Recovery and Climate Experiment (GRACE) is a dedicated satellite mission whose objective is to map the global gravity field with a spatial resolution of 400 km to 400,000 km every thirty days. GRACE was launched on March 17, 2002, with an intended lifetime of 5 years [*Watkins et. al., 2000; Tapley et. al.,2001*]. The GRACE mission is a joint project between NASA (National Aeronautics and Space Administration) and DLR (Deutsches Zentrum für Luft- und Raumfahrt). It has been proposed to NASA's Earth System Science Pathfinder project (ESSP) in 1996 [*Tapley.,1996*].

The GRACE mission consists of two identical satellites in near-circular orbits at ~ 500 km altitude and 89.5° inclination, separated from each other by approximately 220 km along-track, and linked by a highly accurate inter-satellite, K-Band microwave ranging system, Figure (4-12). Each satellite, in addition to the inter-satellite ranging system, also carries Global Positioning System (GPS) receivers and attitude sensors [*Dunn et. al., 2003*] and high precision accelerometers [*Touboul et. al.,1999*].

4.2.1.3.1.1 Spacecraft Components

These components are illustrated as follows:

- a- K-Band Ranging System (KBR):** Provides precise (within $10 \mu\text{m}$) measurements of the distance change between the two satellites needed to measure fluctuations in gravity.

-
- b- Ultra Stable Oscillator (USO):** Provides frequency generation for the K-band ranging system.
 - c- Superstar Accelerometers (ACC):** Precisely measures the non-gravitational accelerations acting on the satellite.
 - d- Star Camera Assembly (SCA):** Precisely determines the two satellites orientation by tracking them relative to the position of the stars.
 - e- Coarse Earth and Sun Sensor (CES):** Provides omnidirectional, reliable, and robust, but fairly coarse, Earth and Sun tracking. Used during initial acquisition and whenever GRACE operates in safe mode.
 - f- Center of Mass Trim Assembly (MTA):** Precisely measures the offset between the satellite's center of mass and the "acceleration-proof" mass and adjusts center of mass as needed during the flight.
 - g- Black-Jack GPS Receiver and Instrument Processing Unit (GPS):** Provides digital signal processing; measures the distance change relative to the GPS satellite constellation.
 - h- Globalstar Silicon Solar Cell Arrays (GSA):** Covers the outer shell of the spacecraft and generates power

[www.csr.utexas.edu/grace/gallery/gravity/].

- i- Laser Retro-Reflector (LRR):** The GRACE laser retro reflector (LRR) will be provided by GFZ and is identical with the CHAMP LRR. It is a simple passive payload instrument consisting of 4 prisms manufactured from high-grade fused glass, glued into fixing rings mounted within an aluminium-alloy structure. The LRR is used to reflect short laser pulses of visible or near-infrared wavelengths transmitted by dedicated Laser ground stations. The direct distance can be measured

with an accuracy of 1 - 2 cm (depending on the technological status of the ground station). The LRR data will be used for

- Precise orbit determination in combination with GPS tracking data for gravity field recovery
- Calibration of the on-board GPS Space Receiver,
- Technological experiments such as two-colour ranging

The idea of the two-colour ranging principle is to demonstrate the possibility of differential ranging with a few mm single-shot precision and thus to verify existing tropospheric correction models.

[http://www-app2.gfz-potsdam.de/pb1/op/grace/index_GRACE.html]

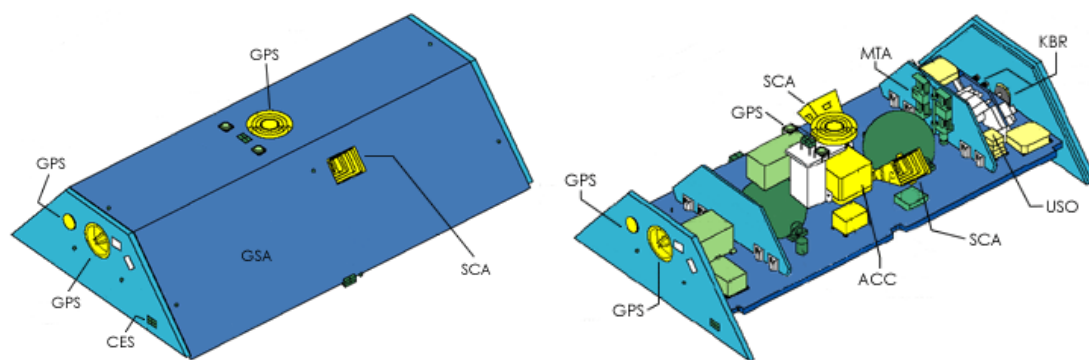


Figure (4- 12): The Components of GRACE

The twin GRACE satellites use the low-low satellite-to-satellite tracking configuration to measure the distance between them. Like CHAMP, the GRACE satellites are also tracked by high-Earth orbiting (GNSS) satellites (hl-SST) giving a near-global coverage. Figure (4-13)

[<http://adt.curtin.edu.au/theses/available/adt.WCU20071112.131832/unrestricted/10appendices.pdf>]. The satellite altitude decays naturally (~30 m/day) so that the ground track does not have a fixed repeat pattern. The satellites are nominally held in a 3-axis stabilized, nearly Earth-pointed

orientation, such that the K-Band antennas are pointed precisely at each other. Except for the K-band ranging system, there is considerable heritage in the satellite design from the CHAMP mission [Reigber *et. al.*,1999].

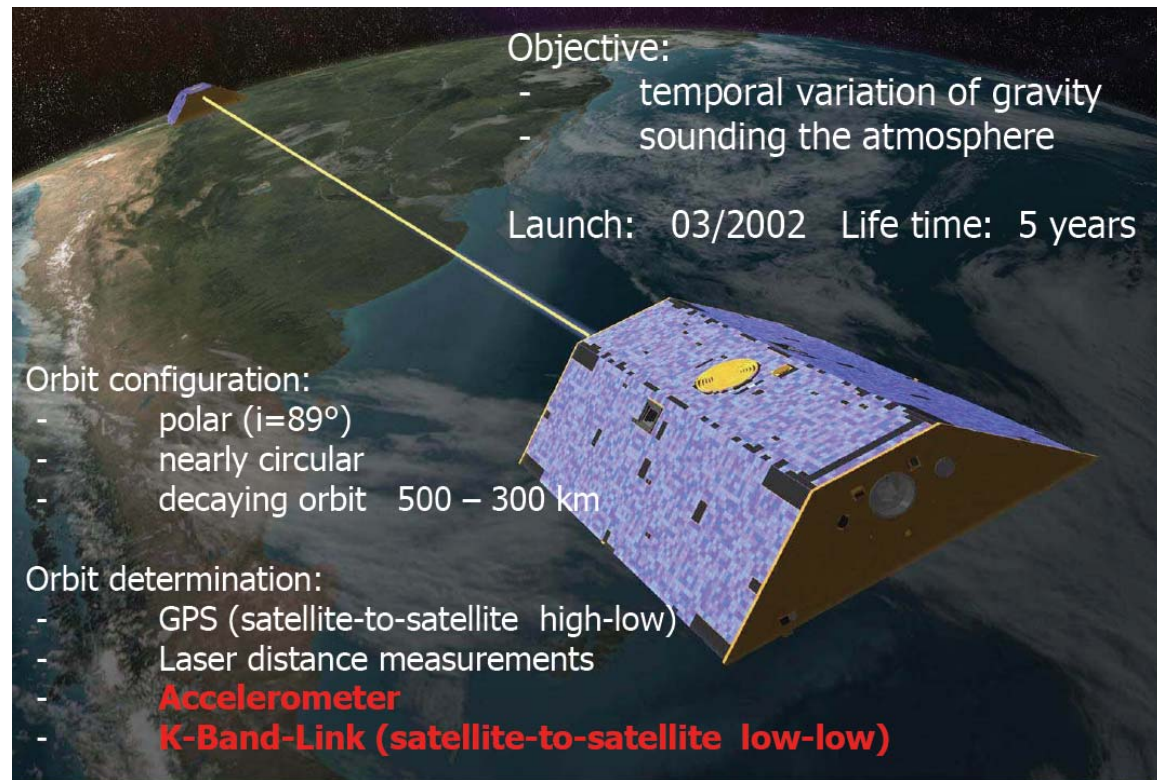


Figure (4-13): The GRACE Satellites

In order to achieve the necessary precision, the dual-frequency one-way K-Band phase measurements transmitted and received by both spacecraft are combined during ground processing to produce an ionosphere-free 'dual one-way range' measurement that largely removes the effects of oscillator instability [Dunn *et. al.*,2003].

The effects of the non-gravitational forces acting on the satellite are removed using the precise accelerometers that measure the surface force acceleration. The GPS receivers on each satellite enable precise time-tagging of the measurements used in extracting the inter-satellite range change and provide absolute positions of the satellites over the earth. The

attitude sensors provide high precision estimates of the inertial orientation of the spacecraft [Tapley, B.D., et. al., 2004].

4.2.1.3.1.2 The Workings of GRACE

GRACE is different from most Earth observing satellite missions, Terra and Aqua for example, because it doesn't carry a suite of independent scientific instruments on board. It does not make measurements of the electromagnetic energy reflected back to it from the Earth's surface. Instead, the two GRACE satellites themselves act in union as the primary instrument. Changes in the distance between the twin satellites are used to make gravitational field measurements.

The two identical satellites orbit one behind the other in the same orbital plane at approximate distance of 220 kilometers (137 miles). As the pair circles the Earth, areas of slightly stronger gravity (greater mass concentration) affect the lead satellite first, pulling it away from the trailing satellite Figure (4-14). As the satellites continue along their orbital path, the trailing satellite is pulled toward the lead satellite as it passes over the gravity anomaly. The change in distance would certainly be imperceptible to our eyes, but an extremely precise microwave ranging system on GRACE detects these minuscule changes in the distance between the satellites. A highly accurate measuring device known as an accelerometer, located at each satellite's center of mass, measures the non-gravitational accelerations (such as those due to atmospheric drag) so that only accelerations caused by gravity are considered. Satellite Global Positioning System (GPS) receivers determine the exact position of the satellite over the Earth to within a centimeter or less. Members of the GRACE science team can download all this information from the

satellites, and use it to construct monthly maps of the Earth's average gravity field during the planned five-year mission

[www.csr.utexas.edu/grace/gallery/gravity/].

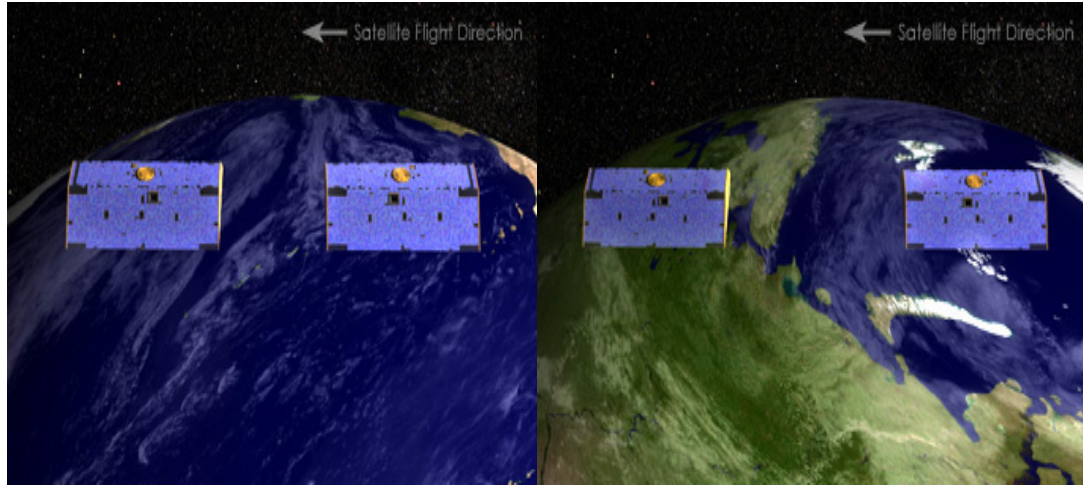


Figure (4-14): Shape of the GRACE Satellites above Different Regions

GRACE provides, for the first time, global coverage of the Earth's gravity field every 30 days from a single source.

GRACE is already able to measure the gravity field with a level of precision that is at least 100 times greater than any existing measurement, and continued improvements are expected as the mission progresses. The finer details of the geoid that have evaded scientists for so long are on the verge of being revealed. GRACE also gives us our best opportunity to date to study time-variable gravity effects. As the mission progresses and more data are added to the model, the resolution of the geoid will improve even further. As the geoid map becomes more detailed, the accuracy of satellite altimetry, synthetic aperture radar interferometry, and digital terrain models covering large land and ice areas all used in remote sensing applications and cartography, will improve. These techniques provide critical input to many scientific models used in

oceanography, hydrology, geology, and related disciplines, and will be used for a variety of applications including:

- Measuring the changing mass of polar ice caps;
- Measuring changes in water resources on land;
- Understanding shallow and deep ocean current transport;
- Understanding sea level change resulting from ocean temperature and water mass changes;
- Understanding atmosphere-ocean mass exchange;
- Understanding the forces that generate Earth's geomagnetic field; and
- Understanding internal Earth forces that move tectonic plates and result in earthquakes and volcanic eruptions

[www.csr.utexas.edu/grace/gallery/gravity/]

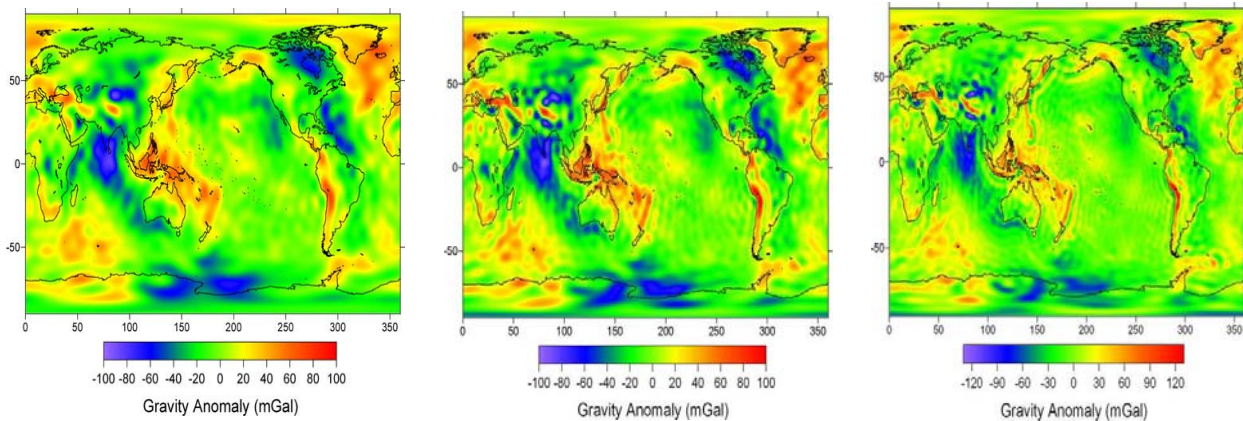
4.2.1.3.1.3 Global Gravity Field Models from GRACE

1- EIGEN-GRACE01S

EIGEN-GRACE01S is the first GRACE gravity model EIGEN-GRACE01S was released on July 25, 2003. It is based on 39 days of preliminary GRACE flight instrument data gathered in August and November 2002. This model is about 5 times more accurate than the latest CHAMP field and about 50 times more accurate than pre-CHAMP satellite only gravity models (at 1000 km half wavelength).

Prior to GRACE and CHAMP, the long-wavelength part of the Earth's gravity field from space was determined from various tracking measurements of a greater number of Earth orbiting satellites. These measurements were of considerably varying vintage and quality, and of incomplete geographical coverage. Consequently the accuracy and resolution of the resulting Earth gravity field models were limited, with

most of the satellite contributions limited to wavelengths of 1000 km or longer. At shorter wavelengths, the errors were too large to be useful. Only broad geological features of the Earth's structure could be detected. As a result, improvements to the Earth gravity models at medium and short wavelengths had to come from the use of measurements of terrestrial, marine- and air-gravimetry also of varying vintage, quality and geographic coverage. Since the launch of CHAMP (CHAllenging Minisatellite Payload Mission) in July 2000 a new epoch in gravity modeling has begun.



Fig(4-15a): Gravity anomaly map derived from tracking data of 30 Earth orbiting satellites over more than 20 years (GRIM5-S1 model)

Fig(4-15b): Gravity anomaly map derived from 16 months of CHAMP data only (EIGEN-CHAMP02S model)

Fig(4-15c): Gravity anomaly map derived from 39 days of GRACE data only (EIGEN-GRACE01S model)

[\[www-app2.gfz-potsdam.de/pb1/op/grace/results/index_RESULTS.html\]](http://www-app2.gfz-potsdam.de/pb1/op/grace/results/index_RESULTS.html)

Model	Year	Degree	Data
EIGEN-GRACE01S	2003	140	S(Grace)

[\[http://icgem.gfz-potsdam.de/ICGEM/ICGEM.html\]](http://icgem.gfz-potsdam.de/ICGEM/ICGEM.html)

2- EIGEN-GRACE02S

EIGEN-GRACE02S is GRACE satellite-only Earth gravity field model complete to degree and order 150 released on February 13, 2004 to the GRACE Science Team and August 9, 2004 to the public. A medium-wavelength gravity field model has been calculated from 110 days of GRACE tracking data, called EIGEN-GRACE02S. The solution has been derived solely from GRACE inter-satellite observations and is independent from oceanic and continental surface gravity data which is of great importance for oceanographic applications, as for example the precise recovery of sea surface topography features from altimetry.

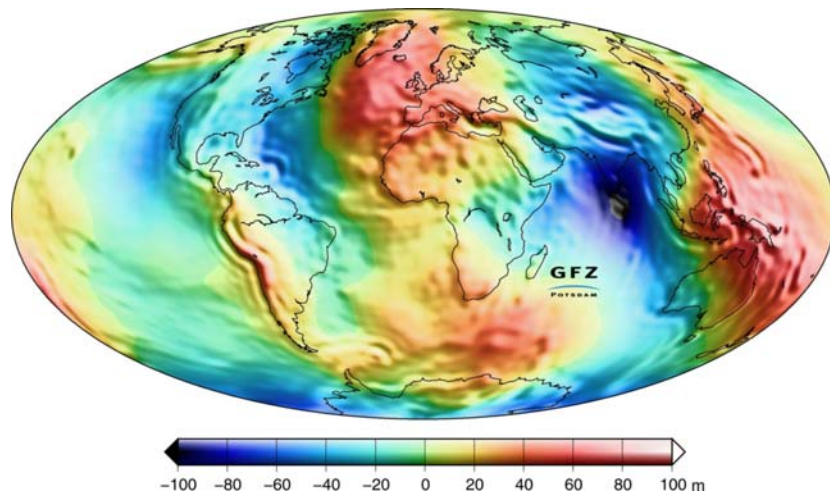


Figure (4-16): EIGEN-GRACE02S Geoid Heights

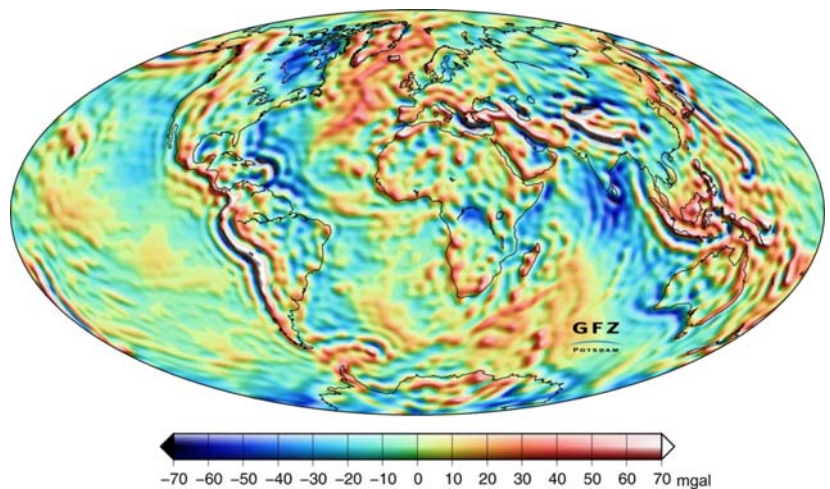


Figure (4-17): EIGEN-GRACE02S Anomalies

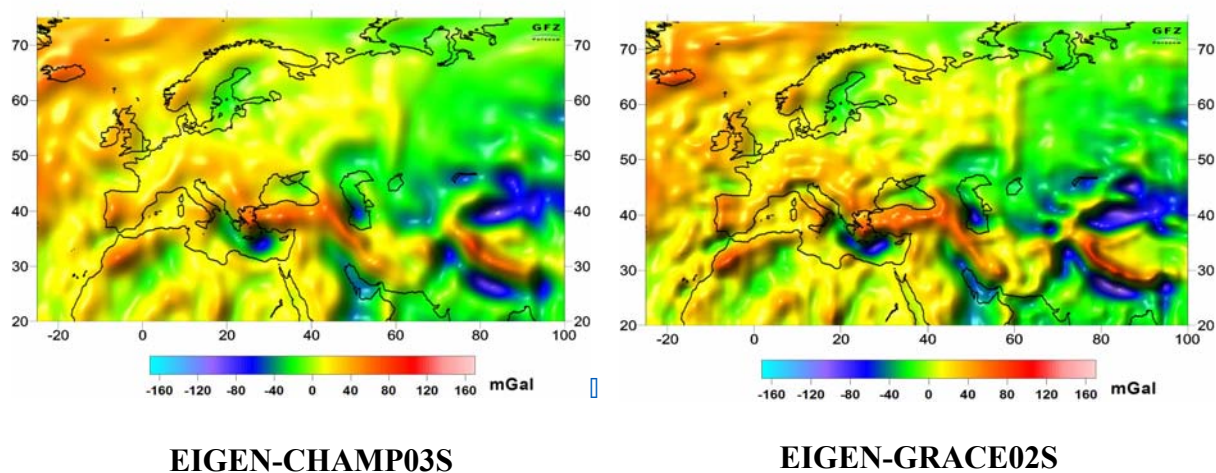


Figure (4-18): Gravity Anomalies (mGal) derived from the EIGEN-CHAMP03S (Left) and EIGEN-GRACE02S (Right) models

Model	Year	Degree	Data
EIGEN-GRACE02S	2004	150	S(Grace)

[\[www-app2.gfz-potsdam.de/pb1/op/grace/results/index_RESULTS.html\]](http://www-app2.gfz-potsdam.de/pb1/op/grace/results/index_RESULTS.html).

3- EIGEN-GL04S1

EIGEN-GL04S1 is Satellite-only gravity model complete to degree and order 150 from GRACE and LAGEOS data, released May 24, 2006. On March 31, 2006 the high-resolution gravity field model EIGEN GL04C has been released. This model is a combination of GRACE and LAGEOS mission plus 0.5 x 0.5 degrees gravimetry and altimetry surface data and is complete to degree and order 360 in terms of spherical harmonic coefficients. High-resolution combination gravity models are essential for all applications where a precise knowledge of the static gravity potential and its gradients is needed in the medium and short wavelength spectrum. Typical examples are precise orbit determination of geodetic and altimeter satellites or the study of the Earth's crust and mantle mass distribution. But, various geodetic and altimeter applications request also

a pure satellite-only gravity model. As an example, the ocean dynamic topography and the derived geostrophic surface currents, both derived from altimeter measurements and an oceanic geoid, would be strongly correlated with the mean sea surface height model used to derive terrestrial gravity data for the combination model.

Therefore, the satellite-only part of EIGEN-GL04C is provided here as EIGEN-GL04S1. The contributing GRACE and Lageos data are already described in the EIGEN-GL04C description. The satellite-only model has been derived from EIGEN-GL04C by reduction of the terrestrial normal equation system and is complete up to degree and order 150 [www-app2.gfz-potsdam.de/pb1/op/grace/results/index_RESULTS.html].

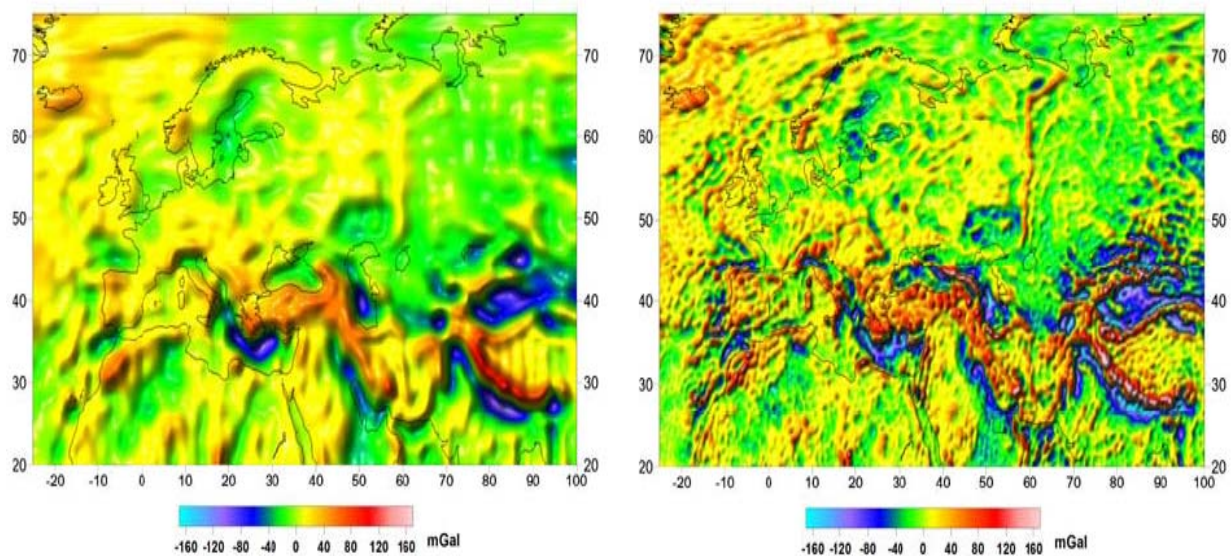


Figure (4-19): Gravity Anomalies (in mgal) Over Europe Derived from the GRACE/LAGEOS Satellite Only Model EIGEN-GL04S1 (Left) and from the Combined Model EIGEN-GL04C (Right) [After, Schmidt, R., et. al.,2007].

Model	Year	Degree	Data
EIGEN-GL04S1	2006	150	S(Grace,Lageos)

(S=Satellite Tracking Data, G = Gravity Data, A = Altimetry Data)

Table (4-3): Root Mean Square (RMS) About Mean of GPS / levelling
Minus Gravity Field Model Derived Geoid Heights [m]

Model	Nmax	USA 6169 points	Canada 1930 points	Europe 1235 points	Australia 201 points
EIGEN-GRACE01S	140	0.765 m	0.705 m	0.936 m	0.553 m
EIGEN-GRACE02S	150	0.739 m	0.643 m	0.828 m	0.538 m
EIGEN-GL04S1	150	0.630 m	0.576 m	0.748 m	0.464 m

[<http://icgem.gfz-potsdam.de/ICGEM/ICGEM.html>]

4.2.1.3.1.4 Combined Global Gravity Field Models from CHAMP and GRACE

1- EIGEN-CG01C

EIGEN-CG01C is combined gravity field model complete to degree and order 360 from CHAMP, GRACE and surface gravity data, released on October 29, 2004.

a. Input Data

CHAMP (860 days) and GRACE (200 days) satellite gravity data have been combined with 0.5 x 0.5 deg surface data (gravimetry and altimetry) to generate the high resolution global gravity field model EIGEN-CG01C

b. Results

Gravitational potential of the Earth in terms of 130317 spherical harmonic coefficients complete to degree and order 360 and resulting representation of the global geoid and the global free air gravity anomalies down to spatial features of 100 km full wavelength.

c. Applications

This highly accurate new gravity field model and global geoid model, respectively, will allow geodesists and cartographers to precisely link the various height datums around the globe together, will allow Space geodesists and satellite operators to determine orbits of near Earth satellites and to navigate satellites with much higher accuracy and will allow solid Earth scientists to much more accurately infer the Earth's internal structure and at finer resolution than was ever before possible from Space. Ocean scientists can combine this gravity model with ocean height measurements from satellite altimeters to study global ocean circulation on a finer scale than has been previously possible .

This will, in turn, enable a better understanding of the processes that drive the Earth's dynamic system (solid Earth, ocean and atmosphere), thus leading to better analysis and predictions of climate change and natural hazards (e.g., Earthquakes).

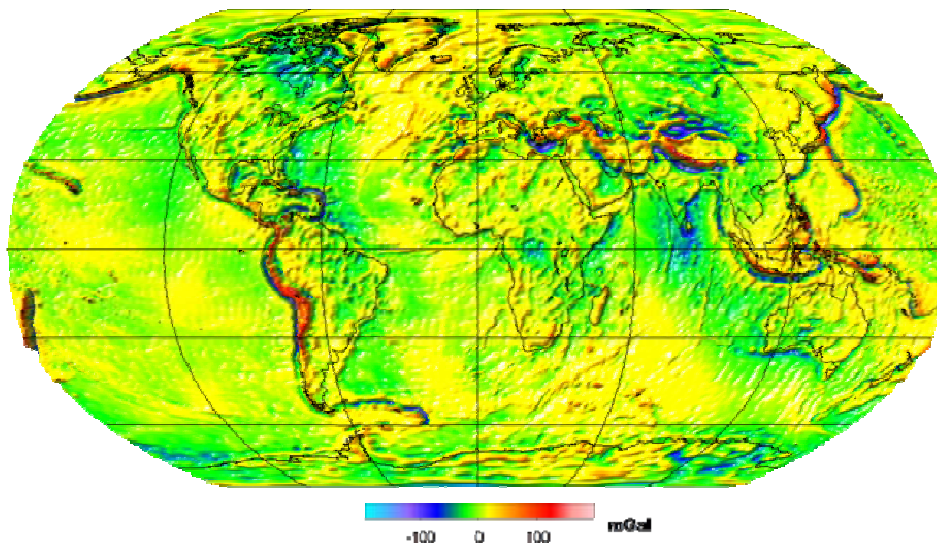


Figure (4-20): EIGEN-CG01C Free Air Gravity Anomalies
[http://op.gfz-potsdam.de/champ/index_CHAMP.html]

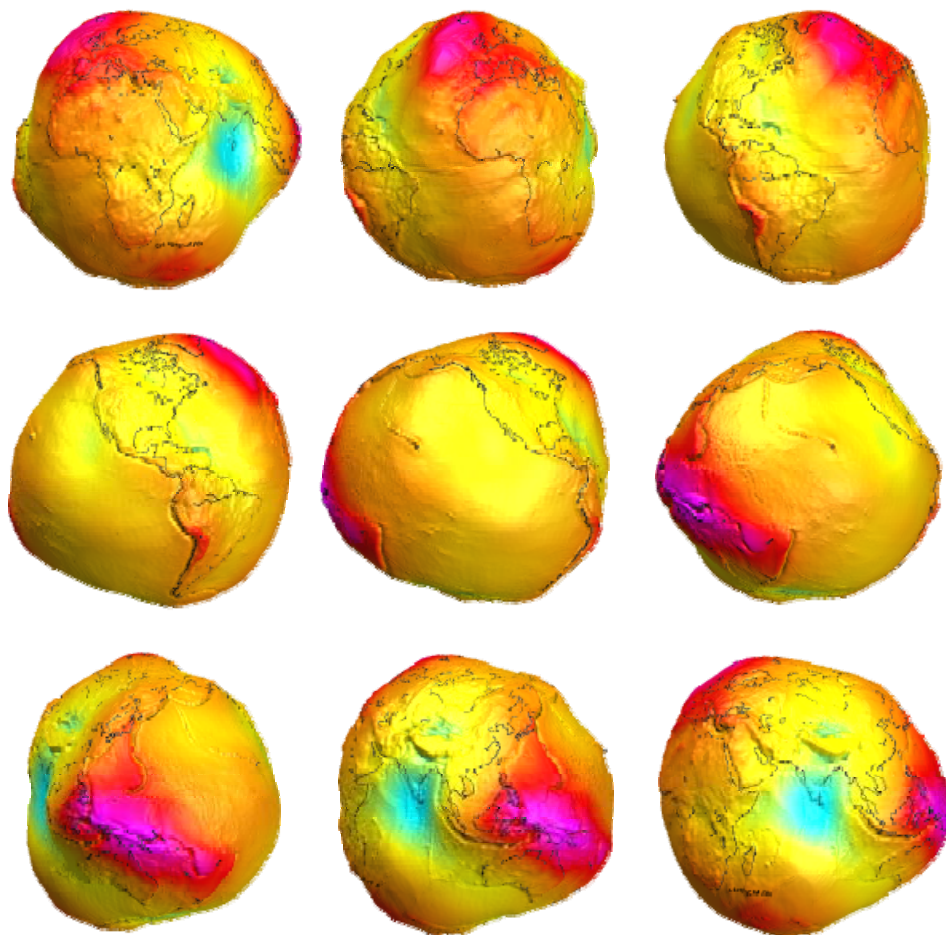


Figure (4-21): EIGEN-CG01C Geoid
[http://op.gfz-potsdam.de/champ/index_CHAMP.html]

Model	Year	Degree	Data
EIGEN-CG01C	2004	360	S(Champ,Grace),G,A

(S=Satellite Tracking Data, G = Gravity Data, A = Altimetry Data)

[<http://icgem.gfz-potsdam.de/ICGEM/ICGEM.html>].

2- EIGEN-CG03C

EIGEN-CG03C is combined gravity field model complete to degree and order 360 from CHAMP, GRACE and surface gravity data, released on May 12, 2005. The gravity field combination model EIGEN-CG03C is an upgrade of EIGEN-CG01C. The model is based on the same CHAMP mission and surface data (0.5 x 0.5 deg. gravimetry and altimetry), but takes into account almost twice as much GRACE mission data. Instead of 200 days now 376 days out of February to May 2003, July to December 2003 and February to July 2004 have been used.

EIGEN-CG03C is complete to degree and order 360 in terms of spherical harmonic coefficients and resolves geoid and gravity anomaly wavelengths of 110 km. A special band-limited combination method has been applied in order to preserve the high accuracy from the satellite data in the lower frequency band of the geopotential and to form a smooth transition to the high frequency information coming from the surface data

[www-app2.gfz-potsdam.de/pb1/op/grace/results/index_RESULTS.html]

Model	Year	Degree	Data
EIGEN-CG03C	2005	360	S(Champ,Grace),G,A

(S=Satellite Tracking Data, G = Gravity Data, A = Altimetry Data)

Table (4-4): Root Mean Square (RMS) About Mean of GPS / Levelling
Minus Gravity Field Model Derived Geoid Heights [m]

Model	Nmax	USA 6169 points	Canada 1930 points	Europe 1235 points	Australia 201 points
EIGEN-CG01C	360	0.351 m	0.270 m	0.370 m	0.263 m
EIGEN-CG03C	360	0.346 m	0.306 m	0.355 m	0.260 m

[<http://icgem.gfz-potsdam.de/ICGEM/ICGEM.html>]

4.2.1.3.1.5 Combined Global Gravity Field Models from GRACE, LAGEOS and Surface Gravity Data

1- EIGEN-GL04C

EIGEN-GL04C is combined gravity field model complete to degree and order 360 from GRACE, LAGEOS and surface gravity data, released on March 31, 2006. The gravity field combination model EIGEN-GL04C is an upgrade of EIGEN-CG03C. The model is a combination GRACE and LAGEOS mission plus 0.5 x 0.5 degrees gravimetry and altimetry surface data. The satellite data have been analysed by GFZ Potsdam (GRACE for February 2003 - July 2005 without January 2004) and GRGS Toulouse (GRACE and LAGEOS for February 2003 - February 2005). The used surface data are identical to EIGEN-CG03C except of the geoid undulations over the oceans which have been derived from a new GFZ mean sea surface height (MSSH) model minus the ECCO sea surface topography (EIGEN-CG03C: CLS01 MSSH minus ECCO).

EIGEN-GL04C is complete to degree and order 360 in terms of spherical harmonic coefficients and thus resolves geoid and gravity anomaly wavelengths of 110 km.

[www-app2.gfz-potsdam.de/pb1/op/grace/results/index_RESULTS.html]

Model	Year	Degree	Data
EIGEN-GL04C	2006	360	S(Grace,Lageos),G,A

(S=Satellite Tracking Data, G = Gravity Data, A = Altimetry Data)

[<http://icgem.gfz-potsdam.de/ICGEM/ICGEM.html>]

2- EIGEN-5C

EIGEN-5C complete to degree and order 360 from GRACE, LAGEOS and surface gravity data, released on September 29, 2008. The combined gravity field model EIGEN-5C is an upgrade of EIGEN-GL04C. The model is a combination of GRACE and LAGEOS mission data plus 0.5 x 0.5 degrees gravimetry and altimetry surface data. The combination of the satellite and surface data has been done by the combination of normal equations, which are obtained from observation equations for the spherical harmonic coefficients.

The satellite data have been processed by GFZ Potsdam (GRACE for February 2003 - January 2007) and GRGS Toulouse (GRACE for August 2002 - January 2007 and LAGEOS for January 2002 - December 2006). The used surface data are identical to EIGEN-GL04C except of new gravity anomaly data sets for Europe, the latest Arctic Gravity Project gravity anomaly data and newer Australian gravity anomalies.

Combined gravity field models, EIGEN-5C is complete to degree and order 360 in terms of spherical harmonic coefficients which corresponds to a spatial resolution of 55 km on the Earth's surface.

[www-app2.gfz-potsdam.de/pb1/op/grace/results/index_RESULTS.html]

Model	Year	Degree	Data
EIGEN-5C	2008	360	S(Grace,Lageos),G,A

(S=Satellite Tracking Data, G = Gravity Data, A = Altimetry Data)

[<http://icgem.gfz-potsdam.de/ICGEM/ICGEM.html>]

3- EGM2008

EGM2008 has been recently release to public by the U.S. Geospatial-Intelligence Agency (NGA) EGM Development Team. It is developed up to degree and order 2159, and contains additional spherical harmonics coefficients extending to degree 2190 and order 2159 *[Tocho,C.,et .al.,2008]*.

Model	Year	Degree	Data
EGM2008	2008	2190	S(Grace),G,A

(S=Satellite Tracking Data, G = Gravity Data, A = Altimetry Data)

Table (4-5): Root Mean Square (RMS) About Mean of GPS / Levelling
Minus Gravity Field Model Derived Geoid Heights [m]

Model	Nmax	USA 6169 points	Canada 1930 points	Europe 1235 points	Australia 201 points
EIGEN-GL04C	360	0.339 m	0.253 m	0.336 m	0.244 m
EIGEN-5C	360	0.341 m	0.251 m	0.303 m	0.244 m
EGM2008	2190	0.248 m	0.126 m	0.208 m	0.217 m

Nmax: The maximum degree

[<http://icgem.gfz-potsdam.de/ICGEM/ICGEM.html>]

4.2.2 Satellite Gradiometry

Gradiometry measures the difference in acceleration of test masses over small distances with two accelerometers for each direction. In this way, components of the gravity tensor can be measured, which will mainly provide information on the high-degree spherical harmonics of the Earth's gravity field [*Rummel and Colombo, 1985*].

Non-conservative forces will act on all test masses in an almost similar way and this influence can therefore be neglected from the gradiometer observations. The GOCE satellite will be the first satellite carrying a gradiometer on board. The launch of the satellite is scheduled for 2009, with an expected lifetime of two years. It will fly at a low-altitude (250 kilometers) and will be equipped with GPS receivers, laser reflectors (SLR), and a gradiometer [*Fehringer, M., et. al., 2007*].

4.2.2.1 GOCE

The Gravity field and steady-state Ocean Circulation Explorer Mission (GOCE) will be the first Core Earth Explorer mission in the context of ESA's Living Planet programme [*Fehringer, M., et. al., 2007*]. is scheduled to take place on Wednesday 10 September 2008 [www.space.gs/08/22-aug-2008-goce.html]. But this date scheduled for launch is changed to February 2009 due to a failure in the guidance and navigation system of the launcher's Upper Stage. The anomaly was discovered during the spacecraft's launch preparation tests on 7 September 2008 in Plesetsk, which subsequently led to the postponement of the launch. The cause of the anomaly in the guidance and navigation system has meanwhile been identified and reproduced. The necessary hardware changes will require a minimum of two months of additional

work by the manufacturer. As a consequence, GOCE launched on 17 March 2009.

[www.esa.int/SPECIALS/GOCE/SEM8VARTKMF_0.html]. GOCE will measure highly accurate, high spatial resolution gravity gradients in three dimensions along a well characterized orbit. The mission objectives are to obtain gravity gradient data such that new global and regional models of the static Earth's gravity field and of the geoid can be deduced with high spatial resolution and accuracy. The goal is to achieve an accuracy of 1mGal for gravity anomalies and 2cm for the geoid at length scales down to 100km. Such an advance in the existing knowledge of the Earth's gravity field will help develop a more comprehensive understanding of the physics of the Earth's interior, the interaction between continental plates and the ocean circulation. Further, GOCE products will have broad application in the fields of geodesy, oceanography, solid-earth physics and glaciology *[Fehringner, M., et. al.,2007]*.



Figure (4-22): Artist's Impression of the GOCE Satellite.

4.2.2.1.1 Mission Orbit

GOCE will fly in a sun-synchronous, circular dawn/dusk low Earth orbit (with an inclination of 96.5°). Scientific measurements will be conducted at 250 km and 240 km in two measurement phases. Each measurement phase is separated by a long-eclipse period during which time the satellite will be placed in hibernation [www.esa.int/livingplanet/goce].

4.2.2.1.2 Mission Profile

The nominal mission duration is 20 months, including a nominal 3 month commissioning and calibration phase; and two science measurement phases (each 6 month duration) separated by a long-eclipse hibernation period [www.esa.int/livingplanet/goce].

4.2.2.1.3 GOCE Spacecraft Elements

To meet the required accuracy and resolution, GOCE will fly in low Earth orbit (~250 km) to counteract altitude-related gravity-field Electrostatic Gravity Gradiometer instrument for the first time in space. Gradiometry was conceived to measure 3d gravity gradients between pairs of accelerometers in the x, y, z directions. Meanwhile, the GOCE spacecraft will be tracked continuously from above by Global Navigation Satellite Systems. Precise three-dimensional “high-low” GPS tracking information, together with the gradiometer measurements.

a- Electrostatic Gravity Gradiometer (EGG)

The principle of operation of the EGG is based on the measurement of the forces needed to maintain a proof mass at the centre of a cage. Each pair of identical accelerometers, mounted on the ultra-stable carbon-carbon structure about 0.5m apart, form a “gradiometer arm”. The three identical arms are mounted orthogonal to one another. The gradiometer axes so defined are nominally aligned in the along-track, cross-track and a third direction pointing approximately towards the Earth’s centre

b- Satellite to Satellite Tracking Instrument (SSTI)

The objective of the SSTI is to provide support to the gravity field recovery, by using the positioning provided by the simultaneous tracking of up to 12 GPS satellite signals, Figure (4-23).

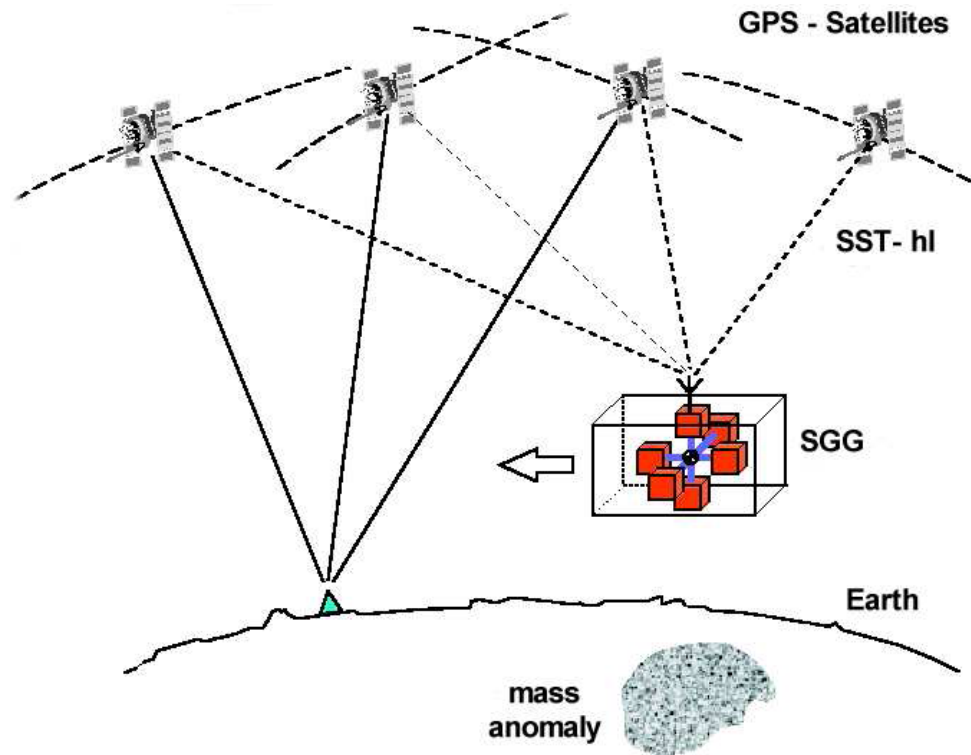


Figure (4-23): Schematic Illustration of the Combined Satellite Gravity Gradiometer (SGG) and Satellite-to-Satellite (High-Low) Tracking Mission Concept.

c- Laser Retro-Reflector (LRR)

The LRR allows acquisition of a supplementary data set of satellite laser ranging (SLR) observations (by the existing SLR ground network) as backup for precise orbit determination post-processing. The LRR is a corner-cube array capable of reflecting laser pulses back along the incident light path.

d- Satellite Attitude Control

1- Ion Propulsion Assembly

The Ion Propulsion Assembly (IPA) consists of an ion thruster, a gas feed system and related power and control electronics. The Ion Thruster

Assembly is the primary actuation device on board GOCE and functions solely to compensate drag in the along-track direction.

2- Magnetometers

Magnetometers aligned in the x, y, and z direction may be used to realign the spacecraft axes with respect to the Earth's magnetic field.

3- Sensors

The sensors responsible for providing information on the satellite attitude are the star trackers, a 3-axis magnetometer, a digital Sun sensor, and a coarse earth and sun sensor. The star trackers (STR), are used to provide data about the orientation and angular rate of the spacecraft at a rate of 2Hz [*Fehring, M., et. al.,2007*].

4.2.2.1.4 GOCE Measurement System

The GOCE satellite measures the earth's gravity field in two ways, by satellite-satellite tracking (SST) plus accelerometer, and by gradiometer. The former is the more familiar technique (the same as that used by CHAMP). The acceleration of the satellite is due to a combination of gravitational forces and body forces (such as atmospheric drag and thruster forces). Using the onboard accelerometers to determine the acceleration due to body forces, the GPS tracking of the satellite then constrains the estimation of gravitational accelerations, permitting the earth's gravitational field to be determined. This technique is particularly suited to longer wavelength parts of the gravity field. The second method used by GOCE is gradiometry, and it is this method which permits the recovery of short wavelength features in the gravity field. Gradiometry uses a pair of accelerometers to measure the difference in gravitational acceleration between two nearby points (separated by 0.5m for GOCE).

There are three such pairs in GOCE, arranged along mutually orthogonal axes, resulting in a full measurement of the three-dimensional gradient of gravity (9 numbers, each representing the gradient of one component of gravity along one particular direction) [*Hughes, C. W. and R. J. Bingham, 2006*].

4.2.2.1.5 Mission Objective

The Earth's gravity field is a fundamental physical force for every dynamic process on its surface and its interior. Since the start of the satellite era, the determination of the global gravity field and the associated geoid (i.e. the reference equipotential surface) has been considered a high priority goal. With GOCE we are aiming to achieve a significant step in characterization of the high-resolution static component of the Earth's gravity field. The new knowledge which is occurred will help advance our present understanding of how the earth works and will have a number of important practical applications.

Figure (4-24) shows the accuracy required by GOCE to improve the geoid and gravity field where significant improvements can be expected in oceanography, solid-earth physics and geodesy applications of the data. It also shows the status of gravity field knowledge in time when the GOCE mission was proposed (see EGM96 curve) through the present day (indicated by the GRACE curves in Figure (4-24)). For instance, since gravity is directly linked to the distribution of mass within the Earth, an accurate global geoid model including high harmonics contributes to an improved understanding of key features of ocean circulation, which plays an important role in energy exchanges around the globe (Figure (4-24a)). Similarly, a higher-resolution gravity-field map of the anomalous density structure of the lithosphere and upper mantle will provide new insights

into the physics and dynamics of processes in zones impacted by natural hazards such as volcanoes and earthquakes (Figure (4-24b)). Such information will provide better constraints for modelling the Earth's interior. Together the new GOCE data products will lead to the possibility for global unification of height systems (Figure (4-24c)), using 'pseudo levelled' or orthometric heights referenced to a common GOCE-derived geoid.

The aim of the GOCE mission is therefore to determine the gravity anomalies and geoid heights. It shall do this, by:

- Measurement of the Earth's gravity anomaly field with an accuracy of better than 1–2 mGal ($1 \text{ mGal} = 10^{-5} \text{ ms}^{-2}$) via combination of gravity gradients and satellite to satellite tracking.
- Determining (from the measured gravity anomaly field) the geoid (i.e. the equipotential surface of a hypothetical ocean at rest) with a radial accuracy better than 1-2 cm.
- Achieving both these measurements at a length scale of 100 km or less (i.e. degree and order equal to or higher than 200 in a spherical harmonics expansion of the field). A summary of the scientific applications of the GOCE data are shown below in Table (4-6) [*Fehringer, M., et. al.,2007*].

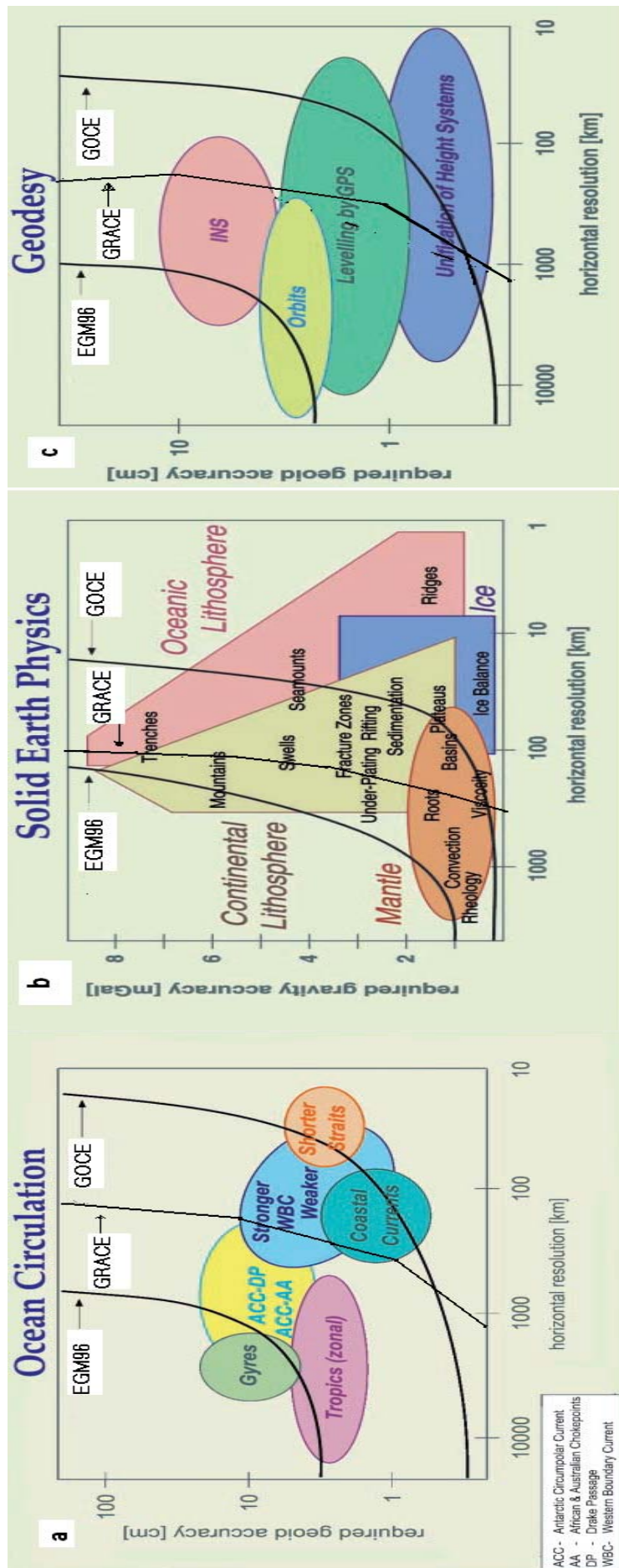
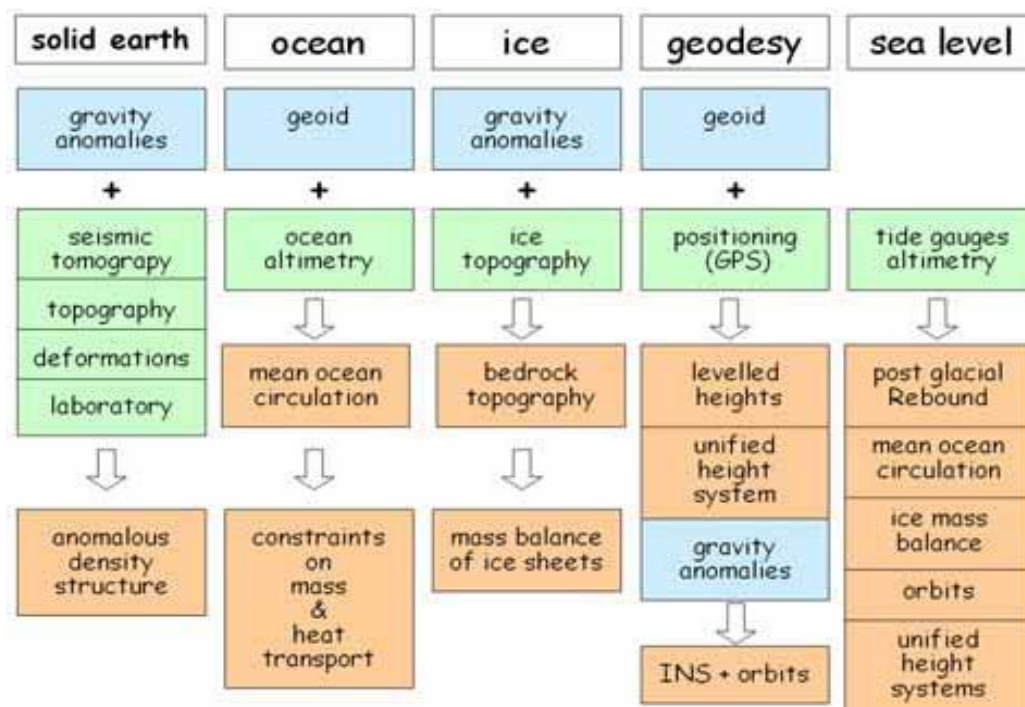


Figure (4-24): Schematic diagram showing geoid accuracy and scale, or horizontal resolution, required to characterise (a) ocean circulation features; (b) solid-earth processes; and for (c) geodesy applications. and illustrate the GOCE curve indicate the expected improvement over the existing EGM96 and more recent GRACE geoid and gravity model.

Table (4-6): Summary of Science Applications Areas Using GOCE Data

[After, Fehringer, M., et. al., 2007].



4.2.3 Satellite Altimetry

Satellite altimetry is a method to estimate the sea surface height, by measuring the distance between the satellite and the sea surface using an on board altimeter. Possible error sources in this height estimation are the observation error itself (including atmospheric delays), its spatial averaging and the positioning of the satellite. Moreover, one does not measure the geoid, but the sea surface height, which in general will not coincide. The difference is called dynamic topography. However, satellite altimetry provides very accurate data over the oceanic regions, where surface gravity data is absent. It has contributed to many combination solutions, e.g., EGM96 [Lemoine et. al., 1998] and EGM08 [Pavlis et. al., 2008].

Examples of altimetry satellites are the GEOS-3 (1975-1978), SEASAT (1978), GEOSAT (1985-1990), ERS-1 (1991-2000), ERS-2 (1995-),

TOPEX/Poseidon (1992- 2005), Jason-1 (2001-) and Envisat (2002-) satellites. Just recently (June 2008), the Jason-2 satellite is put into orbit [*Loon,J.,2008*]. Table (4-7) illustrates the history of satellite altimetry

4.2.3.1 Measurement Method

In concept, radar altimetry is among the simplest of remote sensing techniques. Two basic geometric measurements are involved. In the first, the distance between the satellite and the sea surface is determined from the round-trip travel time of microwave pulses emitted downward by the satellite's radar and reflected back from the ocean. For the second measurement, independent tracking systems are used to compute the satellite's three-dimensional position relative to a fixed Earth coordinate system. Combining these two measurements yields profiles of sea surface topography, or sea level, with respect to the reference ellipsoid. In practice, the various measurement systems are highly sophisticated and require expertise at the cutting edge of instrument and modeling capabilities. This is because accuracies of a few centimeters must be achieved to properly observe and describe the various oceanographic and geophysical phenomena of interest. Figure (4-25) shows a schematic of the Topex/Poseidon (T/P) satellite altimeter system. Launched in 1992 as a joint mission of the American and French Space agencies (and still operating as of 2001). Its microwave radars measure the distance to the sea surface with a precision of 2 cm. Two different frequencies are used to solve for the path delay due to the ionosphere, and a downward-looking microwave radiometer provides measurements of the integrated water vapor content which must also be known. Meteorological models must be used to estimate the attenuation of the radar pulse by the atmosphere, and other models correct for biases created by ocean waves. Three different tracking systems (a laser reflector, a Global Positioning

System receiver, and a ‘DORIS’ Doppler receiver) determine the satellite orbit to within 2 cm in the radial direction. The result of all these measurements is a set of global sea level observations with an absolute accuracy of 3-4 cm at intervals of 1 s, or about 6 km, along the satellite track. The altimeter footprint is exceedingly small - only 2-3km - so regional maps or ‘images’ can only be derived by averaging data collected over a week or more [Cheney,R.,2001]. The last data were acquired on October 2005, due to a failure in a pitch reaction wheel. The mission ended on 18 January 2006 [Rosmorduc, V., et al.,2006].

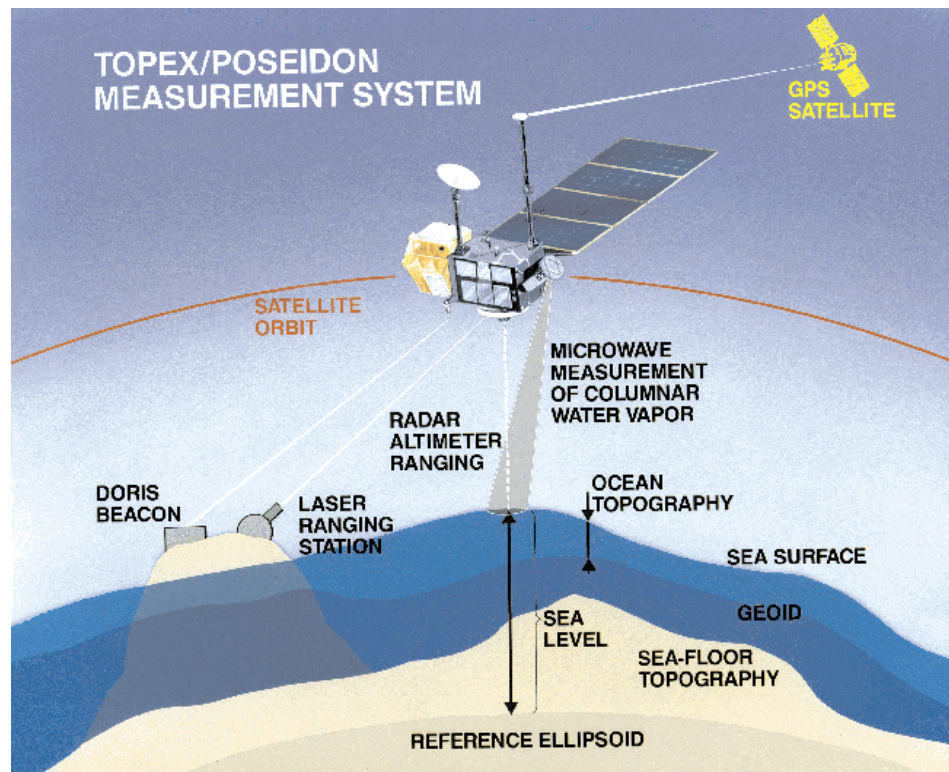


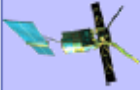









Figure (4-25): Schematic diagram of satellite radar altimeter system

Table (4-7) Illustrates History of Satellites Altimetry [*Rosmorduc, V., et. al.,2006*]

Satellite	Agency	Launch	Altitude	Altimeter	Frequency used	Repetitivity	Inclination	Error budget
 Seasat	NASA	1978	800 km	ALT	Ku-band	17 days?	108°	Range: 5 cm; Orbit: ~100 cm
 Geosat	US Navy	1985	800 km		Ku-band	17 days	108	Range: 4 cm; Orbit: 30-50 cm
 ERS-1	ESA	1991	785 km	RA	Ku-band	35 days (3 days ice phase, 168 days geodetic phase)	98.5°	Range: 3 cm; Orbit: 8-15 cm
 Topex/ Poseidon	NASA / CNES	1992	1336 km	Topex Poseidon-1	Ku and C-band Ku-band	10 days	66°	Range: 2 cm; Orbit: 2-3 cm
 ERS-2	ESA	1995	785 km	RA	Ku-band	35 days	98.5°	Range: 3 cm; Orbit: 7-8 cm
 GFO	US Navy / NOAA	1998	800 km	GFO-RA	Ku-band	17 days	108°	Range: 3.5 cm; Orbit: ? cm
 Jason-1	CNES / NASA	2001	1336 km	Poseidon-2	Ku and C-band	10 days	66°	Range: 2 cm; Orbit: 2-3 cm
 Envisat	ESA	2002	800 km	RA-2	Ku and S-band	35 days	98.5°	Range: 2-3 cm ; Orbit: 2-3 cm
 Jason-2	CNES / NASA / Eumetsat / NOAA	2008	1336 km	Poseidon-3	Ku and C-band	10 days	66°	
 Cryosat	ESA	2009	720 km	SIRAL	Ku-band	369 days	92°	

Chapter 5

Applications for These Satellites in Egypt

In this chapter, some of applications based on using the previously mentioned satellite missions in Egypt are presented.

5.1 Positioning Satellites Applications in Egypt

GPS proved itself as a powerful surveying tool. It is used in Egypt in many surveying and geodetic applications. Stations of large spacing, geodetic networks, are fixed using GPS. Some of these networks are explained in the following sections.

5.1.1 High Accuracy Reference Network (HARN)

GPS observations were planned with both absolute and relative processing requirement in mind. The United States Defense Mapping Agency (DMA) was contacted and agreed to process the data for absolute results by removing the effects of selective availability. The observational requirements suggested by DMA called for a minimum of four observation sessions of at least 4 hours duration. Observations were to be taken during times of good PDOP and observations 1/2 hour either side of sunrise or sunset were to be avoided to reduce any effects of possible increases in solar activity during these time periods. Additionally, DMA requested that observations to be made at a minimum of two different times during the day to eliminate the possibility of biases caused by all measurements coming from the same satellite configuration. A 30 second epoch interval was used and meteorological data (wet and dry bulb temperature as well as barometric pressure) were to be collected every hour.

Fortunately, by this time The International GPS Service for Geodynamics (IGS) had established International Terrestrial Reference Frame (ITRF) Stations and placed phase and pseudorange observations in daily Rinex format on the internet. This development provided the means for creating a

new datum without assistance from DMA thus enabling ESA to continue on with minor alteration and enhanced results. However, GPS observation scenarios were planned for relative accuracies between HARN stations and absolute accuracies as specified DMA. Therefore, these observational scenarios, were not planned for relative accuracies between the HARN stations and ITRF stations [*Powell,S.,1997*].

This procedure worked quite well, the amount of data collected turned out to be an ideal amount for producing a 1:10,000,000 (Order A) relative precision between stations. All original observations of the HARN were completed by MAY 31st 1995. Additional measurements were made in September of 1996 to bring station 0Z00 in the southeast corner of Egypt. Up to the 1:10,000,000 accuracy standard.

No master or fiducial station within Egypt was continuously occupied during each session. However, there are two stations that do have common data with 50% or more of the other stations in the network. The following is a list of these stations and the corresponding stations with common observational times. In addition to these stations, the continuously operating IGS CORE stations, served as fiducial stations [*Powell,S.,1997*].

0Z19 0Z05, 0Z09, 0Z10, 0Z11, 0Z12, 0Z13, 0Z14, 0Z15, 0Z16, 0Z17,
0Z18, 0Z20, 0Z21, 0Z22, 0Z23, and 0Z24.

0Z05 0Z01, 0Z02, 0Z03, 0Z04, 0Z06, 0Z10, 0Z11, 0Z12, 0Z13,
0Z19, 0Z23, 0Z24, 0Z25, 0Z26, 0Z27, 0Z28 and 0Z29.

The relative precision ratios show that all vectors of the HARN do meet Order A or 1:10,000,000 relative precision. Additionally, it shows that all stations of the HARN have 1:100,000,000 or Order AA relative accuracy between Egypt and four ITRF stations. The operational IGS CORE stations

during the time the HARN was observed are shown in Figure (5-1). The coincident data from stations in Matera, Italy ; Maspalomas, Canary Islands; Hartebeesthoek, South Africa ; and Kitab, Uzbekistan were used to produce coordinates for the Egyptian HARN. These stations are the closest IGS stations in each quadrant relative to Egypt for which coincident data was available [Powell,S.,1997].

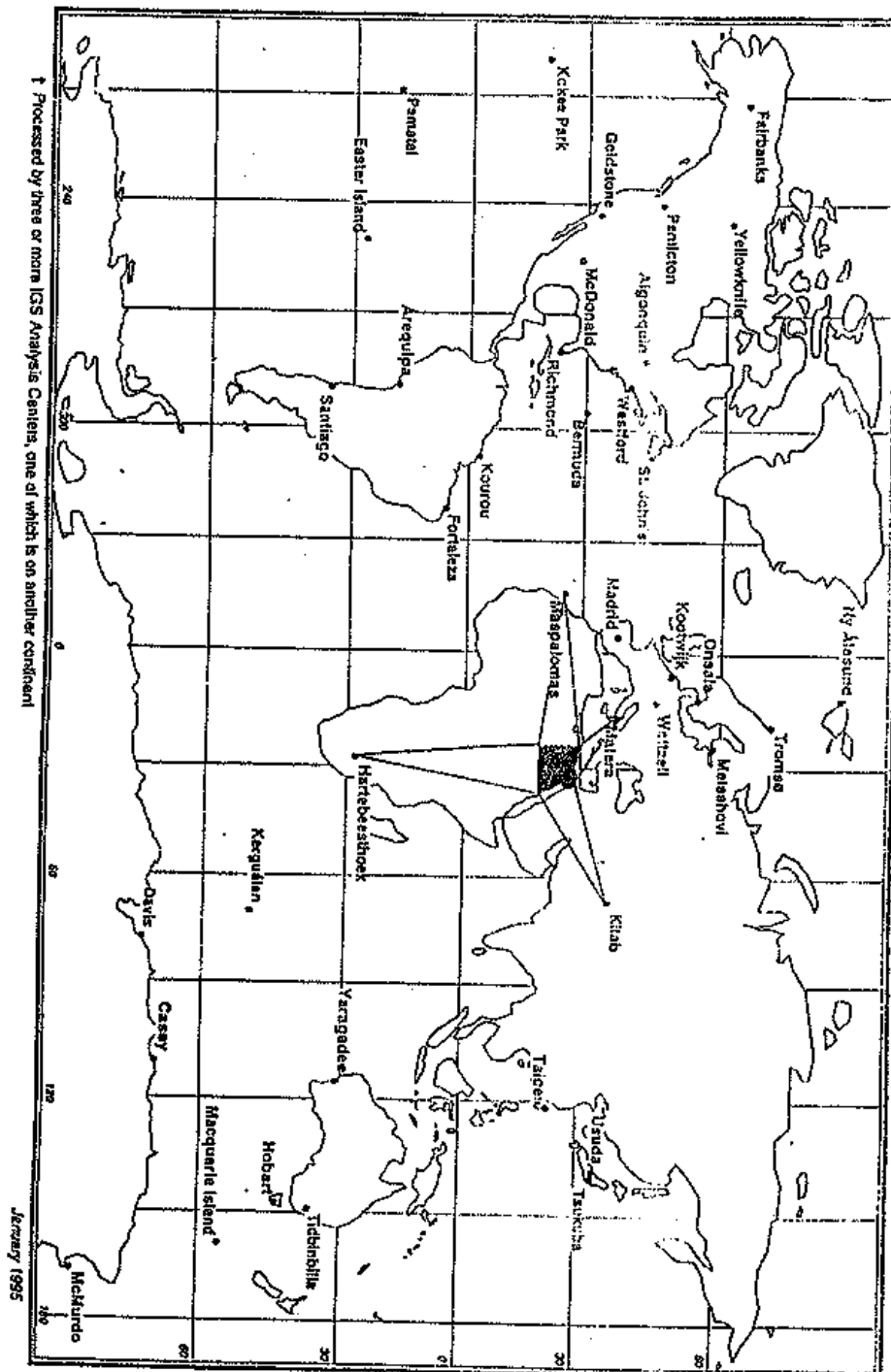


Figure (5-1): GPS Tracking Network of the International GPS Service for
Geodynamics Global Stations

The volume of data was immense. Since there was data from each of ITRF stations to each of the 30 stations of the HARN and each station had between 4 and 10 sessions. Additionally, since between six and eight receivers had been operated simultaneously by ESA, there were as many as 12 receivers for each of 52 sessions of the HARN [Powell,S.,1997].

5.1.2 The National Agriculture Cadastral Network (NACN)

For agricultural development along the Nile valley, the National Agricultural Cadastral Network (NACN) has been established with a precision of 1 part per million. The National Agricultural Cadastral Network (NACN) that is mainly covers the Nile valley and the Delta. NACN consists of 112 stations, with a station separation of 50 Km approximately, whose relative precision is 1:1,000,000 [Gomaa M., and Sherine S.,2005]. Twelve stations of the HARN were occupied during observation of the NACN [Powell,S.,1997].

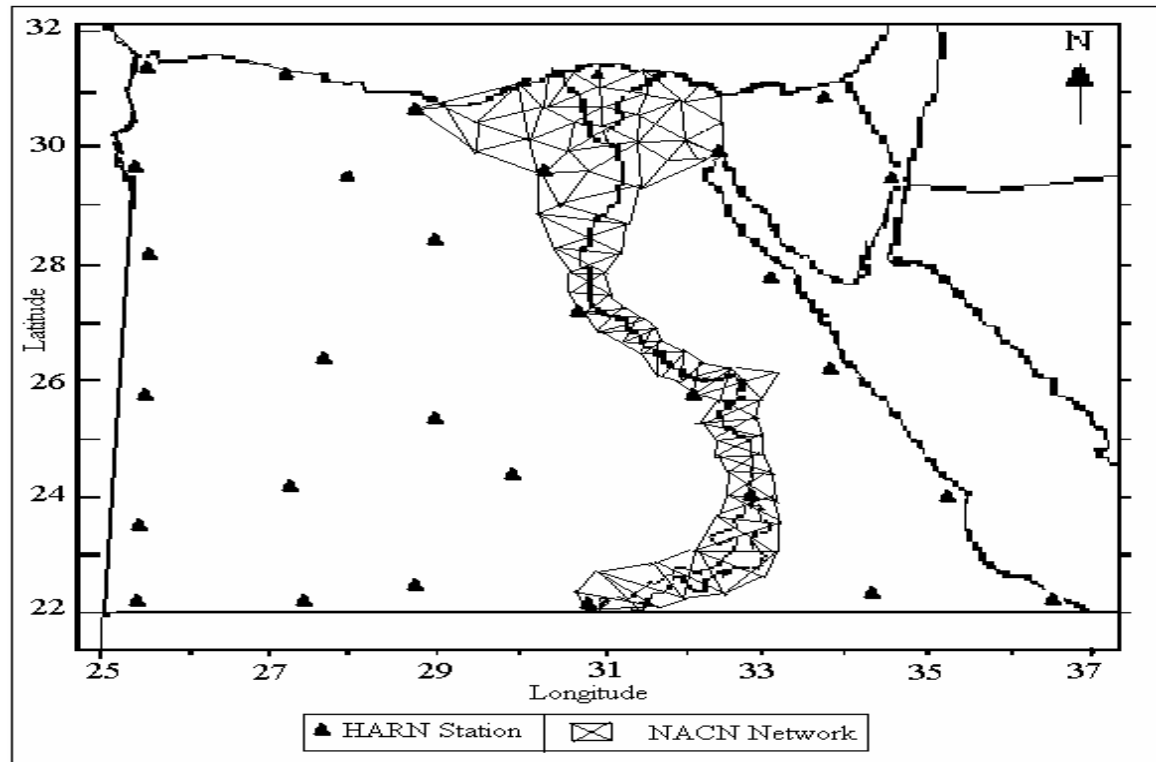


Figure (5-2): Recent Precise GPS Geodetic Control Networks in Egypt
[After, Gomaa M., and Sherine S.,2005].

5.1.3 Radio Beacon Network

In 1997, Beacon Co. of Egypt and the Maritime Systems Business Unit of MacDonald Dettwiler, (formerly the Maritime Information Systems Group of CANAC/Microtel), were awarded a contract to provide a complete turnkey National DGPS system for the Egyptian Ports & Lighthouse Authority. This contract consists of the engineering, procurement, integration, factory testing, delivery, configuration, and site-testing of the Egyptian Marine DGPS [*Rehab,k.,2008*].

a- System Architecture

The system consists of one control monitor station linked to six DGPS control stations via a High Frequency (HF) radio network. Dialing from standard telephone lines provides backup access to the networks.

Each DGPS control station broadcasts DGPS corrections on a standard marine radio beacon frequency as a supplement to the standard GPS signals. The corrections enable the Egyptian and International Maritime commercial to determine their positions to better than 5 meters accuracy [*Rehab,k.,2008*].

The DGPS system implements a fault-tolerant architecture with dual redundancy in all key equipment. If any equipment were to fail, the system architecture would ensure continued operation. All irregularities in operations are reported immediately to the control monitor.

Table (5-1): Egypt Marine DGPS Station Data
[\[www.Trimble/findbeacon.asp\]](http://www.Trimble/findbeacon.asp)

SITE	MACHINE NAME	Station ID	Range (KM)	Station ID	Freq (KHz)	Baud (Bps)
Port Said	Port Said 1 Port Said 2	321	324	442,443	290.0	200
Alexandria	Alexandria 1 Alexandria 2	320	278	440,441	284.0	200
Mersa Matrouh	Mersa 1 Mersa 2	324	278	448,449	307.0	200
Ras Umm Sid	Rasummsid 1 Rasummsid 2	322	234	444,445	293.5	200
Ras Gharib	Ras Gharib 1 Ras Gharib 2	323	278	446,447	298.0	200
Quseir	Quseir 1 Quseir 2	325	482	450,451	314.5	200

b- Remote Monitoring System

Consists of a number of floating monitor receivers (buoys) that continually navigate the integrity of the Radio Beacon system and its corrections. These monitors constantly provide their navigation results to the master stations to generate alarms in case of any irregularity within the system:

- VHF Radio Monitoring System for 24 buoys, Red Sea Port Authority.
- UHF Radio Monitoring System for 16 buoys, Dummitta Port Authority.
- VHF Radio Monitoring System for 9 buoys, Hurghada Port.



Figure (5-3): Radio Beacon Reference Stations in Egypt

[After, Rehab,k.,2008].

5.1.4 Finnmap Project

FINNMAP project is presented in 1989 to produce topographic maps of 1:50,000 scale for eastern desert Figure (5-4). Geodetic control over project area was established using relative satellite positioning with Global positioning System (GPS). Total of 389 stations were positioned *[Finnmap project.,1989]*.

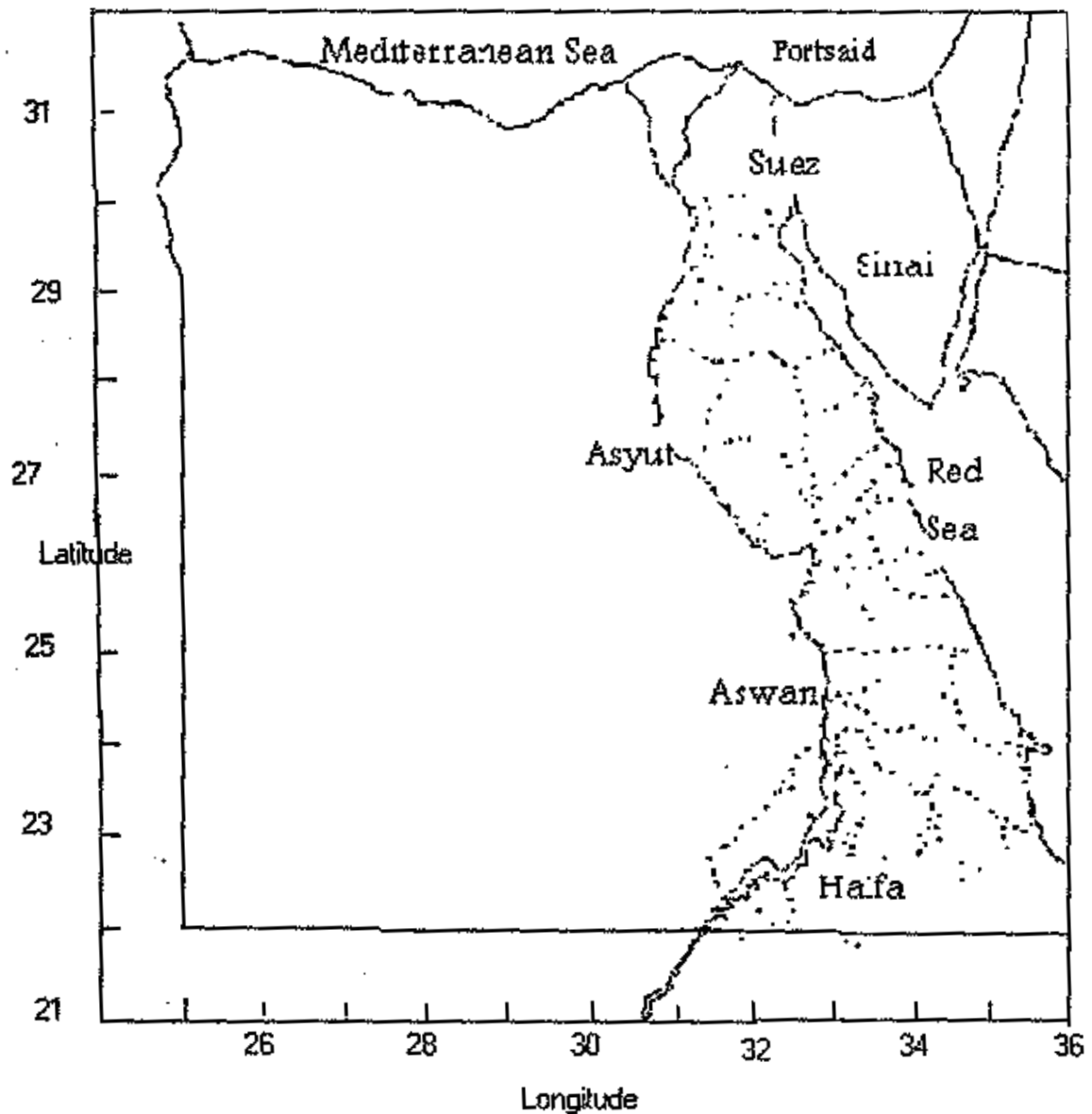


Figure (5-4): General Layout of (Finnmap) GPS Satellite Network

[After, Finnmap project., 1989].

GPS observations were accomplished using six single frequency, 5-channel Trimble 4000sx GPS- receivers. Observations included 1st and 2nd order observation sessions. Features of different observation sessions are shown in Table (5-2) and (5-3).

Table (5-2): 1st Order Observation Sessions

Name of Session	Length of Session (min)	Observed satellites	Average PDOP in Session
B	90	6, 8, 9, 12, 13	5
C	105	3, 6, 9, 12, 13	5

Table (5-3): 2nd Order Observation Sessions

Name of Session	Length of Session (min)	Observed satellites	Average PDOP in Session
A	70	6, 8, 9, 11, 13	20
B	70	6, 8, 9, 12, 13	5
C	70	6, 3, 9, 12, 13	5

Vertical angle (cut-off) was 18 degrees in all sessions. In 1st order observations average length of a baseline was 112 km. That for 2nd order observations was approximately 50 km

Total number of successfully observed stations is 389. This includes

31 1st order stations (of which 6 are initial stations)

340 2nd order stations

16 3rd order stations

2 photo stations

a- Primary Network

13 observation days including 26 sessions were used for observation primary net which was to be classified as 1st order net. Total 87 baselines were computed so that most of the baselines have double determination. Approximate coordinates for all stations were computed using station E7 Gebel Hamid's pseudo-ranging coordinates as origin.

RMS-value in adjustment is 0.88 meters. When dividing this by mean length of a baseline, 112.5 km, we get

Relative accuracy = $0.88 \text{ m} / 112.5 \text{ km} = 1 / 127,840$

For 1st order we should, according to specifications, have relative accuracy $1 / 100\,000$. Since $1 / 127,840$ is better than $1 / 100,000$.

Primary net is observed according to specifications of 1st order.

For 2nd and 3rd order station we should have

2nd order $< 1 / 50,000$

3rd order $< 1 / 20,000$

- 340 2nd order stations and 16 3rd order stations were obtained in densification surveys. 2 stations didn't meet specifications and were classified as photo stations [*Finnmap project.,1989*].

5.1.5 Civil Aviation Project

GPS network for Civil Aviation Authority, CAA, has been established. Eighty one GPS stations were constructed for national and international Civil Aviation Services. The established GPS network covers 18 airports and 9 navigational aids outside the airports. The measurements were performed in 1997 and 1998. WGS84 reference frame was utilized to be the basic datum of the produced coordinates, which were gained directly from GPS. The established GPS geodetic network is divided into three sub-nets, Net 1, Net 2 and Net 3. Net 1, is considered the base network for the whole CAA GPS networks. This net consists of five local stations which is located in five airports distributed along the boundary and the center of Egypt at, AlArish (02AR), Cairo (20CA), Asyut (31AS), Abo Simble (56AB), and Sidi Barani (70AB), Figure (5-5). In addition these stations are connected to two IGS and one HARN stations. The selected IGS stations are located at Manama, Bahrain (BAHR) and Matera, Italy (MATE). The HARN station E7 is one of the high accuracy reference network stations, Figure (5-6) [*ElSagheer,A.,2005*].

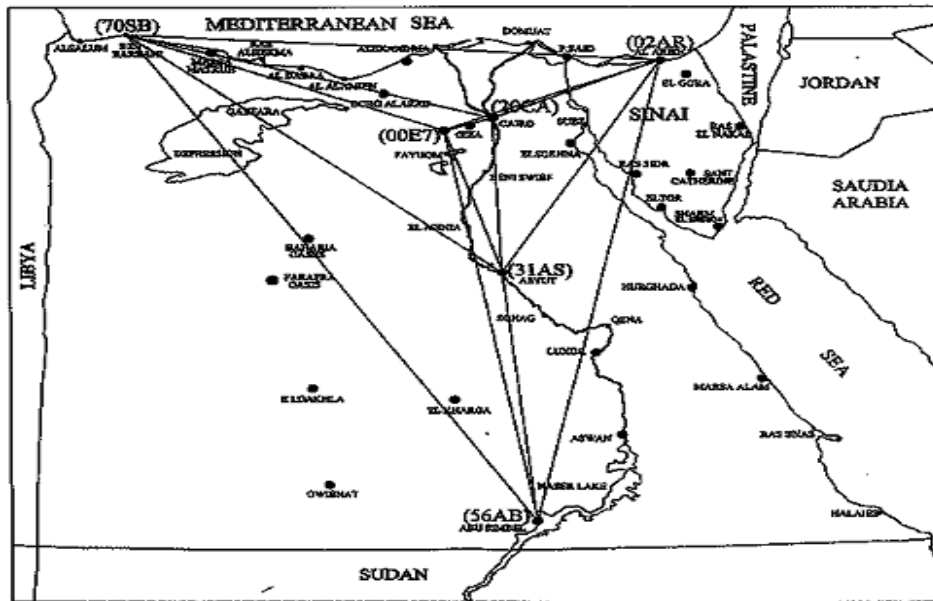


Figure (5-5): Basic Civil Aviation Authority Network, CAA-Net1

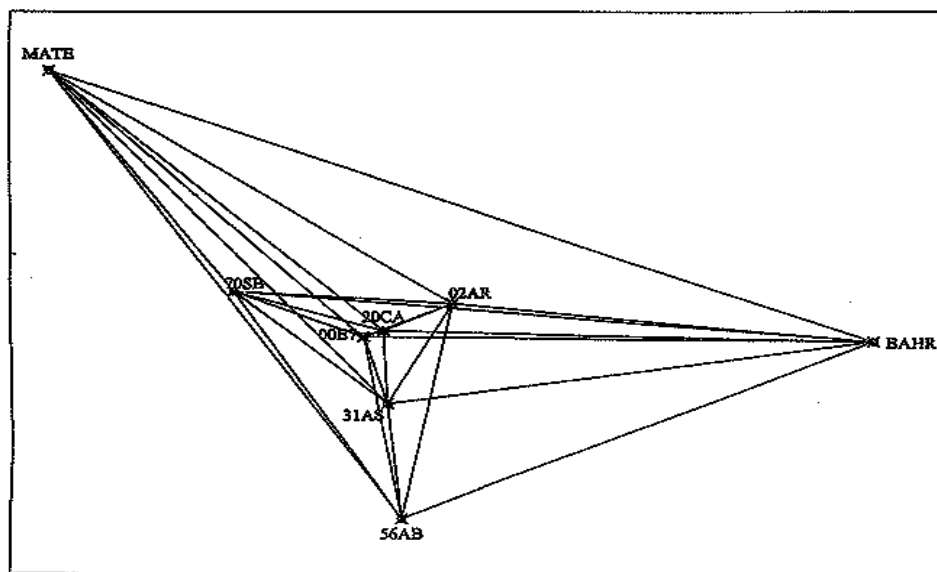


Figure (5-6): Basic Civil Aviation Authority Network, CAA-Net1,
Connected to IGS and HARN Reference Stations.

The measurements were performed at 1997, Table (5-4). The network stations were observed three times, every time was continuous 24 hours, with duration of three weeks apart between every session. Precise ephemeris obtained from the IGS stations was used during the data processing. The observation criteria for the observing sessions were as follows:

Observed Technique: Static

Data Type : Unsmoothed Carrier Phase on Dual Frequency Receivers

Data Sampling Rate : 30 Seconds

Elevation Mask : 15 Degree

Session Duration : Continuous 24 Hours

Repeatability : 3 Observing Sessions

Time Spacing : 3 weeks

Table (5-4): GPS Observation Date and Session Duration at Every Investigated Station [*After, ElSagheer,A.,2005*].

Station	Start time	Day	End time	Day	Remarks
56AB	09:46:30	21/07/1997	11:33:30	22/07/1997	Abo Simble Airport
31AS	09:51:30	21/07/1997	11:35:00	22/07/1997	Asyut Airport
02AR	09:55:30	21/07/1997	11:40:30	22/07/1997	AlArish Airport
20CA	09:57:00	21/07/1997	11:33:00	22/07/1997	Cairo Airport
70SB	10:00:30	21/07/1997	11:32:30	22/07/1997	Sidi Barani N.A.*
E7	10:00:00	21/07/1997	14:00:00	21/07/1997	HARN station
BHAR	02:00:00	21/07/1997	23:00:00	22/07/1997	IGS station
MATE-97	02:00:00	21/07/1997	23:00:00	22/07/1997	IGS station
MATE-05	02:00:00	01/01/2005	02:00:00	02/01/2005	IGS station

N.A.: Navigation Aids. [ElSagheer,A.,2005].

5.2 Remote Sensing Satellites Applications in Egypt

The remote sensing satellites imagery is used in different applications in Egypt, the following sub sections illustrate some projects.

5.2.1 Estimation of Water Loss from Toshka Lakes Using Remote Sensing and GIS

Toshka area is located to the west of Lake Nasser, in the Western Desert of Egypt. By the end of 1998, water in the River Nile has entered Toshka depressions for the first time when the Lake Nasser water level exceeded 178 m above sea level. Intermittently, water continued to discharge into the

depression until the end of year 2001. As a result the lake continued to aerially expand until the end of year 2001, but thereafter the lakes are shrinking. An assessment of the lakes droughts using an integration of remote sensing and GIS technique is performed. A set of remote sensing images were collected and processed to show the lakes aerial extend shrinkage from 2002 up to 2006. Spatially variable bathymetry (i.e. depths) has been interpolated from contour topographic maps surveyed prior to the filling of these depressions with water from Lake Nasser. At a given time, the water volume of the lakes was calculated given the aerial extend derived from the images and the spatially variable depths of these lakes derived from the DEM analysis. Spatial analysis of bathymetry DEM reveals that loss rate is around 2.5 m/year, and the lakes stored around 25.26 billion cubic meters of water in 2002. But in 2006 the stored water was greatly reduced to 12.57 billion cubic meters [El Bastawesy, M., et. al., 2007].

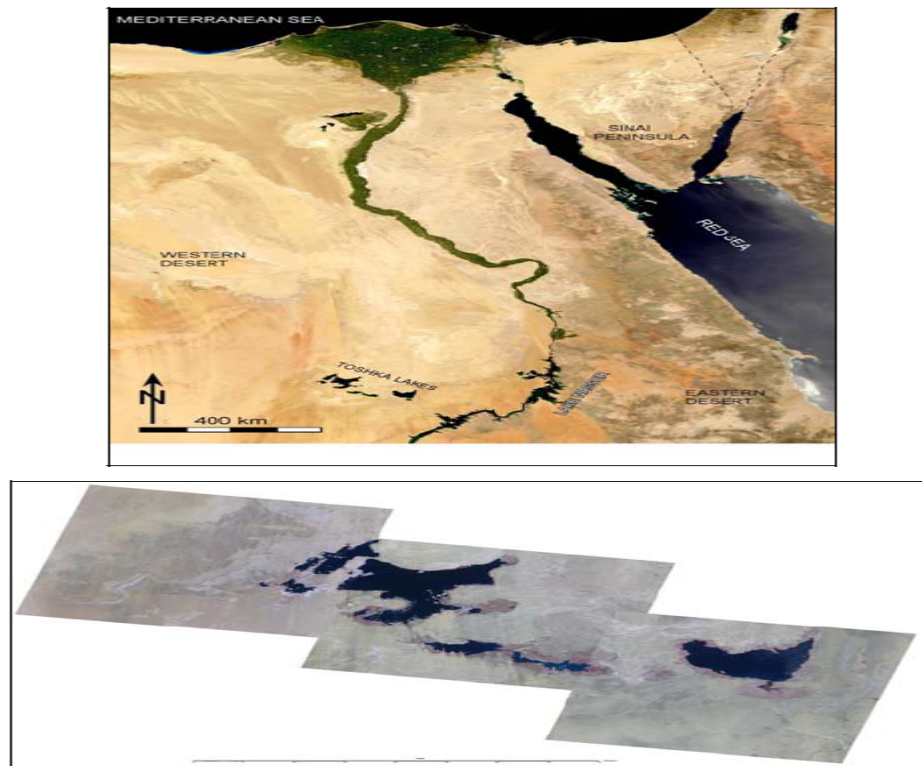


Figure (5-7): Location Map of Toshka Lakes
[After, El Bastawesy, M., et. al., 2007].

a- Data and Methods

Toshka lakes water loss modeling required various types of data from different sources. Three Aster images acquired in February 2002 and four Spot4 images of February 2006 were collected, preprocessed and processed to delineate lakes surface areas. The images were rectified into Universal Transverse Mercator (UTM), zone 36. Then they were enhanced in a way to discriminate between lakes and surroundings. The scenes of 2002 and 2006 were mosaiced and classified in order to compute the lakes surface area reduction during the given time span, Figure (5-8). However, water volume of each lake at a given date requires, in addition, water depths. Usually, bathymetry is estimated using a sonic depth finder instrument.

But for Toshka lakes there are topographic maps of scale 1: 100,000 surveyed prior to the formation of the Lakes, Figures (5-9). Therefore, these topographic maps were digitized, and DEM was generated to simulate lakes bed bottom topography and surroundings Figure (5-10). The DEM is of 20 m resolution, and was interpolated in Arc Info Topogrid's module using digitized contours, drainage networks and spots heights layers. The DEM was used to estimate the elevation.

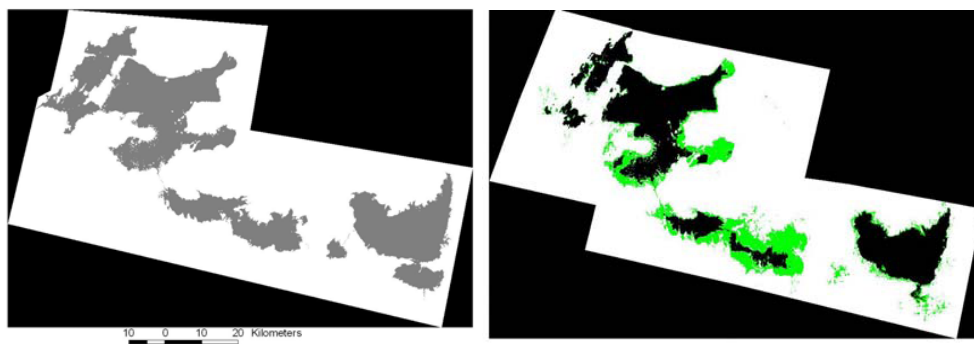


Figure (5-8): Toshka Lakes Surface Area Change from 2002 (Left) to 2006 (Right) [After, El Bastawesy, M., et. al., 2007].

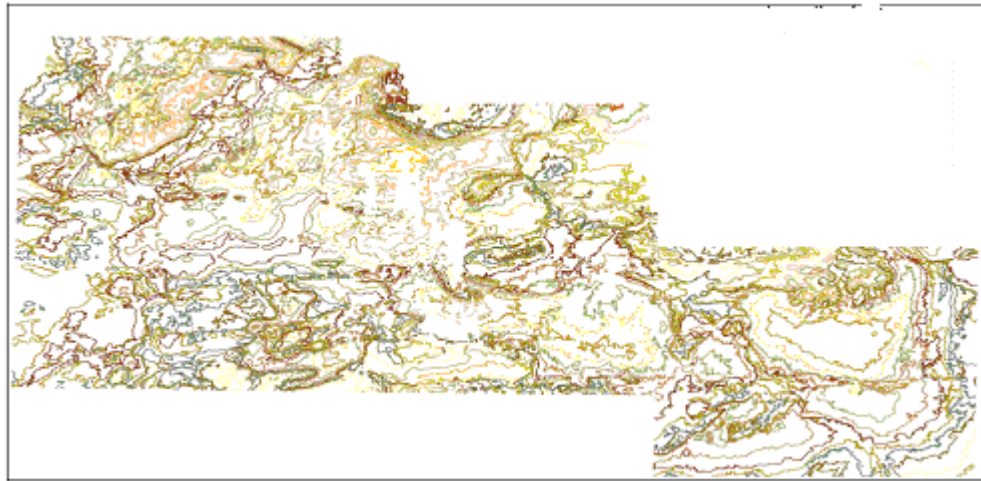


Figure (5-9): Digitized Contours of Topographic Maps for The Study Area
[After, El Bastawesy, M., et. al., 2007].

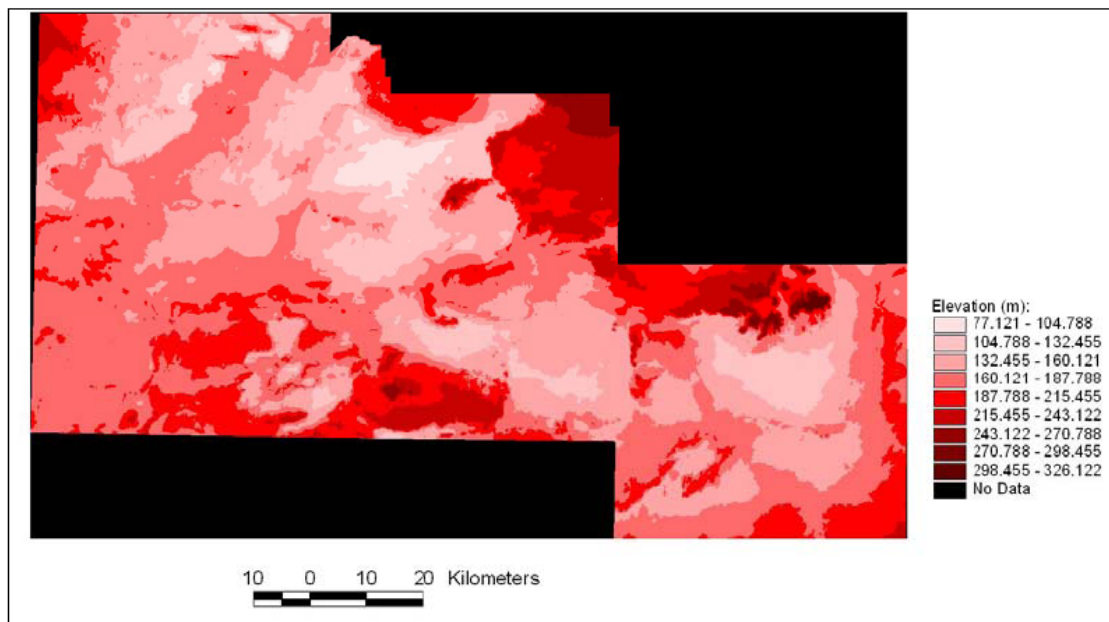


Figure (5-10): DEM of the Toshka Area Prior To the Formation of Lakes
[After, El Bastawesy, M., et. al., 2007].

b- Results

The estimated total surface area of Toshka lakes in 2002 was 1541 km² distributed on lakes 1, 2, 3 and 4 respectively as follow: 449, 20, 265 and 807 km². But in 2006 the lakes surface area were greatly reduced and reached

937 km². Lake 2 is completely vanished, and surface areas of lakes 1, 3 and 4 were calculated to 286, 101, and 550 km² respectively Figure (5-11). The analysis of DEM revealed that lakes surface stands on different elevation levels. Where lake 1 surface level in 2002 is estimated as 153 m above sea level and the lakes 2, 3 and 4 levels were 151, 141, and 140 m respectively. However, the rate of drop in the lakes surface level from the year 2002 to 2006 is almost similar, it is approximately 10 m in 4 years. Therefore, lake 1 surface level in 2006 stands at 143 m above sea level, and lakes 3 and 4 stand at 131 and 130 m a.s.l respectively. The calculated water volumes in Toshka lakes 1, 2, 3, and 4 for the year 2002 are 6.78, 0.044, 2.21, and 16.23 billion m³, and for the year 2006 are 3.45, zero, 0.44, and 8.78 billion m³ respectively Figure (5-12). This significant rate and volume of water loss can be attributed to both evaporation and infiltration, since there is no human exploitation of water from Toshka lakes with the exception of very minimal activity around lake 1. The annual evaporation rate is estimated as 2, 3 m/year data where it was measured in the field by the General Authority for the High Dam from September 2003 to August 2004. Therefore, most of Toshka lakes water is lost through evaporation with very limited amount being percolated to the ground water [El Bastawesy, M., et. al., 2007].

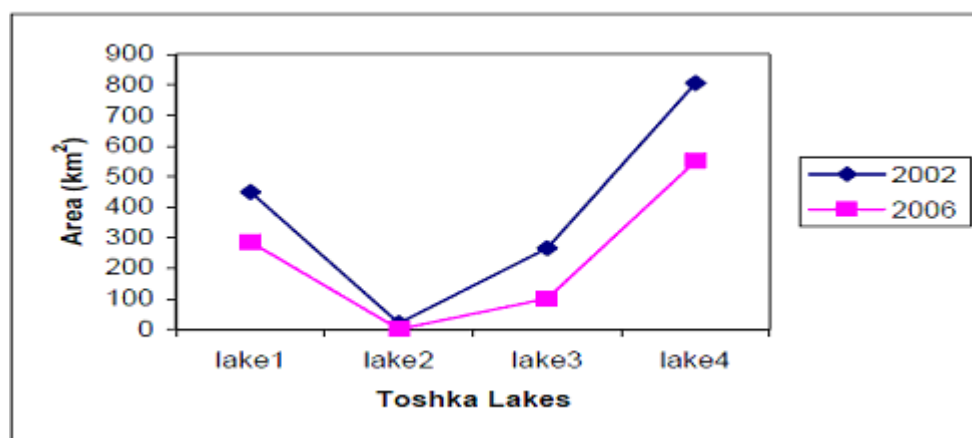


Figure (5-11): Toshka Lakes Surface Area Change from 2002 to 2006

[After, El Bastawesy, M., et. al., 2007].

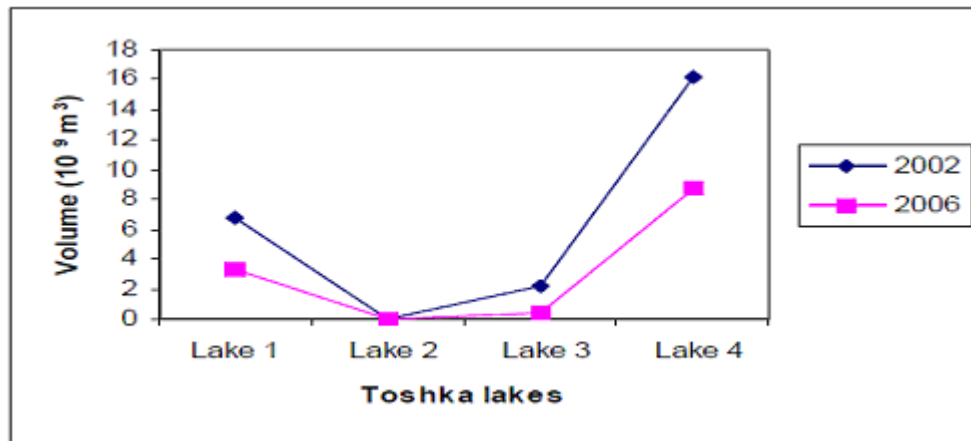


Figure (5-12): Toshka Lakes Water Volumes Change from 2002 to 2006

[After, El Bastawesy, M., et. al., 2007].

5.2.2 Middle Egypt Survey Project 2004

a- Methodology

This survey used Landsat and Corona satellite imagery to locate 70 archaeological sites in the survey area, which were then visited in a major survey. Without previous satellite imagery analysis, it is doubtful that the same results could have been achieved, due to a large survey area (450 kilometers squared). Middle Egypt is an area that has not been surveyed with the same intensity as other regions in Egypt, especially certain parts of the Delta and Luxor. The general lack of knowledge regarding existing sites on the west bank made it ideal for applying satellite remote sensing analysis in locating new and "lost" places of archaeological interest.



Figure (5-13): Landsat Satellite Image Used During the Middle Egypt Survey (Delta and Luxor).

After the initial computer analysis, each area was mapped that registered as an archaeological site. Using modern site names, the Napoleonic survey and other place name studies, only 30 places which had appeared as potential archaeological sites in the Landsat and Corona images seemed to be genuine (a success rate of 50 percent for the initial analysis); actual ground-truthing would test the validity of the remaining 30+ sites. Though other material from the west bank suggested that sites would be very late in date, it would be important to determine if any archaeological material remained from Pharaonic times and its nature and relationship to surrounding major sites such as Tell el-Amarna, Ashmunein and later sites like Kom el-Nana.

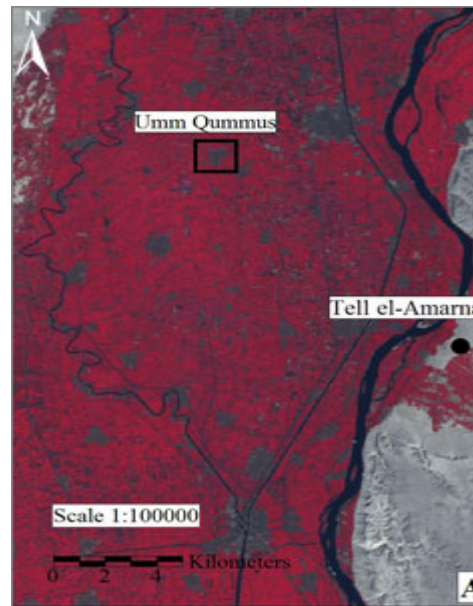


Figure (5-14): Close-up photo of the survey region. The red represents agricultural areas and the grey, towns.

b- General Survey Results

Using a GPS to determine exact eastings and northings, a detailed site location log was created which would record site size, extent as well as any material culture remains. Comparing the satellite images to modern maps allowed the exact placement of each potential site; subsequent location with GPS points made it possible to determine remaining site size. This was important as many sites existed within small sections of large cities and towns, and without the precise coordinates of the site from the satellite images up to a week could have been spend in each town searching for them. [\[www.amarnaproject.com/pages/recent_projects/survey/middle_egypt/2004.shtml\]](http://www.amarnaproject.com/pages/recent_projects/survey/middle_egypt/2004.shtml).

Results from the ground-truthing survey have shown the increased archaeological importance of the area between Malawi and Dairut, namely during the Late Roman Period.

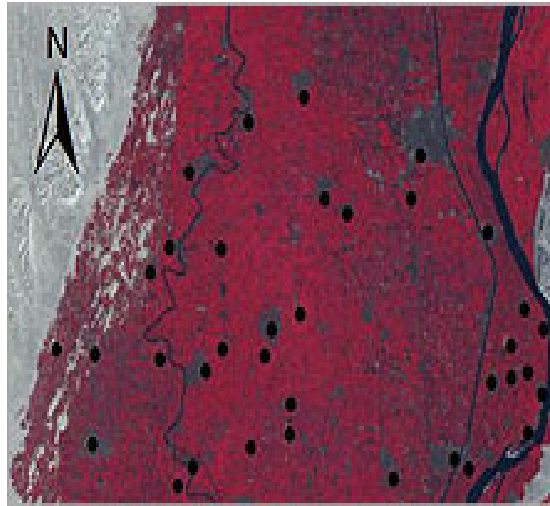


Figure (5-15): Satellite image of the survey area. The red areas represent archaeological places of interest and the circles mark the locations of the sites surveyed in the 2004 season.

[www.amarnaproject.com/pages/recent_projects/survey/middle_egypt/2004.shtml].

5.2.3 Remote Sensing and GIS for Integrated Coastal Zone Management

A case Study: The Coral Reefs in the Northwestern Red Sea (HURGHADA, EGYPT)

Remote sensing is very suitable for coral reef monitoring as it provides information about the configuration and composition of the coral reef; enables the monitoring of the biophysical parameters of the seas and oceans in which the coral reefs occur; and supports the detection of changes over time of these elements. This remote sensing-derived data is integrated in a Geographic Information System (GIS) together with additional environmental information. The GIS does not only form an inventory of all available information but is also used as a tool to analyze this information in order to support integrated coastal zone management (ICZM). The example is given of a risk assessment map constructed for the coral reefs offshore Hurghada, Egypt, indicating the coastal zones most endangered by human

activities. It is shown that about 86% of the marine, coastal area near Hurghada is at medium to high risk of being deteriorated [Vanderstraete, T., et. al., 2005].

a- Study Area

The coastal zone near Hurghada (Egypt) ($27^{\circ}14'N$ $33^{\circ}54'E$), situated in the north-western part of the Red Sea, is chosen as test site Figure (5-16). These coral reefs are located in a unique natural environment as the Red Sea is completely surrounded by deserts, has almost no water input from rivers and, hence, very stable physical characteristics such as salinity, temperature and water quality. Although the coral reefs are not under great natural threat, they are suffering from the negative effects of booming tourism and urban coastal development projects mainly for tourist accommodation and in support of the Egyptian relocation policy

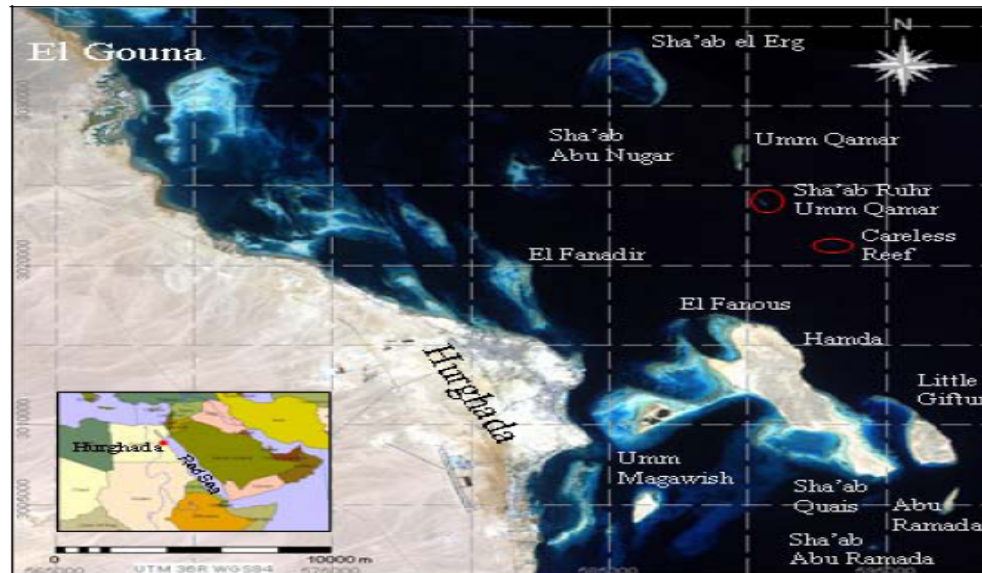


Figure (5-16): Overview of the Study Area on a Landsat 7 ETM [After, Vanderstraete, T., et. al., 2005].

b- Methodology

1- Integration of Remote Sensing-Derived Products into A GIS

Figure (5-17) gives an overview of some remote sensing-derived products and additional information resources useful for monitoring the status and health of a coral reef system. Based on these data layers, a local or regional coral reef monitoring system is set up. The Coral Reef-GIS forms the main working tool within this monitoring system. It does not only collect all available information, but is also used to analyze the different input products and delivers different decision support products to come to ICZM.

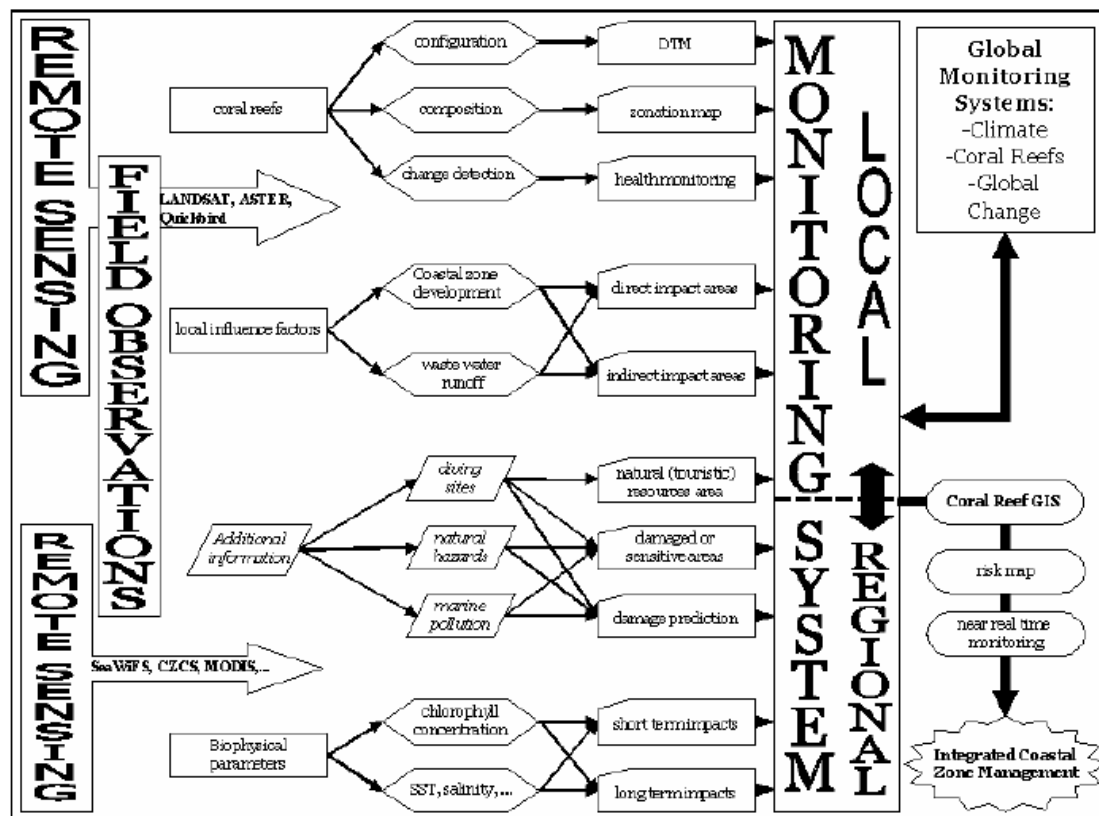


Figure (5-17) Schematic Overview of the Integration of Remote Sensing-Derived Products Together with Additional Information into a Monitoring System linked with a Coral Reef-GIS [After, Vanderstraete, T., et. al., 2005].

2- Risk Assessment Mapping

One of these decision support products is a risk assessment map in which is shown to what level of stress the coral reef systems are potentially up to due to the human activities in the coastal area these risk levels are commonly grouped into three classes, being: ‘low risk’, ‘medium risk’, and ‘high risk’.

c. Result

Two main risk zones could be discriminated on the overall risk assessment map shown in Figure (5-18). A high risk zone is present in the north of the study area due to the occurrence of two near shore drilling platforms. The common medium risk zone up to 10km offshore is mainly caused by the presence of tourist resorts and urban settlements along the entire coastline. The small spots of high and medium risk distributed over the area are linked to the most important known diving sites. This shows that physical damage to the coral reefs by divers is relatively localized but potentially severe. Remark that a ‘no risk’ class was not distinguished. As the Red Sea is an important shipping route and oil exploitation area, the entire coastline is considered at low risk of oil pollution or a shipping accident [Vanderstraete,T., et. al.,2005].

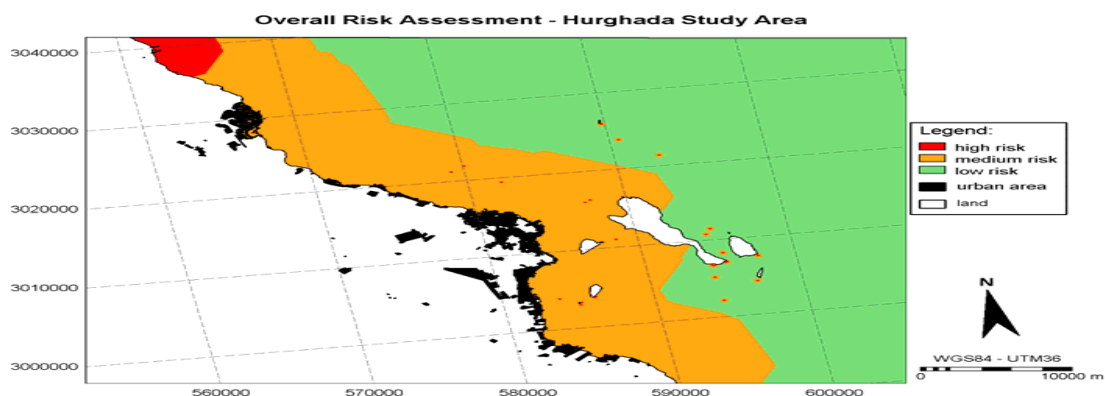


Figure (5-18) Overall Risk Assessment Map of the Hurghada Study Area
[After, Vanderstraete,T., et. al.,2005].

Chapter 6

Practical Application

This research presents study using a satellite image of Landsat TM-5 to obtain a soil classified map for Northern Sinai using the supervised classification techniques. These techniques depend on taking the training areas (signatures) on the image from reference geological map for the same area of scale 1:250 000 (geological map of Sinai (Sheet No.5)). Three techniques of supervised classification are used, (Minimum Distance, Mahalanobis Distance and Maximum Likelihood) with different number of classes. Firstly, the maximum number of classes (32) has been used and then reducing the number of classes in each classification gradually, by neglecting small areas of classes in the reference soil map in each stage. The number of classes used in these techniques was 32, 28, 24, 20 and 16, respectively using ENVI 4.4 software. The output results of classification techniques have been compared with the available geological map. The comparison indicates that the method of Maximum Likelihood gives the best results in all used number of classes.

6.1 Study Area, and Data Sources

The test was carried out for apart from the Northern Sinai which located in the northern east of Egypt, Figure (6-1). Geographical coordinates of the investigated area lies between 30° 00' to 32° 15' N and 32° 15' to 33° 45' E.

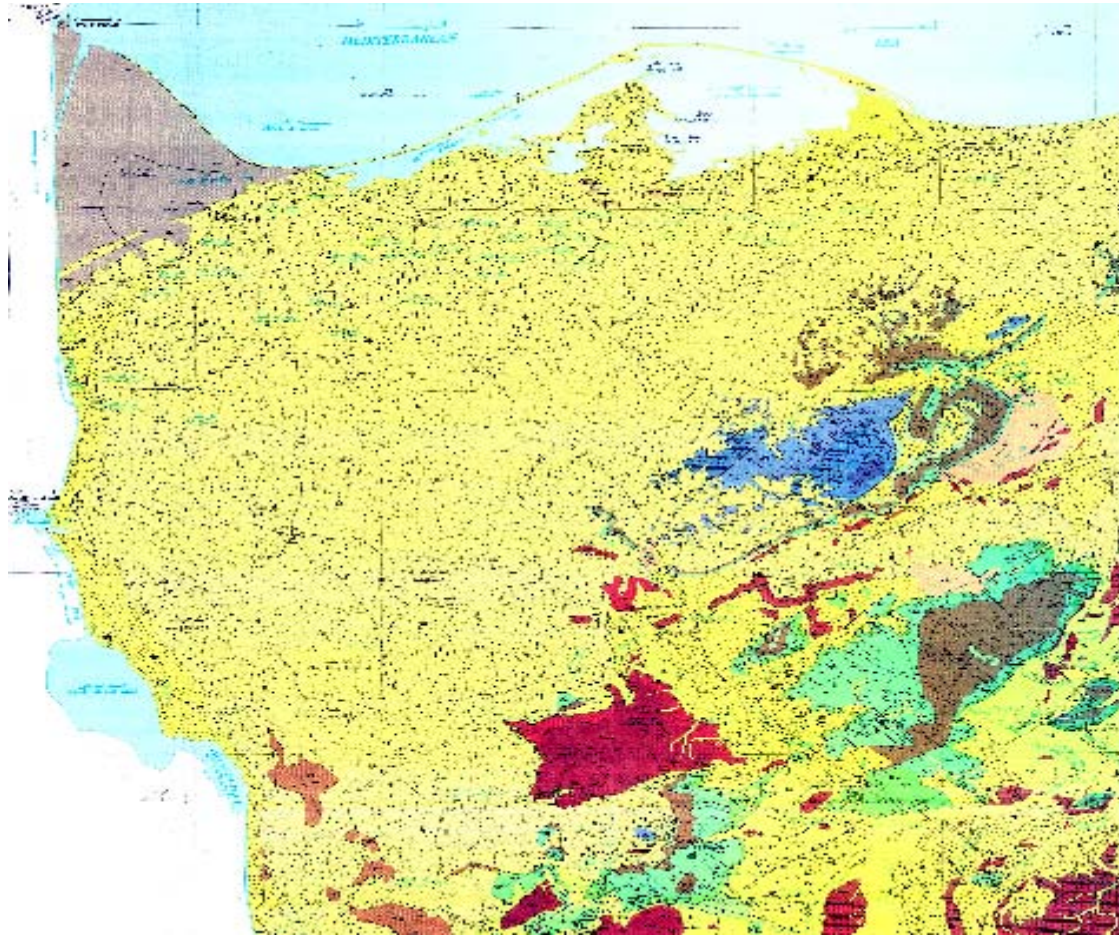


Figure (6-1): Geological Map of Sinai, Arab Republic of Egypt (Sheet No.5).

The following data sources are available for the study area:

- a- A multispectral Landsat TM-5 image of Sinai Peninsula, acquired on 1990, was used for this investigation Figure (6-2), which has three spectral bands with 28.5 spatial resolutions.
- b- Geological map of the area of the area study (Sheet No.5), 1: 250 000, 1992, sponsored by Academy of Scientific Research and Technology (Sinai Development Research Council).

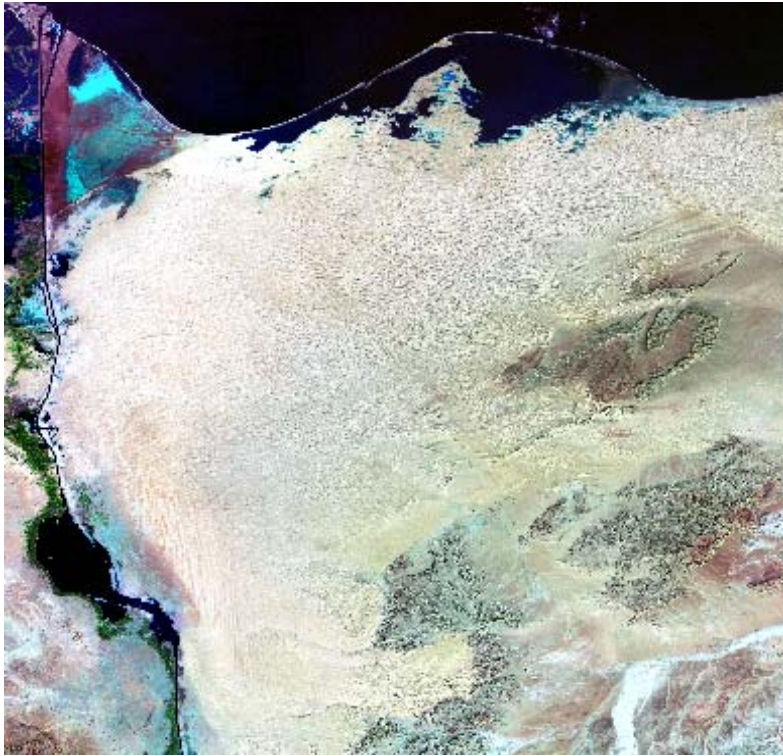


Figure (6-2): Landsat TM-5 Satellite Data for Northern Sinai Peninsula, Egypt.

6.2 Methodology

Soil classification map of investigation of the study area will be developed according to the following stages:

1. Scanning the available existing hard copy of the geological map (Sheet No.5), 1: 250 000.
2. Georeferencing the scanned map.
3. Image to map georeferencing.
4. Supervised classification using the following techniques:
 - a. Minimum distance technique.
 - b. Mahalanobis distance technique.
 - c. Maximum likelihood technique.

In the following subsections a brief discussion of the above mentioned stages is given.

6.2.1 Scanning the Available Existing Hard Copy of the Geological Map

Scanning is a very common procedure used for transforming hard copy maps into a digital format. The 1:250 000 hard-copy geological map has been scanned using Xerox scanner. The scanned image of geological map is in TIFF format with resolution of 200 dpi (dot per inch).

6.2.2 Georeferencing the Scanned Map

The process involved georeferencing of geological map to the Universal Transverse Mercator projection (UTM) using map corner coordinates in ENVI 4.4 software, where the projection information are, Project type is UTM, Reference Ellipsoid is WGS-72 and Zone Number is 36. The total Root Mean Square Error (RMSE) was 110 meter as shown in Table (6-1).

Table (6-1): Registration Map Reference Points (MRPs)

point	Base X	Base Y	Warp X	Warp Y	Predict X	Predict Y	Error _x	Error _y	Error _{xy}
1	571413.00	3457550.32	6063.50	429.25	6064.27	425.63	0.77	-3.62	3.70
2	428587.00	3457550.32	1489.25	410.25	1488.48	413.87	-0.77	3.62	3.70
3	427663.22	3319021.20	1448.00	4782.25	1448.76	4778.67	0.76	-3.58	3.66
4	572336.78	3319021.20	6084.50	4787.00	6083.74	4790.58	-0.76	3.58	3.66
Average Error _{xy} : 3.68									

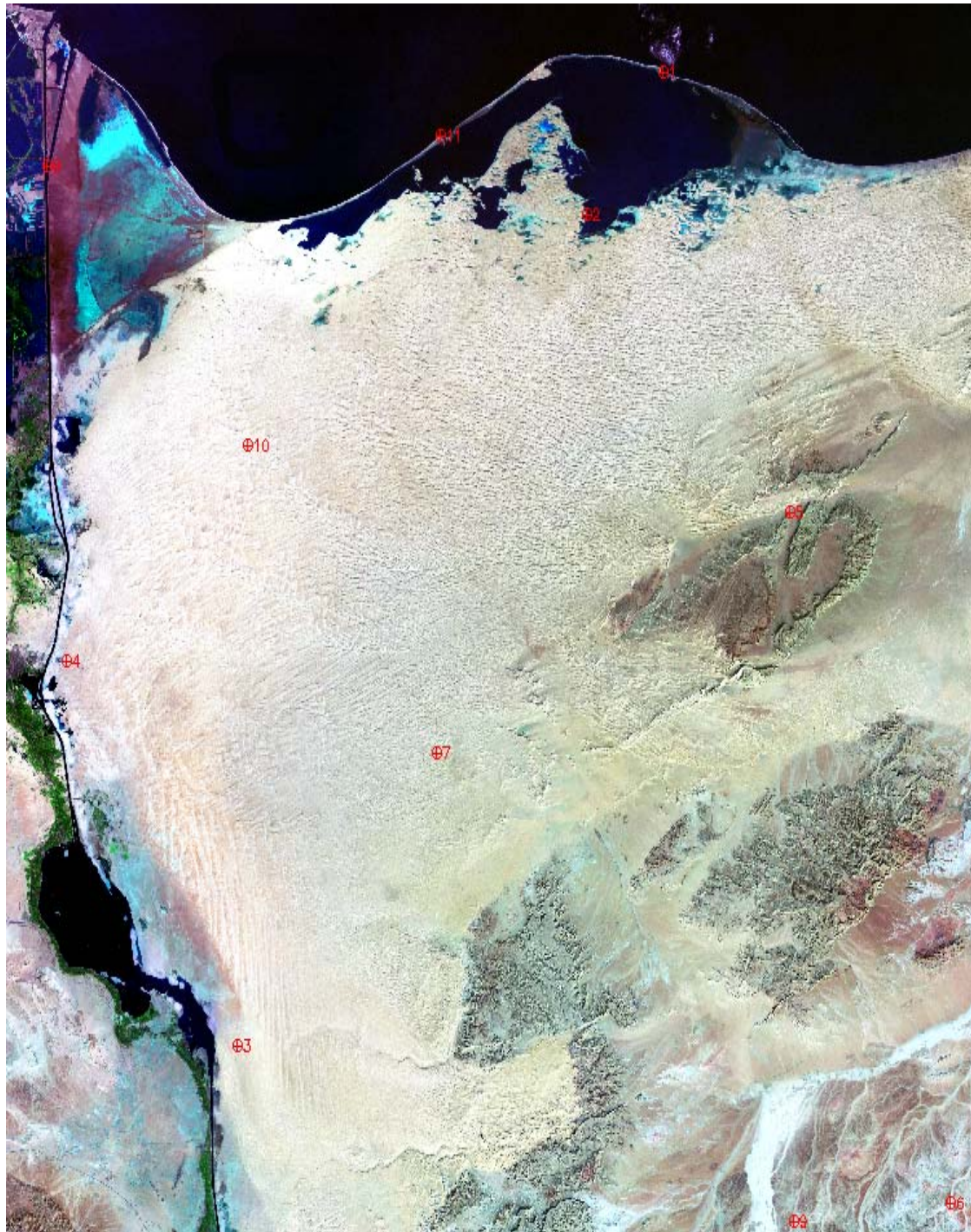
Where $Error_{xy} = \sqrt{(Error_x)^2 + (Error_y)^2}$, since pixel size is 30 x 30 meter, the average $Error_{xy} = 3.68$ is 110 meter

6.2.3 Image to Map Georeferencing

Georeferencing was done by performing image registration and geometric correction utilities to reference pixel-based (raster) images to geological map. The geological map is a georeferenced image in UTM coordinates

map projection. Map Reference Points (MRPs) are selected from the geological map as master/ base image to rectify the Landsat TM-5 image. It is necessary to spread MRPs throughout the study area on clearly identifiable points on both the master image and warp image for tie points in the image to image registration, Figure (6-3). After selecting enough MRPs, the images were warped using second order polynomial with Nearest Neighbour option to make a geometric correction or georeferenced image. The Root Mean Square Error (RMSE) obtained is 14.281 meter from 11 ground control points. The (RMSE) of the selected MRPs are shown in Table (6-2). For polynomial warping, the degree available is dependent on the number of MRPs defined where $\# \text{ MRPs} > (\text{degree} + 1)^2$ [*ENVI 4.4 Help*].

Therefore the required MRPs for rectification should be more than 9 points.



⊕ Ground control points

Figure (6-3): Distribution of the Map Reference Points over the TM-5 Image.

Table (6-2): Error in Coordinates of Control Points.

point	Base X	Base Y	Warp X	Warp Y	Predict X	Predict Y	Error _x	Error _y	Error _{xy}
1	12807.50	14916.50	4575.00	532.00	4575.4471	531.8281	0.4471	-0.1719	0.4790
2	12411.00	15488.00	4214.00	1043.00	4212.7197	1043.4878	-1.2803	0.4878	1.3701
3	10588.00	18837.20	2542.00	4039.75	2541.9166	4039.7383	-0.0834	-0.0117	0.0842
4	9701.75	17290.25	1742.00	2649.75	1742.0023	2649.8176	0.0023	0.0676	0.0677
5	13468.00	16690.00	5169.07	2125.74	5169.2216	2125.6555	0.1516	-0.0845	0.1736
6	14301.00	19471.75	5918.00	4628.00	5918.0929	4627.9766	0.0929	-0.0234	0.0958
7	11625.25	17658.00	3490.15	2987.30	3490.6001	2987.2680	0.4501	-0.0320	0.4512
8	9601.00	15291.00	1662.00	860.00	1661.9524	860.0387	-0.0476	-0.0387	0.0614
9	13488.00	19545.00	5180.25	4690.75	5180.0704	4690.7995	-0.1796	0.0495	0.1863
10	10643.25	16418.25	2602.59	1872.35	2602.4931	1872.1961	-0.0969	-0.1539	0.1819
11	11651.00	15170.25	3523.00	757.00	3523.5529	756.8442	0.5529	-0.1558	0.5745
Average Error _{xy} : 0.50									

Since image resolution 28.5 x 28.5 meter, the average Error_{xy} = 0.50 is 14.2 meter.

Remotely sensed imagery can be digitally classified through two means: unsupervised and supervised classification techniques. These methods differ in that an unsupervised classification involves separation of spectral classes by the software with the user then classifying each range into a class while a supervised classification utilizes user inputted training sites to classify each pixel in the image into the various corresponding training sites [Schnitzer,P.,2007]. In this research the supervised classification was used.

6.2.4 Supervised Classification

The procedure of supervised classification will be more controlled by the user than unsupervised classification. Supervised classification starts with training, which results in various signatures, and followed by class assignment using a decision rule [ERDAS Field Guid , 1997].

Training is the process of defining the criteria by which patterns are recognized [Hord, 1982]. The computer must be trained to recognize patterns in the data. Training samples for each land-use type are first selected by use of ground truth data, aerial photos, and maps. Signatures

for each class are then generated from the training samples. Signatures are statistical criteria for the corresponding classes. Finally the pixels in the image are sorted into classes based on the signatures, by use of a classification decision rule. The decision rule is a mathematical algorithm that performs the actual sorting of pixels into distinct classes [ERDAS Field Guide, 1997]. In this research Training samples for each land-use type are selected by the use of the only available mean i.e., geological map.

In this research, the Gaussian Minimum Distance, Mahalanobis Distance, and Maximum Likelihood/ Bayesian methods/classifier were utilized to classify the image using ENVI 4.4 image processing software. These decision rules are discussed in the following sections

6.2.4.1 Minimum Distance Classifier

The mean spectral value in each band for each information class is determined. These spectral values comprise the mean vector for each class [Lillesand, T.M., and Kiefer, R.W. ,2001]. The minimum distance decision rule calculates the spectral distance between the measurement vector for the pixel to be classified and the mean vector for each signature [Erlangung,Z.,1999]. The unclassified pixel is assigned to class membership based on the closest mean class value, or minimum distance [El-Gafy,M.,2005].

The equation for classifying by spectral distance is based on the equation for Euclidean distance

$$SD_{xyc} = \sqrt{\sum_{i=1}^n (\mu_{ci} - X_{xyi})^2} \quad (6-1)$$

where:

n : number of bands (dimensions)

i : a particular band

c : a particular class

X_{xyi} : data file value of pixel x,y in band i

μ_{ci} : mean of data file values in band i for the sample for class c

SD_{xyc} : spectral distance from pixel x,y to the mean of class c

When spectral distance is computed for all possible values of c (all possible classes), the class of the candidate pixel is assigned to the class for which SD is the lowest [Swain, Philip H., and Shirley M. Davis., 1978].

6.2.4.2 Mahalanobis Distance Classifier

The Mahalanobis distance algorithm assumes that the histograms of the bands have normal distributions. In addition to the mean value of the signature class the covariance matrix (covariance and variance) is included in the calculation [Andersen, G., 1998].

Mahalanobis distance is similar to minimum distance, except that the covariance matrix is used in the equation. Variance and covariance are figured in so that clusters that are highly varied lead to similarly varied classes, and vice versa. For example, when classifying urban areas—typically a class whose pixels vary widely—correctly classified pixels may be farther from the mean than those of a class for water, which is usually not a highly varied class [Swain, Philip H., and Shirley M. Davis., 1978].

The equation for the Mahalanobis distance classifier is as follows:

$$D = (X - M_c)^T (Cov_c^{-1}) (X - M_c) \quad (6-2)$$

Where:

D : Mahalanobis distance

c : a particular class

X : the measurement vector of the candidate pixel

M_c : the mean vector of the signature of class c

Cov_c : the covariance matrix of the pixels in the signature of class c

Cov_c^{-1} : inverse of Cov_c

T : transposition function

The pixel is assigned to the class, c , for which D is the lowest [ERDAS Field Guide, 2005].

6.2.4.3 Maximum Likelihood/Bayesian Classifier

This classification method uses the training data as a means of estimating means and variances of the classes, which are then used to estimate probabilities. Maximum likelihood classification considers not only the mean or average values in assigning classification, but also the variability of brightness values in each class [Campbell, J., 2001].

The maximum likelihood algorithm is the most common decision rule for supervised classification. This decision rule is based on the probability that a pixel belongs to a particular class. It assumes that these probabilities are equal for all classes, and that the input bands have normal distributions [Erlangung, Z., 1999].

If you have a priori knowledge that the probabilities are not equal for all classes, you can specify weight factors for particular classes. This variation of the maximum likelihood decision rule is known as the Bayesian decision rule [*Hord, 1982*]. Unless you have a priori knowledge of the probabilities, it is recommended that they not be specified. In this case, these weights default to 1.0 in the equation.

The equation for the maximum likelihood/Bayesian classifier is as follows:

$$D = \ln(a_c) - [0.5 \ln(|Cov_c|)] - [0.5 (X-M_c)^T (Cov_c^{-1}) (X-M_c)] \quad (6-3)$$

D : weighted distance (likelihood)

c : a particular class

X : the measurement vector of the candidate pixel

M_c : the mean vector of the sample of class c

a_c : percent probability that any candidate pixel is a member of class c (defaults to 1.0, or is entered from a priori knowledge)

Cov_c : the covariance matrix of the pixels in the sample of class c

| Cov_c | : determinant of Covc (matrix algebra)

Cov_c⁻¹ : inverse of Covc (matrix algebra)

Ln : natural logarithm function

T : transposition function (matrix algebra)

The pixel is assigned to the class, c, for which D is the lowest [*ERDAS Field Guide, 2005*].

6.2.5 Accuracy Assessment

Accuracy assessment is done by comparing the supervised classification maps with the available geological map, this geological map represented

the reference of training areas (signatures) taking on the image [<http://members.chello.nl/~r.sugardiman/ThesisRu/08CH5.pdf>].

Accuracy assessment forms the most important integral part of the classification process. No classification is complete until its accuracy has been assessed [*Chatterjee, B., 2006*]. The following are two methods commonly used to do the accuracy assessment.

6.2.5.1 The Error Matrix

Error Matrix is the most effective way of representing map accuracy in which the individual accuracies of each category are mainly described along with both error of commission and error of omission. User's accuracy, producer's accuracy and overall accuracy can be judged with the help of error matrix method. The brief description of the accuracy indexes are given below [*Chatterjee, B., 2006*].

A- Overall Accuracy

The proportion of the reference pixels which are classified correctly is known as the overall accuracy. It is computed by dividing the total number of correctly classified pixels by the total number reference pixels. It is a very coarse measurement and does not provide the information about the classes that are classified with good accuracy [*Chatterjee, B., 2006*]. Table (6-3) are illustrate the error matrix for the maximum likelihood soil classification map with the 16 class and the value for the overall classification accuracy and overall Kappa Statistics for this soil classification map.

B- Producers Accuracy

Producer's accuracy is the probability of a reference (training) pixel being correctly classified, i.e., a measure of omission error. It is the number of

pixels correctly classified as a land cover class divided by the total number of reference pixels for that land cover class [*Jiang Li and Ram M. Narayanan., 2004*].

C- User's Accuracy

User's accuracy indicates reliability, or the probability that a pixel classified in the image is really that land cover class on the ground. It is the number of pixels correctly classified as a land cover class divided by the total number of pixels that were classified in that land cover class [*Jiang Li and Ram M. Narayanan., 2004*]. Table (6-4) are illustrates the producers accuracy and the user accuracy for the maximum likelihood classification map with 16 class.

Table (6-4): Illustrates the Producer's Accuracy and User Accuracy For the Maximum Likelihood Classification Map Used 16 Classes.

Class	Prod. Acc .(Percent)	User Acc .(Percent)	Prod Acc. (Pixels)	User Acc. (Pixels)
Water	95.94	97.90	3457601/3603746	3457601/3531924
Qst	36.76	89.46	266590/725217	266590/298004
Qsd	45.25	93.23	5193026/11475037	5193026/5570141
Telmn	52.22	25.86	173654/332545	173654/671437
Khll	18.18	15.08	112492/618742	112492/745923
Qfg	57.97	14.85	109647/189152	109647/738513
Jmj	41.86	13.07	56119/134060	56119/429445
Qw	13.93	81.74	92624/664912	92624/113316
Kwt	7.35	9.29	49445/672417	49445/532132
Qh	33.29	26.05	552361/1659035	552361/2120751
Qqn	71.49	21.18	324076/453339	324076/1530018
Tplhj	70.11	3.55	98734/140831	98734/2782204
Ksd	29.46	18.80	250830/851488	250830/1334058
Jbgh	34.94	9.78	32938/94276	32938/336673
Teleg	48.37	8.72	84529/174751	84529/969267
Jsh	63.94	19.59	24225/37890	24225/123632

6.2.5.2 Kappa Statistics

Overall Kappa statistics and individual Kappa values for each class are calculated for the thematic maps. Kappa coefficient measures the difference between the agreement of the reference data and classification results and the chance agreement of the reference data and a random classifier [Gregory, J *et. al.*, 2003]. It provides a better measure of the accuracy of a classifier than the overall accuracy, and it takes into account the whole confusion matrix rather than the diagonal elements alone [Pal, M., 2002].

6.3 Results and Analysis

The main aim of this investigation is to assess the relative performance of three classification approaches in remote sensing, which are, maximum likelihood, mahalanobis distance and minimum distance methods, by using different number of classes which, affect their performance in terms of the overall classification accuracy. Tables (6-5), (6-6) and (6-7) show

the overall accuracy and kappa results obtained for the three classifier methods in the study area.

These tables indicate that the obtained classification results from the maximum likelihood classifier are the best of the three methods for all different classes. In this method the number of 16 classes gives the best overall accuracy. Finally, the produced classified map based on this technique is shown in Figure (6-4) and the other figures are illustrates the different methods classification with various classes.

Water is almost classified perfectly because that both the producer's and user's accuracy are high based on the higher compatibility between the reference geological map and the spectral resolution in the image classified in the water class this interpreter the harmony in the water signatures and lager size of signature.

Table (6-5): Accuracy of Maximum Likelihood Classification at the Various Numbers of Classes

Number of classes	Overall accuracy %	Kappa coefficient %
32	40.2584	31.50
28	44.2044	34.39
24	45.1891	35.31
20	47.3693	37.21
16	49.8404	39.08

Table (6-6): Accuracy of Mahalanobis Distance Classification at the Various Numbers of Classes

Number of classes	Overall accuracy %	Kappa coefficient %
32	34.6370	25.93
28	37.6138	28.08
24	38.4872	28.72
20	42.8203	32.40
16	45.3723	34.30

Table (6-7): Accuracy of Minimum Distance Classification at the Various Numbers of Classes

Number of classes	Overall accuracy %	Kappa coefficient %
32	26.8647	20.79
28	27.5227	21.25
24	27.8866	21.52
20	29.4393	22.47
16	38.6305	27.02

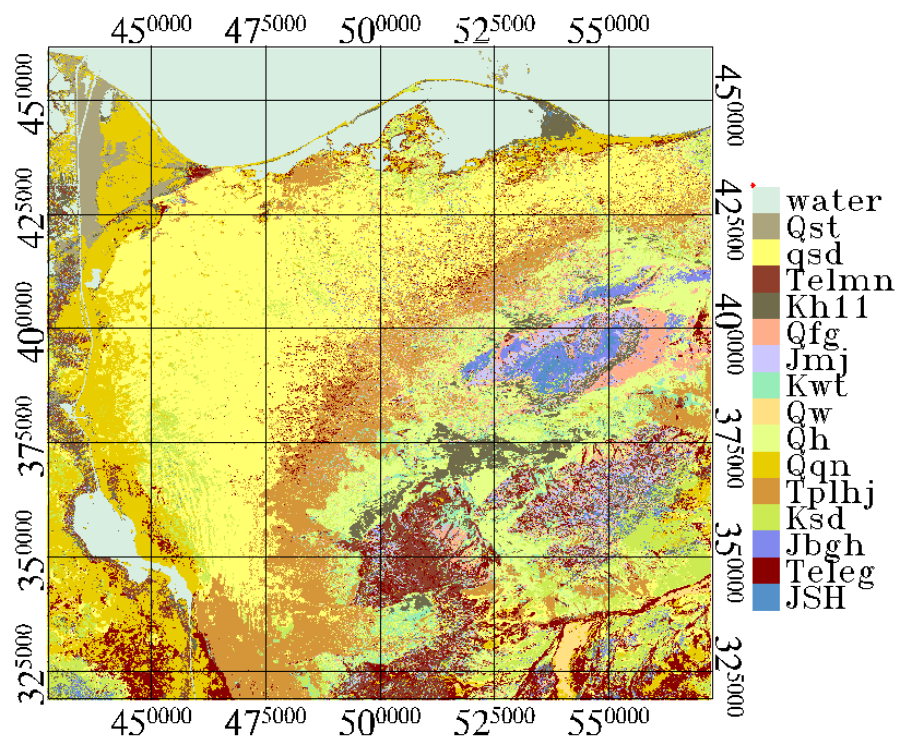


Figure (6-4):Maximum likelihood Classified Landsat-5 image with 16 class

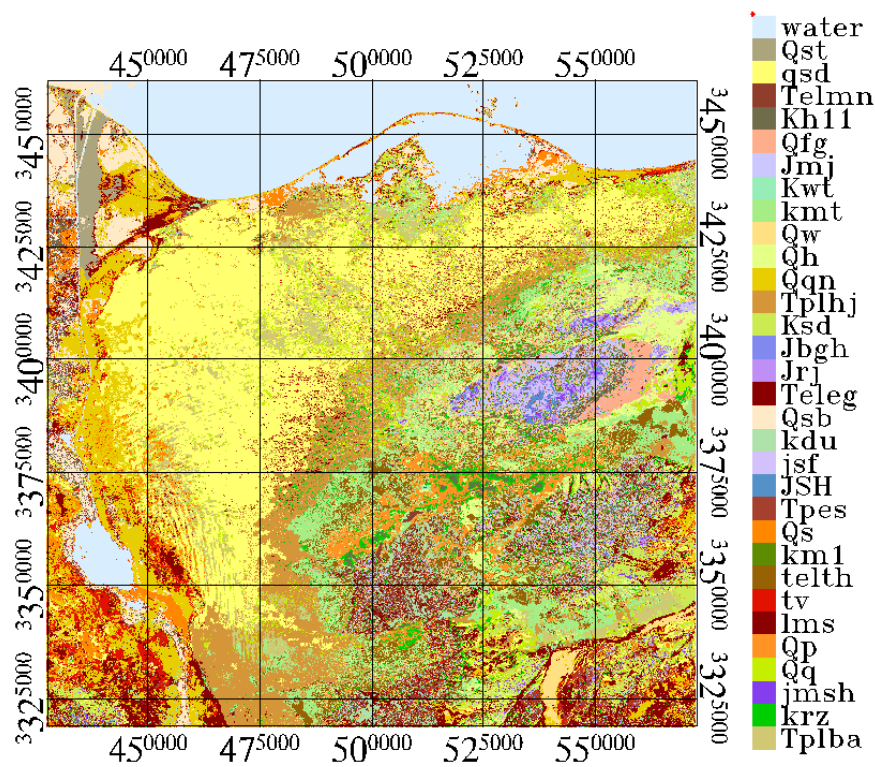


Figure (6-5):Maximum likelihood Classified Landsat-5 image with 32 class

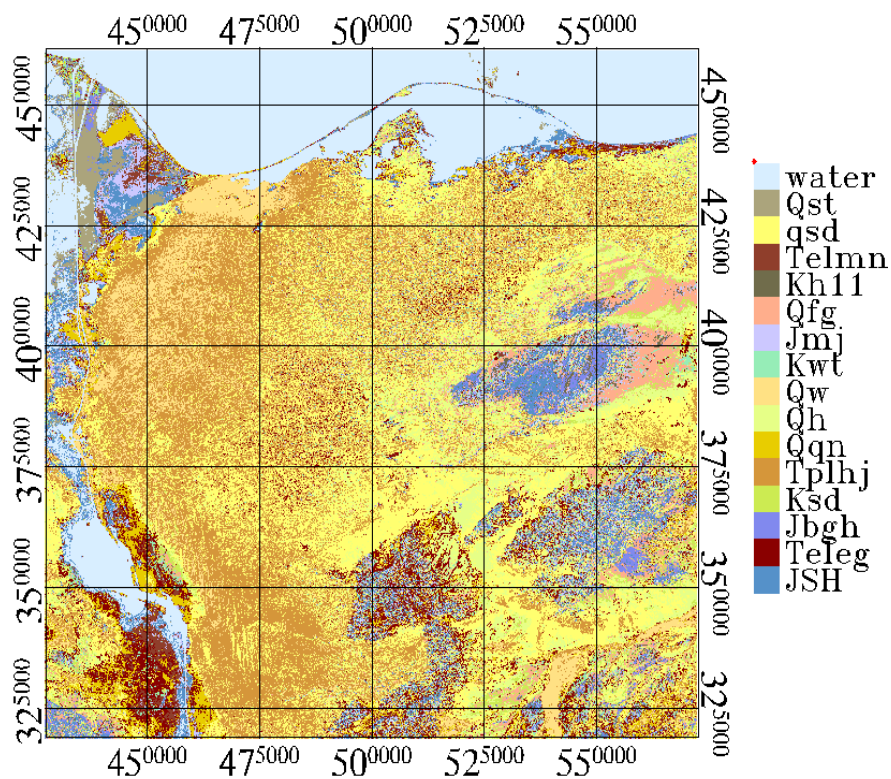


Figure (6-6):Minimum Distance Classified Landsat-5 image with 16 class

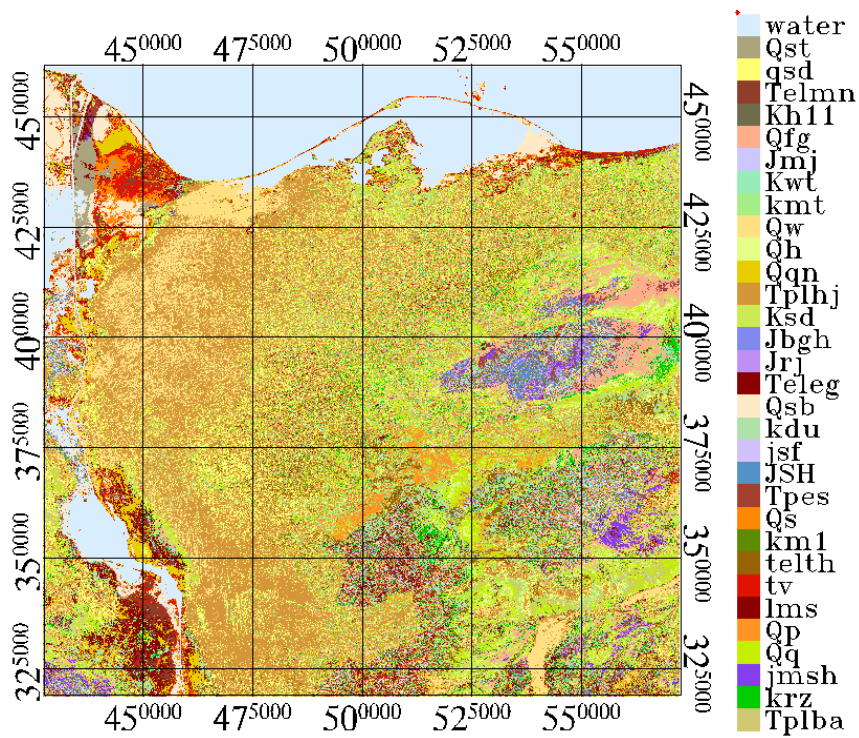


Figure (6-7): Minimum Distance Classified Landsat-5 image with 32 class

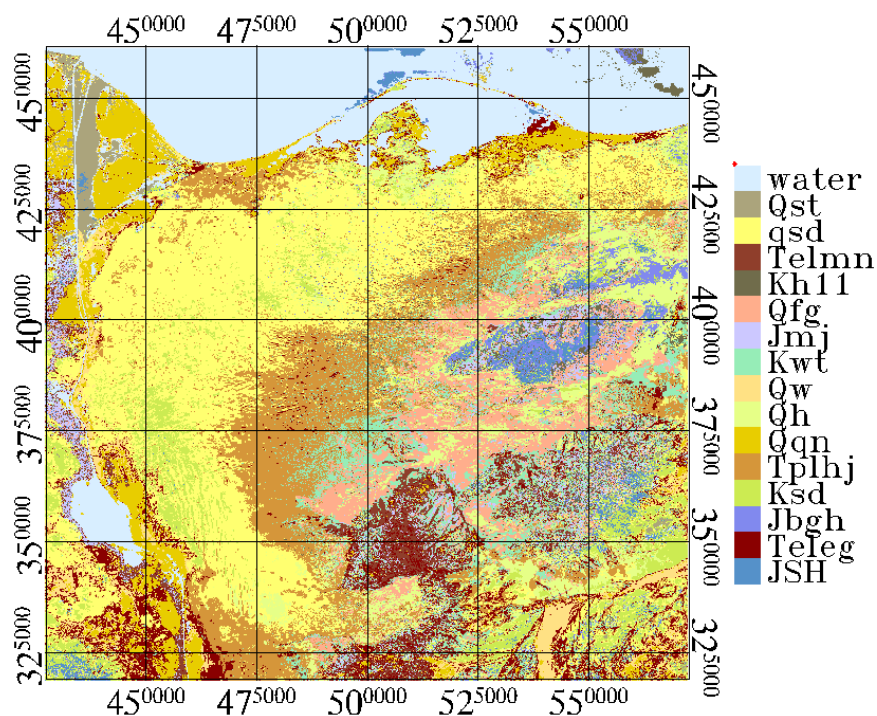


Figure (6-8): Mahalanobis Distance Classified Landsat-5 image with 16 class

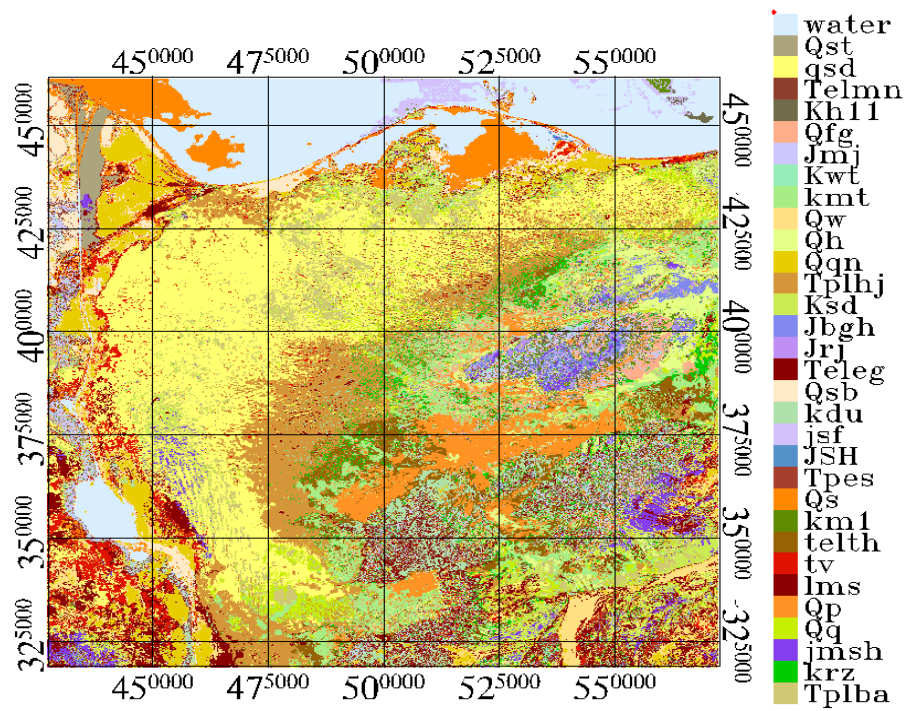


Figure (6-9): Mahalanobis Distance Classified Landsat-5 image with 32 class

Table (6-3): Error Matrix for the Maximum Likelihood Map Produced From Landsat-5 Image Used 16 Classes

	Ground Truth (Pixels)																
Class	Water	Qst	Qsd	Telmn	Khll	Qfg	Jmj	Qw	Kwt	Qh	Qqn	Tplhj	Ksd	Jbgh	Teleg	Jsh	Total
Water	3457601	41069	8139	699	2070	0	0	0	864	10	20652	0	817	1	0	2	3531924
Qst	19034	266590	8221	33	1032	0	1	122	1314	108	154	0	1313	0	91	0	298004
Qsd	1019	2133	5193026	2517	23813	1533	1267	60995	23307	93327	40088	28032	84883	1526	12475	200	5570141
Telmn	8904	6565	100713	173654	40630	2902	4083	43296	111473	86895	18867	1534	61305	166	10367	83	671437
Khll	50057	28521	279949	24681	112492	2635	8925	13911	66666	114595	13829	33	18464	4984	4637	1544	745923
Qfg	86	209	282529	12093	76108	109647	19294	13341	70550	106627	38	423	35877	8574	2684	433	738513
Jmj	725	155	84826	25821	101189	10991	56119	5279	87469	38532	245	361	12718	1893	2836	286	429445
Qw	71	1	1345	98	41	0	0	92624	46	3927	109	0	12523	0	2531	0	113316
Kwt	947	793	269674	12680	22123	3539	3080	28763	49445	106058	385	1218	30016	1251	2022	138	532132
Qh	104	298	1158456	9731	62787	39620	10344	82534	68875	552361	48	762	115266	15550	3237	678	2120751
Qqn	61481	365892	602572	3937	4736	5	13	43118	5917	31234	324076	2632	54991	6	29397	11	1530018
Tplhj	332	2141	2396129	4680	23979	1178	3041	55063	37483	91415	7409	98734	57286	1087	2220	27	2782204
Ksd	259	2076	717228	5272	38512	714	3327	79924	38676	171066	1444	4011	250830	6011	11011	2597	1334058
Jbgh	122	1131	64289	1970	41804	8340	17562	6602	18389	118716	207	95	11036	32938	5940	7532	336673
Teleg	2339	7568	302930	53348	39885	7927	1861	137216	83426	122499	25648	2991	96059	907	84529	134	969267
Jsh	665	75	5011	1331	27550	21	4043	2124	8517	21665	140	5	8104	19382	774	24225	123632
Total	3603746	725217	11475037	332545	618742	189152	134060	664912	672417	165903	453339	140831	851488	94276	174751	37890	21827438

Overall Classification Accuracy = (10878891/21827438) = 49.8404%

Overall Kappa Statistics = 39.08%

Chapter 7

Summary, Conclusions and Recommendations

7.1 Summary

This research concerns with studying the satellite developing technology in different fields of surveying. Positioning satellites, remote sensing satellites and gravity field satellites are investigated. The practical part in this research introduced a soil classification map for the northern Sinai Peninsula from satellite image and illustrated the best method used in this classification.

The first chapter is considered as a general introduction to the thesis, where a brief background on the subject matter is given first. Then, history of the satellites in different fields of surveying in three branches, positioning, remote sensing, and gravity field the modernization in the used satellites is introduced. The main objective of this research are explicitly defined.

Chapter (2) is devoted to the description of the positioning satellites which divided into two components, the first is global positioning satellites such as TRANSIT, NAVSTAR, GLONASS, GALILIO and BEIDOU-2 and the second is regional positioning satellites such as, BEIDOU-1, QZSS and IRNSS. Additionally, other satellites are contributing to increase the efficiency of the positioning satellites, these satellites are called augmentation satellites. Space based augmentation system, divided into two components, the first is global space based augmentation system, OmniSTAR, StarFire and VueStar. The second is regional space based augmentation system, EGNOS in Europe, WAAS in the USA and MSAS in Japan. Several other SBAS systems are now in study or development phase for the coverage of other regions (GAGAN in India, CWAAS in Canada and SNAS in China. Nigeria is also planning NIGCOMSAT, Russia is also planning SDCM this is Wide-area (Russia)

and ground based augmentation systems such as LAAS. Finally, the chapter illustrates the modernization of receivers.

Chapter (3) concentrates on the description of the two main types of Remote Sensing Technology. Firstly, Aerial Photography, passive remote sensing using such as Panchromatic scanners, Multispectral scanners, Hyperspectral scanners Thermal scanners and Passive Microwave scanners. Secondly, Active Remote Sensing Technologies such as Radio Detection And Ranging (RADAR), Synthetic Aperture Radar (SAR), Interferometric Synthetic Aperture Radar (IfSAR), Light Detection And Ranging (LIDAR) and Sound Navigation And Ranging (SONAR). The satellite orbits which include: geostationary orbits and polar orbits are explained. The image resolution is illustrated in spatial resolution, spectral resolution, temporal resolution and radiometric resolution. The digital image and its processing are manipulated. Satellite platforms and most common optical land imaging satellites in Egypt are illustrated.

Chapter (4) is oriented to the presentation and discussion of the basic gravity field quantities, Gravity field determination from satellite data, Satellite tracking, High-Low Satellite-to-Satellite Tracking (hl-SST) as CHAMP, Low-Low Satellite-to-Satellite Tracking (ll-SST) as GRACE, Satellite Gradiometry as GOCE and Satellite Altimetry. This chapter explains in details the components and the theory of operation, applications for the above systems and illustrates, global gravity field models from the CHAMP, global gravity field models from GRACE, combined global gravity field models from CHAMP and GRACE, combined global gravity field models from GRACE, LAGEOS and Surface Gravity Data.

Chapter (5) presents some proposals which could be done by those satellites separately or integrated in different fields of applications in Egypt. GPS proved itself as a powerful surveying tool. It is used in Egypt in many surveying and geodetic applications. Stations of large spacing, geodetic networks, are fixed using GPS such as High Accuracy Reference Network (HARN), National Agriculture Cadastral Network (NACN), Radio Beacon Network and FINNMAP Project. Remote sensing satellites imagery are suggested to be used for more applications in Egypt such as estimation of water loss from Toshka Lakes using remote sensing and GIS, middle Egypt survey project 2004 and Remote Sensing and GIS for Integrated Coastal Zone Management, a case Study: The Coral Reefs In The Northwestern Red Sea (HURGHADA, EGYPT).

Chapter (6) presents the practical part of this research which uses supervised classification techniques for producing recent geological map for northern Sinai Peninsula from Landsat TM-5 medium resolution image. Then the obtained results will be analyzed and checked out against a reference geological map of northern Sinai Peninsula. The obtained results illustrated the best method which is maximum likelihood.

Chapter (7) summarizes the basic work performed in this research. Then, the important conclusions, as deduced from the obtained results are stated. Finally, appropriate recommendations, associated with the stated conclusions, are suggested for the future researches connected with the applications using these satellites.

7.2 Conclusions

Based on the obtained results in our investigation contained herein, the following conclusions may be stated

- The modernization for the GPS will increase the accuracy using three civil frequencies will allow users to remove the ionospheric delay, which is the largest GPS error source. More specifically, the new signals will enable the following performance hierarchy:
 - a- Legacy users will continue to operate as before. Some will derive an ionospheric estimate from the single frequency ionospheric model included in the GPS navigation message. Others will use differential GPS to remove most of the ionospheric error, but with the cost of a reference receiver and data link. Single frequency users of SBAS will continue to use the real time ionospheric model contained in that data stream.
 - b- The traditional L1/L2 combination and the new L1/L5 combination will be the best, because the frequency differences are 348 and 399 MHz respectively. The L2/L5 combination will be less effective for ionospheric estimation, because the frequency difference is only 51 MHz.
- The future of high accuracy GNSS must recognise the following issues:
 - a- Experience with real-time GPS surveying shows that performance improves when more satellites are available.
 - b- Extra signals are not only useful for ionospheric correction; they also increase the number of observations available for ambiguity resolution, which delivers high accuracy sooner and with greater reliability. Therefore, dual frequency measurements have proved very useful in GPS surveying,

hence being able to use three frequencies will increase performance even more.

- c- Any extra signals carrying a civilian code can be accessed by less complicated receivers than is currently the case. This should lead to a new generation of less expensive receivers capable of delivering high accuracy.
- d- The techniques employed in real-time GPS surveying are already addressing other applications, including the field of machine guidance servicing construction, mining and agriculture. These industries have high marginal costs and therefore require high levels of reliability and very robust solutions.
- Remotely sensed data are commonly used for the classification and mapping of vegetation over large spatial scales, replacing traditional classification methods, which require expensive and time-intensive field surveys.
- Recent experiments of a project that deals with the combined use of high resolution satellite images, Quickbird, and laser scanner data to analyze urban images. The aim of the project is to recognize buildings and point out the occurrence of new buildings or detect new compartments within old constructions, based on a more comprehensive description of the visible objects within the image.
- The use of hyper-spectral imagery to detect oil spills in water and soil has a lot of advantages in the field. It can be used to monitor oil facilities and therefore prevent worst scenarios when a leak in the facility is found. Also can be used to help planning the cleanup

of the area, by quickly identifying the affected areas and possible path of the spill to be one step ahead.

- Soil erosion, which directly effects on the development of human society, is the one of important problems human being faces, so nations in the world pay attention to the soil erosion conservation. Remote Sensing Interpretation is monitoring the soil erosion.
- New global gravity field models derived from the satellite missions CHAMP, GRACE and GOCE are expected to significantly improve the long wavelength gravity spectrum.
- Launches of the CHAMP and GRACE satellite missions have produced a new generation of global geopotential models (GGMs). The performance of seven recent GGMs has been analyzed using a local geodetic dataset (terrestrial gravity and GPS/ leveling points) in Egypt. The results show that the EIGEN-CG01C model is best at representing the long and medium wavelengths of gravity field in Egypt.

7.3 Recommendations

According to the above stated conclusions, and the findings in the present research, the following recommendations can be suggested:

- A nationwide network of GPS Continuously Operating Reference Stations, known as the National CORS is proposed. CORS is a GPS augmentation established by the National Geodetic Survey that supports non-navigation, post-processing applications. Typical uses of National CORS are for land management, coastal

monitoring, civil engineering, boundary determination, mapping, and geographical information systems, and both geophysical and infrastructure monitoring as well as future improvements to weather predicting and climate monitoring. An enhancement to the basic GPS signal known as Differential GPS (DGPS) provides much higher precision and increased safety in its coverage areas.

- Use GPS to help in surveying road and highway networks, by identifying the location of features on, near, or adjacent to the road networks. These include service stations, maintenance and emergency services and supplies, entry and exit ramps, damage to the road system, etc. The information serves as an input to the GIS data gathering process. This database of knowledge helps transportation agencies to reduce maintenance and service costs and enhances the safety of drivers using the roads.
- Studying certain endemics, various endemics can be captured by the spatial, temporal, and spectral resolutions of RS satellite onboard sensors. Remote sensing, combined with other technologies like GPS (Global Positioning System), capable of spatially locating the event.
- Over the past 2 decades, the development of airborne and satellite hyperspectral sensor technologies has overcome the limitations of multispectral sensors. In Egypt many applications can depend on this technologies because narrow bandwidths characteristic of hyperspectral data permit an in-depth examination of earth surface features which would otherwise be 'lost' within the relatively coarse bandwidths acquired with multispectral data. Hyperspectral data at a finer spectral resolution can be used to improve vegetation

classification, by detecting biochemical and structural differences in vegetation

- Salinization is a major form of land degradation in agricultural areas, where information on the extent and magnitude of soil salinity is needed for better planning and implementation of effective soil reclamation programs from Remotely sensed data
- Using carrier phase differential GPS, a network of receiver modules can be installed in order to perform monitoring and surveillance operations for small movements. Typical applications for this type of sensor network include monitoring of structures such as buildings, dams, bridges, as well as measuring the movement of landslides and rock formations.
- Technologies such as laser scanners and other technologies, hyperspectral technology, etc. can be used to measure the Nile river environments and prepared Nile river environment information maps.
- The reference datum for GNSS is WGS84 where heights are referred to a theoretical "mathematical" ellipsoid, not to real-life terrain or geopotential surface. Hence, in order to reference GNSS-derived heights to terrain, the geoid–ellipsoid separation must be known to be used in the famous equation of $h = H + N$. using GNSS/Benchmark data in Egypt (geoid separation) to evaluate the recent geoid models produced from the gravity field satellites and chose the optimum geoid model compatible with GNSS/Benchmark data

- Shoreline mapping and shoreline change detection are critical in many coastal zone applications. Shorelines can be extracting from satellite imagery and any change in shoreline can be computed by using many satellite images at different dates for the same region.
- Soil Classification Maps for certain desert areas, can be prepared by using remote sensing techniques and digital image analysis.
- It is recommended to compare of recent GGMs with terrestrial gravity data, GPS/ leveling points in Egypt to choose the best model used to improve the related applications.

References

REFERENCES

- **Aggarwal,S.,(1997):**" Earth Resource Satellites" Photogrammetry and Remote Sensing Division, Indian Institute of Remote Sensing, 1997.
- **Aggarwal,S.,(1998):**"Principles of Remote Sensing " Photogrammetry and Remote Sensing Division Indian Institute of Remote Sensing, Dehra Dun,1998.
- **Alan Zor., (2002):** " GPS Modernization", Dynamics Research Corporation Systems Engineering Group 60 Frontage Road Andover, MA 01810, 30 October 2002.
- **Alspaugh, D., 2004:** A brief history of photogrammetry, in McGlone, J.C., Mikhail, E.M., Bethel, J. and Mullen, M., eds., Manual of Photogrammetry: Bethesda, MD, American Society of Photogrammetry and Remote Sensing, p. 1-14.
- **Andersen,G.,1998:** " Classification and Estimation of Forest and Vegetation Variables in Optical High Resolution Satellites: A Review of Methodologies", International Institute for Applied Systems Analysis, Laxenburg, Austria, October 1998
- **Balmino G., R. Sabadini, C.C. Tscherning, and P. Woodworth.,(1998):**" Tutorial # 3",1998
- **Berkes, U., (2002):** "GALILEO System Update", European CGSIC Meeting - Eurocontrol, 5-6 December 2002, Brussels.
- **Borjesson,J., (2000):** " GLONASS Contributions to Space Geodesy" Department of Radio and Space Science ,Chalmers University of Technology, Goteborg, Sweden 2000.
- **Campbell, J. B. (2002):**" Introduction to remote sensing" 3rd edition. Taylor and Francis press. 620 p.

- **Campbell,J.,2001:** " Digital Image Classification Geography 4354 – Remote Sensing, December 10, 2001.
- **Carroll,J.,(2004):**" A Survey of Possible Methods for Mitigating the Impact of Radio Frequency Interference on Satellite Navigation Systems Used for Precision Approach", Volpe National Transportation Systems Center, Cambridge, Mass. USA, April 29, 2004.
- **Chatterjee,B.,(2006):** "Satellite Based Monitoring Of the Changes in Mangroves in South Eastern Coast and South Andaman Islands of India - A Tsunami Related Study", January, 2006.
- **Chou,H.,(2006):** " An Introduction to Satellites Navigation ,Ph.D, Project Management Institute, April 25,2006.
- **Christoph ABART(2005):**"Assessment of Solution Strategies for GRACE Gravity Field Processing", Master Thesis, Institute of Navigation and Satellite Geodesy Graz University of Technology, Graz, March 2005.
- **Christoph Reigber, Hermann Lühr, Peter Schwintzer GeoForschungsZentrum Potsdam (2001):**" Announcement of Opportunity for CHAMP", gfz-potsdam, May 28, 2001.
- **Crane, M., Clayton, T., Raabe, E., Stoker, J., Handley, L., Bawden, G., Morgan, K. and Queija, V., 2004:** Report of the U.S. Geological Survey LIDAR Workshop Sponsored by the Land Remote Sensing Program and held in St. Petersburg, FL, November 2002: U.S. Geological Survey, Open-file Report 04-106, 72 p.
- **Crews,M., (2008):** " Long-Term Future of GPS", Institute of Navigation (ION)San Diego, Col Mark Crews,28 January 2008.

-
- **Daras,I,(2008):** " Determination of a gravimetric geoid model of Greece using the method of KTH, M.Sc. Thesis in Geodesy No. 3102 TRITA-GIT EX 08-002, Royal Institute of Technology (KTH) School of Architecture and the Built Environment 100 44 Stockholm, Sweden, January 2008.
 - **Dempster,A.,(2007):**" The "System of Systems" Receiver: an Australian Opportunity, International Global Navigation Satellite Systems Society IGNSS Symposium 2007, The University of New South Wales, Sydney, Australia 4 – 6 December, 2007.
 - **Drobnjak,S., Tomić,S., Pejić,M.,2006:** " Analysis of Methods of Automatic Extraction Vegetation From The Satellite Images, 2006.
 - **Dumesnil, N., (2007):**" European Global Navigation System Services Programme", N. Dumesnil , September 2007.
 - **Dunn, C., et al. (2003):** " Instrument of GRACE: GPS augments gravity measurements", GPS World, 14(2),16-28,2003.
 - **Eicker,A.,(2008):** " Gravity Field Refinement by Radial Basis Functions from In-situ Satellite Data", Erlangung des akademischen Grades Doktor_Ingenieur (Dr._Ing.), Institut für Geodäsie und Geoinformation der Universität Bonn, 30. Januar 2008.
 - **Eissfeller,B., Ameres,G., Kropp,V., Sanroma,D., Munchen,(2007):** "Performance of GPS, GLONASS and GALILEO" ,2007.
 - **El Bastawesy,M., et. al., (2007):** " Estimation of Water Loss from Toshka Lakes Using Remote Sensing and GIS", National Authority for Remote Sensing and Space Science (NARSS), Cairo, Egypt, 2007.

-
- **El-Gafy,M.,(2005):** " Environmental Impact Assessment of Transportation Projects: An Analysis Using An Integrated GIS, Remote Sensing, And Spatial Modeling Approach ", The Florida State University College of Engineering, Spring Semester, 2005.
 - **El-Rabbabny, A.,(2002):** "Introduction to GPS:The Global Positioning System" Artech House, Boston. London, www.Artechhouse.com.
 - **ElSagheer,A.,(2005):**" Practical Evaluation of the Influence of: GPS Error Sources, Processing Strategies, Reference Stations, and Adjustment Criterion on Positioning Accuracy", Shoubra Faculty of Engineering, 2005.
 - **Enderle,W.,(2009):** "Benefits of Galileo for Future Space Missions", 7th IAA Symposium on Small Satellites for Earth Observation, 07/05/2009.
 - **ENVI 4.4 Help.**
 - **ERDAS Field Guide 1997**
 - **ERDAS Field Guide,2005**
 - **Erlangung,Z.,1999:** " A New Information Fusion Method for Land-Use Classification Using High Resolution Satellite Imagery", der Johannes Gutenberg-Universität in Mainz, Germany
 - **Featherstone,W.,(2003):**" Improvement to long-wavelength Australian gravity anomalies expected from the CHAMP, GRACE and GOCE dedicated satellite gravimetry missions,2003.
 - **Fehringer, M., Mark R. Drinkwater, R. Haagmans, D. Muzi, A. Popescu, R. Floberghagen, and M. Kern,(2007):**"The GOCE Gravity Mission: ESA'S First Core Earth Explorer", Proceedings of the 3rd International GOCE User Workshop, 6-8 November,

-
- 2006, Frascati, Italy, ESA Special Publication, SP-627, ISBN 92-9092-938-3, pp.1-8, 2007.
- **Finnmap Project (1989):**" Egyptian Survey Authority", Final Report, Eastern Desert Topographic Mapping Project.
 - **Fitzgerald, R. W., and Lees, B. G. (1994):** "Assessing the classification accuracy of multisource remote sensing data. Remote Sensing of the Environment", 47, 362-368.
 - **Ford, J.P., Blom, R.G., Coleman, J.L. Jr., Farr, J.J., Plaut, H.A. and Sabins, F.F., Jr., (1998):** Radar Geology, in Henderson, F.M. and Lewis, A.J., eds., Principles and Applications of Imaging Radar: New York, John Wiley & Sons, p. 511-559.
 - **Francois, R.,(2007):**"Critical Analysis Report (Public Version)", European GNSS Supervisory Authority, HARMLESS,19/04/2007.
 - **Franklin, S.E. (2001):** "Remote sensing for sustainable forest management", CRC Press. 407 p.
 - **Geo Yan,(2003):** "Pixel based and object oriented image analysis for coal fire research" ITC, Netherlands.
 - **Giannon,F.,(2006):**" A Rigorous Model for High Resolution Satellite Imagery Orientation" PhD, University of Rome "La Sapienza" Faculty of Engineering, Department of "Idraulica e Trasporti e Strade" "Geodesia e Geomatica" Rome, 2006.
 - **Gomaa M., and Sherine S.,(2005):**" Enhancing the Integrity of the National Geodetic Data Bases in Egypt", FIG Working Week 2005 and GSDI-8, Cairo, Egypt April 16-21, 2005.
 - **Gregory, J., Siamak Khorram, Donald F. Stallings, Halil Cakir, (2003):**" High Resolution Mapping Land Cover Classification of the Hominy Creek Watershed", Center for Earth Observation North

-
- Carolina State University, CEO Technical Report 220, November 24, 2003.
- **Grewal ,M. S., Weill ,L. R., and . Andrews ,A. P., (2007):** " Global Positioning Systems, Inertial Navigation, and Integration",2007.
 - **H.R. Matinfar. et al (2007):**" Comparisons of Object-Oriented and Pixel-Based Classification of Land Use/Land Cover Types Based on Landsat7, Etm+ Spectral Bands (Case Study: Arid Region of Iran)", 1H.R. Matinfar, 2F. Sarmadian, 3S.K. Alavi Panah and 4R.J. Heck, 1University of Lorestan, Iran 2Department of Soil Science, University of Tehran, Iran 3College of Geography, University of Tehran, Iran 4Land Resource Science Department, University of Guelph, Iran.
 - **Hoffmann-Wellenhof, B., H. Lichtenegger, and J. Collins,(2001):** "Global Positioning System: Theory and Practice", 5th ed., New York: Springer-Verlag, 2001.
 - **Hord, R. Michael. (1982):** "Digital Image Processing of Remotely Sensed Data" New York: Academic Press.
 - **<http://adt.curtin.edu.au/theses/available/adt.WCU20071112.131832/unrestricted/10appendices.pdf>**
 - **http://calval.cr.usgs.gov/documents/LDGST_overview_LDCM.pdf**
 - **http://dprg.geomatics.ucalgary.ca/files/Courses/435/435_CH3_6.pdf**
 - **http://dspace.unitus.it/bitstream/2067/77/3/cmraposo_tesid.pdf**
 - **http://en.wikipedia.org/wiki/GPS_modernization**.
 - **http://faculty.missouristate.edu/x/XinMiao/class/GRY551/Classification_Methods.pdf**.
 - **<http://geodesy.eng.ohio-state.edu/course/g609/>**.
 - **http://geog.tamu.edu/~liu/courses/g489/note7_1.pdf**

- <http://geog.tamu.edu/~liu/courses/g661/orbits.pdf>
- <http://icgem.gfz-potsdam.de/ICGEM/ICGEM.html>
- <http://members.chello.nl/~r.sugardiman/ThesisRu/08CH5.pdf>
- http://op.gfz-potsdam.de/champ/index_CHAMP.html
- http://op.gfz-potsdam.de/champ/results/index_RESULTS.html
- <http://pnt.gov/public/2006/2006-06-zambia/ken2.ppt>
- http://sedac.ciesin.columbia.edu/remote_sens/RemoteSensing.pdf
- http://space.skyrocket.de/index_frame.htm?http://space.skyrocket.de/doc_sdat/nigcomsat-1.htm
- http://spacegrant.nmsu.edu/statewide/projects/remote_sensing.pdf
- [http://telecom.tlab.ch/~zogg/Dateien/GPS_Compendium\(GPS-X-02007\).pdf](http://telecom.tlab.ch/~zogg/Dateien/GPS_Compendium(GPS-X-02007).pdf)
- http://volkskunde.at/alp_2006/report_red_team.pdf
- <http://www.fmv.se/upload/Bilder%20och%20dokument/Publikationer/rapporter/Galileo.pdf>
- <http://www.geoinfo.rs/Pdf/NavCom/vuestar.pdf>
- <http://www.navcomtech.com/StarFire/>
- <http://www.space.gov.za/conferences/alc2007/programme/Alale.pdf>
- http://www-app2.gfz-potsdam.de/pb1/op/grace/index_GRACE.html
- **Hughes, C. W and R. J. Bingham,(2006):** " An oceanographer's guide to GOCE and the geoid", Proudman Oceanographic Laboratory, 6 Brownlow St., Liverpool L3 5DA, UK, 20 September 2006
- **Hung, Chih-Cheng, and Kim, 1992:** " The Application of Agglomerative Clustering In Image Classification Systems", Southeastcon '92, Proceedings, IEEE, vol.1, pp.23-26, 1992.

-
- **¹Jiang Li and ²Ram M. Narayanan (2004):**"Integrated Information Mining and Image Retrieval in Remote Sensing" ¹Department of Computer Science and Information Technology Austin Peay State University, ²Department of Electrical Engineering The Pennsylvania State University University Park.
 - **JAXA (2007):** "Quasi Zenith Satellite System Navigation Service" ,Japan Aerospace Exploration Agency, January 22, 2007.
 - **JAYARAMAN, K.S., (2006):** "India To Develop Regional Navigation System",22 May 2006.
 - **Jekeli, C. (1999):**" The determination of gravitational potential differences from satelliteto- satellite tracking",Celestial Mechanics and Dynamical Astronomy, 75, p. 85- 101.
 - **Jensen, John R. (1996):** Introductory Digital Image Processing. Prentice Hall, 2nd. Edition, New Jersey, NY, 750 p.
 - **Jensen, L.L.F. and B.G.H. Gorte, (2001):** "Principle of remote sensing", Chapter 12 Digital image classification, ITC, Enchede, 2nd Edn. The Netherlands.
 - **Kemppi,p.,(2007):**"Next generation satellite navigation systems", VTT Technical Research Centre of Finland, Finland, 2007.
 - **Kishimoto,M.,(2007):** "Quasi-Zenith Satellite System:Status and Design", Japan Aerospace Exploration Agency (JAXA),2007.
 - **Kulkarni,M.,(2000):**" THE GLOBAL POSITIONING SYSTEM AND ITS APPLICATIONS" Prof. Madhav N. Kulkarni, Department of Civil Engineering Indian Institute of Technology, Bombay.2000.
 - **Kumar,M.,(1997):**"Digital Image Processing", Photogrammetry and Remote Sensing Division, Indian Institute of Remote Sensing, Dehra Dun,1997.

- **Leick, A., (2005):**" GPS Satellite Surveying" Third Edition. Hoboken, NJ: John Wiley and Sons.
- **Lemoine, F.G., S.C. Kenyon, J.K. Factor, R.G. Trimmer, N.K. Pavlis, D.S. Chinn, C.M.Cox, S.M. Klosko, S.B. Luthcke, M.H. Torrence, Y.M. Wang, R.G. Williamson, E.C. Pavlis, R.H. Rapp, T.R. Olsen (1998):**"The development of the joint NASA GSFC and the National Imagery and Mapping Agency (NIMA) geopotential model EGM96", NASA Technical paper NASA/TP-1998-206861, Goddard Space Flight Center, Greenbelt.
- **Lillesand, T.M., and Kiefer, R.W. ,2001:** " Remote Sensing and Image Interpretation", 4th ed, John Wiley and Sons, inc. USA, 2001,
- **Lindstrom,G., Gasparini,G.,(2003):**" The Galileo satellite system and its security implications, Gustav Lindstrom and Giovanni Gasparini, Paris, April 2003.
- **Loon,J., (2008):**" Functional and stochastic modelling of satellite gravity data", **NCG** Nederlandse Commissie voor Geodesie Netherlands Geodetic Commission, Delft, October 2008.
- **Louden, E.I., 2003:** Use of the three-dimensional laser scanner at Texas Tech University as a documentation tool at the Statue of Liberty, and diverse historic sites, in HABS 70th Anniversary Symposium: Technology and Architectural Documentation, 6p.
- **Lucas,R., (2006):** "Galileo", Rafael Lucas, March 2006, ESA.
- **Ludwig,D.,(2007):** " European GNSS Programmes" , Dr Daniel Ludwig ,Second meeting of the International Committee on Global Navigation Satellite System (ICG-02), Sept.4-7, 2007, Bangalore, India.

-
- **Matthews, N.A., Breithaupt, B.H. and Moore, R. E., 2001a:** Laser technology meets dinosaur paleontology, in 2001: A fossil odyssey: Partners for a new millennium: The 6th Fossil Resource Conference, Abstracts with Programs, 10 p.
 - **Miller, J. J., (2006):**"Space-Based PNT Modernization Update", India, June 6, 2006
 - **Mohinder S. Grewal, Lawrence R. Weill, Angus P. Andrews,(2001):**"Global Positioning Systems, Inertial Navigation, and Integration", Mohinder S. Grewal, Lawrence R. Weill, Angus P. Andrews,2001.
 - **Nair,M.,(2006):**"SATELLITES FOR NAVIGATION", G Madhavan Nair, PRESS INFORMATION BUREAU GOVERNMENT OF INDIA BANGALORE,10.08.2006 .
 - **NovAtel, (2006):** "GPS+ Reference Manual" ,2006.
 - **NovAtel,(2006):** "2006 Annual Report, Developing Tomorrow's Technology Today".
 - **Ouattara T., R. Couture, P.T. Bobrowsky, and A. Moore.,2004:**" Remote Sensing and Geosciences" , Geological Survey of Canada, 2004.
 - **Pal,M.,2002:** " Factors Influencing The Accuracy of Remote Sensing Classification: A comparative Study", University of Nottingham, May 2002.
 - **Parkinson,B.,(2007):**" The Future of Satellite Navigation (PNT)", Professor Brad Parkinson, Stanford University, July 2007.
 - **Pat Norris,(2006):**" Global Navigation Satellite Systems (GNSS)", Pat Norris, London ,30 May 2006.
 - **Pavlis, N.K., S.A. Holmes, S.C. Kenyon, J.K. Factor (2008):**"An Earth gravitational model to degree 2160: EGM2008" oral

presentation at the EGU General Assembly 2008, 13-18 April, 2008, Vienna.

- **Peckham, R., (2006):** "Galileo Status", Galileo Masters Competition
- **Pereira, C., (2006):** "Estimating and Mapping Forest Inventory Variables Using the K-NN Method: Mocuba District Case Study-Mozambique", Universita Tuscia, January, 2006.
- **Powell,S.,1997:** "Results of the Final Adjustment of the New National Geodetic Network", Egyptian Survey Authority, 10/23/1997.
- **Prinja,R.,(2003):** "Global Positioning Systems – An Introduction"(Graduate Student) (Department of Computer Science,University of Minnesota.
- **Pullen,S.,(2008):**" Worldwide Trends in GNSS Development and their Implications for Civil User Performance and Safety", Department of Aeronautics and Astronautics, Stanford University, Sam Pullen,2008.
- **Radhakrishnan, (2007) :** " Use of Equatorial orbit for Indian Satellite Navigation Indian Satellite Navigation Program , 13th February 2007
- **Randall B. Smith,(2006):**" Introduction to Remote Sensing of Environment (RSE)" Ph.D., MicroImages, Inc., USA, 23 August 2006, <http://www.microimages.com>.
- **Rebhan, H., M. Aguirre, and J. Johannessen (2000):** "The Gravity Field and Steady-State Ocean Circulation Explorer Mission – GOCE",ESA Earth Observation Quarterly 66, 6–11.
- **Rehab,k.,(2008):** "Performance Study of Wide Area Differential GPS (WADGPS), M.Sc. Thesis, Submitted to the Faculty of Engineering Ain Shams University, Cairo, Egypt, 2008.

-
- **Reigber, C., P. Schwintzer, H. Lühr (1999):** "The CHAMP geopotential mission", *Bollettino di Geofisica Teorica ed Applicata*, Vol. 40, No. 3-4, p. 285-289.
 - **Revnivkykh, S., (2007):** "GLONASS Status and Progress", 47-th CGSIC Meeting, Fort Worth, Texas, September 24-25, 2007.
 - **Richards, J. A., and Jia, Xiuping 1999:** "Remote Sensing Digital Imagery Analysis: An Introduction", Third Edition, Springer-Verlag, Germany, 1999.
 - **Rizos, C., (2007):** "The Future of Global Navigation Satellite Systems", School of Surveying & Spatial Information Systems, University of New South Wales, AUSTRALIA.
 - **Robert Cheney (2001):** "Satellite Altimetry", Laboratory for Satellite Altimetry, NOAA, E/Ra31 SSML3, Room 3260 1315 East-West Highway, Silver Spring, Maryland 20910-3282, USA
 - **Rolf Knig, Ludwig Grunwaldt, Christoph Reigber, Roland Schmidt, Peter Schwintzer (2004):** "SLR and the CHAMP Gravity Field Mission", GeoForschungsZentrum Potsdam (GFZ), Department 1: Geodesy and Remote Sensing Telegrafenberg, 14473 Potsdam, GERMANY, 2004.
 - **Rosmorduc, V., J. Benveniste, O. Lauret, M. Milagro, N. Picot (2006):** "Radar Altimetry Tutorial", December 2006.
 - **Rummel, R. and O.L. Colombo (1985):** "Gravity field determination from satellite gradiometry", *Bulletin Géodésique*, 59, p. 233-246.
 - **Russell G. C., Green K., 1998:** "Assessing the Accuracy of Remotely Sensed data: Principles and Practices, Levis, ISBN: 0-87371-986-7, 1998.
 - **S. Raman, L. Garin, (2005):** "Performance Evaluation of Global Differential GPS (GDGPS) for Single Frequency C/A Code

- Receivers", in Proc. ION GNSS 2005, Long Beach, CA, USA, September 2005.
- **Sandwell,D.,(2007):**"Overview Of Remote Sensing", David Sandwell,2007.
 - **Satoshi KOGURE,(2007):**" QZSS / MSAS Status", CGSIC –47th Meeting ,Fort Worth, Texas September25, 2007, OGURE Satoshi, Japan Aerospace Exploration Agency QZSS Project Team .
 - **Schill, S., D. Rundquist, A. Fillippi, K. Kvamme, J. Cothren, and J. Tullis, (2005):** "Platforms and Sensors Volume of the Manual of Remote Sensing Chapter 11: In situ Sensors and Field Methods", July 2, 2005.
 - **Schmidt, R., Förste, Ch., R. Stubenvoll, F. Flechtner, Ul. Meyer, R. König, H. Neumayer, R. Biancale, J.-M. Lemoine, S. Bruinsma, S. Loyer, F. Barthelmes, S. Esselborn(2007):**"The GFZ/GRGS Satellite and Combined Gravity Field Models EIGEN-GL04S1 AND EIGEN-GL04C", GeoForschungsZentrum Potsdam (GFZ), Department 1 ‘Geodesy and Remote Sensing’, Telegrafenberg A17, 14473 Potsdam, Germany, foer@gfz-potsdam.de
 - **Schnetzer,P.(2007) :**" Supervised Classification: A Landsat 7 ETM+ Scene Covering Portions of New Brunswick, Prince Edward Island and Nova Scotia", December 7, 2007.
 - **Short, N.M, 2006:** The Remote Sensing Tutorial: Greenbelt, MD, National Aeronautics and Space Administration, CD-ROM.
 - **Simonovic,S.,(2002):**" Role of remote sensing in Disaster Management", Nirupama, Ph.D. Post-doctoral Fellow, Institute for Catastrophic Loss Reduction The University of Western Ontario, September 2002.

-
- **Slater, J.A., P. Willis, W. Gurtner, W. Lewandowski, C. Noll, R. Weber, G. Beutler, R. Neilan, G. Hein, (1999):** The International GLONASS Experiment (IGEX-98): Organization, Preliminary Results and Future Plans, Proceedings ION GPS-99, Nashville, Sept. 14-17, 1999, pp. 2293-2302, Inst. of Navigation.
 - **Soanes,C., (2004):** "Orbital Navigation Systems Present and Future Systems", The Dynamic Positioning Centre London and Singapore, September 28-30, 2004.
 - **Steciw,A.,(2008):**" ESA Global Navigation Satellite Systems
 - **Stoney, W.E., 2006:** Guide to Land Imaging Satellites, PECORA 16, Global Priorities in Land Remote Sensing: Sioux Falls, American Society of Photogrammetry and Remote Sensing, CD-ROM.
 - **Story, M., and Congalton, R. G. (1986):** "Accuracy assessment: a user's perspective. Photogrammetric Engineering and Remote Sensing", **52**, 397-399.
 - **Swain, Philip H., and Shirley M. Davis. 1978:** "Remote Sensing: The Quantitative Approach",New York: McGraw Hill Book Company.
 - **Tae-Suk Bae (2006):** Near Real-Time Precise Orbit Determination of Low Earth Orbit Satellites Using An Optimal GPS Triple-Differencing Technique. Presented in Partial Fulfillment of the Requirements for the Degree Doctor of Philosophy in the Graduate School of The Ohio State University, The Ohio State University,2006.
 - **Talbot,N.,(2006):** "The Impact of GNSS Modernization on Precise Positioning, 2006.
 - **Tapley, B. and Ch. Reigber (2001):** " The GRACE Mission: Status and future plans, Eos Trans. AGU, 82(47), Fall Meet. Suppl.,G41 C-02,2001.

-
- **Tapley, B. D. (1996):** "Gravity Recovery And Climate Experiment (GRACE)", Proposal, University of Texas, Austin, Texas. Proposal to NASA's Earth System Science Pathfinder Program.
 - **Tapley, B.D., S. Bettadpur, J.C. Ries, P.F. Thompson, M.M. Watkins (2004a):** "GRACE Measurements of Mass Variability in the Earth System", *Science*, 305, p. 503-505.
 - **Tapley, B.D., S. Bettadpur, M. Watkins, C. Reigber (2004b):** "The Gravity Recovery and Climate Experiment: Mission Overview and Early Results", *Geophysical Research Letters*, 31, L09607, doi:10.1029/2004GL019920.
 - **Tapley, B.D., S. Bettadpur, M. Watkins, Ch. Reigber (2004):** "The Gravity Recovery and Climate Experiment: Mission Overview and Early Results, American Geophysical Union, 2004.
 - **Tocho, C., G. S. Vergos, M.G. Sideris (2008):** "Further Improvements in the Determination of the Marine Geoid in Argentina by Employing Recent GGMs and Sea Surface Topography models", M.G. Sideris Department of Geomatics Engineering, University of Calgary, Calgary, Alberta, Canada.
 - **Touboul, P., E. Willemenot, B. Foulon, and V. Josselin (1999):** "Accelerometers for CHAMP, GRACE and GOCE space mission: synergy and evolution", *Boll. Geof. Teor. Appl.*, 40, 321-327, 1999.
 - **Touti, T., (2004):** "Review Paper: Geometric Processing of Remote Sensing Images: Models, Algorithms and Methods" Natural Resources Canada, Canada Centre for Remote Sensing.
 - **Vanderstraete, T., et. al., 2005:** "Remote Sensing and GIS for Integrated Coastal Zone Management A case Study: The Coral Reefs in the Northwestern Red Sea (HURGHADA, EGYPT), Presented at the Eighth International Conference on Remote

- Sensing for Marine and Coastal Environments, Halifax, Nova Scotia, 17-19 May 2005
- **Vincent, N.,(2007):**" Telespazio France vision on Galileo applications" June 2007, N. Vincent, France.
 - **Visser, H., (2006):** "OmniSTAR Satellite Services", OmniSTAR BV Dillenburgsingel 69,2263HW Leidschendam, The Netherlands, 2006, Email: h.visser@omnistar.nl.
 - **Walton B. Campbell ,Joann M. Nault ,Robert A. Warner,(1997):**" Remote Sensing for Coastal Resource Managers: An Overview" USA, February 1997.
 - **Wang, Y. and Dahman, N.A., 2002:** Active sensors and modern photogrammetry: Geospatial Solutions, Online, www.geospatial-online.com.
 - **Watkins, M. and S. Bettadpur (2000):** " The GRACE mission: challenges of using micron-level satellite-to-satellite ranging to measure the Earth gravity field, Proc. of the International Symposium on Space Dynamics, Biarritz, France, 26-30 June 2000,Centre National d'Etudes Spatiales (CNES), Delegation a la Communication (pub1), June 2000.
 - **Wilkinson, G. G. (2000):** "Processing and classification of satellite images", Encyclopaedia of Analytical Chemistry, Edited by R. A. Meyers. John Wiley and sons, 8679-8693.
 - **www.aa.washington.edu/courses/aa420/references/GPS_intro_2.pdf**
 - **www.aars-acrs.org/acrs/proceeding/ACRS2007/Papers/TS40.5.pdf**
 - **www.amarnaproject.com/pages/recent_projects/survey/middle_eg_ypt/2004.shtml**.
 - **www.amesremote.com/section2.htm**

-
- www.amsa.gov.au/Marine_Environment_Protection/National_Plan/Environment_and_Scientific_Coordinators_Toolbox/Workshop_Proceedings/2004/Day1/Remote_flyer.pdf.
 - www.csc.noaa.gov/crs/rs_apps/sensors/ikonos.htm.
 - www.csc.noaa.gov/crs/rs_apps/sensors/spot.htm
 - www.csc.noaa.gov/products/sccoasts/html/tutlid.htm
 - www.csr.utexas.edu/grace/gallery/gravity
 - www.dnr.wa.gov/htdocs/plso/gps_guidebook_version_1.pdf.
 - www.esa.int/esaCP/SEM9GD2QGFF_index_0.html.
 - www.esa.int/livingplanet/goce.
 - www.esa.int/SPECIALS/GOCE/SEM8VARTKMF_0.html
 - www.evergladesplan.org/pm/pm_docs/qasr/qasr_ch_09.pdf
 - www.evergladesplan.org/pm/recover/recover_docs/qasr/qasr_sec_09_2006.pdf
 - www.faa.gov/about/office_org/headquarters_offices/ato/service_units/techops/navservices/gnss/gps/controlsegments.
 - www.faa.gov/about/office_org/headquarters_offices/ato/service_units/techops/navservices/gnss/waas/news/.
 - www.gdgps.net.
 - www.gim-international.com/files/productsurvey_v_pdfdocument_21.pdf.
 - www.gitta.info/PrimSources/en/multimedia/remotesensing.pdf.
 - www.glonass-ianc.rsa.ru/i/glonass/ICD02_e.pdf.
 - www.gmat.unsw.edu.au/snap/work/2005/cr36-05proj.pdf.
 - www.gs.rmit.edu.au/commimg/Surveying%20using%20the%20GNSS.pdf.
 - www.isprs.org/caravan/documents/Lao_Basic_RS.pdf
 - www.iss-eu.org/occasion/occ44.pdf.

-
- www.lsespace.com/missions/champ.php.
 - www.matimop.org.il/1/foreign/Galileo%20Signal.pdf.
 - www.navcomtech.com/Products/GPS/vuestar.cfm.
 - www.realvista.it/products/docs/P_S.pdf.
 - www.researchplanning.com/pubs/RemoteSensing.pdf.
 - www.sani-ita.com/pdf/SatelliteGuide.pdf.
 - www.scanex.ru/en/publications/pdf/publication22.pdf.
 - www.sinodefence.com/strategic/spacecraft/beidou1.asp.
 - www.sinodefence.com/strategic/spacecraft/beidou2.asp.
 - www.space.gs/08/22-aug-2008-goce.html
 - www.Trimble/findbeacon.asp
 - www.unoosa.org/pdf/icg/2007/algeria/01.pdf.
 - www.unoosa.org/pdf/publications/icg_book01E.pdf.
 - www.usace.army.mil/publications/eng-manuals/em1110-1-1003/c-5.pdf.
 - www.usyd.edu.au/su/agric/acpa/GRDC/GPS%20webpage.pdf.
 - www.usyd.edu.au/su/agric/acpa/people/james/Thesis/Chapter%203_Taylor2004.pdf.
 - www.waterandfood.org/gga/Lecture%20Material/SKSrivastav_Overview.pdf.
 - www-app2.gfz-potsdam.de/pb1/op/champ/more/newsletter_CHAMP_016.html.
 - www-app2.gfz-potsdam.de/pb1/op/grace/results/index_RESULTS.html
 - **Zhang, Y.,(2004):**" Understanding Image Fusion", Department of Geodesy and Geomatics Engineering, University of New Brunswick, Canada, June 2004.
 - **Zhou, Q.,(1999):** " Digital Image Processing and Interpretation", Department of Geography, Hong Kong Baptist University, 1999.

1972

1-

2000

1957

.5-



/

-

• •

-

-

•

-

-

•

-

-